THE

PHYSICAL REVIEW

A JOURNAL OF EXPERIMENTAL AND
THEORETICAL PHYSICS

SEP 14

CONDUCTED BY

THE

AMERICAN PHYSICAL SOCIETY

BOARD OF EDITORS

Managing Editor John T. Tate, University of Minnesota, Minneapolis

G. Breit, P. W. Bridgman, L. W. McKeehan; I. S. Bowen, R. S. Mulliken, H. D. Smyth; E. U. Condon, C. J. Davisson, F. K. Richtmyer

SEPTEMBER 1, 1929

Electron Scattering in Atomic and Molecular Hydrogen – – – Gaylord P. Harnwell

Absorption Coefficient for Slow Electrons in Alkali Metal Vapors – – Robert B. Brode

Electron Emission and Diffraction by a Copper Crystal – – – H. E. Farnsworth

Spark Spectra of Germanium – – – – – – – – – – – – R. J. Lang

Spectrum of Gallium II and the $(4s4p^2)$ Configuration in Gallium I and Indium I – – – – – – – – – – – – – – – – R. A. Sawyer and R. J. Lang

Intensity Measurements in the Raman Effect and the Distribution Law of Maxwell-Boltzmann – – – – – – – – – – – – – – – L. S. Ornstein and J. Rekveld

Secondary Diffraction Maxima of Spectral Lines – – – – – – A. G. Shenstone

Near Infra-Red Absorption Spectra of Some Halogen Derivatives of Ethane – – – – – – – – – – – – – – – B. J. Spence and M. A. Easley

Dissociation of Nitrogen by Electron Impact – – Louis A. Turner and E. W. Samson

Excitation Potential of the Negative Bands of Nitrogen – Louis A. Turner and E. W. Samson

Search for Element 87 by Analysis of Positive Rays – – – – K. T. Bainbridge

Conductivity of Ions in Crossed Electric and Magnetic Fields – – – Leigh Page

Barkhausen Effect in Iron, Nickel and Permalloy. I. Measurement of Discontinuous Change in Magnetization – – – – – – – – – – – – Richard M. Bozorth

Total Radiation from Nickel and Cobalt – – – – – – – – C. L. Utterback

Influence of Surface Conditions and Space Charges on the Conductivity of Poor Conductors – – – – – – – – – – – – – – – – K. F. Herzfeld

Constrictions in Acoustical Conduits – – – – – – – – – – R. B. Lindsay

Letters to the Editor – – – – – – – – – – – – – – – –

Book Reviews – – – – – – – – – – – – – – – – – –

PUBLISHED BY THE AMERICAN PHYSICAL SOCIETY

OFFICERS OF THE SOCIETY

[illegible] C. Gault — University of Chicago, Chicago, Ill.
[illegible] A. Kraus — Bartol Research Foundation, Philadelphia, Pa.
[illegible] Mendenhall — Columbia University, New York City
[illegible] Pupin — Columbia University, New York City
[illegible] T. Ware — University of Minnesota, Minneapolis, Minn.

[illegible] Kelly — University of California, Berkeley, Calif.

THE PHYSICAL REVIEW

[illegible] Physical Society at 450 Ahnaip St., Menasha, Wis.
[illegible] of Minnesota, Minneapolis, Minn. Two volumes annually, [illegible]

[illegible] July 1, 1896, to January 1, 1913, the Review was conducted by Ed[illegible] Merritt and Frederick Bedell, with the financial support of Cor[illegible] The first four volumes were issued annually; subsequent volumes, semi[illegible] volumes in all.

On January 1, 1913, the Review was transferred to the American [illegible] as announced on the first page of the new series which was then begun. [illegible] now conducted by a Board of Editors elected by the Society. Semi[illegible] eight in January and July. Since July 1, 1913, the Review has been issued

[illegible] are referred to page 2 of the advertisements for further information.

[illegible] throughout the Postal Union, $5.00 in advance.

[illegible] of current volume, $6.

[illegible] $3.00, in advance.

[illegible] per volume; Back Numbers, $1.10 per copy for issues prior to [illegible], $.60 per copy for issues subsequent thereto. Postage is free [illegible] below; otherwise postage is extra. No bound volumes can be [illegible] Review's Second Number of First Series, Vol. 1, No. 1 [illegible], Series, Vol. 1, No. 1, January 1916; Vol. 7, No. 2, February [illegible] 1916; and Vol. 7, No. 5, May 1916 (at $0.60 each).

[illegible] will be supplied by the Editor on request. Copy for each num[illegible] Minneapolis, two weeks prior to the date of issue; all copy in [illegible] Send electrotypes direct to the printer, George Banta [illegible]

[illegible] payable in advance; subscription agencies will purchase of the American

[illegible] Complaints of failure to receive the Review, in the case of [illegible] should be addressed to the Treasurer; in the case of [illegible] Menasha, Wis.; or to the Editor. New copies can [illegible] to complaints of non-delivery only if notice of non-delivery is [illegible] of date of issue.

[illegible] should be addressed to the Physical Review, University of [illegible]

Second Series *September 1, 1929* *Vol. 34, No. 5*

THE

PHYSICAL REVIEW

ELECTRON SCATTERING IN ATOMIC AND MOLECULAR HYDROGEN

By Gaylord P. Harnwell*
Palmer Physical Laboratory, Princeton University

(Received July 27, 1929)

Abstract

An apparatus for generating an electron beam of known energy was designed to rotate about an axis perpendicular to the beam, and through which it passed. Those electrons scattered in the neighborhood of the axis through a given angle entered an analyzer in which an energy spectrum was obtained. The scattering gas was hydrogen admitted from the center of a discharge tube. When the discharge was in operation it was estimated that more than 60 percent of the hydrogen was in the atomic condition. At a given electron velocity and angular setting the electron energy spectrum could be analyzed into component peaks which were interpreted as due to elastic, inelastic and ionizing collisions. One inelastic loss of about 8 volts was found to occur and several were observed in the neighborhood of 12.5 volts. From the areas under these peaks the number of electrons scattered through the particular angle could be computed. From these results the number of electrons scattered elastically was plotted as a function of the angle both for the case of atomic and molecular hydrogen. The scattering in both cases was very similar. In the former case the results agreed well within the experimental error with the theoretical curves predicted by quantum mechanics.

THE field of electron scattering is one of particular interest at present for in it modern quantum mechanics is able to make certain definite predictions which are at variance with the older theories and these predictions are capable of direct experimental verification. In fact, one of the chief supports of this theory is its complete and accurate agreement with the results obtained by Davisson and Germer, G. P. Thomson, and others working with electrons scattered by metal surfaces. An additional test of the theory from a slightly different angle is provided by the scattering of electrons in gases. The present writer[1] working in several gases found the scattering much larger than could be accounted for classically, and E. G. Dymond[2] has obtained electron scattering curves in helium in excellent agreement with theorectical curves calculated by N. F. Mott.[3] In view of these re-

* National Research Fellow in Physics.

[1] G. P. Harnwell, Phys. Rev. **33**, 559 (1929).

[2] E. G. Dymond, Proc. Roy. Soc. **A122**, 571 (1929).

[3] N. F. Mott, Nature **123**, 717 (1929).

sults it was thought to be of particular interest to investigate the phenomenon of electron scattering in atomic hydrogen. Theoretically it is much the simplest case. The calculations are free from the approximations necessary in the present state of the theory when dealing with more complicated atoms or molecules. From this point of view it is the most satisfactory gas in which to work, but unfortunately the experimental difficulties are considerable. The most important of these is the difficulty in obtaining a large concentration of atomic hydrogen in the scattering chamber. Also, as it is not possible to have the hydrogen completely in the atomic condition, it is important to know what fraction is dissociated. However, it was not found possible to measure this quantity accurately and various methods of estimation had to be used, as will be discussed later. During the course of this work the scattering in molecular hydrogen was investigated in some detail and several points of interest were found.

The apparatus used was very similar to that described in a previous paper.[2] The scattering chamber is indicated diagrammatically in Fig. 1.

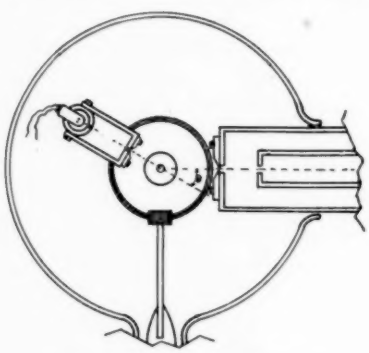

Fig. 1. Scattering chamber.

The electrostatic analyser is not shown. The alterations were mainly in the nature of refinements. The electron gun was redesigned with several points in view. The form of the filament was changed to that of a very narrow hairpin in the hope of decreasing the magnetic field due to the filament current. It was completely enclosed in a copper cylinder in the front of which a slit was cut. This was done in order to decrease the amount of thermal ionization and dissociation in the scattering region, and also to decrease the area of glass wall exposed to the filament as it could not be completely out-gassed. The exit slit of the electron gun was adjustable and made much finer so that the emerging electron beam was more accurately defined. As in the previous apparatus the electrons were accelerated to the first slit by a constant field and then retarded to the desired velocity by an opposing field between the first and second slit. The rotation was obtained by means of a clock gear upon which the gun was mounted and which in turn was supported by arms (not shown) extending from the analyser. This engaged a pinion mounted in a ground glass stopper which could be turned from outside the bulb. A pointer which moved over an angular scale was attached

to the stopper and owing to the gear ratio of 21:4 the angles could be measured more accurately than had been possible previously. Those electrons scattered through an angle θ entered the analyser. This was an electrostatic analyser identical with that described in the paper already referred to. The slits were made as fine as possible for increased accuracy though this entailed a decrease in intensity of the electron beam reaching the Faraday cylinder. For this reason it was found possible to work only with electrons with energies above one hundred volts, though the electrometer sensitivity was increased considerably over that previously used. The inside of the scattering chamber was sputtered with platinum to make it conducting and avoid any errors due to stray electrostatic charges. The electron gun rotated about a hollow axis and along this axis the scattering gas was admitted to the chamber through a short length of glass tube about two millimeters in diameter. A few centimeters above this jet was a large pumping exit, this was arranged so that it could be disconnected if desired. When this was disconnected the gas was pumped out only through the narrow slit in the front of the analyser, and the pressure in the bulb was much higher and also presumably much more uniform in the scattering region. The necessity for this will be seen later. The gas admitted through this small tube was drawn from the center of a Wood's discharge tube. This tube was of fairly small bore and about two meters in length. The hydrogen was admitted to this tube through artificial leaks from the high pressure reservoir. It was generated electrolytically and when atomic hydrogen was being investigated it was passed through no drying agents. When working with molecular hydrogen the gas was stored over P_2O_5 and passed through a liquid air trap. As before the scattering chamber was placed in the center of a framework of coils to neutralize the effect of the earth's and any stray magnetic fields. The current in the coils and the zero position of the gun were determined empirically as described in the paper previously referred to.

Unfortunately it was not found possible to counteract completely the effect of all stray magnetic fields. The main difficulty was caused by the filament current. When the angular setting of the electron gun was changed or when the filament current was increased as was found necessary at large angles the entire energy scale was shifted by a few volts. This, however, was not of great importance if the scale remained uniform. By comparing curves obtained under different conditions this was found to be the case as nearly as could be determined. The maximum error which could be introduced in this would be of the order of two or three percent. Also the heat of the filament and the electrons emerging from the gun undoubtedly ionized and dissociated a certain amount of the hydrogen when the Wood's tube was not in operation. As these effects were undoubtedly small and could not even be estimated they have been neglected. An additional complicating effect was introduced by the scattering of electrons from the front slit of the analyser at small angles. This, however, could be measured accurately by removing the hydrogen from the apparatus and it has been allowed for in the subsequent work. It was only apparent below ten degrees and the correction

to be applied was less than five percent. An additional correction had to be applied at angles below ten or fifteen degrees as the gas pressure was apparently not uniform throughout the effective scattering region. When the pumping exit from the scattering chamber was open apparently a large amount of the hydrogen entered the pumping exit directly from the jet without ever colliding with the walls of the bulb. Thus the pressure decreased radially from the axis about which the electron gun rotated. This was checked by closing this pumping exit thereby increasing the pressure in the scattering chamber and reducing the rate of flow of gas. This made the pressure throughout the bulb quite uniform and by adjusting the pressure to its former value the curves obtained under the two conditions for molecular hydrogen could be compared and the correction to be applied in the former case determined. This correction was found to be of the order of ten percent at small angles and has been applied to the curves which will be given later.

The voltage scale of the analyser was checked by comparing it directly with the accelerating voltage of the electrons. This was done by decreasing the accelerating voltage in small steps and recording the analyser voltage at which the elastically scattered peak appeared. However, even with this calibration, errors of as much as four or five percent might occur in the voltage scale due to unsteady conditions in the scattering chamber particularly when the discharge tube was in operation. This is probably less than the error arising from the uncertainty in the analysis of the curves obtained. The energy losses in hydrogen are so close together that even with the greatest resolution which could be obtained the peaks were not completely resolved. It was thus necessary to analyse the curves obtained into their component peaks which introduced a certain amount of uncertainty as to their intensity and exact position. The error made in position was probably larger than that in intensity.

The fraction of the hydrogen in the scattering chamber which was in the atomic state when the Wood's tube was in operation could not be measured directly. But from the work of Wood,[4] Bonhoeffer,[5] and Kaplan,[6] an estimate of this quantity could be formed. They found the optimum pressure for the formation of atomic hydrogen in a discharge to be about 0.5 mm. Unfortunately the most favorable pressure in the scattering chamber was from 0.02 mm to 0.05 mm. Due to the small tube through which the hydrogen was admitted from the discharge tube to the scattering chamber the pressure in the discharge tube was probably two or three times this, but undoubtedly less than the optimum. However, the center of the discharge tube when it was in operation gave every evidence of the presence of a large amount of atomic hydrogen. The tube exhibited a deep purple color and small bits of metal which had fallen in were raised to incandescence. The Balmer series from this portion of the tube was very strong and the second-

[4] R. W. Wood, Proc. Roy. Soc. **A102,** 1 (1922).
[5] K. F. Bonhoeffer, Zeits. Physik. Chem. **113,** 199 (1924).
[6] J. Kaplan, Phys. Rev. **30,** 639 (1927).

ary spectrum could hardly be discerned visually. Probably at least 90 percent of the hydrogen in that region was atomic. A certain amount of recombination undoubtedly occurred in passing into the scattering chamber. The rate of flow was such, however, that the time taken in passing from the discharge to the scattering region was about a fifth of a second. Part of this distance was through a narrow tube. When the tube was performing most favorably little bits of the sputtered coating in the pumping exit from the scattering chamber could be seen to glow, though not brightly, showing that some of the hydrogen passed through the scattering bulb in the atomic condition. Taken in conjunction with the evidence from the scattering curves themselves which will be mentioned later it was estimated that about sixty percent of the hydrogen was dissociated.

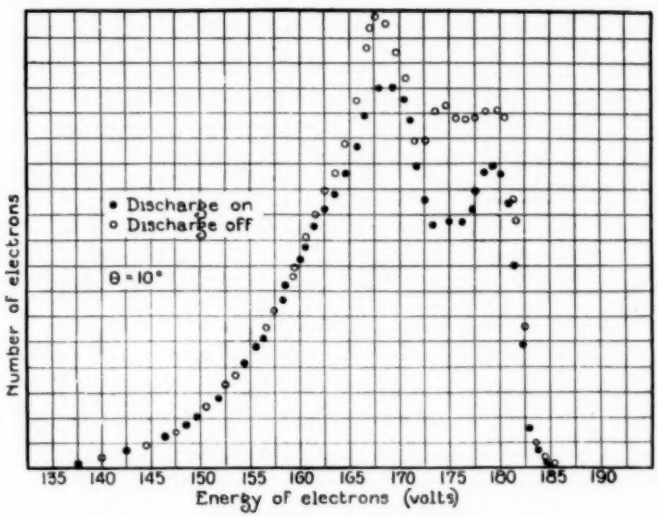
• Discharge on
o Discharge off
θ = 10°
Number of electrons
135 140 145 150 155 160 165 170 175 180 185 190
Energy of electrons (volts)

Fig. 2. Typical curve showing energy losses at 10° scattering. Energy of incident electrons 180 volts.

Before discussing the intensity of electron scattering as a function of the angle there are some points of interest in connection with the types of energy losses observed. A typical curve is given in Fig. 2. In obtaining such a curve the angular setting of the electron gun and the accelerating voltage of the electrons are kept constant while the potential across the plates of the analyser is varied. The electrometer current is plotted against the energy of the electrons in volts as calculated from the analyser potential. The curve in Fig. 2 is quite representative of all those obtained though, of course, the relative intensities of the peaks vary with angle. This curve was obtained with 180 volt electrons deflected through 10°. The circles represent points obtained when the discharge tube was not in operation and hence represent the scattering from molecular hydrogen. The peak on the right at the 180 volt abscissa represents those electrons which have been scattered elastically and will be referred to as the primary peak. About five volts to the left is another peak of approximately the same height. Upon analysing the curve

this is seen to be somewhat farther away and considerably smaller and represents an energy loss which will be discussed a little later. Another slightly unsymmetrical peak occurs about 12.5 volts to the left of the primary peak. At 10° this is seen to be considerably larger than the primary peak and is probably made up of several components. There appear to be several smaller and more doubtful energy losses between 14 and 25 volts which will be referred to later. Beyond 25 volts the points seem to lie on a smooth curve gradually approaching zero about 45 volts to the left of the primary peak. All the curves obtained show these salient characteristics with only small variations. Many curves were taken at each angular setting and in the discussion which follows, values obtained from the averages of these curves will be given.

It is necessary to analyse a curve such as Fig. 2 into its component peaks. It was found that the peaks obtained with this apparatus were quite symmetrical so the process can be carried out with little ambiguity. When this is done it is seen that the first peak to the left of the primary peak represents an energy loss of between 5.5 and 7.5 volts. This is a somewhat surprising result. The current views of the structure of the hydrogen molecule such as given by Heitler and London,[7] Winans and Stueckelberg,[8] and Condon and Smyth[9] give no reason for expecting a characteristic energy loss of this value. Due to the proximity to the primary peak it is difficult to fix this critical potential accurately. However, the lowest recognized critical potentials are three or four volts greater than this, well beyond the limits of error. The energy of dissociation of the hydrogen molecule, though never observed as a characteristic energy loss, is calculated to be about 4.5 volts. The peak observed appears to lie somewhat higher than this though it is possible that there is some undiscovered correction that would lower it by the volt or so necessary for agreement. It is possible that this is the correct explanation but in view of the work of Jones and Whiddington [10] this does not seem particularly promising. These investigators worked with hydrogen in an apparatus approximately equivalent to the present one when the electron gun is set at $\theta = 0$. They analysed their scattered electrons magnetically. They obtained the same type of curves given in this paper though their accuracy was probably greater and there were many differences in the conditions of the experiments. They also obtained a peak in the neighborhood of 7 or 8 volts and their accuracy was such that it probably could not be due to a loss of 4.5 volts. They observed this peak only when the original energy of the electrons was between 26 and 14 volts. The peak due to the 12.5 volt critical potential was present from about 13 volts up, but the 8 volt peak rose rapidly to approximate equality with the 12.5 volt peak with 18 volt electrons and then dropped to zero at about 26 volts. With the present apparatus it was not possible to work at these voltages and the 8 volt

[7] W. Heitler and F. London, Zeits. f. Physik **44**, 455 (1927).
[8] J. G. Winans and E. C. G. Stueckelberg, Proc. Nat. Acad. **14**, 867 (1928).
[9] E. U. Condon and H. D. Smyth, Proc. Nat. Acad. **14**, 871 (1928).
[10] Jones and Whiddington, Phil. Mag. **6**, 889 (1928).

peak was never observable at a gun setting of $\theta = 0$. It was observed only at larger angles and there was always much smaller than the 12.5 volt peak. The apparent ratio of this peak to the 12.5 volt peak decreased as the voltage increased though this effect was not large. Jones and Whiddington advanced the suggestion that this was a hitherto unobserved characteristic energy loss of the hydrogen molecule. The theory that it is an effect due to the molecule receives considerable support from the type of curve obtained in the presence of atomic hydrogen as will be discussed later. The possibility of its being due to adsorbed hydrogen on the slits was considered but in view of its intensity and the geometry of the apparatus this seems unlikely. For its variation with angle is very nearly the same as the 12.5 volt peak which would not be true if it were caused by an adsorbed layer on the slit surfaces. That it is not a characteristic of the apparatus is shown by the fact that it is absent in work that has been done in helium and though there is evidence of such a peak in nitrogen it is smaller and of a somewhat different character. In the same way this is evidence against the possibility of its being due to a nitrogen impurity. Water vapor was undoubtedly present to some extent in all the work but in greatly varying amounts, and this seemed to have no effect on the intensity of the peak. At present it seems to be a real though unexplained phenomenon and further work with this peak at lower voltages is in progress.

The next large peak to the left represents a loss of approximately 12.5 volts. It appears, however, not to be a simple peak and contains at least one large, two small components. The small component on the right represents a loss of about 11 volts and the one on the left between 13 and 14 volts. The dependence on pressure and angle of all these components seems to be the same, and when the dependence on angle is discussed later the sum of these peaks will be the quantity referred to. This group of peaks appears to represent the well-known series of critical potentials lying in this region. They are discussed in detail in the paper of Jones and Whiddington already referred to. To the left of this large peak the curve does not seem to be perfectly smooth but is best analysed into a broad peak of small intensity lying between 15 and 25 volts, and a continuous portion extending on to the left. Some indication as to the nature of this broad peak is given by its variation in intensity with the pressure. When the pressure in the scattering chamber is varied through as large a range as possible this peak varies more rapidly than the first inelastic peaks discussed. The first inelastic peaks vary approximately linearly with the pressure but this peak varies as some higher power. Also the variation in intensity of this peak with angle is less than for the others. Hence this peak is probably caused by those electrons which have suffered two inelastic collisions. As can be seen they occur in the approximately correct region of the energy scale.

The points to the left of these peaks appear to lie on a smooth curve which slopes gradually to the axis at about 135 volts. This continuous portion is probably due to electrons which have suffered one ionizing collision.

The shape of this peak in conjunction with some earlier work[11] gives some interesting evidence on the energy distribution between the electron which does the ionizing and the electron which is ejected. For with a slightly different arrangement of potentials capable of detecting electrons entering the analyser with very small energies a peak very near the zero on the energy scale can be obtained. The slope of this curve on the high voltage side is very similar to the slope of the curve in Fig. 2 between 135 and 155 volts. Owing to the difficulty in working in this low voltage region the results are not of great accuracy. But if the correct explanation is that the continuous curve above 135 volts is due to one of the electrons from the ionization process and the peak near zero to the other the shapes are of interest in connection with the energy distribution. The inference from the slopes would be that at an ionizing collision the energy is not distributed equally between the two electrons, but that one or the other emerges with nearly the total excess of original energy over the ionizing energy. From the curves there would be a certain finite probability of energy sharing between the two electrons which would drop off fairly sharply from the maximum probability of one electron having all the energy.

A typical scattering curve when the Wood's tube is in operation is such as is given by the solid dots in Fig. 2. There are certain obvious changes in character indicating a fairly large proportion of atomic hydrogen. The primary peak is somewhat reduced in magnitude which was an effect almost always observed. This means that the elastic scattering in atomic hydrogen is less than in the molecular form. This is in a general way in agreement with the theoretical prediction. The next peak to the left representing the electrons which have been scattered with a loss of 6 or 7 volts is seen to have dropped very greatly in intensity. It was never possible to obtain a curve in which it had disappeared completely but there seemed to be a rough correlation between the behavior of the Wood's tube and the intensity of this peak. At some times the atomic hydrogen seemed to be produced more efficiently than at others and during these periods the peak was at its minimum. This is the strongest evidence obtained that this peak was due to an energy loss directly attributable to the molecule. The peak at 12.5 volts is seen to be altered also, the apex is no longer at 12.5 but is nearer 11 volts. On analysis it is seen that the component in the neighborhood of 10 or 11 volts has risen very much and the 12.5 volt peak has dropped. The lower characteristic energy loss is what would be expected in atomic hydrogen where the first critical potential is 10.5 volts. The behavior of these peaks in conjunction with the evidence already mentioned is the basis on which the proportion of atomic hydrogen in the scattering chamber has been estimated. The rest of the curve is very similar to that obtained without the discharge, in fact, within the limits of experimental error they are the same.

In passing it might be mentioned that the ratios of these component peaks to one another are of some interest in connection with the probability of ionization or excitation at a collision. The areas of these peaks at a single

[11] G. P. Harnwell, Phys. Rev. 33, 632 (1929).

angular setting can not be compared directly as they vary differentially with angle as will be mentioned in connection with Fig. 3. However, with the aid of these two types of curves an estimate of the total number of electrons scattered by elastic, inelastic, and ionizing collisions can be made. The ratio of each of these to their sum gives the probability of the various types of collisions. As the results are very uncertain at small angles the process is not susceptible of great accuracy. An estimate was made of these probabilities with 180 volt electrons, with these approximately 30 percent of the collisions result in excitation and about 25 percent in ionization. This last is in fairly good agreement with the results obtained by Compton and Van Voorhis.[12] This means that out of 20 collisions approximately 9 are elastic 6 inelastic, and 5 result in ionization.

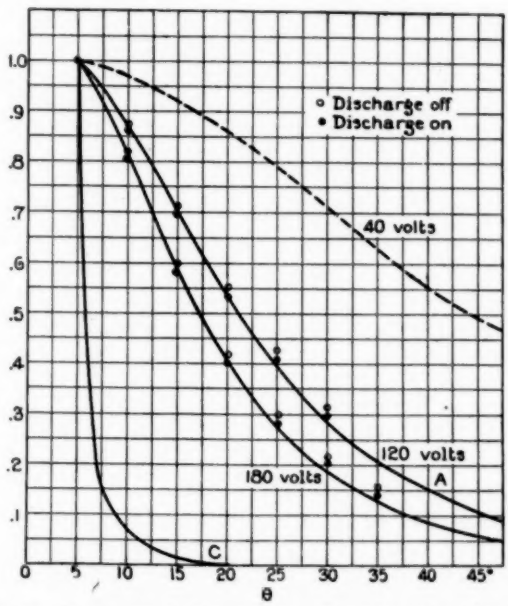

Fig. 3. Intensity of scattered electrons as a function of angle of scattering.

Figure 3 represents the intensity of the scattered electrons as a function of the angle of scattering. As in Fig. 2 the circles represent the case of molecular hydrogen and the dots that of atomic and molecular hydrogen combined. The ordinates of these points are proportional to the areas under the component peaks of Fig. 2 multiplied by the $\sin^2$ of the angle. One of the sine factors is for the variation in effective scattering volume which decreases as the angle increases, the other factor is for reduction to solid angles. As has been mentioned previously there were two corrections to be applied to these areas. The first is that due to the scattering from the slits of the analyser and the second due to the variation in pressure in the scattering region. It has been indicated how these corrections could be determined

[12] K. T. Compton and C. C. Van Voorhis, Phys. Rev. **27**, 724 (1926).

and they have been applied to the points given in Fig. 3. The conditions were so complicated at angles below 5° due to the original electron beam that it was thought best to omit that region. It gave no indication of the maximum of these curves as the results were completely masked by those electrons which entered the analyser without having collided at all. In view of this the curves have all been reduced arbitrarily so as to pass through the unit ordinate at 5°.

The two solid lines marked A in Fig. 3 have been plotted from the formula given by Born.[13]

$$\psi_r=(1/4)(a/r)^2\{(2+z_0^2)/(1+z_0^2)^2\}^2.$$

In this formula ψ_r is proportional to the number of electrons scattered in the solid angle between θ and $\theta+d\theta$, θ being measured from the original beam.

$$z_0=a\kappa_0\sin\theta/2 \qquad \text{and} \qquad a=h^2/4\pi^2me^2$$
$$\kappa_0=2\pi/\lambda_0$$

λ_0 is the deBroglie wave-length associated with the electron and the other quantities have their usual significance. This formula applies only to elastic scattering from atomic hydrogen. An equivalent formula has been given by Sommerfeld.[14]

$$|(\psi'/\psi)|^2=(\epsilon^2z/2Er)^2/(\sin^2\theta/2+\alpha^2)^2$$

where $\alpha=\lambda Z/2\pi a$. In deriving this formula he considered a hydrogen atom with Z electrons in the first quantum state. As a first approximation this might be expected to indicate the changes to be expected in the scattering for the case of the molecule. This would in general correspond to an increase in Z which would not only increase the total amount of scattering, but would also decrease the rate of change with angle. These two effects are observed in the experimental curves.

As can be seen by Fig. 3 there is little difference in the behavior of the electrons scattered in atomic or in molecular hydrogen. Both sets of points lie very well on the proper curves. The points obtained in molecular hydrogen, however, lie farther away than those obtained when atomic hydrogen was present. If it were assumed that 75 percent of the hydrogen was atomic and that hence these points lay partway between the values for molecular hydrogen and the correct values the points would be in slightly better agreement with the theoretical curves, but in either case they agree with them well within the limits of error. The deviations, such as they are, are amply accounted for by the variations in the discharge conditions and hence changes in the relative concentrations of the atomic and molecular states. The agreement affords very interesting evidence in favor of the most recent developments of the quantum mechanics. It is another very interesting point that the scattering by the molecule agrees so closely with that predicted

[13] M. Born, Gottinger, Nachr. p. 146 (1926).

[14] Atombau und Spektrallinien Wellenmechanischer Ergänzungsband, p. 231.

for the atom. Dymond[2] also found that the scattering in helium bore a very close resemblance to that predicted for atomic hydrogen. Of course nothing is shown about the absolute values by these curves because of the convention that had to be adopted in plotting them but the general forms are seen to be very similar.

The apparatus which had been used previously was less accurate but capable of working at much lower electron voltages. With this apparatus curves were obtained with electrons whose original energy was as low as 20 volts. Apparently there were some complicating effects in the region below 40 volts, either due to the apparatus or inherent in the scattering process. Above that value, the curve for which is indicated by the broken line in Fig. 3, the points all lay fairly well on their respective curves. The electron

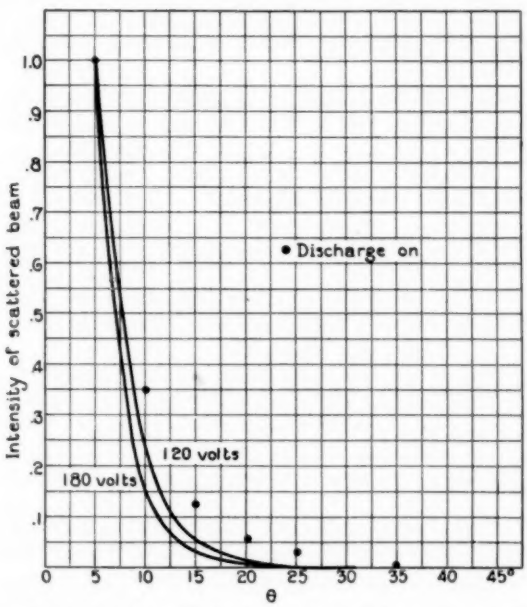

Fig. 4. Intensity of inelastically scattered electrons as a function of the angle of scattering.

energies used were 40, 75, and 100 volts. The points obtained at the lower voltages all lay above those of the higher voltages, but the accuracy was not such as to warrant their inclusion in Fig. 3. They would have occupied the region between the 120 volt curve and the broken line. The steepest curve on the left indicates the values which would be obtained from an inverse square law scattering center, plotted with the same convention as to passing through the unit ordinate at 5°. This is the curve which is approached as the electron velocity is increased. This can be seen from the theoretical expression. An increase in velocity corresponds to a decrease in α, and when α is zero this becomes the well-known Rutherford scattering formula.

Figure 4 is plotted on the same scale as Fig. 3 and with the same convention as to passing through the unit ordinate as 5°. The experimental points

represent the combined areas under the peaks due to inelastically scattered electrons. They are from the curves obtained using electrons of 180 volts energy. The data for this voltage and for 120 volts are the same within the limits of error. The complication of peaks is such that it did not seem fruitful to attempt an analysis of them into those due to molecular and those due to atomic hydrogen. The points given were obtained in the presence of the discharge. The solid lines have been plotted from the formula given by Born[13] for the angular scattering of those electrons which at the scattering encounter have excited the hydrogen atom to the second quantum state. This formula is:

$$\psi_a = 0.9886(a/r)^2(\kappa_1/\kappa_0)/\left\{z_1^2(1+z_1^2)^5\right\}.$$

Here $z_1 = 2a/3\ (\kappa_0^2+\kappa_1^2-2\kappa_0\kappa_1\cos\theta)^{\frac{1}{2}}$; κ_0, θ, and a have the same significance as before, and $\kappa_1 = 2\pi/\lambda_1$, where λ_1 is the deBroglie wave-length associated with the scattered electron.

It can be seen that the experimental points do not lie on the predicted curve. This is not at all surprising as by far the largest contribution to these points is made by the electrons scattered by the hydrogen molecule with a loss of about 12.5 volts. The remarkable thing is that they lie as closely as they do in the region of the theoretical curves. It can be seen that the curve defined by these points is much steeper than the elastic scattering curves. This means that at large angles many more electrons are scattered elastically than inelastically. This is a general characteristic of all the experimental curves which have been obtained. From a macroscopic view point this is rather surprising, for it would seem reasonable to suppose that an exciting or ionizing collision would represent a "more complete" interaction between the atom or molecule and the colliding electron than a collision which left the atom unchanged. If this were so one would be tempted to assume that the original trajectory of the electron would be less important among those factors determining its ultimate direction of ejection. This, however, is not the case. An electron appears to have a better chance of continuing on in its original direction if it has collided inelastically than if it has had a perfectly elastic encounter. In this the results are quite in agreement with the new quantum theory. This same general phenomenon has been observed in nitrogen as will be reported later. It has also been observed by Dymond[2] in helium, though, of course, for these more complicated cases theoretical curves are not available.

In conclusion it is a great pleasure to express my appreciation to Professor K. T. Compton for the privilege of working in the laboratory, and to him and the other members of the department, particularly Professor Condon, for their interest and many helpful suggestions.

THE ABSORPTION COEFFICIENT FOR SLOW ELECTRONS IN ALKALI METAL VAPORS

By Robert B. Brode
University of California, Berkeley

(Received July 27, 1929)

Abstract

The absorption coefficient for electrons has been measured in the vapors of the alkali metals, Na, K, Rb, and Cs. Measurements were made with a beam of electrons bent by a magnetic field through a series of slits arranged on a circle so as accurately to determine the velocity. The path length was kept constant while the pressure was varied by changing the temperature of the metal. The actual value of the vapor pressure is not known accurately and consequently the magnitude of the absorption coefficient is a little uncertain. The shape of the curve is independent of this uncertainty. The absorption coefficient for all the alkali metals increases monotonically from high to low velocity except in the region of the critical potentials where a sharp peak is superimposed on the monotonic rise.

THE absorption coefficient for slow electrons has been measured in most of the stable gases. A satisfactory theoretical interpretation of the results has not been possible because the molecules are of complicated structure. Because of experimental difficulties the simplest atom, monatomic hydrogen, can not easily be studied. The alkali metal atoms are in structure similar to hydrogen and the results of measurements on them may be interpreted by the theoretical discussions of the absorption coefficient for electrons in hydrogen.

Apparatus

The apparatus and method employed in this experiment are the same as previously used for the determination of the absorption coefficient in other substances.[1,2] Fig. 1 shows a cross-section of the apparatus. The source of electrons was a 3 mil tungsten filament, F, in the center of a cylinder, C, 7 mm in diameter. A longitudinal slit in the cylinder, S_c, 0.2 mm wide and 5 mm high, let through a fine beam of electrons. This beam passed through a series of slits arranged on a circle 15 mm in radius. The last slit, S_5, was 1 mm wide and 10 mm high. The other slits were 2 mm wide and 10 mm high. The apparatus was made of tantalum as this metal is non-magnetic and does not alloy or react with the alkali metal vapors.

A large pair of Helmholtz coils neutralized the earth's magnetic field. The magnetic field required for bending the electrons in the circular path was produced by a solenoid whose axis was perpendicular to the plane of the apparatus shown in Fig. 1.

[1] R. B. Brode, Phys. Rev. **25**, 636 (1925).

[2] R. B. Brode, Proc. Roy. Soc. August (1929). The same apparatus as used here is described in more detail in this paper.

The apparatus was enclosed in a Pyrex bulb to which a tube for holding the alkali metal was attached. The tube and the bulb were heated by separate furnaces so that the temperature of the bulb could be maintained above that of the tube. The electrical heating wires of the furnaces were wound so that there was no magnetic field resulting from the heating current. The temperature of the bulb and tube was measured by thermocouples attached to copper cylinders which were in close contact with the glass. The thermocouples were calibrated by comparison with a Bureau of Standards certificated thermocouple.

The Pyrex bulb and apparatus were evacuated and baked at 500°C for several hours. Any residual gas in the metal was driven out by heating the metal parts by an induction furnace to a bright yellow. The metal to be studied was prepared in vacuum by heating the purified salt of the metal

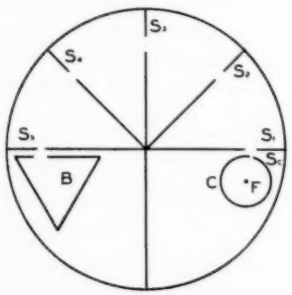

Fig. 1. Diagram of apparatus.

with metallic calcium. Some of the metal thus formed was distilled slowly into the tube attached to the bulb. The apparatus was then sealed off from the pumps. The completeness of the evacuation was shown by the constancy of the results obtained over a period of several weeks. After the measurements were completed with one metal the tube was washed out with dilute HCl and distilled water and then the evacuation process repeated.

The pressure of the metal vapor in the apparatus was determined from the vapor pressure of the metal at the temperature of the tube corrected for thermal effusion between the tube and the bulb. The uncertainty in the absolute magnitude of the values of the absorption coefficients is due almost entirely to the inaccurate values of the vapor pressure constants. The values given by different observers for these constants result in values of the absorption coefficient differing by as much as 2 or 3 fold. The values used here are those given in the International Critical Tables.[3]

Method

The absorption coefficient is determined by use of the equation $I = I_0 e^{-\alpha x p}$ where I_0 is the initial electron current in the beam, I the current at the end of the path x, p the pressure and α the absorption coefficient at unit pressure. It is not possible to measure I_0 under the same conditions as I is measured. For this reason the total emission of electrons through the slit in the cylinder

[3] International Critical Tables, Vol. III, p. 205.

has been used as proportional to I_0. By taking observations at two different pressures the factor of proportionality relating the total emission and the initial current in the beam can be eliminated and the value of α computed. From several determinations, each at a different pressure, identical values of α were obtained. This was found to be true even at velocities corresponding to less than 1 volt accelerating potential.

The velocity of the electrons was determined by the magnetic field used to bend the beam through the slits. Using accelerating potentials between 100 and 400 volts, where the contact e.m.f. was negligible, a linear relation was found between the square root of the potential and the current producing the magnetic field. When plotted, the straight line resulting from this linear relation passed through the origin.

Most of the measurements were made with the filament coated with the alkali metal and emitting at a low temperature. When the filament was heated hot enough to drive off the alkali metal there was a large change in the contact e.m.f. By using the magnetic field to determine the velocity, identical values of the absorption coefficient were obtained at corresponding velocities from both filaments. Because of the very large absorption coefficients for low velocity electrons the pressure of the vapor had to be maintained at about 10^{-5} mm of Hg. The coating of potassium and sodium on the filament could not be maintained when the filament was heated hot enough to give a suitable current for measurements at the lowest velocities. When possible, measurements were made with both types of filament.

Bruche[4] has criticised this simplification of Ramsauer's method as not being capable of results comparable in accuracy with the two-chamber method. The single-chamber method which he uses and describes as "qualitative" can not be expected to give accurate results as the initial current is not measured and any change in the number of photoelectrons emitted due to the introduction of the gas is neglected. The careful study made in the experiments described here, of the relation between the pressure and the resulting values of the absorption coefficient, shows that the simplified method is capable of giving quantitative results throughout the entire range of velocities studied. The two-chamber method employed by Ramsauer and Bruche uses a path about 15 mm long defined by slits 1 mm wide and 10 mm high. The absorption coefficient depends on the length of path and the limiting angle through which an electron can be deflected and still reach the last chamber. Curves with a disagreement in magnitude of 10 to 20 percent, with agreement in form, are described by Bruche as being in contradiction. With measurements of this type not made with the same apparatus some disagreement is to be expected due to a different geometry of the path.

Measurements

The metal was first brought to a temperature giving a suitable pressure while the apparatus was maintained at from 10° to 20° C higher so as to avoid

[4] E. Bruche, Ann. d. Physik **81**, 557 (1926); **83**, 1097 (1927).

condensation on the seals. The accelerating potential was applied between the filament and the cylinder and then the magnetic field varied until a maximum of current was observed by the galvanometer connected to the box B. This maximum was quite sharp at all except the lowest velocities. At low pressure and at velocities corresponding to over 100 volts, more than half of the electrons leaving the cylinder arrived at the box B. The current leaving the slit in the cylinder and that arriving at the box B were measured by galvanometers of a sensitivity of about 10^{-11} amperes per division. In most cases the currents were of the order of 10^{-9} amperes. The two

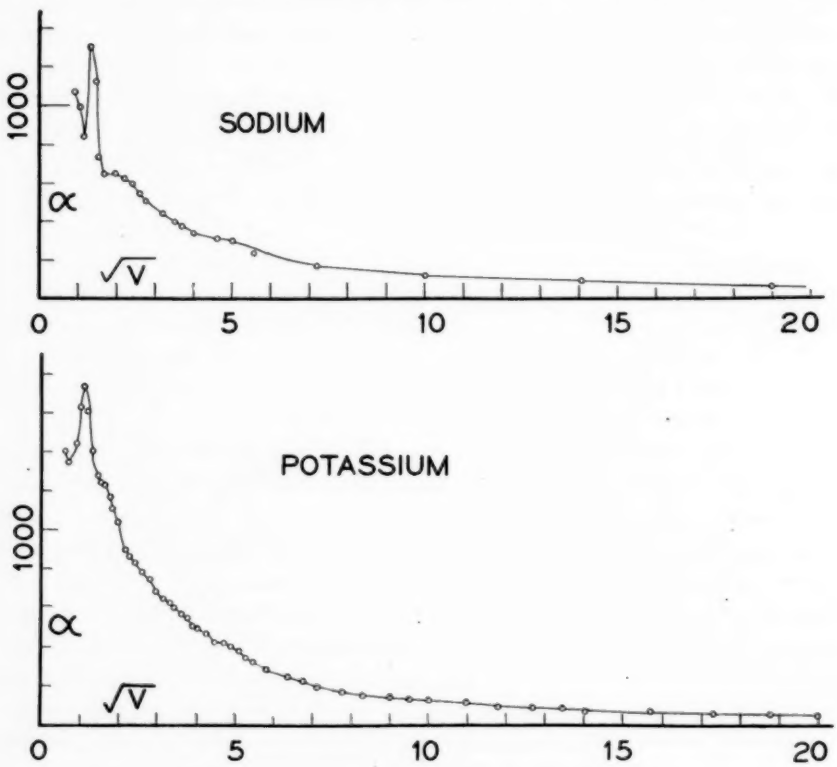

Fig. 2. The absorption coefficient α for electrons in sodium and potassium as a function of the velocity of the electrons.

galvanometer readings, the magnetic field current, the accelerating potential and the temperature of both furnaces were recorded. At each reading the zero points of the galvanometers were observed in order to allow for leakage currents. The efficiency of the guard rings was shown by the fact that with an accelerating potential of 400 volts and with sodium vapor in the apparatus at 300°C only small leakage currents were observed.

The temperatures were then changed and after equilibrium was reached the measurements were repeated throughout the range of potentials used. From 5 to 8 different pressures were used with each metal. The value of α could be computed from readings of the same velocity taken at any two dif-

ferent pressures. The average of the resulting values of α was computed for each velocity and the results plotted in Figures 2, and 3. The value of α is expressed in square centimeters per cubic centimeter of vapor at a pressure of 1 mm of Hg at 0°C. The individual values of α for velocities above 4 volts differed in no case from the average by more than 10 percent. In most cases

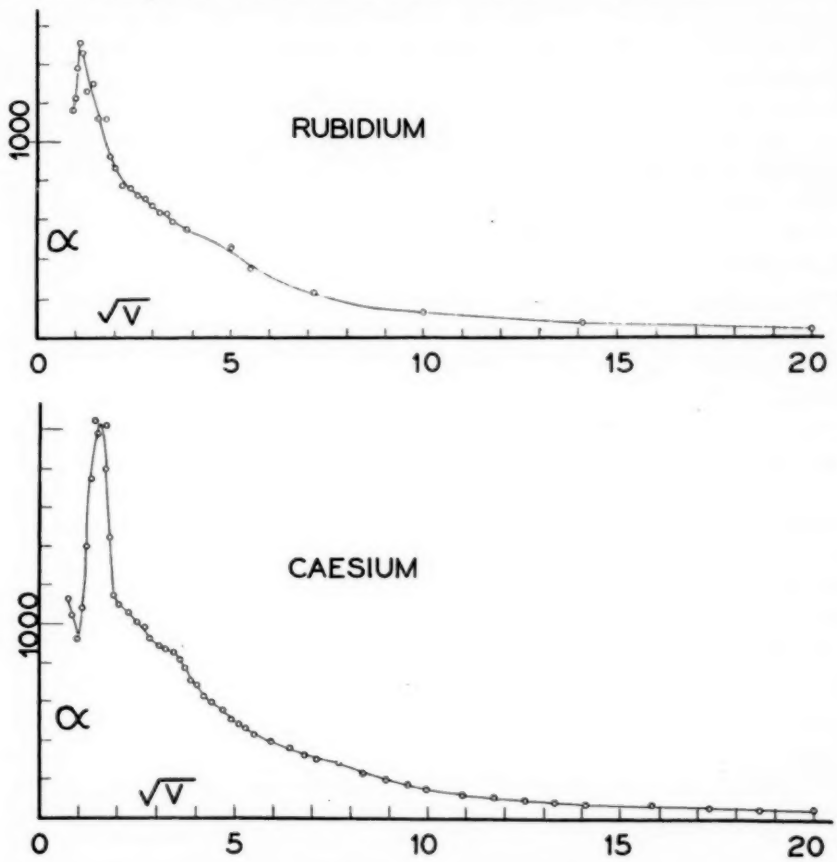

Fig. 3. The absorption coefficient α for electrons in rubidium and caesium as a function of the velocity of the electrons.

this difference could be almost completely removed by assuming that the temperature was measured in error by not more than 1/4° C. Below 4 volts the results were somewhat less consistent but never in greater deviation than 15 percent from the average value.

Discussion

The shape of the observed curves can be described as due to a curve rising monotonically with decreasing velocity to which is added a curve which begins to rise at about the first resonance potential, reaches a sharp maximum and falls rapidly in the region of the ionization potential of the alkali metal. The absorption coefficients of the alkali atoms are much larger than those for

any other materials previously measured. The effective radius of the disk within which the passing electron is deflected out of the beam is given by the relation, radius in angstroms $=0.30\,(\alpha)^{1/2}$. This radius is as large as 10 or 12 angstroms for electrons below 2 volts. Atoms of this size are consistent with the relatively large atomic volumes of the alkali atoms. By either Pauling's[5] or Hartree's[6] method of finding the electron probability distributions, there is an appreciable probability of finding the valence electron between 8 and 10 angstroms from the nucleus.

A treatment of the problem by classical mechanics in terms of the polorization of the atom by the passing electron is difficult. The time of passage is so short that the polarization may not be able to follow the electron. Another difficulty is that the passing electron enters into the same region in which the valence electron is to be found.

Two solutions have been given for the hydrogen atom by the wave mechanics. Elsasser[7] has concluded that the variation of the absorption coefficient with velocity of the electron should consist of a monotonic increase with decreasing velocity superimposed on which is another system of curves begining at the resonance potentials, rising rapidly to maxima and then decreasing with increasing velocity. Oppenheimer[8] by a more general solution has shown that neglecting the polarization effect, the absorption coefficient for electrons in monatomic hydrogen should rise monotonically with decreasing velocity. With a complete solution in which the polarization is introduced it would be reasonable to expect that a type of resonance effect would appear in the region of the critical potentials as is here actually observed.

[5] L. Pauling, Proc. Roy. Soc. **A114,** 181 (1927).
[6] D. R, Hartree, Proc. Cam. Phil. Soc. **24,** 89 and 111 (1928).
[7] W. Elsasser, Zeits. f. Physik **45,** 522 (1927).
[8] J. R. Oppenheimer, Phys. Rev. **32,** 361 (1928).

ELECTRON EMISSION AND DIFFRACTION BY A COPPER CRYSTAL*

By H. E. Farnsworth
Brown University, Providence, R. I.

(Received July 19, 1929)

Abstract

Correlation between changes in slope of secondary electron curve, and position of diffraction beams.—A narrow beam of electrons of variable speed is incident normally on the (100) face of a copper crystal. Measurements of the total secondary electron current are obtained under the same conditions as the angular distribution of scattered electrons for bombarding potentials from 0 to 250 volts, and after the crystal has been thoroughly degassed at red heat in an exceptionally good vacuum. The total secondary electron curve shows two maxima at 3 and 10.5 volts, respectively, and many sudden changes in slope in the region between 10.5 and 250 volts. Intense beams of full-speed electrons are found to issue from the crystal at such voltages as to account for the maxima, and for many of the changes in slope. Other beams are to be expected in the direction of the normal to the crystal, and hence are outside the solid angle of observation; they, however, contribute to the total secondary current, and appear sufficient to account for the remaining changes in slope. It thus appears that changes in the electron emission at potentials corresponding to energy levels within the atom are, at most, relatively unimportant in the production of sudden changes in slope in this region.

Diffraction beams.—With two exceptions, all of the expected diffraction beams which are the x-ray analogues in the two principal azimuths, and in the range below 250 volts are found. In addition, 20 sets of beams are found, 12 of which satisfy the conditions required by a wave of one-half the length given by $\lambda = h/mv$, or by a double grating spacing. These beams appear not to be due to gas. A temperature effect is observed for both types of beams. One additional set of beams at 3 volts does not appear in either of the two principal azimuths, and is not accurately reproducible. Most of the beams are very intense and sharp. In the case of a 70-volt beam, the background scattering of full-speed electrons in azimuth under the best vacuum conditions is found to be only 4.3 percent of the maximum intensity of the beam.

Refractive index.—Both types of classified beams require a refractive index greater than unity. The value of ϕ, however, in the expression $\mu = (1+\phi/V)^{1/2}$ is not constant, but increases from 6 or 7 volts for beams at the lowest voltages to about 25 volts for the beams above 200 volts.

Energy of scattered electrons.—After making correction for an error inherent in the method of measurement, it appears that the diffraction beams are composed entirely of full-speed electrons. These electrons in the case of the 70 volt beam comprise about 50 percent of all the electrons moving in the direction of the beam. *Evidence of a selective angular distribution of emitted electrons*, differing from that of the scattered electrons, is also obtained.

IN A series of investigations[1] the writer has previously shown that the sudden changes in slope in the low-voltage region of the secondary electron curve

* A preliminary account of some of the results reported here is given in Nature **123**, 941 (1929).

[1] H. E. Farnsworth, Phys. Rev. **25**, 41 (1925); **31**, 419 (1928).

(total secondary electron current as a function of bombarding potential) of polycrystalline copper are a function of the arrangement of the surface atoms, and not directly of the structure of the atoms themselves. Since the development of the idea of electron diffraction, it appears natural to attribute these results to the wave nature of the electron. Some evidence of this has already been furnished by experiments[2] in which a change was observed in the angular distribution of the secondary electrons concomitant with the appearance of the changes in slope, mentioned above, which resulted from critical heat-treatment of the target. It appeared advisable, however, to carry out a more direct experiment by measuring the total secondary emission from a single copper crystal under the same conditions as the angular distribution of scattered electrons, and thus make possible a correlation between the voltages corresponding to the changes in slope of the secondary electron curve and the voltages corresponding to the diffraction beams.

This was the original object of the experiments reported here. However, during the course of the experiments there have been certain developments which made it advisable to investigate, in addition, other points of importance. Among these is the subject of refractive index. The results of Davisson and Germer[3] for the (111) face of a nickel crystal require a refractive index in accord with the equation $\mu=(1+\phi/V)^{1/2}$ where V is the bombarding voltage, and ϕ is the inner potential of the crystal which has the constant value of about 18 volts, except for a voltage range in which μ appears anomalous. On the other hand, the results of Rose[4] for the (111) face of an aluminum crystal require a refractive index of unity. Although Rupp,[5] from a study of the transmission of slow electrons through thin metal films, has reported a refractive index greater than unity, G. P. Thomson[6] has shown that Rupp's reasoning was in error, and that his results furnish no information in regard to refractive index. The above experiments leave the subject of refractive index unsettled.

Results on certain other important points which have been investigated are also contained in this report.

Apparatus and Procedure

The essential parts of the apparatus are shown diagramatically in Fig. 1. They are constructed of molybdenum to eliminate magnetic effects. The earth's magnetic field is compensated by Helmholtz coils of 1 meter diameter. A special type of electron gun *SFAB* is used to obtain an intense beam of electrons at the low voltages. It is essentially the same as that previously described,[7] except for the construction of the part *B*. In the present case the construction is such as to permit the maximum possible motion of the

[2] H. E. Farnsworth, Phys. Rev. **31**, 414 (1928).
[3] Davisson and Germer, Phys. Rev. **30**, 705 (1927); Proc. Nat. Acad. Sc. **14**, 619 (1928).
[4] D. C. Rose, Phil. Mag. **6**, 712 (1928).
[5] E. Rupp, Ann. d. Physik **85**, 981 (1928).
[6] G. P. Thomson, Phil. Mag. **6**, 939 (1928).
[7] H. E. Farnsworth, J.O.S.A. and R.S.I. **15**, 290 (1927).

Faraday box *G*. In addition, a ring is attached to *B* which covers the space between *A* and *B*, and thus prevents stray electrons from leaving at this place. The primary electrons strike, at normal incidence, the (100) face of the copper crystal *T* which is placed at the center of the drum *C*. One edge of the drum is made with a slot so that some electrons, after leaving the crystal, may pass through it, and into the opening of the double Faraday box which may be rotated in a horizontal plane from the plane of the target to within 13° of the incident beam. The double box is made with a rectangular cross-section. The sides of each box are made in one piece, properly folded; the ends have projecting pieces which fit snugly over the sides, and hold them in place. The two boxes are insulated from each other by quartz strips. The whole arrangement is assembled with cleaned metal tweezers so that all parts of the box are free from contamination. A fine platinum wire which makes contact with the inner box is shielded by quartz tubing, and passes outward

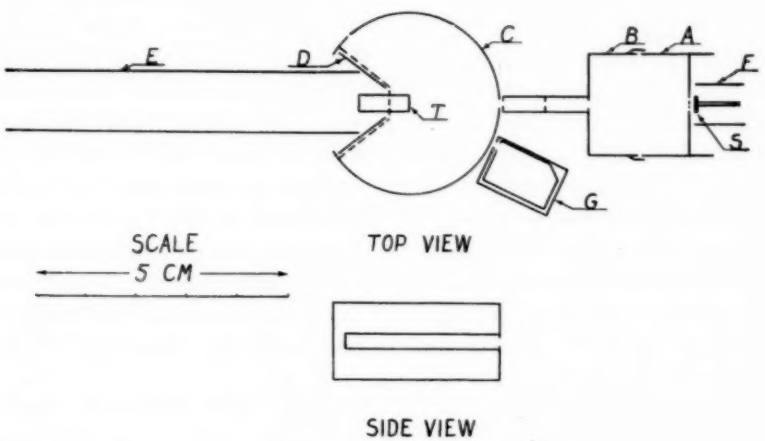

Fig. 1. Apparatus.

from the drum along the axis of revolution. During observations on angular distribution the potential of the inside Faraday box is so adjusted that electrons which have lost more than one volt at the crystal are excluded from the box.

The crystal is mounted on a quartz strip which is rigidly attached to the end of a Pyrex tube by means of a tungsten rod sealed into the end of the tube. The axis of the tube is perpendicular to the face of the crystal. This tube may be rotated or slid in guides parallel to its axis, thus rotating the crystal in azimuth, or removing it into a side tube where it may be heated at red heat. A molybdenum strip, making good thermal contact with the back of the crystal, is heated by electron bombardment, and the crystal is thus heated by conduction. This method of heating was found to decrease the amount of recrystallization which occurred at the place of bombardment of the copper crystal. The crystal was heated so that copper evaporated freely from the surface. A trap-door may be raised in the side tube, after

withdrawing the crystal, to prevent copper vapor from entering the apparatus proper, and thus contaminating insulating surfaces.

The moving parts are operated by two magnetic controls which are sufficiently far removed (from 10 to 12 inches) to cause no measurable effect at the target. The bearings are molybdenum on molybdenum and molybdenum on Pyrex glass.

The metal parts are enclosed in a Pyrex tube in the form of a 3 inch bulb with properly arranged side tubes. The inside of the bulb was made conducting by evaporation from a molybdenum filament. The coating is sufficiently thin to permit observation through it when properly illuminated. This serves as an electrostatic shield, and also permits a measure of the electrons which escape through the slot in the drum. The various metal parts, with the exception of the cylinder E and the target T, are mounted on a Pyrex framework. E and T are mounted on another framework. These two frames were inserted in opposite side tubes, and were brought together in proper alignment by guides attached to the frames. When in place, the crystal is at the center of the bulb.

The total primary current is obtained by measuring the current to the cylinder E and crystal, with the crystal withdrawn to the back end; or by measuring the total current to target, shield, drum and diaphragm D, with the target in the forward position. Since both methods give the same result, the latter is used in practice. The total secondary current is then obtained in the usual manner by subtracting the current to the target from the total current. With the crystal withdrawn, no current is observed to the drum C or diaphram D, thus insuring that the primary beam is not scattered.

The total primary and secondary currents are measured with a galvanometer of sensitivity 10^{-9} amperes per mm on a scale at 1 m distant. The current to the Faraday box is measured by a Compton electrometer of sensitivity about 1000 mm per volt shunted with India ink resistances so as to give a current sensitivity of approximately 10^{-12} amperes per mm on a scale at 1 m distant.

All metal and glass parts of the tube were thoroughly cleaned with chromic acid and distilled water either before or after mounting in place. Where mounting was necessary after cleaning, the parts came in contact with only cleaned rubber gloves or metal tweezers. The tube was baked and pumped for several days.

The pumping system consists of two Pyrex diffusion-pumps and an oil-pump, in series. The mercury shut-off is placed between the two diffusion-pumps so that the minimum length of large glass tubing, which includes a mercury-vapor trap in liquid air, separates the experimental tube from the first diffusion-pump. The diffusion-pumps are kept running during observations. It was originally intended to seal the tube from the pumping system, but the vacuum conditions obtained are sufficiently good without. Under the best conditions no pressure is observable on a sensitive McLeod gauge (a distance of 0.75 mm in the top of the gauge capillary corresponds to 10^{-6} mm Hg) while the crystal is at red heat. Also, the tube has remained as long as

48 hours after stopping the pumps with no pressure observable on the gauge at the end of this time. The good vacuum conditions are attributed, in part, to an additional condensing trap in liquid air which is placed between the oil-fore-pump and the diffusion-pumps, thus preventing any oil vapor from contaminating the mercury in the pumps, and from entering the other liquid-air trap.* This second trap is made of small tubing, and is placed beside the large trap so that one liquid-air container serves to cool both traps.

The crystal was heated separately at red heat for several minutes after baking the whole tube so as to remove the layer of oxide on the crystal face. A series of observations, extending over a period of several weeks, was then made to locate diffraction beams in the two principal azimuths, and in the voltage range from 0 to 150 volts. This consisted in taking colatitude curves for various bombarding potentials so that the complete range was covered in steps of a few volts, and also in obtaining several azimuth curves for the beams. During this period the crystal was not heated; it was probably not well degassed since the total time of heating had been rather short. The time of heating the crystal was purposely made short since two other copper crystals had been damaged by heat-treatment. After the above procedure the crystal was further heated at red heat until it was thoroughly degassed, and the same complete range again investigated. Since the intensity of the electron beams decreased gradually with time, the procedure was adopted of heating the target at red heat each day for about one minute, one-half hour previous to beginning observations. Results were obtained below 150 volts in at least two opposite angles of each azimuth, and over parts of the range in all four angles of each azimuth. The observations were later extended to 250 volts in one of each of the two principal azimuths.

Preparation and Geometry of the Crystal

The copper crystal was obtained from the General Electric Co. It was made by melting and slow cooling in an atmosphere of hydrogen. The approximate orientation of the crystal was determined by a method described by Bridgman.[8] Etching in ammonium persulphate develops both the (100) and (111) faces. A piece of the crystal to be used for the target was carefully cut, with a jeweler's saw, so that one geometrical face was as nearly parallel as possible to a (100) plane. To make the face more nearly parallel to this plane, the following method was used. The crystal was mounted in a wooden holder on the tool-post of a lathe so that the crystal plane in question was approximately perpendicular to the axis of the lathe. After reflection from a small mirror, a narrow beam of light was sent along the axis of the lathe, and reflected by the crystal back to a telescope placed just behind and to one side of the mirror. The adjustment consisted in changing the orientation of the crystal until the crystal facets flashed out in the field of the telescope. The crystal plane in question was then perpendicular to the axis of the lathe. A fine grinding wheel was then mounted on the lathe

* This idea developed during a conversation with Mr. Theodore Soller.

[8] P. W. Bridgman, Proc. Am. Acad. Sc. 60, 313 (1925).

so that it rotated about an axis parallel to the axis of the lathe. Without changing its orientation, the crystal was brought into contact with the grinding wheel which was slowly rotated until a flat surface was produced on the crystal. By re-etching the surface and repeating the above process a few times the desired result was obtained to sufficient accuracy.

After the target has been cut and surfaced it is essential that it be etched sufficiently to remove all broken pieces from the surface. Unless this is done these small crystals will grow at the expense of the larger crystal during subsequent heating.

Since the copper crystal is a face-centered cube, it follows that for normal incidence on the (100) plane there exist four-fold symmetry and two principal azimuths. The azimuths parallel to the cube sides will be denoted as the (100) azimuths, and those parallel to the face-diagonals as the (111) azimuths, in accord with Fig. 2a. When viewed from a direction perpendicular to a (100) plane, the rows of atoms perpendicular to this plane intersect it in points which are represented by circles and crosses in Fig. 2b. If the circles

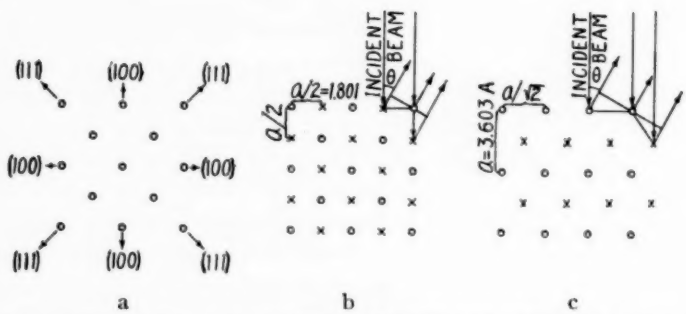

Fig. 2 Structure of the crystal. a—The (100) face and azimuth designation. b—The (100) azimuth. c—The (111) azimuth.

denote atoms lying in the plane of the paper, then the crosses represent atoms lying in front or in back of this plane by an amount $a/2 = 1.801$A. When viewed from a direction perpendicular to a (110) plane, the rows of atoms perpendicular to this face intersect it in points which are shown in Fig. 2c. If the circles represent atoms lying in the plane of the paper, then the crosses represent atoms lying in front or in back of this plane by an amount $a/2(2)^{\frac{1}{2}} = 1.275$. The azimuths lying in or parallel to the plane of the paper are then the (100) and (111) azimuths for Figs. 2 b and 2c, respectively. The (111) azimuth is also the (110) azimuth.

The positions of the theoretical or Laue beams were determined by applying the conditions for constructive interference to radiation coming from rows or lines of atoms perpendicular to the azimuths in question.

Referring to Fig. 2b for the (100) azimuth, the radiation is incident on the crystal in the vertical direction. Let the direction making an angle θ with the vertical, as shown by the arrows, be one in which there is constructive interference. It is seen that if the conditions of constructive interference are satisfied by the three rows of atoms considered, then they will also be satisfied

by all other rows of atoms. These conditions may be stated in the form of the two equations

$$n_1\lambda = 1.8015 \sin\theta, \qquad n_2\lambda = 1.8015(1+\cos\theta),$$

where n_1 and n_2 may have any integer values. Solving these two equations simultaneously, one obtains the corresponding values of λ and θ for various values of n_1 and n_2. The graphical method is given here since it offers a simple method of designating the orders to which the various points correspond. The plots of λ against sin θ obtained from the above equations for various

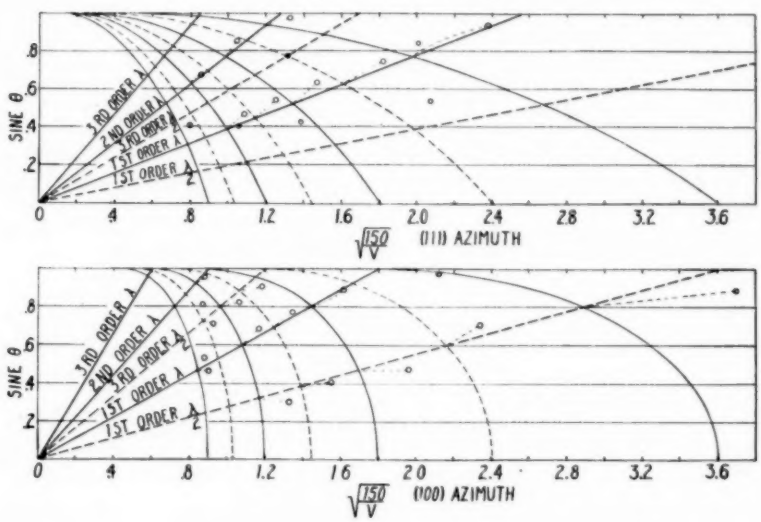

Fig. 3. Location of experimental and theoretical diffraction beams on a plot of sine θ against $\lambda = (150/V)^{1/2}$. Positions of experimental beams are denoted by circles and of theoretical λ-beams by the intersections of continuous curves. Intersections of broken lines with either broken or continuous lines denote the positions of theoretical $\lambda/2$-beams.

values of n_1 and n_2 are shown by the continuous lines in Fig. 3. The positions of the theoretical beams are then given by the intersections of these lines. Referring to Fig. 2c, by a similar consideration for the (111) azimuth, the following two equations are obtained:

$$n_1\lambda = 2.55 \sin\theta, \qquad n_2\lambda = 1.8015 + 2.2070 \cos(\theta + 35°15.6').$$

The plots of λ against sin θ obtained from these two equations are also shown by continuous lines in Fig. 3. These lines determine the positions of the theoretical beams in the (111) azimuth by their points of intersection.

The angular positions and voltages of the diffraction beams occurring in the (1̄00) and (111) azimuths and in the region from 0 to 250 volts are shown in Table I and in the plot of Fig. 3. The theoretical voltages in column 2 of Table I are obtained from the expression $V = 150/\lambda^2$, where λ is the wavelength of the theoretical beams taken from Fig. 3. The voltage differences give the values of ϕ which appear in the expression $\mu = (1+\phi/V)^{\frac{1}{2}}$ for refractive

TABLE I. *Diffraction Beams.*

Experimental voltage of electron beam	Theoretical voltage for $\mu=1$. $V=150/\lambda^2$	Voltage difference	Colatitude angle
	(*100*) *Azimuth*		
57.2	72.3	15.1	63.0°
110.0	129.0	19.0	43.5°
186.5	212.2	25.7	27.5°
196.5	218.0	21.5	72.5°
	"Additional Beams"		
11.0	18.1	7.1	62.5°
27.5	32.4	5.9	45.0°
33.5	—	—	78.0°
39.0	52.5	13.5	28.0°
62.5	77.6	15.1	24.0°
82.5	96.8	14.3	50.0°
85.0	109.0	24.0	17.5°
107.5	133.6	26.1	65.0°
132.5	162.7	30.2	56.0°
176.5	198.0	21.5	45.0°
194.0	—	—	32.0°
199.0	—	—	54.0°
	(*111*) *Azimuth*		
26.5	38.8	12.3	70.0°
70.0	84.0	14.0	39.3°
85.0	105.1	20.1	77.0°
128.0	153.5	25.5	27.8°
135.5	155.8	20.3	56.5°
206.5	234.0	27.5	42.5°
—	245.0	—	—
—	266.0	—	—
	"Additional Beams"		
35.0	—	—	32.5°
37.5	—	—	57.0°
45.5	58.5	13.0	48.0°
79.0	—	—	25.0°
87.5	87.5	0	50.8°
96.0	115.3	19.3	32.7°
137.0	—	—	23.5°
236.5	—	—	24.0°

index. In addition to the beams for which there are x-ray analogues, several others are observed which have been tabulated under "additional beams." Many of these beams occupy the approximate positions which would be expected for a wave of one-half the length given by the expression $\lambda=h/mv$ or for a space grating of twice the spacing for a copper crystal. For convenience of notation such beams will be referred to as $\lambda/2$-beams. Positions of the theoretical beams to which these $\lambda/2$-beams correspond are given by the intersections of broken lines with either broken or continuous lines. The broken lines are obtained from the same equations that give the continuous lines, except that λ is replaced by $\lambda/2$. Hence, the continuous lines of any particular order coincide with broken lines of twice the order. Davisson and Germer[9] have also observed beams which satisfy the same relation, but which are plane grating beams instead of space grating beams. These beams dis-

[9] Davisson and Germer, Phys. Rev. **30**, 705 (1927); L. H. Germer, Zeits. f. Physik **54**, 408 (1929).

appeared with further heating of the nickel crystal, and hence were attributed to a surface gas grating having twice the spacing of the nickel grating.

The "additional beams" which are observed for the copper crystal do not appear to be due to gas for the following reasons: (1) They are space grating beams instead of surface grating beams, i.e., they are sharp in co-latitude angle as well as voltage, and of the same order of intensity as other beams. (2) They are observed under the best vacuum conditions which must be of the order of 10^{-8} mm Hg, and show no indication of decreasing in intensity with further heating of the crystal. (3) They are observed only a few minutes after the crystal has been heated at red heat, i.e., while it is still considerably above room temperature, and exhibit a temperature effect similar to that of the other beams. They attain their maximum intensity about one-half hour after heating, which then decreases very slowly (see Temperature Effect below). (4) Three sets of the "additional beams" fall on first order lines i.e., they are not "half order" beams. They appear too intense to be attributed to a second order beam from a double spaced surface grating. (5) Two sets of beams not satisfying the relation of the majority of the "additional beams" were found to disappear with further heating of the crystal. These may have been due to gas or a trace of copper oxide on the surface.

As mentioned above, these results appear to require an additional wave-length or an additional grating spacing. In either case, the absence of many "additional beams" which are required to satisfy all of the $\lambda/2$-relations is unaccounted for. If the results are attributed to the grating it must be a volume effect, as pointed out above. The type of beams in (4) above would then require the constructive interference of radiation from a surface grating of single spacing with that from a depth grating of double spacing. The fact that most of these beams appear in the (100) azimuth makes it seem that the structure of the crystal is responsible for them.

The following is a summary of the electron beams found to issue from the crystal in the two principal azimuths and in the region 0 to 250 volts:

Ten sets of electron beams are found which are the x-ray analogues, and which require a refractive index greater than unity. This includes three 1st order and three 2nd order sets of beams in the (111) azimuth; three 1st order and one 2nd order sets of beams in the (100) azimuth. One 3rd order and one 1st order set in the (111) azimuth which should appear in this voltage range are missing. In addition, 12 sets of beams appear in the (100) azimuth, 8 of which satisfy the $\lambda/2$-relation, and require a refractive index greater than unity. Three of the remaining beams are very weak. The fourth is quite strong, and falls near one of the x-ray beams which is associated with another electron beam. In the (111) azimuth, three sets are accounted for by the $\lambda/2$-relation, one of which requires a refractive index of unity. There are 4 other sets in this azimuth, all of which are very weak. Besides the above, the observed set of 3 volt beams does not appear in either azimuth, and is not accurately reproducible.

Some of the typical beams are shown in both colatitude and azimuth in Figs. 4, 5, and 6. It is to be noted that the beam in Fig. 6 is an "additional beam" to which statement (4) above applies. The effect of heating the crystal

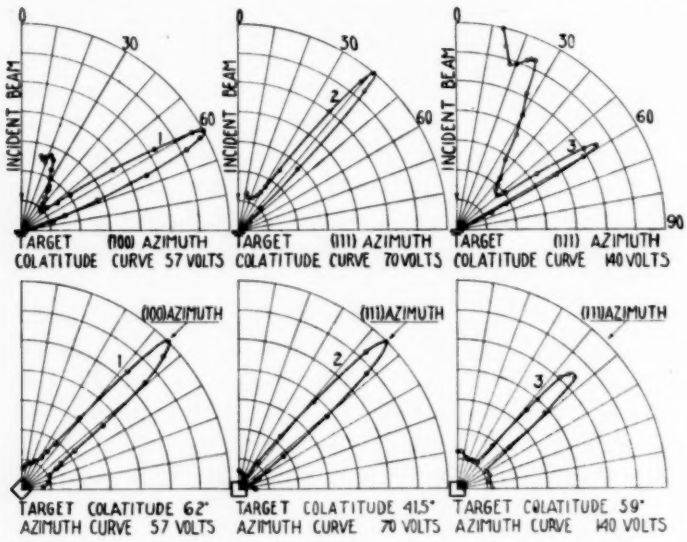

Fig. 4. Beams 1 and 2 are 1st order λ-beams. Beam 3 is a 2nd order λ-beam.

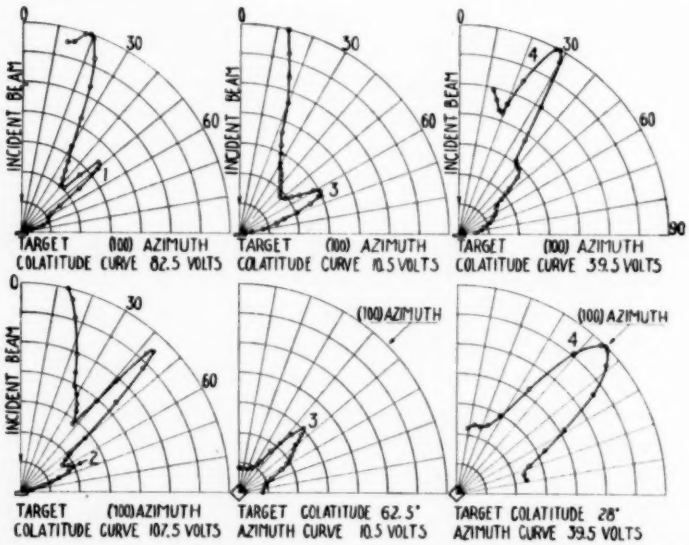

Fig. 5. Beam 1 is a λ/2-beam on the 1st order λ-line. Beam 2 is a 3rd order λ/2-beam. Beams 3 and 4 are 1st order λ/2-beams.

has been to increase the intensity and sharpness of the beams. Some weak beams, which were not found after the initial heating, appeared after subsequent heating. No correction has been made to the colatitude angles to

take into account the effect of background scattering since it is small for most of the beams.

A variation in the colatitude angles for the different beams of a single set indicates that the normal to the crystal face makes an angle of about 2.5° with the incident beam in the plane of a (100) azimuth. The positions of the beams in Fig. 3 and Table I have been corrected for this imperfect alignment. The lack of exact symmetry in azimuth, as shown in Fig. 6, is attributed to this tilt of the crystal face. This lack of symmetry varies in amount with the colatitude angle of the beam, and hence produces an observed variation in azimuth for beams of different colatitude angles.

No attempt has so far been made to make an accurate comparison of intensities of the different beams. Such a comparison would require a knowledge of the actual values of total primary current as well as the values of

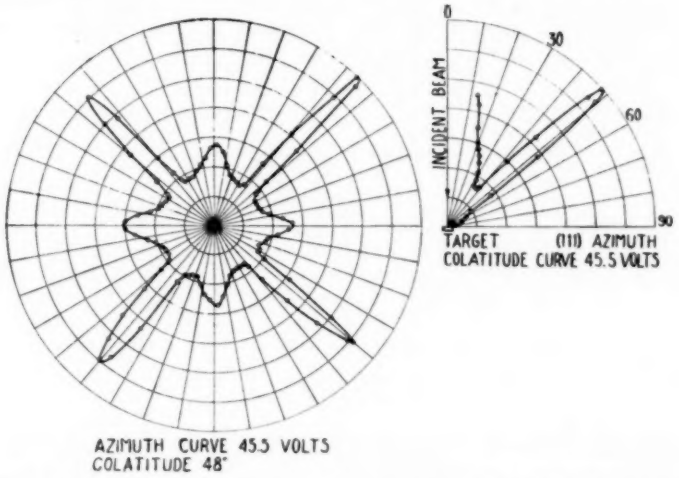

Fig. 6. A λ/2-beam showing symmetry in azimuth, and position in colatitude.

the corresponding currents to the Faraday box, since the total primary current cannot be held constant for all of the beams. In addition, a correction would be necessary for background scattering which differs for each beam.

The values of the voltage difference ϕ given in column 3 of Table I are plotted against the theoretical voltage in Fig. 7. This curve shows that the voltage difference ϕ, instead of being constant, decreases for the lower bombarding potentials, and approaches a limiting value for the higher potentials. This statement also applies to the "additional beams." It is believed that the deviation of the individual values from a smooth variation may well be due to various errors involved. It is impossible to determine the voltage for maximum development of some of the beams with a possible error of less than a few volts. The growth or decay of neighboring beams may falsify the voltage as well as the angular position of any one beam. In my note to "Nature," 30 volts was given for the upper value of ϕ. Although one of the beams does appear to require this value, later observations at higher potentials indicate that 25 volts is more nearly the average for this upper value.

Davisson and Germer[10] found ϕ for nickel to have the constant value of 18 volts, but their observations include only two beams below 100 volts at 54 and 65 volts, respectively. Davis[11] has recently found that a value of 4 or 5 volts for ϕ is required in correlating maxima in the low voltage region of the secondary electron curve of polycrystalline cobalt with bands computed by the application of the Bragg formula to important sets of cobalt planes. From Fig. 7 it appears that the full value of this inner potential ϕ of the crystal is not effective unless the incident electron speed exceeds a certain value. This suggests that ϕ depends on the depth of penetration of the surface layer.

In making observations on total secondary electron emission from a metal target, it is found that after the target has been heated at red heat the apparent reflection coefficient passes through a minimum at a bombarding potential of about one volt, and then rapidly increases as the voltage is further decreased. In the past this has been attributed to a contact potential between the degassed target and the surrounding metal electrodes. Thus, if the target assumes a negative potential of one volt with respect to its

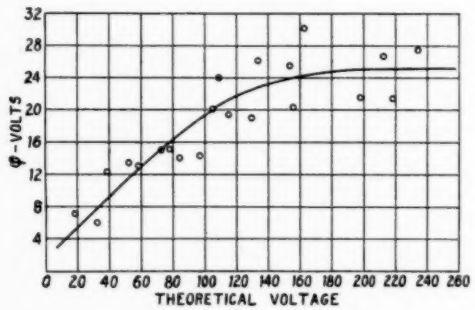

Fig. 7. Inner potential ϕ of the crystal as a function of theoretical voltage of electron beams.

surroundings as a result of heat-treatment, then all primary electrons having an energy less than one equivalent volt are turned back from the target, and consequently increase the apparent reflection coefficient. To compensate for this effect the target has been placed at a positive potential of the correct amount. This is one volt for the copper crystal in the present experiments. However, recent theoretical investigations by Nordheim,[12] in terms of the new quantum mechanics, make it appear that an appreciable reflection coefficient is to be expected for very low-speed electrons. If this result is found to be in accord with experiment, then the effect observed is the combined effect of a contact potential difference and of a reflection coefficient. The present experimental arrangement affords no means of distinguishing between the two possibilities. In case the reflection coefficient proves to be responsible for an appreciable part of the effect, a correction must be applied to all experimental voltages in this paper. The effect of this correction would

[10] Davisson and Germer, Proc. Nat. Acad. Sc. **14**, 619 (1928).
[11] Myrl N. Davis, Nature **123**, 680 (1929).
[12] L. Nordheim, Zeits. f. Physik **46**, 833 (1928); Proc. Roy. Soc. **121**, 626 (1928).

be to decrease the values of ϕ, given in column 3 of Table I, by an amount not greater than one volt.

An experiment is now being planned by the writer by which it is hoped that a distinction may be made between the above possibilities, and the effect of each separately determined.

Total Emission

A comparison of the total secondary electron curve for the (100) face of a single copper crystal, as shown in Fig. 8, with that previously obtained for a polycrystalline copper surface[1] shows the presence of many more sudden changes in slope in the curve for the single crystal, although both curves show maxima and minima in the low-voltage region. It is also to be noted that the positions of the sudden changes in slope of the curve for

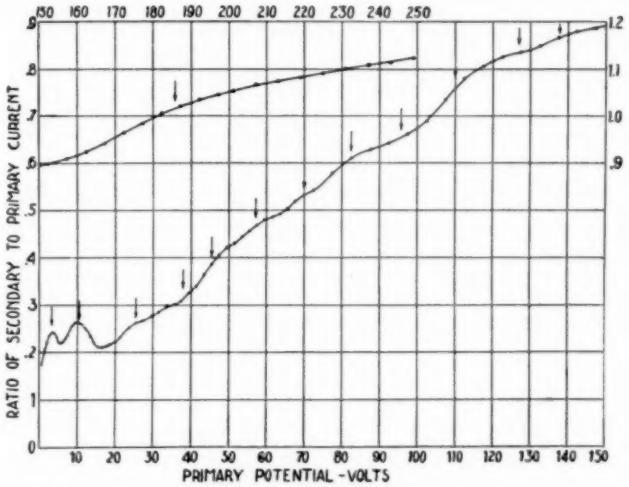

Fig. 8. Total secondary electron curve for the (100) face of a copper crystal. The upper curve is a continuation of the lower curve, and is plotted to the scales at the upper and right sides.

the single crystal do not coincide in voltage with any of those of the curve for the polycrystalline surface. These results confirm the statements in the first paragraph of this article. The arrows indicate the voltages at which intense diffraction beams are found to leave the crystal. They are such as to account for the two maxima and for many other changes in slope. Other beams are to be expected in the direction of the normal, and hence are outside the solid angle of observation; they, however, contribute to the total secondary current. For a refractive index of unity these beams in the region 0 to 250 volts would occur at 11.6, 46.3, 104.2, and 185 volts. Taking into account the actual refractive index, from Fig. 7, these beams should occur at approximately 7.5, 36, 84, and 160 volts. Similarly, there may be "additional beams" satisfying the $\lambda/2$–relation, for which the theoretical voltages are 26.0, 72.4, and 141.5 volts. When the values of refractive index are taken into account, these voltages should have the approximate values of

19, 57, and 118 volts. Although these values are only very approximate, a comparison with Fig. 8 shows that they are in satisfactory agreement with the curve, and appear to account for the changes in slope not accounted for by the observed beams.

The sharpness of the changes in slope of the curve is decreased by the fact that each electron beam is present over a range of several volts. This sharpness is still further decreased by the tilt of the target, which causes the voltages for the maximum development of the four beams in the four different angles of the same azimuth to have different values. When these factors are taken into account, it appears that most, if not all, of the departures from a smooth curve may be accounted for by the diffraction beams. In the low-voltage region, where the emission is negligible, these beams produce actual maxima in the curve. At higher voltages maxima do not occur because of the rapid increase in the number of emitted electrons with increase in voltage.

Temperature Effect

Davisson and Germer[9] have reported the effect of temperature of the nickel crystal on the intensity of the diffraction beams. A similar effect is observed in the present experiments for a copper crystal. The purpose of the curves in Fig. 9 is to verify the statement, previously made, that the "additional beams" show a temperature effect similar to that of the beams having x-ray analogues. The curves shown were obtained within five minutes after heating the target at red heat; hence the target was several hundred

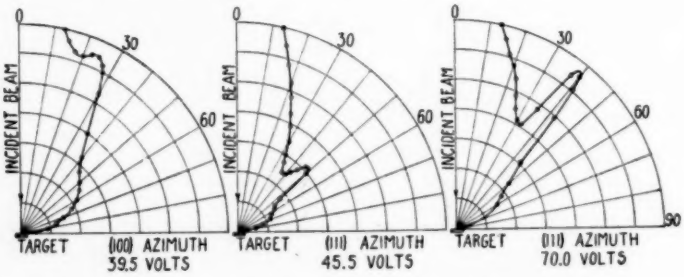

Fig. 9. The effect of increase in temperature of crystal on the relative strength of electron beams.

degrees C above room temperature during the observations. All of the beams investigated were found to be very weak in comparison with their relative intensity at room temperature, as shown in Figs. 4, 5, and 6. The intensity of the beams increases rapidly as the target cools; it attains a maximum value in about one-half hour, after which it decreases very gradually (only a few percent over a period of several hours).

Resolving Power of Crystal and Apparatus

In general, the voltage range over which an electron beam is observable depends on the intensity of the beam and the value of the bombarding

potential. For example, the 26.5 volt beam can just be detected at 23.5 and at 30.5 volts. This gives a ratio of the observed range, expressed in wave-length difference, to the wave-length of the beam at maximum development of $\Delta\lambda/\lambda = .125$. The corresponding values for the 70.0 volt beam are 52.5 to 77.5 volts and $\Delta\lambda/\lambda = .205$; for the 135.5 volt beam they are 125.5 to 145.5 volts, and $\Delta\lambda/\lambda = .072$.

The beams at the lower voltages move toward smaller colatitude angles as the voltage is increased, such that $V^{1/2} \sin\theta$ remains approximately constant, but the beams at higher voltages grow and decay in a total angular displacement which is much smaller than the above relation requires. In fact, in some cases the position of the beam remains very nearly the same. Davisson and Germer attribute this failure to obey the plane grating formula to the lack of sufficiently wide crystal lattices.

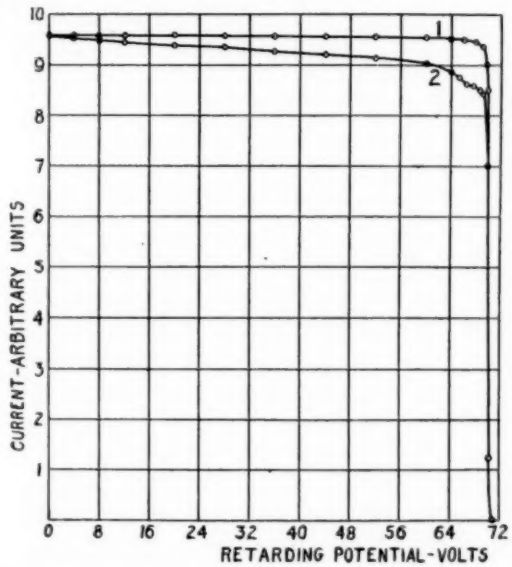

Fig. 10. Curve 1 shows correct energy distribution of primary electrons. Curve 2 shows apparent energy distribution of primary electrons.

The ratio of the background scattering to the maximum intensity of the diffraction beams is, in general, much smaller than the ratio observed by Davisson and Germer for a nickel crystal. This ratio for the 70 volt beam was found to be only 4.3 percent in azimuth under the best vacuum conditions. The beams for copper are also generally sharper in colatitude and azimuth than those for nickel, although some of the "additional beams" lack this extreme sharpness. Only a part of this difference for the two metals may be attributed to the difference in resolving power of the two pieces of apparatus.

The resolving power of the apparatus, as determined by the size of the opening in the Faraday box and its distance from the target (a 1 mm opening at 19 mm from the target), is less than the effective resolving power under

the conditions of observation. This results because the effective opening of the outer Faraday box is decreased by the retarding potential difference which exists between the boxes, i.e., only those high-speed electrons which are directed at a circular area somewhat smaller than the actual area of the opening, and concentric with it, are able to enter the inner box. That this is the case is shown by measurements with a similar arrangement on the primary beam whose correct energy distribution is known. The arrangement used for measurements on the primary beam is shown in Fig. 1. The primary beam passes through a 1 mm opening in the last diaphragm of the cylinder *B*, and then through an adjacent concentric opening of 2 mm diameter in the drum. By applying a retarding potential to the drum *C* and the electrodes *D* and *E* behind it, the shape of the field at the entrance of the drum should very closely approximate that at the entrance of the inner Faraday box, for the same potential differences. Curve 2, Fig. 10, shows the results of measurements of current to *C*, *D*, *T*, and *E* for various retarding potentials, and with a fixed primary voltage. The ratio of the difference between the ordinates of the two curves to the ordinate of the correct curve, at any particular retarding potential, should give the effective decrease in area for that retarding potential and for the primary potential used. This assumes, of course, a uniform distribution of current density over the area previous to the application of the retarding potential.

Energy Distribution of Scattered Electrons

Referring again to Fig. 10, the energy distribution of the primary electrons, as expressed by curve 2, shows the presence of the main group of full-speed electrons and, in addition, a smaller group of nearly full-speed electrons. From the considerations contained in the previous paragraph, it follows that this second group is only apparent, and is caused by the geometry of the arrangement used for the measurements. Measurements on the energy distribution of scattered electrons by the method in question are hence subject to the same error, and require a correction. This correction may be approximately obtained from a comparison of the apparent and correct energy distributions of the primary beam. The correction may then be applied to the apparent energy distribution of the scattered electrons to obtain the correct energy distribution. This method of correction assumes the same distribution of current density across the primary and scattered beams that are being measured. Although this requirement is not fulfilled, at least an approximate correction can be made.

Taking the case of the 70 volt diffraction beam, curve 1 of Fig. 11 shows the current to the inner Faraday box as a function of the retarding potential between the two boxes. This curve represents the apparent distribution due to the sum of the emitted electrons, the background scattering, and the diffraction beam itself. The effects of the first two are eliminated by subtracting curve 2 which represents the apparent distribution of the emission and background scattering for the same voltage and colatitude angle, but different azimuth. Although the background scattering varies somewhat

with azimuth, the shape of the curve should not be very different. Similar estimates of the background scattering were also obtained by keeping the azimuth and coalitude angles unchanged, and varying the voltage. A curve obtained by the former method is shown here because it furnishes unexpected information regarding the emission. Comparison of curves 1 and 2 in the low-voltage region shows that there are more low-speed electrons in the azimuth-angle which does not contain the diffraction beam. Since the low-speed electrons are interpreted as emitted electrons, it follows that the emission is considerably greater in the azimuth-angle not containing the diffraction beam, and hence there is an angular distribution of emitted electrons which does not coincide with the angular distribution of scattered

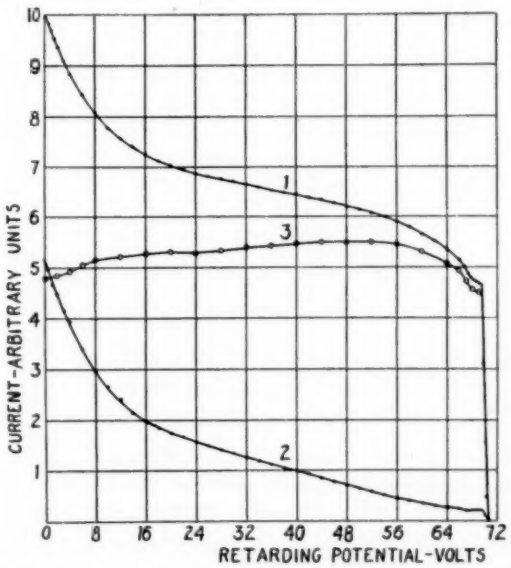

Fig. 11. Curve 1 shows apparent energy distribution of electrons in the 70 volt beam. Curve 2 shows apparent energy distribution of electrons for the same voltage and colatitude angle, but for azimuth angle differing by 22.5°. Curve 3 is obtained by subtracting curve 2 from curve 1.

electrons. This point has not been investigated in detail. The negative slope of curve 3 in the low-voltage region is, of course, a result of the distribution just mentioned. Returning now to a consideration of the scattered electrons, we see that, in addition to a group of full-speed electrons, there is an apparent group of nearly full-speed electrons similar to that shown in curve 2 of Fig. 10 for the primary beam. From the close similarity of these two curves it appears that this group of nearly full-speed electrons is entirely due to the defect in the method of measurement. Taking this, the background scattering, and the emission into account, it may be concluded that all of the electrons contributing to the diffraction beam considered are full-speed electrons.

Figure 12 shows two uncorrected energy distribution curves both of which are taken at the positions of the maximum development of diffraction beams.

A similar distribution is observed in these cases, although a smaller percent of full-speed electrons is present. In the case of the 70 volt beam the remarkable result is observed that at least 50 percent of all the electrons moving in the direction of the beam are full-speed electrons.

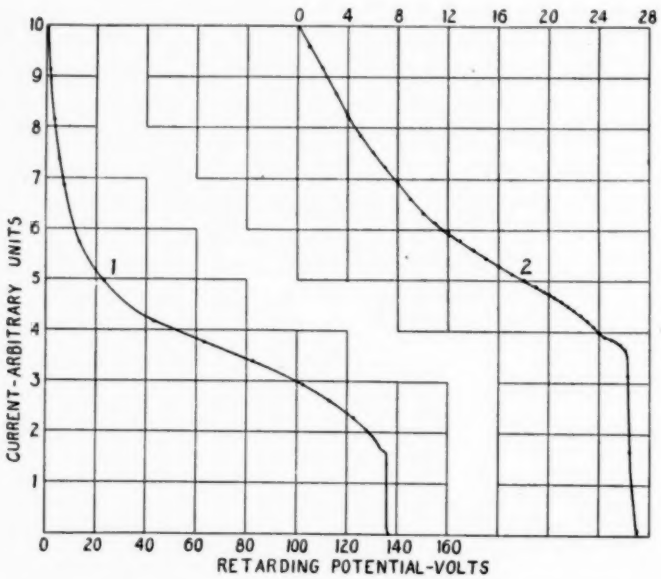

Fig. 12. Curve 1 shows apparent energy distribution of electrons in the 136 volt beam. Curve 2 shows apparent energy distribution of electrons in the 26.5 volt beam.

I have been greatly aided in these experiments by my research assistant, Mr. Newton Underwood. Most of the reducing and plotting of data has been done by Mr. Vernon Goerke. It is a pleasure to record here my sincere thanks to several Providence friends who have made this assistance possible. I am also indebted to the General Electric Co. for furnishing the copper crystal from which the target was cut.

THE SPARK SPECTRA OF GERMANIUM

By R. J. Lang
University of Alberta, Edmonton

(Received May 24, 1929)

Abstract

The first three spark spectra of germanium have been extended by the discovery of many new terms and combinations as follows: Ge II $s4p^2\ ^2S$ and $p^3\ ^2P$. Ge III $s4s\ ^1S_0\ s5s\ ^1S_0\ s4p\ ^1P_1\ s5s\ ^1P_1\ s4d\ ^1D_2\ s4f\ ^1F_3\ p4p\ ^1D_2\ p4d\ ^1P_1\ ^1F_3\ ^1D_2\ d4d\ ^1D_2$ and possibly $s5g\ ^3G\ ^1G$. Ge IV $d^{10}\ 6p\ ^2P\ d^{10}\ 5g\ ^2G$, $d^9\ s^2\ ^2D$.

THE first and second spark spectra of germanium were investigated for the first time by the writer[1] over a year ago and this work was followed by the work of Rao and Narayan.[2] The detailed agreement of the results of these two investigations is very gratifying and leads to a good measure of confidence in the term scheme there proposed. In these reports, however, not much more was attempted than an outline of the first two or three terms of each series from the normal configurations and in neither were the normal G terms recorded.

This report records the results of an attempt to extend these term schemes, especially for the singlet system of Ge III, but in the course of this work certain new terms were located also in Ge II and IV. These results are discussed separately for each stage of ionization throughout the body of the report. At the end of the report a complete list of all the classified lines of Ge II, III and IV is given.

The condensed spark between metallic germanium electrodes in vacuo and in an atmosphere of hydrogen with various amounts of inductance in series has been employed as a source and the spectra were resolved by means of a two-meter grating having 30000 lines per inch mounted in a vacuum spectrograph. In the case of the spark in hydrogen the spark chamber was separated from the main body of the spectrograph by means of a thin disk of fluorite which was cemented over the slit. The hydrogen was placed only in the spark chamber and usually at a pressure of one atmosphere. Ordinary commercial hydrogen was used and it was found that when the gas was placed in the spectrograph proper as well as in the spark chamber no radiation reached the photographic plate shorter than λ1600A or so on account of the absorption of the gas in the light path of 4 meters length.

For photographs of the vacuum spark between germanium electrodes in the region between λ5000A and λ2450A the writer is indebted to Professor Stanley Smith of this laboratory. Plates were taken on a two meter grating in a Rowland mounting and also on a Hilger E 178 one meter interchangeable prism spectrograph.

[1] Lang, Proc. Nat. Acad. Sci. **14**, 32 (1928).
[2] Rao and Narayan, Proc. Roy. Soc. **A119**, 607 (1928).

In the tables which follow, the wave-lengths are given in I.A. (air) above λ2000A and I.A. (vacuum) below that value while all the wave-numbers have been reduced to values in vacuum. The wave-lengths of about ten lines in the Schumann region are taken from data by Carroll.[3]

The notation used throughout this report is in accordance with the recent recommendations of the committee on notation[4] in so far as these have been understood by the writer.

The First Spark Spectrum, Ge II

No extensive investigation of this spectrum has been attempted here chiefly because the available sources are not well adapted to the excitation of the first spark spectrum beyond a few low-lying terms. It appears, however, that a doublet P and a doublet S term from the $4s4p^2$ configuration have been located. The doublet D term had already been located.

Table I. *Predicted and empirical terms in Ge II.*

Configuration	Predicted Terms	Empirical Terms and Term Values
	^4P	
$s4p^2$	^2D	$^2D_{1\frac{1}{2}}$ 63623 $^2D_{2\frac{1}{2}}$ 63454
	^2S	$^2S_{\frac{1}{2}}$ 42240
	^2P	$^2P_{\frac{1}{2}}$ 37625 $^2P_{1\frac{1}{2}}$ 36518

In Table I all the terms expected from this configuration are given together with all the empirical terms which have been found. The term values are taken relative to an assumed value of $s^24f^2F = 28320$ cm^{-1}. This value was chosen by Rao and Narayan[2] and seems to be of about the proper value. The ^2D and ^2P terms were given in the previous report of the writer,[1] with slightly different absolute values, but are repeated here for completeness

Table II. *New combinations in Ge II.*

$s4p^2$			$s^24p\ ^2P_{\frac{1}{2}}$ 128635		$s^24p\ ^2P_{1\frac{1}{2}}$ 126871
$^2S_{\frac{1}{2}}$	42241		86397 (3) 3		84627 (3) −3
$^2P_{\frac{1}{2}}$	37625		91012 (7) 2		89249 (5) 3
		1107			
$^2P_{1\frac{1}{2}}$	36518		92119 (7) 2		90355 (8) 2

and also to point out that but one of the suggested P terms given by Rao and Narayan was correct. The separation of their two suggested P terms was much too great.

[3] Carroll, Trans. Roy. Soc. **A225,** 357 (1926).

[4] Russell, Shenstone and Turner, Phys. Rev. **33,** 900 (1929)

In Table II the combinations of these $s4p^3$ terms with the s^24p^2P terms are given. In this table the levels are designated at the heads of the columns and at the left side for the rows; in the body of the tables are the wave-numbers of the observed lines followed in parentheses by their intensities. Below each wave-number is the discrepancy between the observed wave-number and the wave-number calculated from the values assigned to the levels.

Ge III

Some of the important states and terms expected on the Hund theory in the spectrum of doubly-ionized germanium are given below.

Configuration	Terms		Configuration	Terms
$s4s$	^1S		$s5s$	^3S ^1S
$s4p$	^3P	^1P	$p4p$	^3P ^1S D
$s4d$	^3D	^1D	$p4d$	^3P D F; ^1P D F
$s4f$	^3F	^1F	$p4f$	^3D F G; ^1D F G
$s5g$	^3G	^1G		

The empirical terms and term values of Ge III which have been located are given in Table III. These term values depend upon an arbitrary choice of 65500 cm^{-1} for the value of the $^3F_4$ term. There are successive members

TABLE III. *Empirical terms and term values of Ge III.*

Odd Terms		Even Terms	
Terms	Term Values	Terms	Term Values
$s4p\ ^3P_0$	214303	$s4s\ ^1S_0$	276036
$s4p\ ^3P_1$	213540	$s4d\ ^1D_2$	131064
$s4p\ ^3P_2$	211898	$p4p\ ^3P_0$	128345
$s4p\ ^1P_1$	184163	$p4p\ ^3P_1$	127392
$s5p\ ^3P_0$	94165	$p4p\ ^1D_2$	127260
$s5p\ ^3P_1$	93997	$p4p\ ^3P_2$	125663
$s5p\ ^3P_2$	93538	$s5s\ ^3S_1$	117459.8
$s5p\ ^1P_1$	91727.2	$s4d\ ^3D_1$	113185.0
$p4d\ ^1D_2$	78914	$s4d\ ^3D_2$	113114.2
$s4f\ ^3F_2$	65580.7	$s4d\ ^3D_3$	113007.7
$s4f\ ^3F_3$	65563.3	$s5s\ ^1S_0$	108586
$s4f\ ^1F_3$	65505.	$s6s\ ^3S_1$	64887
$s4f\ ^3F_4$	65500	$s5d\ ^3D_1$	62902.8
$p4d\ ^1P_1$	63677	$s5d\ ^3D_2$	62872.2
$p4d\ ^1F_3$	62457	$s5d\ ^3D_3$	62828.0
		$s5g\ ^1G_4$	41126.?
		$s5g\ ^3G$	41108
		$d4d\ ^1D_2$	40128

of series which may be used to calculate limits but in all cases these combinations fall rather far in the extreme ultra-violet and since there are but two members in any case the results of such calculations may be looked upon merely as a rough guide in making the choice for the basic term value. The comparison of term values for the isoelectronic sequence given in Table IV shows clearly that this choice has been made with reasonable accuracy. In this table the term values for Ga II have been taken from unpublished work by Dr. R. A. Sawyer and the writer and those for As IV and Se V from the results of Sawyer and Humphreys.[5] On the other hand Rao and Narayan

[5] Sawyer and Humphreys, Phys. Rev. **32**, 583 (1928).

based their term values upon an assumed value of 63000 cm^{-1} for $^3F_4$. This value is almost certainly too small by 2000 cm^{-1}. The estimate seems to have been made on the assumption that the $4F$ orbits are non-penetrating and that these term values can therefore be estimated on the basis of a Coulomb field; but while this is the case for lighter elements it does not seem to be justified for Ge III and still less for Pb III.

All of the term values given are measured from one origin; namely, the $3d^{10}4s^2S_1$ term of Ge IV, for while the $4p4p$, the $4p4d$ and the $4p4f$ terms all converge to the limit $3d^{10}4p^2P$ of Ge IV, no sequence of terms for any of these has been obtained to enable one to estimate the true term values as measured from the proper limits.

The ionization potential of Ge III as estimated by means of the 4^1S_0 term is 34.07 volts.

The comparison of term values made in Table IV will serve to show not only that the term values form a very uniform sequence for the various ions

TABLE IV. *Comparison of term values.*

	$N=$	4	5	6	7
	$R/N^2=$	6858.56	4389.48	3048.25	2239.53
S_1	Zn		22094.4	10334.4	6020.5
	Ga/4		15629	8111	4991
	Ge/9		13051	7030	—
	As/16		12443	—	—
	Se/25		12094	—	—
P_2	Zn	43455.0	14519.4	7695.8	
	Ga/4	29177	11683	—	
	Ge/9	23544	10393	—	
	As/16	21232	—	—	
	Se/25	19793	—	—	
D_3	Zn	12997.6	7187.0	4553.3	
	Ga/4	12896	7069	4481	
	Ge/9	12556	6981	—	
	As/16	13018	—	—	
	Se/25	13268			
F_4	Zn	6931.3	4442.3		
	Ga/4	7031	4494		
	Ge/9	7278	—		

and thus constitute a proof of the essential correctness of the choice of the term values, which, in all cases but Zn I, rest upon an arbitrary basis, but also to show the increasing departure, not only of the D terms, but also the F terms from the value derived for a purely hydrogenic orbit. In this connection we may compare the results with those for the sequence of ions beginning with Rb I[6]. Here it was found that in the Moseley diagram the line for the $4D$ terms was no longer parallel to the line for the $4F$ terms but diverged in such a way that it crossed both the $5P$ and $5S$ lines before the second stage of ionization had been reached. Here we can see that exactly the same thing is happening. In Zn I the $4D$ terms are smaller than either

[6] Bowen and Millikan, Phys. Rev. **28**, 923 (1926).

TABLE V. *Combinations and intensities in the spectrum of Ge III.*

Even Terms \ Odd Terms		$s4p\ ^3P_0$	$s4p\ ^3P_1$	$s4p\ ^3P_2$	$s4p\ ^1P_1$	$s5p\ ^3P_0$	$s5p\ ^3P_1$	$s5p\ ^3P_2$	$s5p\ ^1P_1$	$p4d\ ^1D_2$	$s4f\ ^3F_2$	$s4f\ ^3F_3$	$s4f\ ^1F_3$	$s4f\ ^3F_4$	$p4d\ ^1P_1$	$p4d\ ^1F_3$
		214303	213540	211898	184163	94165	93997	93538	91727.2	78914	65580.7	65563.3	65505	65500	63677	62457
$s4s\ ^1S_0$	276036	0	9		40				2							
		−2	0		0				−113							
$s4d\ ^1D_2$	131064		8	20*	6					00	2		10			
			0	3	0					−4	−2		0			
$p4p\ ^3P_0$	128345		10						3?							
			0						−3							
$p4p\ ^3P_1$	127392	12	8	15						3					0	
		4	0	0						0					−1	
$p4p\ ^1D_2$	127265		8	3							0	0		00	0	1
			−5	−6							−1.3	−1.7		1	9	−5
$p4p\ ^3P_2$	125663		10	8	00					1					1	
			2	0	−5					−5					−1	
$s5s\ ^3S_1$	117459.8	8	12	12	0	150	200	200	15							
		−2.2	−0.2	−2.2	−1	−0.6	−0.1	−2.2	2.4							
$s4d\ ^3D_1$	113185.0	12	10	2		3	3	0	4		15				2	
		−2.0	4.0	−2.0		−1.6	−0.2	2.2	−0.2		−1.6				0	
$s4d\ ^3D_2$	113114.2		15	10			5	10	10	3	2	15	15		4	1
			3.2	0.2			0.3	−0.2	−0.3	2.9	−0.6	−0.8	−6.5		−2.9	1
$s4d\ ^3D_3$	113007.7			15				18				1	25	25		2
				1.7				0.3				−1.1	0.5	−2.5		−1
$s5s\ ^1S_0$	108586		2		4					5						
			4		−4					−2.1						
$s6s\ ^3S_1$	64887	0	1	2		20	40	40	2							
		−2	−12	−13		2.5	1.6	2.3	1.4							
$s5d\ ^3D_1$	62902.8	1				25	25	3	1							
		−4.2				2.6	1.5	0.9	0.8							
$s5d\ ^3D_2$	62872.2		2	00			35	20	8							
			−12.8	−5.8			0.8	1.2	0.2							
$s5d\ ^3D_3$	62828.0			3				40								
				−13				2.5								
$s5g\ ^1G_4$	41126?									0			50			6
										−2			0			3.7
$s5g\ ^3G$	41108?										30	35		40		0
											−1.8	−1.8		3.2		−0.2
$d4d\ ^1D_2$	40128								0		0	2			12	
									−2.2		−0.7	−0.2			−0.8	

* Classified also as Ge II.

$5P$ or $5S$ but before Ga II is reached $4D$ has exceeded $5P$ and has practically reached $5S$ at Ge III and exceeds it in As IV and Se V. This may be taken as evidence of the increasing penetration of the $5D$ orbits. The steady *increase* rather than decrease of the comparative term values for the F terms is found here exactly as it was in the Rb sequence.

In Table V the combinations in the spectrum of Ge III are given. The levels are designated at the heads of the columns and rows together with the term values referred to an arbitrary value $s4f^3F_4 = 65500$. In the body of the table the intensities of the observed combinations are given and below each intensity the discrepancy (observed value minus calculated value) between the observed wave-number and the wave-number calculated from the positions assigned to the levels.

Table V together with the table of classified lines at the end of the report exhibits fully all the data in connection with the spectrum of Ge III but since the singlet system and the resonance lines form such an important part of any spectrum and since only a few lines are involved it was thought wise to place these in a separate table (Table VI) for ease of reference in connection with the discussion which follows.

TABLE VI. *Singlet terms and combinations in Ge III.*

Combination	(I.A. vac)	I	ν	Term	Values
$s4s\ {}^1S_0 - s5p\ {}^1P_1$	542.90	2	184195	$s4s\ {}^1S_0$	276036
$s4p\ {}^3P_1 - s5s\ {}^1S_0$	952.76	2	104958	$s4p\ {}^1P_1$	184163
$s4s\ {}^1S_0 - sp\ {}^1P_1$	1088.46	20	91873	$s4d\ {}^1D_2$	131064
$s4p\ {}^1P_1 - s5s\ {}^1S_0$	1323.22	4	75573	$s5s\ {}^1S_0$	108586
$s4d\ {}^1D_2 - s4f\ {}^1F_3$	1525.38	10	65559	$s5p\ {}^1P_1$	91728
$s4s\ {}^1S_0 - sp\ {}^3P_1$	1600.09	9	62496	$s4f\ {}^1F_3$	65505
$s4p\ {}^1P_1 - s4d\ {}^1D_2$	1883.26	6	53099		

It is necessary of course to assume the identification of several of the singlet lines in order to make a start on the analysis of the singlet spectrum. However, since the leading triplet terms were already known and also since the singlet spectrum of Ga II has been analysed thus making the irregular doublet law data available (Table VII) it is now possible to choose these

TABLE VII. *Irregular doublet law.*

	${}^1S_0 - {}^1P_1$ Difference		${}^1S_0 - {}^3P_1$ Difference		${}^1P_1 - {}^1D_2$ Difference	
Zn I	46745	23954	32502	15316	15713	21305
Ga II	70699	21174	47818	14678	37018	16081
Ge III	91873		62496		53099	

singlet lines with a fair amount of assurance. The last three lines in Table VI are prominent in the spark in hydrogen and are the only three unclassified Ge lines of any considerable intensity in this region. They occur also in

the vacuum spark with about equal intensity. The resonance line seems to be almost certainly chosen correctly not only because the line itself has the proper characteristics but also because it fits so well into Table VII. The line at λ1733.8 suggested by Rao and Narayan does not appear on my plates at all and no other line appears which can possibly be used that would approximate to the requirements of Table VII. The line given in the writer's previous report also was much too long in wave-length. The choice for the singlet line D–F leads to a term value for ^1F which differs from $^3F_4$ by but 5 units of wave-number. In Ga II these terms are separated by 8 units and in Zn I they have probably not been separated. We must thus conclude that in Ge III the intercombination lines D–F are blended with two lines of the triplet spectrum $^3D_3$–$^3F_4$ and $^3D_1$–$^3F_2$ as they are in Ga II and probably in Zn I also. This blending of these lines is indicated in Table V by entering the intensities of the lines in both spaces and in the table of classified wave-lengths by writing both classifications opposite the blended line. It may be stated in connection with these and other lines in the germanium spectrum which are supposed to be blends of two or more lines, that a new vacuum spectrograph capable of accommodating a grating of three meters radius has been completed and it is hoped shortly to attempt to resolve many of such lines in the Schumann region.

The intercombination lines between triplet and singlet terms are but few in number and some of these are weak. This weakness of intercombination lines is characteristic of lighter elements. In Al II but four such lines were found[7] including the resonance line and no singlet P or triplet S terms were involved. Thus in Ge III we actually have an increase in the number and intensity of these lines. In Pb III we find a further pronounced increase in the intensity of intercombination lines[8] over those in Ge III. This increasing intensity is associated with the increasingly wide triplet intervals in these spectra.

A peculiar feature of the spectrum of Ge III is the fact that the $s5p\,^1P_1$ term gives stronger intercombinations than $s4p\,^1P_1$. This may be partially accounted for by the fact that the combinations of $s4p\,^1P_1$ term with the second triplet D terms are very far in the ultra-violet but the absence of combinations with the first triplet D terms is quite abnormal.

In Table III possible values for the $s5g\,^3G$ and ^1G terms are given. Just in the region about λ4100A where the 4^3F–5^3G combination is expected there are four very intense lines which occur in two pairs with nearly equal separations. These four lines certainly belong together for changes of inductance alter all four in the same way. Besides the photographs taken in connection with this work those shown by Lunt[9] were available. On the plates used by the author all these lines have about the same characteristics as other strong Ge III lines in the neighborhood as for example the triplet $5S$–$5P$. These lines are all fairly broad and the measurement of them is not a highly accurate

[7] Sawyer and Paschen, Ann. d. Physik **84**, 1 (1927).
[8] Smith, Phys. Rev. **34**, 393 (1929).
[9] Lunt, Roy. Astro. Soc. **85**, 38 (1924).

one so it could not be decided absolutely whether the separations involved are those of the ^3F levels or not. Certainly they are approximately so if we use the three shortest lines for the ^3F–^3G combination assuming that ^3G is unresolved. This leaves the fourth line (λ4100A) to be accounted for and if the foregoing is true this can be no other than 4^1F–5^1G. This results in a value for ^1G slightly greater than ^3G. In support of the assignment there are two further combinations, the triplet and singlet G terms each combining with $p4d\,^1F_3$.

Rao and Narayan have given two terms suggested as two members of the $p4p\,^3P$ term but while the first of these agrees with the $^3P_1$ in the table the writer is of the opinion that the other is unreal since the pair of lines on which it was based turn out upon more accurate measurement not to have the correct separation. The singlet D term expected from this configuration is thought to have been found although it is higher in this case than in most similar spectra where it usually lies below the $s4d\,^3D$ terms. It may have been this singlet D term which was found in Sn III at 99650 cm^{-1} but this is hard to decide since both this and the normal singlet D terms may combine with the normal $4s4p$ and $4s4f$ terms only.

The terms of the $p4d$ configuration may combine with those from $s4s$, $s4d$, $p4p$, $p4f$ whenever the inner quantum numbers permit. The three singlet terms seem clearly to be the P, D and F terms expected from this configuration. The D term is expected to lie somewhat lower than the P term. The combinations of this D term are comparatively intense and plentiful. The variations in the wave-numbers with respect to the calculated values are irregular and somewhat large, a feature which seems to be characteristic of all these terms from higher states. The question of the reality of the term given as $^1G_4$ is not clarified at all by these data since the only combination expected, if it really is a G term, is masked by a very strong arc line and one combination may be present (with $p4d\ ^1D_2$) which would be forbidden in such a case. Some traces of the triplet P term of this configuration have been found also but these were too fragmentary to place in the tables.

Some other terms have been located which come from either the $d4d$ or $p4f$ configurations. Unfortunately the terms from these two configurations may combine with exactly the same terms out of all those which have been identified thus far so that one cannot distinguish between them by means of their combinations alone. But one of these terms will be given here; it is given tentatively as arising from the $4d4d$ state.

Evidence for Change of Coupling

If the ratio of the two intervals in the triplet P terms of C III,[10] Si III,[11] Ge III, Sn III[12] and Pb III[13] be compared as in Table VIII a progressive increase is clearly evident in these interval ratios for both the first and

[10] Bowen and Millikan, Phys. Rev. **26**, 316 (1925).
[11] Fowler, Trans. Roy. Soc. **A225**, 1 (1925).
[12] Green and Loring, Phys. Rev. **30**, 574 (1927).
[13] Smith, Nat. Acad. Sci. Proc. **14**, 878 (1928).

second P terms and the effect is much more marked in the second case. When the electronic spins of all the electrons involved in the production of the spectrum (in this case two) combine to form a resultant magnetic moment s and the moments of each electron in its orbit taken separately are combined to form a resultant moment l and when these two resultants combine to give a total resultant j we have the familiar Russell-Saunders coupling which leads to the interval rule of Landé. For triplet P terms we therefore expect the intervals to have a ratio of 2:1. An increase in this ratio is taken to indicate a change from the Russell-Saunders coupling toward the (jj) coupling in which the electronic spin of each electron forms a resultant moment with the magnetic moment of ts orbital motion and the resultants for each electron combine to give the final moment of the system.[14] The

TABLE VIII. *Progressive change in triplet interval ratios.*

	First P terms	Second P terms
C III	Unresolved	2.34
Si III	1.85	2.22
Ge III	2.15	2.72
Sn III	2.45	4.43
Pb III	3.66	30.12

failure of the Landé interval rule is far more pronounced for the second P terms than for the first P terms. This can only mean that the (jj) coupling tends to predominate for a $4s$ and $5p$ electron over a $4s$ and $4p$ electron. Thus when the total quantum numbers are the same for the two electrons the failure of the Russell-Saunders coupling is not so pronounced as when these numbers are different. This is borne out also by the fact that for the P terms of the $p4p$ state in Ge III the interval ratio is 1.81. One finds the same result in the arc spectra[15] of the elements mentioned at the beginning of this paragraph. Here the failure of the Landé interval is very marked for the $p5s^3P$ terms but not nearly so complete for the $3p^{23}P$ terms. It would seem that the explanation for this increasing departure from the Russell-Saunders coupling is simply that the influence of the rest of the electrons on the more loosely bound radiating electron is lessened when the latter is in the higher states. It then tends to act more as an independent unit and less in association with neighboring electrons.

GE IV

The third spark spectrum of germanium arises from the stripped atom and is therefore the simplest of the three, the normal spectrum comprising an ordinary doublet system. This normal doublet spectrum has been studied by Carroll[3] Rao and Narayan[2] Smith[16] and the writer[17] and the lowest two or three terms of each configuration are well known.

[14] Goudsmit and Humphreys, Phys. Rev. **31**, 960 (1928).
[15] Gartlein, Phys. Rev. **31**, 782 (1928).
[16] Smith, Nature, Nov. 19 (1927).
[17] Lang, Phys. Rev. **30**, 762 (1927).

In Table IX all the known term values of Ge IV are given and in Table X the observed intensities of all lines assigned to this spectrum; below each

TABLE IX. *Empirical terms and term values of Ge IV.*

Odd Terms			Even Terms		
Configuration	Term	Value	Configuration	Term	Value
$d^{10}4p$	$^2P_{\frac{1}{2}}$	287386	$d^{10}4s$	$^2S_{\frac{1}{2}}$	368701
$d^{10}4p$	$^2P_{1\frac{1}{2}}$	284598	$d^{10}4d$	$^2D_{1\frac{1}{2}}$	178094
$d^{10}5p$	$^2P_{\frac{1}{2}}$	142242	$d^{10}4d$	$^2D_{2\frac{1}{2}}$	177840
$d^{10}5p$	$^2P_{1\frac{1}{2}}$	141304	$d^{10}5s$	$^2S_{\frac{1}{2}}$	169432
$d^{10}6p$	$^2F_{2\frac{1}{2}}$	111205	d^9s^2	$^2D_{1\frac{1}{2}}$	108759
$d^{10}4f$	$^2F_{3\frac{1}{2}}$	111200	d^9s^2	$^2D_{2\frac{1}{2}}$	104256
$d^{10}6p$	$^2P_{\frac{1}{2}}$	85080	$d^{10}5d$	$^2D_{1\frac{1}{2}}$	102064
$d^{10}6p$	$^2P_{1\frac{1}{2}}$	84938	$d^{10}5d$	$^2D_{2\frac{1}{2}}$	101984
			$d^{10}6s$	$^2S_{\frac{1}{2}}$	98643
			$d^{10}5g$	^2G	70322

intensity the discrepancy is also given. All of the term values rest upon an arbitrary choice of 111200 cm^{-1} made by Carroll for $d^{10}4f^2F_{3\frac{1}{2}}$. The comparison

TABLE XI. *Comparison of term values.*

	$N=$	4	5	6
	$R/N^2=$	6858.56	4389.48	3048.25
S	Cu	62308.0	19171.1	9459.5
	Zn/4	36222.56	14113.60	7848.47
	Ga/9	27533	11796	6694
	Ge/16	23044	10589	6165
P	Cu	315244	12925.0	—
	Zn/4	23884.13	10820.08	6232.88
	Ga/9	20102	9612	—
	Ge/16	17787	8832	5308
D	Cu	12365.9	6917.1	4413.4
	Zn/4	11982.85	6724.55	4312.08
	Ga/9	11512	6507	
	Ge/16	11115	6374	
F	Cu	6881.6	4400.0	
	Zn/4	6907.01	4422.93	
	Ga/9	6930		
	Ge/16	6950		

of term values made in Table XI shows that this value is as nearly accurate as it can be hoped to make it at present and the results obtained by applying a Rydberg formula to the P or D terms confirm this conclusion.

The $d^9s^{22}D$ terms arise from a configuration characterised only by the absence of one d electron and we expect therefore to find them inverted as they have been found in Cu I.[18] The only normal terms with which they combine according to the combination rules are those from the $d^{10}\,np$ states. An exception occurs in the case of the combination $d^{10}5s^2S_{\frac{1}{2}}-d^9s^{22}D_{1\frac{1}{2}}$. This combination violates both rules but was found by Paschen[19] in Hg II who

[18] Shenstone, Phys. Rev. **28**, 449 (1926).

[19] Paschen, Sitzungsber Berl. Akad. Dec. (1928).

TABLE X. *Combinations and intensities in Ge IV.*

Odd Terms \ Even Terms		$d^{10}4s\ ^2S_{\frac{1}{2}}$	$d^{10}4d\ ^2D_{1\frac{1}{2}}$	$d^{10}4d\ ^2D_{2\frac{1}{2}}$	$d^{10}5s\ ^2S_{\frac{1}{2}}$	$d^9s^2\ ^2D_{2\frac{1}{2}}$	$d^9s^2\ ^2D_{1\frac{1}{2}}$	$d^{10}5d\ ^2D_{1\frac{1}{2}}$	$d^{10}5d\ ^2D_{2\frac{1}{2}}$	$d^{10}6s\ ^2S_{\frac{1}{2}}$	$d^{10}5g\ ^2G$
		368701	178094	177840	169432	108759	104256	102064	101984	98643	70325
$d^{10}4p\ ^2P_{\frac{1}{2}}$	287386	20 −2	8 −3		3 −2					1 443	
$d^{10}4p\ ^2P_{1\frac{1}{2}}$	284598	20 1	4 3	8 −1	3 1					1 423	
$d^{10}5p\ ^2P_{\frac{1}{2}}$	142242	1 −189	30 −1.4		50 1		5 −1.6	30 −1.3		2 −1.5	
$d^{10}5p\ ^2P_{1\frac{1}{2}}$	141304	1 −185	15 −1.5	30 1.7	60 −0.2	5 −0.6	3 4.4	2 0.2	20 0.5	2 −0.6	
$d^{10}4f\ ^2F_{2\frac{1}{2}}$	111205		2 6	6 5							15 1.0
$d^{10}4f\ ^2F_{3\frac{1}{2}}$	111200		2 1	6 0							15 0.5
$d^{10}6p\ ^2P_{\frac{1}{2}}$	85080		3 −3	2 2	0 1						
$d^{10}6p\ ^2P_{1\frac{1}{2}}$	84938				15* 12						

* Classified also as Ge III.

TABLE XII. *Classified lines of Ge II, Ge III and Ge IV.*

Designation	Stage	I.A.	I	ν
$s4p^2\ ^2D_{1\frac{1}{2}} - s^24p^2P_{\frac{1}{2}}$	II	7147.0		13990.9
$s4p^2\ ^2D_{2\frac{1}{2}} - s^24p^2P_{1\frac{1}{2}}$	II	7050.1		14181.0
$s4p^2\ ^2D_{1\frac{1}{2}} - s^24p^2P_{1\frac{1}{2}}$	II	6967.5		14350.4
$s^25p^2P_{\frac{1}{2}} - s^25s^2S_{\frac{1}{2}}$	II	6484.32	6	15417.5
$s^25p^2P_{\frac{1}{2}} - s^25s^2S_{\frac{1}{2}}$	II	6336.31	4	15777.7
$5s^25s^2S_{\frac{1}{2}} - 5s^25p^2P_{\frac{1}{2}}$ } $s4p^2\ ^2S_{\frac{1}{2}} - 4p^3\ ^2P_{\frac{1}{2}\ 1\frac{1}{2}}$ }	II	6021.14	8	16603.6
$5s^25s^2S_{\frac{1}{2}} - 5s^25p^2P_{1\frac{1}{2}}$	II	5893.46	10	16963.2
$s4d^3D_1 - s5p^3P_0$	III	5256.61	3	19018.4
$s4d^3D_2 - s5p^3P_1$	III	5229.37	5	19117.5
$s4d^3D_1 - s5p^3P_1$	III	5210.36	3	19187.8
$s^24d^2D_{2\frac{1}{2}} - s^24f^2F$	II	5178.58	10	19304.9
$s4d^3D_3 - s5p^3P_2$	III	5134.75	18	19470.0
$s^24d^2D_{1\frac{1}{2}} - s^24f^2F$	II	5131.7	10	19481.3
$s4d^3D_2 - s5p^3P_2$	III	5016.88	10	19576.0
$s4d^3D_1 - s5p^3P_2$	III	5087.8	0	19649.4
$s^25p^2P_{\frac{1}{2}} - s^25d^2D_{1\frac{1}{2}}$	II	4824.20	10	20723.0
$s^25p^2P_{\frac{1}{2}} - s^25d^2D_{2\frac{1}{2}}$	II	4814.80	200	20763.5
$s^25p^2P_{\frac{1}{2}} - s^25d^2D_{1\frac{1}{2}}$	II	4742.00	50	21082.3
$s4d^3D_2 - s5p^1P_1$	III	4674.36	10	21387.3
$s4d^3D_1 - s5p^1P_1$	III	4659.04	4	21457.6
$s5s^3S_1 - s5p^3P_0$	III	4291.71	150	23294.2
$s5s^3S_1 - s5p^3P_1$	III	4260.85	200	23462.9
$p4d^1P_1 - d4d^1D_2$	III	4245.41	12	23548.2
$s5s^3S_1 - s5p^3P_2$	III	4178.96	200	23919.6
$s4f^3F_3 - d4d^1D_2$	III	3930.47	2	25435.1
$s4f^3F_2 - d4d^1D_2$	III	3927.64	0	25453.4
$s5s^3S_1 - s5p^1P_1$	III	3884.78	15	25734.2
$s5p^1P_1 - s6s^3S_1$	III	3724.51	2	26841.6
$d^{10}5s^2S_{\frac{1}{2}} - d^{10}5p^2P_{\frac{1}{2}}$	IV	3676.65	50	27191.0*
$d^{10}5s^2S_{\frac{1}{2}} - d^{10}5p^2P_{1\frac{1}{2}}$	IV	3554.19	60	28127.8*
$s5p^3P_2 - s6s^3S_1$	III	3489.09	40	28653.3
$s5p^1P_1 - s5d^3D_1$	III	3468.20	1	28825.2
$s5p^1P_1 - s4d^3D_2$	III	3464.59	8	28855.2
$s5p^3P_1 - s6s^3S_1$	III	3434.03	40	29111.6
$s5p^3P_0 - s6s^3S_1$	III	3414.27	20	29280.5
$s5s^1S_0 - p4d^1D_2$	III	3369.57	5	29668.9
$s5p^3P_2 - s5d^3D_1$	III	3263.18	3	30636.1
$s5p^3P_2 - s5d^3D_2$	III	3259.90	20	30667.0
$s5p^3P_2 - s5d^3D_3$	III	3255.05	40	30712.5
$s5p^3P_1 - s5d^3D_1$	III	3214.95	25	31095.7
$s5p^3P_1 - s5d^3D_2$	III	3211.86	35	31125.6
$s5p^3P_0 - s5d^3D_1$	III	3197.56	25	31264.8
$d^{10}5p^2P_{1\frac{1}{2}} - d^94s^2\ ^2D_{2\frac{1}{2}}$	IV	3071.84	5	32544.4
$s4d^3D_2 - p4d^1D_2$	III	2922.86	3	34203.1
$s4p^2\ ^2D_{2\frac{1}{2}} - s^24f^2F$	II	2845.47	30	35133.3
$s4p^2\ ^2D_{1\frac{1}{2}} - s^24f^2F$	II	2831.77	20	35303.2
$d^{10}4d^2D_{1\frac{1}{2}} - d^{10}5p^2P_{\frac{1}{2}}$	IV	2788.61	30	35850.6*
$d^{10}4d^2D_{2\frac{1}{2}} - d^{10}5p^2P_{1\frac{1}{2}}$	IV	2736.09	30	36537.7*
$d^{10}4d^2D_{1\frac{1}{2}} - d^{10}5p^2P_{1\frac{1}{2}}$	IV	2717.44	15	36788.5*
$d^{10}5p^2P_{1\frac{1}{2}} - d^95s^2\ ^2D_{1\frac{1}{2}}$	IV	2698.08	3	37052.4
$d^{10}5p^2P_{\frac{1}{2}} - d^95s^2\ ^2D_{1\frac{1}{2}}$	IV	2631.78	5	37985.8
$d^{10}5p^2P_{1\frac{1}{2}} - d^{10}5d^2D_{1\frac{1}{2}}$	IV	2547.64	2	39240.2†
$d^{10}5p^2P_{1\frac{1}{2}} - d^{10}5d^2D_{2\frac{1}{2}}$	IV	2542.44	20	39320.5†
$d^{10}5p^2P_{\frac{1}{2}} - d^{10}5d^2D_{1\frac{1}{2}}$	IV	2488.25	30	40176.7†
$d^{10}4f^2F_{2\frac{1}{2}} - d^{10}5g^2G$	IV	2445.71	15	40875.5
$d^{10}4f^2F_{3\frac{1}{2}} - d^{10}5g^2G$	IV	2445.38	15	40881.0
$d^{10}5p^2P_{1\frac{1}{2}} - d^{10}6s^2S_{\frac{1}{2}}$	IV	2343.37	2	42660.4†
$d^{10}5p^2P_{\frac{1}{2}} - d^{10}6s^2S_{\frac{1}{2}}$	IV	2293.0	2	43597.5†
$p4p^3P_2 - p4d^1D_2$	III	2138.65	1	46743.7
$s4d^3D_3 - s4f^3F_3$	III	2107.11	1	47443.3

* Classified by Smith.
† Classified by Rao

TABLE XII. (*Continued*)

Designation	Stage	I.A.	I	ν
$s4d^3D_3 - s4f^3F_4$	III	2104.45	25	47503.2
$s4d^3D_3 - s4f^1F_3$				
$s4d^3D_2 - s4f^3F_2$	III	2103.19	2	47532.9
$s4d^3D_2 - s4f^3F_3$	III	2102.42	15	47549.1
$s4d^3D_1 - s4f^3F_2$	III	2100.05	15	47602.7
$s4d^3D_2 - s4f^1F_3$				
$p4p^3P_1 - p4d^1D_2$	III	2062.14	3	48477.7
$s4d^3D_2 - p4d^1P_1$	III	2022.25	4	49434.3
$s4d^3D_1 - p4d^1P_1$	III	2019.22	2	49508.0
		I.A. vac		
$s4d^3D_3 - p4d^1F_3$	III	1978.22	2	50550
$s4d^3D_2 - p4d^1F_3$	III	1974.02	1	50658
$s5p^1P_1 - d4d^1D_2$	III	1930.10	0	51597
$s4d^1D_2 - p4d^1D_2$	III	1917.69	00	52146
$s4p^1P_1 - s4d^1D_2$	III	1883.26	6	53099
$s4p^1P_1 - p4p^3P_2$	III	1709.55	00	58495
$d^{10}5s^2S_{\frac{1}{2}} - d^9s^2\,{}^2D_{2\frac{1}{2}}$	IV	1648.14	3	60674
$s^24p^2P_{1\frac{1}{2}} - s^25s^2S_{\frac{1}{2}}$	II	1649.26	20	60633
$p4p^1D_2 - s4f^3F_2$	III	1621.19	0	61683
$p4p^1D_2 - s4f^3F_3$	III	1620.74	0	61700
$s4s^1S_0 - s4p^3P_0$	III	1619.92	0	61731
$p4p^1D_2 - s4f^3F_4$	III	1619.01	00	61766
$p4p^3P_2 - p4d^1P_1$	III	1613.30	1	61985
$s^24p^2P_{\frac{1}{2}} - s^25s^2S_{\frac{1}{2}}$	II	1602.56	20	62400
$s4s^1S_0 - s4p^3P_1$	III	1600.09	9	62496
$s^24p^2P_{1\frac{1}{2}} - s4p^2\,{}^2D_{1\frac{1}{2}}$	II	1581.16	3	63245
$s^24p^2P_{1\frac{1}{2}} - s4p^2\,{}^2D_{2\frac{1}{2}}$	II	1576.93	10	63414
$p4p^1D_2 - p4d^1P_1$	III	1572.40	0	63597
$p4p^3P_1 - p4d^1P_1$	III	1569.52	0	63714
$p4p^1D_2 - p4d^1F_3$	III	1543.14	1	64803
$s^24p^2P_{\frac{1}{2}} - s4p^2\,{}^2D_{1\frac{1}{2}}$	II	1538.20	2	65011
$s4d^1D_2 - s4f^3F_2$	III	1527.15	2	65481
$s4d^1D_2 - s4f^1F_3$	III	1525.32	10	65560
$d^{10}4d^2D_{2\frac{1}{2}} - d^{10}4f^2F$	IV	1500.61	6	66640‡
$s4p^1P_1 - s5s^3S_1$	III	1499.2	0	66702
$d^{10}4d^2D_{1\frac{1}{2}} - d^{10}4f^2F$	IV	1494.89	2	66895‡
$s4p^1P_1 - s5s^1S_0$	III	1323.24	4	75573
$s^24p^2P_{1\frac{1}{2}} - s^24d^2D_{1\frac{1}{2}}$	II	1264.68	10	79071
$s^24p^2P_{1\frac{1}{2}} - s^24d^2D_{2\frac{1}{2}}$	II	1261.87	18	79247
$s^24p^2P_{\frac{1}{2}} - s^24d^2D_{1\frac{1}{2}}$	II			
$s4p^3P_2 - s4d^1D_2$	III	1237.05	20	80837
$d^{10}4s^2S_{\frac{1}{2}} - d^{10}4p^2P_{\frac{1}{2}}$	IV	1229.81	20	81313‡
$s4p^3P_1 - s4d^1D_2$	III	1212.47	8	82476
$d^{10}4s^2S_{\frac{1}{2}} - d^{10}4p^2P_{1\frac{1}{2}}$	IV	1188.99	20	84104‡
$d^{10}5s^2S_{\frac{1}{2}} - d^{10}6p^2P_{\frac{1}{2}}$	IV	1185.50	0	84353
$d^{10}5s^2S_{\frac{1}{2}} - d^{10}6p^2P_{1\frac{1}{2}}$	IV	1183.34	15	84506
$s4p^3P_2 - p4p^3P_1$	III			
$s^24p^2P_{1\frac{1}{2}} - s4p^2\,{}^2S_{\frac{1}{2}}$	II	1181.65	3	84627
$s4p^3P_2 - p4p^1D_2$	III			
$s4p^3P_1 - p4p^3P_0$	III	1173.78	10	85195
$s4p^3P_1 - p4p^3P_1$	III	1160.79	8	86148
$s4p^3P_2 - p4p^3P_2$	III	1159.62	8	86235
$s4p^3P_1 - p4p^1D_2$	III	1159.15	8	86270
$s^24p^2P_{\frac{1}{2}} - s4p^2\,{}^2S_{\frac{1}{2}}$	II	1157.44	3	86397
$s4p^3P_0 - p4p^3P_1$	III	1150.55	12	86915
$s4p^3P_1 - p4p^3P_2$	III	1137.92	10	87879
$s^24p^2P_{1\frac{1}{2}} - s4p^2\,{}^2P_{\frac{1}{2}}$	II	1120.45	5	89249
$s^24p^2P_{1\frac{1}{2}} - p4p^2\,{}^2P_{1\frac{1}{2}}$	II	1106.74	10	90355
$s^24p^2P_{\frac{1}{2}} - s4p^2\,{}^2P_{\frac{1}{2}}$	II	1098.76	7	91012
$s4s^1S_0 - s4p^1P_1$	III	1088.45	40	91873
$s^24p^2P_{\frac{1}{2}} - s4p^2\,{}^2P_{1\frac{1}{2}}$	II	1085.55	7	92119

‡ Classified by Carroll.

TABLE XII. (*Continued*)

Designation	Stage	I.A.	I	ν
$d^{10}4d^2D_{2\frac{1}{2}} - d^{10}6p^2P_{\frac{1}{2}}$	IV	1078.02	2	92762
$s^24p^2P_{1\frac{1}{2}} - s^26s^2S_{\frac{1}{2}}$	II	1075.14	3	93011
$d^{10}4d^2D_{1\frac{1}{2}} - d^{10}6p^2P_{\frac{1}{2}}$	IV			
$d^{10}4d^2D_{1\frac{1}{2}} - d^{10}6p^2P_{1\frac{1}{2}}$	IV	1073.44	1	93158
$s4p^3P_2 - s5s^3S_1$	III	1058.91	12	94436
$s^24p^2P_{\frac{1}{2}} - s^26s^2S_{\frac{1}{2}}$	II	1055.08	1	94780
$s4p^3P_1 - s5s^3S_1$	III	1040.99	12	96080
$s4p^3P_0 - s5s^3S_1$	III	1032.62	8	96841
$s^24p^2P_{1\frac{1}{2}} - s^25d^2D_{1\frac{1}{2}}$	II	1017.12	2	98317
$s^24p^2P_{1\frac{1}{2}} - s^25d^2D_{2\frac{1}{2}}$	II	1016.69	8	98358
$s4p^3P_2 - s4d^3D_1$	III	1013.07	2	98710
$s4p^3P_2 - s4d^3D_2$	III	1012.31	10	98784
$s4p^3P_2 - s4d^3D_3$	III	1011.21	15	98892
$s^24p^2P_{\frac{1}{2}} - s^25d^2D_{1\frac{1}{2}}$	II	999.14	5	100086
$s4p^3P_1 - s4d^3D_1$	III	996.50	10	100351
$s4p^3P_1 - s4d^3D_2$	III	995.72	15	100429
$s4p^3P_0 - s4d^3D_1$	III	988.96	12	101116
$s4p^3P_1 - s5s^1S_0$	III	952.76	2	104958
$d^{10}4p^2P_{1\frac{1}{2}} - d^{10}4d^2D_{1\frac{1}{2}}$	IV	938.90	4	106507‡
$d^{10}4p^2P_{1\frac{1}{2}} - d^{10}4d^2D_{2\frac{1}{2}}$	IV	936.70	8	106757‡
$d^{10}4p^2P_{\frac{1}{2}} - d^{10}4d^2D_{1\frac{1}{2}}$	IV	915.00	8	109289‡
$d^{10}4p^2P_{1\frac{1}{2}} - d^{10}5s^2S_{\frac{1}{2}}$	IV	868.30	3	115167‡
$d^{10}4p^2P_{\frac{1}{2}} - d^{10}5s^2S_{\frac{1}{2}}$	IV	847.80	3	117952‡
$s4p^3P_2 - s6s^3S_1$	III	680.28	2	146998
$s4p^3P_1 - s6s^3S_1$	III	672.76	1	148641
$s4p^3P_2 - s5d^3D_2$	III	671.05	00	149020
$s4p^3P_2 - s5d^3D_3$	III	670.88	3	149058
$s4p^3P_0 - s6s^3S_1$	III	669.28	0	149414
$s4p^3P_1 - s5d^3D_2$	III	663.7[illegible]	2	150655
$s4p^3P_0 - s5d^3D_1$	III	660.52	1	151396
$s4s^1S_0 - s5p^1P_1$	III	542.90	2	184195
$d^{10}4p^2P_{1\frac{1}{2}} - d6s^2S_{\frac{1}{2}}$	IV	536.54	1	186378
$d^{10}4pP_{\frac{1}{2}} - d6s^2S_{\frac{1}{2}}$	IV	528.58	1	189186
$d^{10}4s^2S_{\frac{1}{2}} - d^{10}5p^2P_{\frac{1}{2}}$	IV	441.95	1	226270*
$d^{10}4s^2S_{\frac{1}{2}} - d^{10}5p^2P_{1\frac{1}{2}}$	IV	440.11	1	227212*

ascribes it to the very weak field in the specially designed tube used by him as source. However, it is a fact that a line occurs in the spectrum of Zn II, Cd II and Ge IV very close to the position which this line would occupy if it occurs. It seems unlikely that these lines can all be accidental and if not one is forced to conclude that Paschen's explanation is not the correct one for these lines all occur in the vacuum spark source. Shenstone found also the forbidden lines $d^9s^2\,^2D - d^{10}4f\,^2F$ in Cu I but if these occur in Ge IV they lie far in the infra-red.

At the end of the report a table has been arranged of all the classified lines of Ge II, Ge III and Ge IV. In the table the wave-lengths of all lines above 2000A are given in I.A. in air and below that value in I.A. vacuum, while all wave-numbers are reduced to vacuum values. The classification of each line is shown in column one while the stage of ionization of the atom which radiates the line is shown in column two. Lines classified by other observers are indicated in the table.

The writer was greatly assisted in the location of the $d^9s^2\,^2D$ terms in Ge IV by Dr. O. Laporte who sent him the results of his calculations in regard to separations and term values more than a year ago. The calculations were very close to the values obtained by experiment and the writer is greatly indebted to Dr. Laporte for the use of these results of his analysis.

In conclusion the writer wishes to thank Professor Smith for the use of his plates on the germanium spectrum and to acknowledge a grant from the Research Council of Canada.

THE SPECTRUM OF GALLIUM II AND THE $(4s4p^2)$ CONFIGURATION IN GALLIUM I AND INDIUM I

By R. A. Sawyer and R. J. Lang
University of Michigan and University of Alberta

(Received July 19, 1929)

Abstract

The spectrum of gallium has been excited in a hollow cathode discharge in helium and photographed in the region from λ10,000 − λ200. About 90 lines so excited have been classified in singlet and triplet series of Ga II. Peculiarities in the run of intensities in successive members of series have been found due to the excitation by helium which is sufficient to excite only terms greater than 12,000 ν-units in this spectrum. Absolute term values are calculated and the lowest term is $(4s^2)^1S = 165458$ corresponding to an ionization potential for Ga II of 20.43 volts. Tables of classified lines and of term values are given. The lines arising from combinations of $(4p^2)^4P$ and $(4p^2)^2S$ with $(4s4p)^2P$ of Ga I have been identified and values of these terms are given. Preliminary work on the excitation of the indium spectrum in helium has enabled the location of $(4p^2)^4P$ in In I and its term values and combinations with $(4s4p)^2P$ are given.

THE first classifications in the spectra of singly-ionized gallium were published by Lang[1] who from vacuum spark data in the extreme ultraviolet identified the triplet groups $(4s4p)^3P - (4s5s)^3S$, $(4s4p)^3P - (4s4d)^3D$, and $(4s4p)^3P - (4p^2)^3P$ and the singlet resonance line $(4s^2)^1S - (4s4p)^1P$. Rao[2] independently chose the same $(4s4p)^3P - (4p5s)^3S$ triplet and identified the $(4p4d)^3D - (4p4f)^3F$ group in the violet. Lang later from unpublished data chose tentatively a $(4s4p)^3P - (4s6s)^3S$ group and a $(4s4d)^3D - (4s5f)^3F$ group but as is well known the vacuum spark is poorly adapted to the excitation of higher series members. The success of the hollow cathode discharge in helium in exciting the spectrum of Al II[3] suggested the attempt to excite the spectrum of gallium by a similar method.

The use of the hollow cathode source with gallium is somewhat more difficult than with aluminum. Gallium melts at 30°C and so cannot be used directly as cathode. Paschen[4] has found that in the case of metals of low melting point or which vaporize too rapidly, good results may be obtained by placing a small quantity of the metal in a carbon hollow cathode.

Carbon neither vaporizes nor sputters in this discharge and if it is sufficiently carefully purified only the spectrum of the metal in the carbon cylinder will be obtained. In the case of gallium this purification was found to be extremely important. Gallium has a very slight vapor pressure even at red

[1] Lang, Phys. Rev. **30**, 762 (1927).

[2] Rao, Phys. Soc. London Proc. **39**, 161 (1927).

[3] Paschen, Ann. d. Physik **71**, 537 (1923); Sawyer and Paschen, Ann. d. Physik **84**, 1 (1927).

[4] Paschen, Preuss, Akad. Wiss, Berl, Ber. **29**, 207 (1927); Sawyer, Naturwiss. **16**, 765 (1927).

heat and as long as traces of the oxygen or hydrogen compounds of carbon remained in the cathode their band systems were excited while the gallium spectrum was but weakly excited.

The system for the circulation and purification of helium was similar to that previously described.[3] The helium was kept in circulation by a two stage Kurth mercury vapor pump and purified by passing over hot copper oxide to remove hydrogen and over charcoal cooled in liquid air to remove other impurities. Many hours of operation of the tube were found necessary sufficiently to remove the carbon compounds and under the best conditions faint traces of the stronger bands and of the carbon lines in the extreme ultra-violet usually persisted. The gallium itself, obtained from Messrs. Adam Hilger, proved to be very pure and the only impurities in the spectra attributed to it were the strongest lines of the indium spectrum. The only other impurities found in the spectra were the strongest lines of mercury, introduced by the circulating pump, and of neon, in the helium, which is the only gaseous impurity not removed by the purification system.

The spectrum was photographed in the extreme ultra-violet with a vacuum spectrograph similar to the one previously described[5], in the ultra-violet with a Hilger E2 and a Hilger E1 quartz spectrograph and in the visible and near infra-red with a Hilger E1 glass spectrograph. The spectra thus photographed covered the region from λ10,000−λ200 Angstrom units. In the vacuum region the known lines of helium, carbon, neon and mercury occurring in the discharge were used as standards, while in the quartz region and in the visible supplementary copper and iron arc lines were used as comparison spectra, and in the red, neon and argon comparison spectra were used. It is of interest to note that on some plates in the ultra-violet there were observed as many as eight members of the He I series 1^1S-m^1P beginning at λ584 and four members of the He II series 1^2S-m^2P beginning at λ304 were observed. λ584 is by far the strongest line excited and appears broad and strongly reversed up to the fifth order on the vacuum spectrograms, sometimes obscuring other predicted lines. The spectra were not exceedingly rich in lines but about 300 lines were tentatively attributed to gallium. Among these were all but a few of the faint ultra-violet lines of Ga I measured by Uhler and Tanch[6] as well as a few other new lines classified below in the Ga I spectrum and about 90 lines which have been classified in the Ga II spectrum. These 300 lines extended from λ8400 to λ830 and the analysis of the singlets would have been quite impossible without so extensive a spectral region.

Inspection of the vacuum spectrograph data at once revealed higher members of the 4^3P-m^3S and 4^3P-m^3D series.[7] Visual observations with a Gaertner constant deviation spectroscope had shown the two triplets 5^3P-5^3D and 5^3S-5^3P at λλ5425–5338 and λλ6456–6334 respectively and these observations formed a basis for readily completing the triplet analysis.

[5] Sawyer, J.O.S.A. **15,** 305 (1927).

[6] Uhler and Tanch, Astrophys. J. **55,** 291 (1922).

[7] For convenience configurations will not be given from here on in discussion of the normal singlets and triplets.

Three members of the ^3F term sequence, four of ^3D, two ^3P and four ^3S terms were found. Absolute values were assigned to the terms by the aid of Paschen's Rydberg Term Tables[8] in such a way as to make the deviations from true Rydberg type similar to those found in Al II. An inspection of these terms, in Table I, reveals one striking fact. No terms smaller than

TABLE I. *Gallium II terms. Values of term T and Rydberg denominator n^*.*

n^*, T	$m=4$	5	6	7	8
n^*	1.629	2.732	(3.754)	4.762	5.764
$^1S_0$	165458	58802	(31150)	19445	13265
n^*	2.173	3.136	(4.125)	5.120	
$^1P_1$	94758	44918	(25800)	16626	
n^*	2.757	(3.387)	4.125	5.055	
$^1D_2$	57739	(38270)	25764	17021	
n^*	3.963	4.943	(5.940)		
$^1F_3$	28115	17966	(12440)		
n^*		2.650	3.680	4.689	5.694
$^3S_1$		62515	32446	19965	13539
n_2^*	1.940	3.065	(4.095)	(5.110)	
$^3P_0$	118088	47031	(26200)	(16840)	
$\Delta_{0,1}$	446	89			
$^3P_1$	117642	46942			
$\Delta_{1,2}$	934	210			
$^3P_2$	116708	46732			
n_3^*	2.917	3.940	4.948	5.948	
$^3D_1$	51642	28304	17942	12397	
$\Delta_{1,2}$	25	12	8		
$^3D_2$	51617	28292	17934		
$\Delta_{2,3}$	34	17	9		
$^3D_3$	51583	28275	17925		
n^*	3.957	4.941	5.936		
$^3F_4$	28125	17975	12458		

$(4p^2)^3P_0 = 50757$
$(4p^2)^3P_1 = 50233$
$(4p^2)^3P_2 = 49321$

12,000 ν-units appear although in the case of Al II terms as high as $n=20$ and with ν-values as small as 1100 were excited. Furthermore inspection of the classified lines and intensities in Table II shows for the extreme ultra-violet triplets a marked minimum of intensity in the 4^3P-m^3S and 4^3P-m^3D series. Thus 4^3P-6^3S is much weaker than 4^3P-7^3S and 4^3P-5^3D slightly weaker than 4^3P-6^3D. That is, terms of value about 30,000 are less strongly excited than those a few thousand smaller or larger. A similar phenomenon was noticed in the hollow cathode spectra of Al II excited in helium where in many of the series a similar minimum occurred for values of the running term about 12,000 ν-units above the limit. These two facts may be immediately explained if we assume that the lowest level of Ga II is 12,000–15,000

[8] Paschen, J.O.S.A. **16**, 231 (1928).

TABLE II. *Wave-lengths of Ga II excited in hollow cathode discharge in helium.*

I	λ(air)	ν obs.	ν cal	Combination
2	7793.0	12828	821	4^1D-5^1P
7	7198.7	13887	886	5^1S-5^1P
0	7000.0	14282	286	$6^3S-5^3P_2$
3	6456.3	15484	484	$5^3S-5^3P_0$
5	6419.4	15573	573	$5^3S-5^3P_1$
10	6334.2	15783	783	$5^3S-5^3P_2$ S
0	5425.6	18426	428	$5^3P_2-5^3D_1$
1	5421.6	18440	440	$5^3P_2-5^3D_2$
3	5416.8	18456	457	$5^3P_2-5^3D_3$
0	5363.5	18639	638	$5^3P_1-5^3D_1$
2	5360.6	18649	650	$5^3P_1-5^3D_2$
1	5338.3	18727	727	$5^3P_0-5^3D_1$
3	5218.21	19158	154	5^1P-6^1D
10	4261.78	23458	458	$4^3D_3-4^3F_4$ S
6	4255.52	23492	492	$4^3D_2-4^3F_4$
1	4253.74	23502	502	$4^3D_2-4^1F_3$
5	4250.91	23517	517	$4^3D_1-4^3F_2$
9	3924.39	25474	473	5^1P-7^1S S
4	3734.85	26768	767	$5^3P_2-7^3S$
2	3705.85	26977	977	$5^3P_1-7^3S$
1	3693.93	27064	066	$5^3P_0-7^3S$
2	3583.60	27897	897	5^1P-7^1D
0	3472.52	28789	789	$5^3P_2-6^3D_1$
1	3471.46	28798	798	$5^3P_2-6^3D_2$
5	3470.34	28807	807	$5^3P_2-6^3D_3$
2	3447.26	29000	000	$5^3P_1-6^3D_1$
3	3446.46	29007	008	$5^3P_1-6^3D_2$
2	3436.66	29089	089	$5^3P_0-6^3D_1$
0	3375.95	29613	614	$4^1D-4^3F_4$
4	3374.94	29622	624	4^1D-4^1F
1	3158.18	31655	653	5^1P-8^1S
2	3011.90	33192	193	$5^3P_2-8^3S$
1	2992.84	33403	403	$5^3P_1-8^3S$
0	2884.83	33493	492	$5^3P_0-8^3S$
5	2974.77	33606	608	$4^3D_3-5^3F_4$
3	2971.60	33642	642	$4^3D_2-5^3F_4$
1	2971.01	33649	651	$4^3D_2-5^1F_3$
3	2969.41	33667	667	$4^3D_1-5^3F_2$
2	2910.77	34345	335	$5^3P_2-7^3D_4$
(a)	2893.65	34548	545	$5^3P_1-7^3D_4$
0	2886.45	34634	634	$5^3P_0-7^3D_1$
15	2780.15	35958	956	4^1P-5^1S V. S.
20	2700.47	37020	019	4^1P-4^1D V. S.
4	2555.28	39123	125	$4^3D_3-6^3F_4$
3	2552.87	39160	159	$4^3D_2-6^3F_4$
2	2551.26	39184	184	$4^3D_1-6^3F_2$
3	2514.15	39764	764	$4^1D-5^3F_4$
5	2513.55	39773	773	4^1D-5^1F

(a) Coincides with mercury line

TABLE XII. (*Continued*)

I	λ (air)	ν obs.	ν cal	Combination
5	2438.88	40990	988	4^1D-7^1P
2	2377.53	42048	051	5^1S-7^1P
20	2091.34	47816	816	$4^1S-4^3P_1$
15	1845.30 (b)	54192	193	$4^3P_0-5^3S$
10	1813.98	55127	127	$4^3P_1-5^3S$
5	1799.42	55574	570	$4^3P_2-5^3S$
5	1695.85	58969	969	$4^3P_2-4^1D$
3	1669.83	59902	903	$4^3P_1-4^1D$
1	1536.91	65066	066	$4^3P_2-4^3D_1$
5	1536.37	65088	091	$4^3P_2-4^3D_2$
8	1535.40	65125	125	$4^3P_2-4^3D_3$
3	1515.19	65997	000	$4^3P_1-4^3D_1$
5	1514.57	66025	025	$4^3P_1-4^3D_2$
3	1505.01	66446	446	$4^3P_0-4^3D_1$
3	1504.41	66472	471	$4^3P_2-(4p^2)^3P_1$
3	1495.21	66885	885	$4^3P_1-(4p^2)^3P_0$
3	1483.95	67386	387	$4^3P_2-(4p^2)^3P_2$
3	1483.52	67410	409	$4^3P_1-(4p^2)^3P_1$
3	1473.73	67853	855	$4^3P_0-(4p^2)^3P_1$
2	1463.65	68322	321	$4^3P_1-(4p^2)^3P_2$
5	1449.49	68990	994	4^1P-6^1D
20	1414.44	70700	700	4^1S-4^1P
5	1327.81	75312	313	4^1P-7^1S
5	1286.38	77738	737	4^1P-7^1D
0	1227.13	81493	493	4^1P-8^1S
3	1186.81	84259	262	$4^3P_2-6^3S$
2	1173.78	85195	196	$4^3P_1-6^3S$
1	1167.62	85644	642	$4^3P_0-6^3S$
5	1130.81	88432	433 416 404	$4^3P_2-5^3D_i$
3	1119.25	89346	350 338	$3^3P_1-5^3D_i$
1	1113.87	89777	778	$4^3P_0-5^3D_1$
8	1033.69	96741	743	$4^3P_2-7^3S$
5	1023.80	97675	677	$4^3P_1-7^3S$
3	1019.10	98126	123	$4^3P_0-7^3S$
5	1012.38	98777	783 774 766	$4^3P_2-6^3D_i$ $4^3P_1-6^3D_i$
3	1002.95	99706	708 700	
2	998.52	100148	146	$4^3P_0-6^3D_1$
2	969.19	103179	169	$4^3P_2-8^3S$
0	960.57	104105	103	$4^3P_1-8^3S$
2	958.67	104311	311	$4^3P_2-7^3D_i$
2	829.60	120540	540	4^1S-5^1P

(b) From here on λ vac.

ν-units deeper than in Al II. This would also be expected from the fact that the two spectra Zn I, which is isoelectronic with Ga II, and Mg I, isoelectronic with Al II, have values of the deepest term, ^1S, of 75767 and 61672 respectively, leading to the expectation that the analogous term of Ga II will be some 14,000 ν-units deeper than in Al II.

The analysis of the singlets showed this to be the case. The clue to the singlet analysis was provided by the intercombination $4^3P_{1,2}-4^1D$, $\lambda\lambda 1695-1669$. Starting from this and the resonance line 4^1S-4^1P, it was relatively a simple matter to find the only two strong lines having as the difference of their wave-number the thus determined value of $(4^1S-4^1P)-(4^3P_1-4^1D)=(4^1S-4^3P_1)-(4^1P-4^1D)$, $\lambda\lambda 2091$ and 2700, and the argument of the preceding paragraph as to the value of 4^1S fixed the assignment of these lines as $4^1S-4^3P_1$ and 4^1P-4^1D respectively. This led to a value of 4^1S of 165458, or 13598 ν-units deeper than in the case of Al II. The further analysis of the singlets was straightforward and unequivocal but rendered more difficult than in Al II by the above mentioned failure of terms smaller than 12,000 ν-units and by the weakness of terms about 30,000 ν-units. The intercombination lines are however somewhat more numerous than in Al II, as is to be expected with increased atomic number, and substantiate the analysis. Table I gives the values of four terms of the ^1S sequence, three ^1P, and three ^1D and two ^1F terms.

All of the triplet terms based on the Ga III term $(4s)^2S$ which were to be expected in this excitation—having ν greater than 12,000—have been found except 6^3P and 7^3P. The corresponding high ^3P terms in the analogous spectra of Al II and Mg I are also weak although in the isoelectronic spectrum Zn I they are well developed. In Ga II the approximate values of these terms can be calculated—$6^3P=26{,}200$, $7^3P=16{,}840$—and careful search has failed to reveal the expected lines although other terms in the spectrum of nearly the same magnitude are excited. Among the singlet terms four are missing—6^1S, 6^1P, 5^1D, and 6^1F. Of these 6^1S can be predicted to be about 31,150 and so falls at the minimum of excitation mentioned above. 6^1P should be about 25,800 and the reason for its failure is not clear. Likewise 5^1D should be about 38,270, although the wide deviation of the ^1D terms from a Rydberg formula makes exact prediction difficult, and should be excited. 6^1F is at about the lower limit of excitation and its combination with 4^1D and 6^1D would fall at about $\lambda 2200$ and $\lambda 7500$, both weak regions in our photographic spectra.

The lowest terms to be expected in Ga II based on higher terms of Ga III are $(4p^2)^3P$, ^1S, and ^1D which should be expected about 65,000 ν-units above $(4s4p)$ ^3P from the Ga III data;[9] $(4p5s)^3P$, ^1P and $(4p4d)^3P$, ^3D, ^3F, ^1P, ^1D, ^1F, all about 80,000 ν-units above $(4p^2)$. Of these only $(4p^2)$ could be excited in our discharge. $(4p^2)^3P$ was identified by Lang. $(4p^2)^1S$ and ^1D should be above ^3P and our failure to find them leads to the belief that they may lie near our minimum of excitation.

[9] Lang, Phys. Rev. **30**, 762 (1927).

Since no more than four terms were found in any series it was impossible to calculate series limits with great accuracy. However, it may be expected that terms of the various series will depart from Rydberg terms in a manner quite parallel to Al II and the term limits have been chosen with this in mind. The values so determined can hardly be in error by more than 100 units and probably by less than 50. All the series have quantum defects which behave very closely like the analogous Al II with the exception of the ^3F. The ^3F terms in Al II shows a very great deviation from expected value,—successive Rydberg denominators being 3.929, 4.882, 5.745, 6.400, 7.152. This effect was explained by Schrödinger[10] as due to resonance between the 7^3F orbits and the atom-core.

No such effect is found in Ga II. The only anomaly found in Ga II which appeared in Al II also is the very large deviation of ^1D terms from Rydbergian. The lowest term in Ga II, $^1S = 165458$ corresponds to an ionization potential of 20.43 volts

$(4p^2)$ Configuration in Gallium I and Indium I

The spectrographic analysis supplied by Hilger gave a list of several unassigned lines found in the gallium arc. Six of these lines appeared also strongly in our discharge and must be due to Ga I since equally strong Ga II in the same region were not found in Hilger's analysis. Five of the lines obviously are the intercombination $(4s^24p)^2P - (4s4p^2)^4P$. These lines are:

I	λ	ν	Combinations
8	2691.29	37146	$(4s^24p)^2P_{1\frac{1}{2}} - (4s4p^2)^4P_{\frac{1}{2}}$
10	2665.05	37511	$(4s^24p)^2P_{1\frac{1}{2}} - (4s4p^2)^4P_{1\frac{1}{2}}$
10	2632.66	37972	$(4s^24p)^2P_{\frac{1}{2}} - (4s4p^2)^4P_{\frac{1}{2}}$
8	2624.82	38087	$(4s^24p)^2P_{1\frac{1}{2}} - (4s4p^2)^4P_{2\frac{1}{2}}$
5	2607.47	38339	$(4s^24p)^2P_{\frac{1}{2}} - (4s4p^2)^4P_{1\frac{1}{2}}$

The $(4s^2p)$ configuration should give also ^2P, ^2S, ^2D. The term $(4s4p^2)^4P$ is however metastable and its combination with $(4s^24p)^2P$ might be expected to be strong. $(4s^24p)^2P - (4s4p^2)^2P$ is weak in the Al discharge in helium and has not been found here but two lines were found which are apparently $(s^2p)^2P - (sp^2)^2S$. These are:

I	λ	ν	Combinations
6	2534.83	39439	$(4s^24p)^2P_{1\frac{1}{2}} - (4s4p^2)^2S_{\frac{1}{2}}$
5	2482.76	40265	$(4s^24p)^2P_{\frac{1}{2}} - (4s4p^2)^2S_{\frac{1}{2}}$

Taking $(4s^24p)^2P$ as 48380 and 47553 the values of $(4s4p^2)^4P$, ^2S are as follows: $^4P_{\frac{1}{2}} = 10408$; $^4P_{1\frac{1}{2}} = 10042$; $^4P_{2\frac{1}{2}} = 9467$; $^2S_{\frac{1}{2}} = 8115$.

An investigation of the spectrum of In II excited similarly in He is now underway and will be reported later. Inspection of the data on in-

[10] Schrödinger, Ann. d. Physik **77**, 43 (1925).

dium already obtained revealed the $(4s^24p)^2P-(4s4p^2)^4P$ of In I as a group of five strong lines also given by Fowler as unclassified arc lines from Exner and Haschek's data who however apparently observed the reversed components of two of these lines (λλ3051 and 2858) as separate lines. Two more of them (λλ2957 and 2937) they also observed as reversed, only the weakest member of the group being unreversed. This reversal in the arc is of course strong evidence for our assignment of these lines. The group is

I	λ	ν	Combination
8	3051.25	32763	$(4s^24p)^2P_{1\frac{1}{2}}-(4s4p^2)^4P_{\frac{1}{2}}$
10	2957.01	33808	$(4s^24p)^2P_{1\frac{1}{2}}-(4s4p^2)^4P_{1\frac{1}{2}}$
15	2858.74	34971	$(4s^24p)^2P_{\frac{1}{2}}-(4s4p^2)^4P_{\frac{1}{2}}$
15	2836.89	35239	$(4s^24p)^2P_{1\frac{1}{2}}-(4s4p^2)^4P_{2\frac{1}{2}}$
8	2775.39	36020	$(4s^24p)^2P_{\frac{1}{2}}-(4s4p^2)^4P_{1\frac{1}{2}}$

Taking $(4s^24p)^2P$ as 46668 and 44455 the values of $(4s4p^2)^4P$ are as follows: $^4P_{\frac{1}{2}}=11697$; $^4P_{1\frac{1}{2}}=10648$; $^4P_{2\frac{1}{2}}=9216$.

The helium used in this investigation was supplied by the U. S. Bureau of Mines through the courtesy of its Director Dr. F. G. Cottrell. We are indebted to Miss Angelyn Cunningham for assistance in measurement of plates and computation. This work was done in the Physical Laboratory of the University of Michigan.

Mr. Lang wishes to express his appreciation of the courtesy of the Director of the Physical Laboratory of the University of Michigan, Professor H. M. Randall, for extending him guest privileges in the laboratory during the summers of 1928 and 1929.

INTENSITY MEASUREMENTS IN THE RAMAN EFFECT AND THE DISTRIBUTION LAW OF MAXWELL-BOLTZMANN

By L. S. Ornstein and J. Rekveld
Utrecht

(Received July 29, 1929)

Abstract

By a consideration analogous to that which Einstein used in his treatment of Planck's law it is shown that for the ratio of intensities between Stokes and anti-Stokes lines in the Raman effect the following formula holds:

$$\frac{I_S}{I_{AS}}=\frac{\nu-\nu_i}{\nu+\nu_i}e^{h\nu_i/kT}.$$

Intensity measurements on carbon tetrachloride have been made and a good agreement with the theory is found. It is shown that it is possible to develop this method into a precision measurement of the constant h/k.

UP TO the present time only a few measurements have been made to test the validity of the distribution law of Maxwell-Boltzmann in the quantum theory. We may mention those which made use of the absorption measurements on metal vapors or halogens. The Raman effect makes it possible to obtain quantitative data by measuring the ratios of intensities between Stokes and anti-Stokes lines. Some qualitative results have been published by Raman and Krishnan,[1] also by Dadieu and Kohlrausch.[2] In the present paper the authors give a quantitative investigation of this matter.

The problem is as follows: When radiation of frequency ν strikes a molecule, which can exist in two states 1 and 2 with energies ϵ_1 and ϵ_2, a Raman effect may take place in such a way that the frequency ν is increased or decreased by ν_i where $\nu_i=(\epsilon_2-\epsilon_1)/h$, so that the frequencies of the scattered light are $\nu-\nu_i$ and $\nu+\nu_i$, corresponding to a Stokes and an anti-Stokes Raman line.

If the probabilities for the states 1 and 2 of changing by a quantum, when the density of radiation is given by $\rho(\nu)$, expressed in number of energy quantums, are B_{12} and B_{21} and the numbers of molecules in these states are N_1 and N_2 then the intensities of the Raman lines of frequency $\nu-\nu_i$ and $\nu+\nu_i$ are given by the following expressions

$$h(\nu-\nu_i)\rho(\nu)N_1B_{12}d\nu \quad \text{and} \quad h(\nu+\nu_i)\rho(\nu)N_2B_{21}d\nu \tag{1}$$

[1] Raman and Krishnan, Proc. Roy. Soc. **A122**, 29 (1929). Krishnan, Nature **122**, 650 (1928).

[2] Dadieu and Kohlrausch, Phys. Zeits. **12**, 390 (1929).

If the distribution of energy corresponds to the law of Maxwell-Boltzmann, then

$$N_1 = g_1 e^{-\epsilon_1/kT} \quad \text{and} \quad N_2 = g_2 e^{-\epsilon_2/kT}$$

and (1) takes the form

$$h_1(\nu-\nu_i)\rho(\nu)g_1 B_{12}e^{-\epsilon_1/kT}d\nu \quad \text{and} \quad h(\nu+\nu_i)\rho(\nu)g_2 B_{21}e^{-\epsilon_2/kT} \tag{2}$$

Now we shall prove that the quantities g_1B_{12} and g_2B_{21} are equal. To that purpose we shall reason on the same lines as Einstein in deriving the law of Planck.

We consider an equilibrium of radiation, in which the numbers of molecules in the two states are

$$n_1 = g_1 e^{-\epsilon_1/kT} \quad \text{and} \quad n_2 = g_2 e^{-\epsilon_2/kT} \tag{3}$$

and in which the law of Wien holds:

$$\rho(\nu) = (8\pi/c^3)\nu^2 e^{-h\nu/kT} \tag{4}[3]$$

where ρ is expressed in numbers of quantums. The number of quantums of frequency ν is changed by Stokes and anti-Stokes Raman effects, so that the frequency ν becomes $\nu-\nu_i$ and $\nu+\nu_i$, where ν_i means the frequency of transition. The probability for a transition from the state 1 to 2 may be represented by $B_{12}(\nu)$ and in the same way the probability of a transition from 2 to 1 is $B_{21}(\nu)$. The number of quantums disappearing from the frequency ν amounts to

$$\rho(\nu)\{B_{12}(\nu)n_1 + B_{21}(\nu)n_2\} \tag{5}$$

This decrease, however, has to be compensated in equilibrium and this takes place by Stokes lines excited by the striking frequency $\nu+\nu_i$ and by anti-Stokes lines excited by the striking frequency $\nu-\nu_i$ to an extent of

$$\rho(\nu+\nu_i)B_{12}(\nu+\nu_i)n_1+\rho(\nu-\nu_i)B_{21}(\nu-\nu_i)n_2. \tag{6}$$

Putting (5) equal to (6) we get with the help of (4)

$$\begin{aligned}\nu^2 e^{-h\nu/kT}\{B_{12}(\nu)g_1 e^{-\epsilon_1/kT}+B_{21}(\nu)g_2 e^{-\epsilon_2/kT}\\ = (\nu+\nu_i)^2 e^{-h(\nu+\nu_i)/kT}g_1 B_{12}(\nu+\nu_i)e^{-\epsilon_1/kT}\\ +(\nu-\nu_i)^2 e^{-h(\nu-\nu_i)/kT}g_2 B_{21}(\nu-\nu_i)e^{-\epsilon_2/kT}\end{aligned}$$

or in a more simple form

$$\nu^2\{g_2B_{12}(\nu)+g_1B_{12}(\nu)e^{h\nu_i/kT}\} = (\nu+\nu_i)^2 g_1 B_{12}(\nu+\nu_i)+(\nu-\nu_i)^2 g_2 B_{21}(\nu-\nu_i)e^{h\nu_i/kT} \tag{7}$$

[3] When one prefers to apply the law of Planck a generalization must be employed as indicated by Einstein and Ehrenfest.

Now the quantities B_{12} and B_{21} are independent of the temperature, and from (7) there follows therefore the two equations:

$$\left.\begin{aligned} &\text{and} \quad \nu^2 g_2 B_{21}(\nu) = (\nu+\nu_i)^2 g_1 B_{12}(\nu+\nu_i) \\ &\qquad \nu^2 g_1 B_{12}(\nu) = (\nu-\nu_i)^2 g_2 B_{21}(\nu-\nu_i) \end{aligned}\right\} \tag{8}$$

These functional equations for B can be satisfied by

$$\nu^2 g_1 B_{12}(\nu) = \beta_i \quad \text{and} \quad (\nu-\nu_i)^2 g_2 B_{21}(\nu-\nu_i) = \beta_i$$

where B_i depends only on ν_i.

Therefore we get:

$$g_1 B_{12}(\nu) = \beta_i/\nu^2 \quad \text{and} \quad g_2 B_{21}(\nu-\nu_i) = \beta_i/(\nu-\nu_i)^2. \tag{9}$$

In the case of resonance we get from (9) as required by the theory, $g_1 B_{12}(\nu) = g_2 B_{21}(\nu)$.

It follows from (2) and (9) that the formula for the ratio of intensities takes the form

$$\frac{I_S}{I_{AS}} = \frac{\nu-\nu_i}{\nu+\nu_i} e^{h\nu_i/kT}$$

where the intensities are expressed in energies.

We have tried to test this formula by intensity measurements on the Raman effect of carbon tetrachloride. This substance is particularly appropriate for the purpose, because the frequencies of transition are rather small, so that there appear relatively strong anti-Stokes lines (in our experiments the ratio I_S/I_{AS} was never above 12).

The lines were excited by the method of Wood,[4] i.e. the mercury-lamp is placed directly over the tube filled with the liquid under examination. The outer tube was used at the same time as a thermostat. Water was circulated very quickly by means of a centrifugal-pump from a big reservoir. The slight difference of temperature between the reservoir, which was kept at constant temperature, and the outer tube has been measured thermoelectrically and a correction has been applied for it.

The scattered light was observed through a plane window, fused in the inner tube, by means of an achromatic lens projected on the slit of the spectrograph. The spectra were obtained with a Hilger quartz spectrograph (Type E 1). In order to get sharp images it was necessary to keep the room temperature constant to about one degree.

Because of the rather great dispersion of this instrument in the observed region, i.e. 13A per mm from 4047A to 4358A, the continuous background practically vanishes, which is of great advantage. We used the Ilford Special Rapid Plates, which showed themselves most sensitive in the region under consideration. The measurements were made in the usual way by means of

[4] Wood, Phil. Mag. **6**, 731 (1928).

density-marks and have been photometered with the microphotometer of Moll.

The (corrected) temperatures are 274°, 300°, 312°, 323.5° and 339.5°K, and we have measured the ratios of intensity of the Raman lines excited by the mercury-lines 4047A and 4358A, corresponding to frequencies of transition of the amount 645, 936 and 1368×10^{10} sec.$^{-1}$. These last transitions correspond to the (non-measured) infra-red oscillations near 46.5, 32.1 and 21.9μ (see for instance Wood[5]).

The calculated and observed ratios are put together in Tables I and II, where for the theoretical value of h/k has been taken the one given by Michel,[6] i.e. 0.476 degree · sec.

TABLE I. (4358A).

T (absolute)	274°	300°	312°	323.5°	339.5°	
$\nu_1 = 645 \cdot 10^{10}$	2.9 3.1	2.6 2.8	2.5 2.65	2.5 2.55	2.6 2.45	observ. calcul.
$\nu_2 = 936 \cdot 10^{10}$	5.5 5.1	4.2 4.4	4.3 4.15	3.9 3.95	3.8 3.7	observ. calcul.
$\nu_3 = 1368 \cdot 10^{10}$	12.0 12.7	9.7 8.7	— 8.1	8.1 7.4	7.0 6.8	observ. calcul.

TABLE II. (4047A).

T (absolute)	274°	300°	312°	323.5°	339.5°	
$\nu_1 = 645 \cdot 10^{10}$	3.1 3.1	3.0 2.8	2.55 2.65	2.7 2.55	2.4 2.45	observ. calcul.
$\nu_2 = 936 \cdot 10^{10}$	5.4 5.1	4.4 4.4	4.1 4.15	4.4 3.95	3.6 3.7	observ. calcul.
$\nu_3 = 1368 \cdot 10^{10}$	11.9 12.7	9.0 8.7	— 8.1	7.4 7.4	7.0 6.8	observ. calcul.

In order to examine the theoretical formula we have put $\ln (I_S/I_{AS}) = \alpha + \beta T^{-1}$. We have found values of α very near to zero, which means that within the precision of our measurements, the formula

$$\ln (I_S/I_{AS}) = h\nu_i/kT$$

holds.

It results from this, that there is a good agreement between theory and experiment and this makes it possible to put together in one diagram the results of the three Raman transitions. This is done in Fig. 2, where ν_i/T has been chosen as abscissa and $\ln (I_S/I_{AS})$ as ordinate.

[5] Wood, Phil. Mag. **6**, Pl. IX (1928).
[6] Michel, Zeits. f. Physik **9**, 285 (1922).

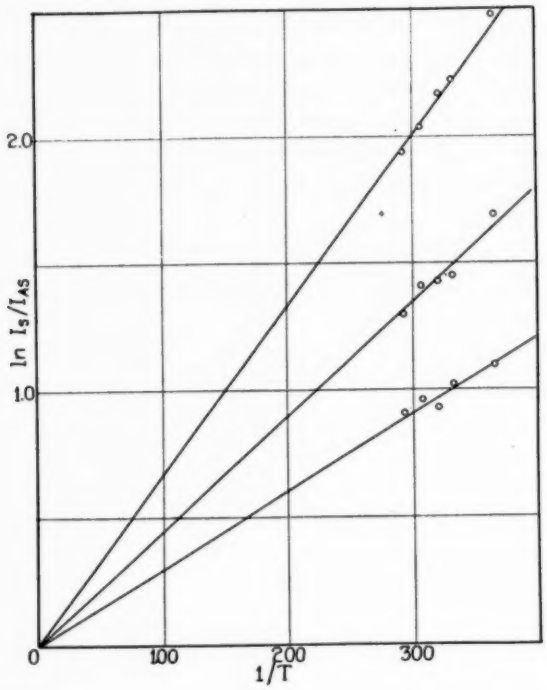

Fig. 1

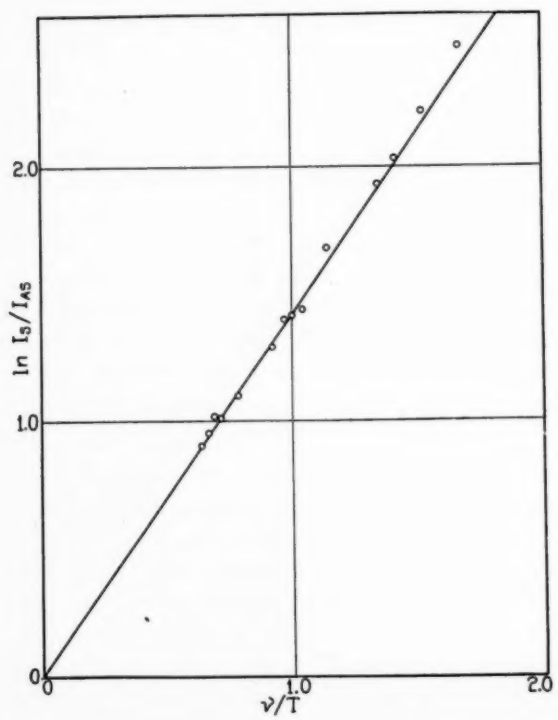

Fig. 2

The line drawn in this figure corresponds to the value which results from our measurements for the constant h/k, which was found to be 0.479 degree·sec., with a mean error of about 2 percent.

It is evident that when the number of the experiments is increased and a greater precision is obtained it is certainly possible to work out this method into a new determination of h/k. With a view to the disagreement between the values of Loschmidt's number which has lately arisen from the comparison of the absolute x-ray wave-lengths (Becklin, Compton) with the value of e obtained by Millikan, it seems to be very interesting to work out this method. Measurements of this kind are already in progress.

Also it seems to be of great importance to apply the Raman effect to obtain results on the distribution of energy over the proper vibrations of crystals. Such measurements are planned as well in our institute.

We are much obliged to Mr. Van Driel for his help during this research.

SECONDARY DIFFRACTION MAXIMA OF SPECTRAL LINES

By A. G. Shenstone
Palmer Physical Laboratory, Princeton University

(Received July 18, 1929)

Abstract

It is shown that the secondary diffraction maxima around a spectral line can be easily photographed under proper conditions. The relative intensities usually do not even approximately agree with Lord Rayleigh's simple theory, indicating that the lenses used in modern spectrographs introduce peculiar forms of aberration. The practical difficulties introduced by the peculiar intensities are discussed.

A WELL-KNOWN laboratory recently returned a spectrograph to the makers because the lines in spectra photographed with it showed a number of satellites. The makers accepted the return of the instrument on those grounds. A paper on the copper spectrum by Stücklen[1] contained measurements on equally spaced bands attached to certain strong ultra-violet lines. Those two cases are quoted to show that some physicists seem to have forgotten that the spectrum line produced by a spectroscope is only the central maximum of a set of diffraction fringes.

The theory was given by Lord Rayleigh.[2] For the case of a slit source and a rectangular aperture the intensity minima fall at distances from the central maximum given by $x = \pm n\lambda f/a$ where λ is the wave-length, f is the focal length of the lens or mirror, and a is the width of the aperture. The maxima fall at $x = 1.43\ \lambda f/a$, $2.46\ \lambda f/a$, etc., and have values relative to the central image 0.05,0.018, etc. The distances are multiplied by a factor $1/\cos\alpha$ if the plate is not normal to the beam. In such a case the fringes are not exactly focussed; but, for the small displacements involved, that fact may be neglected in practice.

The enlargements given in the plate are from photographs taken with a Hilger E.1 spectrograph using as a source a tiny arc between a negative lower 1 mm brass rod and a positive upper 1 cm brass rod. Such a source emits the zinc and lead lines in the visible with extreme sharpness. The light was focussed on the slit of width 0.005 mm by means of a spherocylindrical lens. The photographs have lost considerably in enlarging, but show the detail sufficiently well to illustrate the various points. A description of the patterns accompanies the plate.

A glance is sufficient to show that the fringes certainly do not agree with the simple theory. In numbers 1 and 2 the three parts were photographed with lens apertures of 5 cm, 2.5 cm, 1.25 cm, which should give fringes spaced in the ratios 1:2:4. Measurements on three lines give ratios

[1] Stücklen, Zeits. f. Physik **34**, 562 (1925).
[2] Lord Rayleigh, Phil. Mag. **8**, 261, 403 and 477 (1879); **9**, 40 (1880).

1:2.18:5.5; 1:2.17:5.3; 1:2.19:5.2 which disagree sufficiently with the theoretical ratios to indicate that the difference cannot be due to inaccuracy of measurement. The spacing of the finest fringes agrees very well with theory, the measured value being 0.037 mm and a metre-stick measurement of the dimensions of the apparatus giving 0.036 mm. It is worth mentioning that as many as 25 fringes on one side of a line have been observed by the writer.

The more blatant departure from the simple theory is in the intensities. In all the enlargements it is obvious that there is no regular falling off of in-

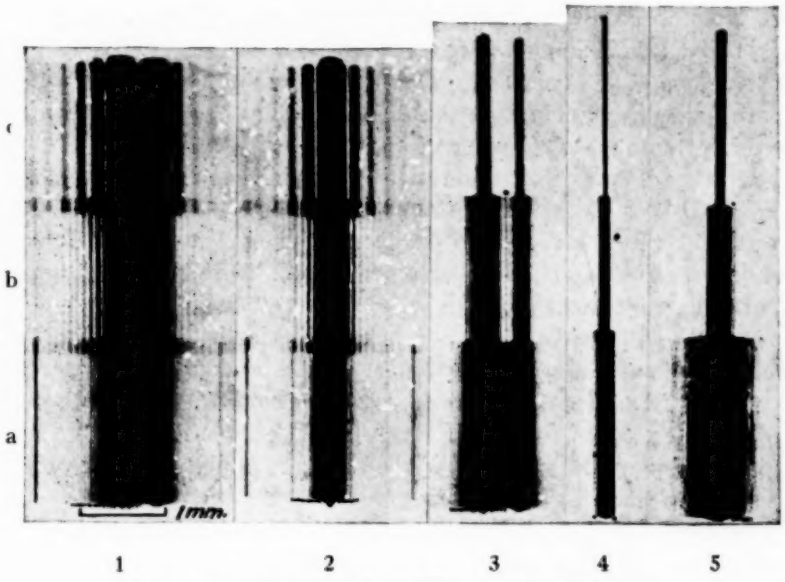

Fig. 1. Source, brass arc at 0.9 amps; slit, 0.005 mm.

1. Hilger E 1. quartz, λλ 4058 Zn and 4062 Cu. (11.2×). (a) 5 cm aperture 15 min. exposure; (b) 2.5 cm aperture 20 min. exposure; (c) 1.25 cm aperture 30 min. exposure.

2. Hilger E 1. quartz, λ3639 Pb. (a), (b), (c) as for 1 (11.2×).

3. Hilger E 1. quartz, λλ 4058 Zn and 4062 Cu. (12.4×). (a), 35 secs. exposure; (b), 3 min. exposure; (c), 15 min. exposure.

4. Hilger E 1. glass, λ4651 Cu (a), (b), (c) as for 3 (13.1×).

5. Hilger E 1. glass, λ4810 Zn (a), (b), (c) as for 3 and 4 (12.8×).

Note: Dots indicate fringes resolved on the original plates.

tensity with distance from the line. No. 2 shows some fringes practically missing and No. 3 illustrates a rather usual case in which groups of 3 or 4 fringes appear with almost equal intensity. Nos. 4 and 5, which were taken with a glass train, exhibit two other intensity anomalies. No. 4 is a common case in which a strong fringe appears as a satellite. In some cases, probably due to poor focus, several strong fringes may fuse to give the appearance of a satellite as much as 3 to 5 wave-numbers from the original line. In No. 5 there is the peculiarity that the inner fringes are uniform but the outer ones have variations of intensity along their lengths.

The first fringes are always of such low intensity relative to the central image that they never appear resolved. This gives a line the appearance of having faint wings. A longer exposure gives the result illustrated by 4b in which the first fringes have been absorbed to form a sharp broad line. No. 5c probably includes the first fringe on each side.

The reason for the departures from the expected ratios of separation for the three lens apertures is not obvious, but the peculiarities of the intensities probably have their explanation in the aberration due to the lens. Lord Rayleigh[3] deals with this question and shows that aberration may not only cause asymmetry in the intensities, but may also shift the position of the line. The more uniform fall of intensity in the case of the small aperture supports this explanation of the anomalies. Lord Rayleigh, however, did not contemplate any form of aberration that could produce such irregularities as are found here. The solution of this problem is one for the physicists employed by the makers of spectrographs.

It is worthy of note that theoretically the fringes should appear exactly the same regardless of the nature of the dispersing system. Lord Rayleigh points out that the aberration will be considerably less for concave mirrors than for lenses; and we should therefore expect more regular intensities in spectra produced by concave gratings.

Not only do all types of spectrographs theoretically produce these secondary maxima, but actually every properly made and adjusted spectrograph should record them if sufficient exposure is given with a suitable source. There is no question of failure of resolution, because it is their separation which gives the resolving power. If they do not appear the spectrograph is not giving its theoretical resolving power.

To the experimental spectroscopist these diffractions patterns are of considerable practical importance. We are all familiar with Lord Rayleigh's definition of resolving power, but it is not generally remembered that it applies only to lines of nearly the same intensity and sharpness. It is not possible to give any definition of resolving power for lines of very different intensities, particularly in the case of an instrument which produces fringes with abnormal intensities. A faint line several angstroms from a strong line may be quite indistinguishable in the diffraction pattern. An example is the marked line in 3b which may be either a real line or simply an abnormally strong fringe. From experience, the writer knows that the identification of faint lines in a fairly dense spectrum is really impossible in the multitude of fringes which are produced when the instrument is being used with its full aperture. It is possible to accomplish some identification of weak lines by making the edges of the aperture curved or saw-toothed or by comparing photographs taken with several different apertures. The apertures of the Hilger small and medium quartz are elliptical and that of the constant-deviation glass instrument is circular, but they all show fringes under proper conditions.

[3] Lord Rayleigh, Phil. Mag. **8**, 477 (1879).

The bearing of this question on fine structure measurements may also be important. The long exposures necessary to bring out fine structure components of very low intensity may be sufficient to register some of the fringes with comparable intensity. An echelon spectrograph is not free from this difficulty especially when it is remembered that the lens system may be such as to produce by aberration some abnormally strong fringes.

In the study of the Raman effect, it is most necessary that the existence of the secondary maxima be not forgotten. The over-exposure of the exciting line always takes place; and great care must, therefore, be exercised in the interpretation of any lines appearing close to it. Exactly the condition that makes it possible to photograph Raman lines near the exciting line is the condition that brings out the fringes, i.e., great homogeneity of the exciting line.

THE NEAR INFRA-RED ABSORPTION SPECTRA OF SOME HALOGEN DERIVATIVES OF ETHANE

By B. J. Spence and M. A. Easley
Northwestern University, Evanston, Illinois

(Received July 17, 1929)

Abstract

The infra-red absorption spectra of the following derivatives of ethane, C_2H_5Br, C_2H_5I, $CH_2Cl \cdot CH_2Cl$, $CH_2Cl \cdot CH_2Br$, $CH_2Br \cdot CH_2Br$, $CH_3 \cdot CHCl_2$, $CH_3 \cdot CHBr_2$, $CH_2Cl \cdot CHCl_2$, $CHCl_2 \cdot CHCl_2$, $CCl_3 \cdot CHCl_2$, $CCl_3 \cdot CCl_3$, $CCl_2 \cdot CCl_2$, $CHBr_2 \cdot CHBr_2$, $CHCl \cdot CHCl$, between 0.8μ and 3μ by means of two different spectrometers, one using a grating of 2500 lines per inch and the other using a grating of 10000 lines per inch. Tables listing spectrometer settings, wave-lengths and wave-numbers are included. A large number of new absorption bands were discovered. It was found that for substances containing no hydrogen no bands existed in the region under investigation. For other substances there was a close similarity in the spectra, particularly where the halogens were interchanged. The bands do not lend themselves to arrangement in a single series, nor does any quantitative relationship exist between the bands in any given substances. No explanation of the mechanism producing the absorption is offered.

ABOUT a year ago, the discovery of a large number of new absorption bands in the near infra-red absorption spectra of a number of the halogen derivatives of methane in liquid form was published from this laboratory.[1] Since then the absorption spectra of a number of the halogen derivatives of ethane have been completed, showing a large number of new absorption bands. Other investigators have studied the absorption spectra of these substances, but owing to the use of spectrometers of low dispersion and resolution, they have failed to observe the numerous absorption bands actually present. It is only with the aid of improved apparatus, such as the many-line grating and more sensitive detecting instruments that it is possible to observe the fine structure of infra-red absorption spectra.

Apparatus and Experimental Procedure

The absorption spectra were observed with a spectrometer which made rapid observations possible. A beam of radiation from a Nernst glower, incident on a concave mirror, was brought to focus on the spectrometer slit 0.25 mm wide. Before the slit was placed a carrier for a quartz absorption cell containing the liquid to be examined. The carrier was so constructed that either the cell or a pair of quartz plates could be placed before the slit. The pair of quartz plates was used to compensate for the absorption of the plates of the cell, thus eliminating the absorption of the quartz from the final results.

[1] M. A. Easley, L. Fenner and B. J. Spence, Astrophys. J. **67**, 185 (1928).

From the slit the radiation passed on to a concave mirror of large aperture and 60 cm focal length, rendered parallel and allowed to fall on a grating of 5×5cm aperture and ruled with 10,000 lines per inch. The dispersed radiation was returned to the mirror and brought to focus on the 0.25 mm wide vane of a sensitive radiometer. The spectrometer ensemble was calibrated by observing the spectrometer settings for the central image of the slit and the first five orders of the sodium line 5890A. The settings were made with an accuracy corresponding to 0.5A. The stability of the radiometer system

TABLE I. *Ethyl Bromide* (C_2H_5Br).

Spectrometer No. 1 setting	λ in μ	Spectrometer No. 2 setting	λ in μ	Waves per cm
		2780	1.1252	8887.3
		2815	1.1392	8778.0
		2865	1.1590	8628.1
		2885	1.1670	8568.9
		2915	1.1787	8483.9
		2935	1.1867	8426.7
		3390	1.3657	7322.2
		3420	1.3772	7261.1
		3445	1.3870	7209.8
		3495	1.4068	7108.3
		3530	1.4206	7039.2
		3605	1.4495	6898.9
		3640	1.4635	6832.9
		3680	1.4787	6762.6
		3710	1.4905	6709.1
		4050	1.6210	6169.0
906	1.666	4170	1.6675	5997.0
		4210	1.6831	5941.4
924	1.698	4250	1.6985	5887.2
935	1.720	4305	1.7190	5817.3
		4370	1.7437	5734.9
		4410	1.7590	5685.0
958	1.762	4440	1.7705	5648.1
		4490	1.7893	5588.7
		4580	1.8234	5484.2
995	1.838	4620	1.8385	5439.2
		4675	1.8590	5379.2
		4775	1.8965	5272.8
		4815	1.9115	5231.4
		4865	1.9300	5181.3
		4915	1.9487	5131.6

was such that observations were free from building tremors and there was no instability of the instrument zero due to temperature effects. The complete range of observations was gone over with cells of thicknesses 1.5 mm, 7 mm, and 14 mm. Different thicknesses were necessary in order to bring out the band characteristics. Some of the compounds were obtained from the Eastman Kodak Company and others were made under the direction of our colleague, F. C. Whitmore, of the Department of Chemistry.

With the arrangement as described above, it was possible to cover the region of the spectrum as far as 2μ. For observations beyond 2μ, it was necessary to set up another spectrometer using a grating of 2500 lines per inch. The use of two spectrometers made it possible to check observations.

The wave-lengths obtained with both spectrometers were in good agreement.

RESULTS

The absorption spectra of the following compounds were investigated between 0.8μ and 3μ: C_2H_5Br, C_2H_5I, $CH_2Cl \cdot CH_2Cl$, $CH_2Cl \cdot CH_2Br$, $CH_2Br \cdot CH_2Br$, $CH_3 \cdot CHCl_2$, $CH_3 \cdot CHBr_2$, $CH_2Cl \cdot CHCl_2$, $CHCl_2 \cdot CHCl_2$, $CCl_3 \cdot CHCl_2$, $CCl_3 \cdot CCl_3$, $CCl_2 \cdot CCl_2$, $CHBr_2 \cdot CHBr_2$, $CHCl \cdot CHCl$.

The wave-numbers of the bands for the different compounds are recorded in the following tables. The results with both spectrometers are

TABLE II. *Ethyl iodide* (C_2H_5I).

Spectrometer No. 1 Setting	λ in μ	Spectrometer No. 2 Setting	λ in μ	Waves per cm
		2835	1.1470	8718.3
632	1.166	2880	1.1650	8583.6
		2920	1.1809	8468.1
648	1.197	2960	1.1968	8355.6
		3375	1.3600	7352.9
		3400	1.3695	7301.9
		3425	1.3792	7250.5
		3455	1.3912	7188.0
		3510	1.4130	7077.1
		3540	1.4243	7020.9
		3635	1.4612	6843.6
		3670	1.4750	6779.6
906	1.668			5995.2
925	1.700			5882.3
950	1.752			5707.7
965	1.778			5624.2
997	1.834			5452.5
1003	1.846			5417.1
1037	1.906			5246.5
1053	1.936			5165.2
1103	2.028			4930.9
1158	2.130			4694.8
1185	2.176			4595.5
1230	2.260			4424.7
1250	2.298			4351.6
1270	2.335			4282.6
1300	2.390			4184.1
1335	2.460			4065.0
1362	2.504			3993.6
1372	2.522			3965.1
1387	2.555			3913.8
1410	2.596			3852.0

recorded, designating the low dispersion instrument as Spectrometer No. 1, and the high dispersion instrument as Spectrometer No. 2. Where the same bands are listed as obtained from each spectrometer, the wave-numbers corresponding to the values obtained with Spectrometer No. 2 is listed, since their value is probably more correct than that obtained with the low dispersion instrument. Two graphs of the results are inserted showing the results as obtained with each spectrometer. The abscissae represent spectrometer settings and the ordinates percent transmission. Ten equally

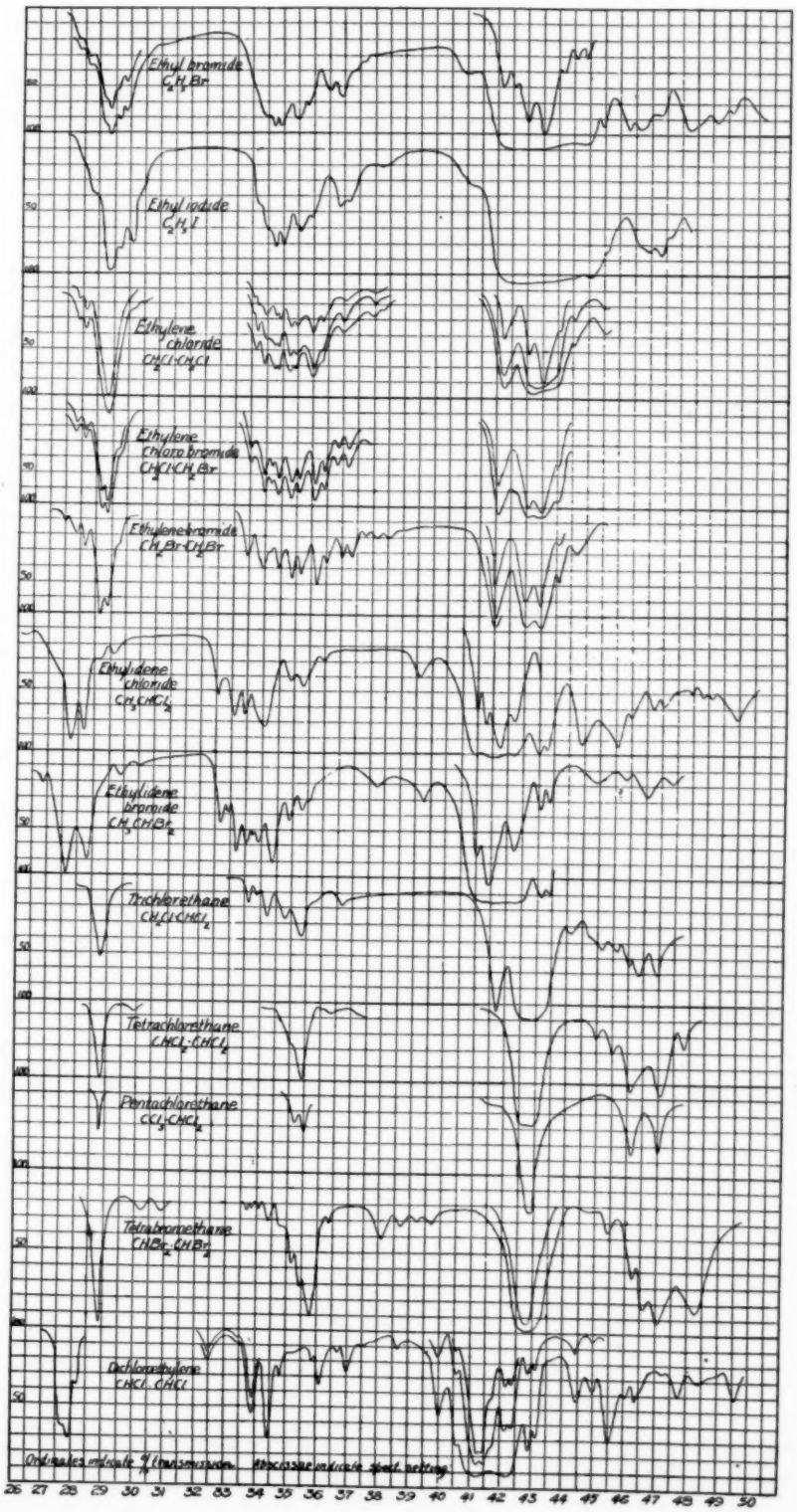
Ethyl bromide
C_2H_5Br
Ethyl iodide
C_2H_5I
Ethylene chloride
$CH_2Cl\cdot CH_2Cl$
Ethylene chlorobromide
$CH_2Cl\cdot CH_2Br$
Ethylenebromide
$CH_2Br\cdot CH_2Br$
Ethylidene chloride
CH_3CHCl_2
Ethylidene bromide
CH_3CHBr_2
Trichlorethane
$CH_2Cl\cdot CHCl_2$
Tetrachlorethane
$CHCl_2\cdot CHCl_2$
Pentachlorethane
$CCl_3\cdot CHCl_2$
Tetrabromethane
$CHBr_2\cdot CHBr_2$
Dichlorethylene
$CHCl:CHCl$
Ordinates indicate % transmission. Abscissae indicate spectr. setting.
26 27 28 29 30 31 32 33 34 35 36 37 38 39 40 41 42 43 44 45 46 47 48 49 50

Fig. 1.

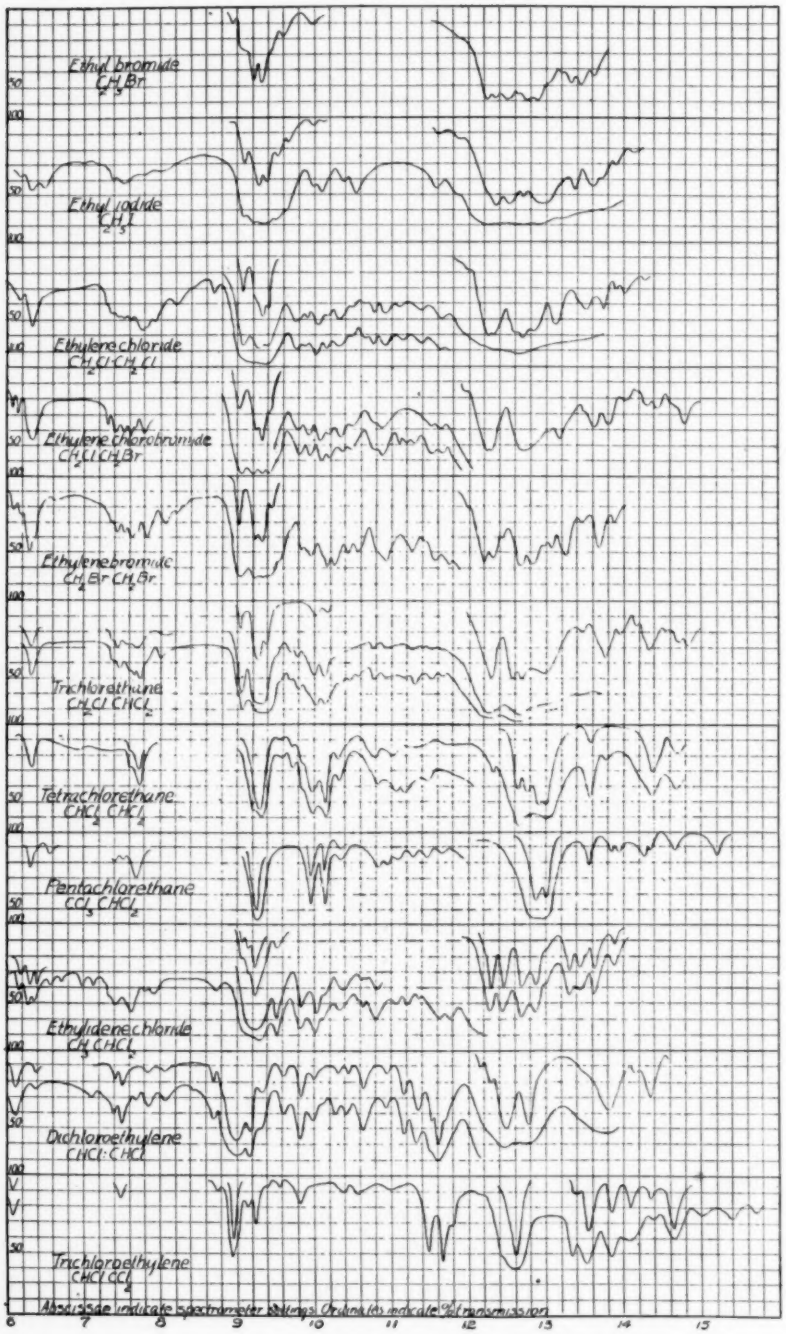
Ethyl bromide
C_2H_5Br
Ethyl iodide
C_2H_5I
Ethylene chloride
$CH_2Cl \cdot CH_2Cl$
Ethylene chlorobromide
$CH_2Cl \cdot CH_2Br$
Ethylene bromide
$CH_2Br \cdot CH_2Br$
Trichlorethane
$CH_2Cl \cdot CHCl_2$
Tetrachlorethane
$CHCl_2 \cdot CHCl_2$
Pentachlorethane
$CCl_3 \cdot CHCl_2$
Ethylidene chloride
$CH_3 \cdot CHCl_2$
Dichloroethylene
$CHCl : CHCl$
Trichloroethylene
$CHCl : CCl_2$
Abscissae indicate spectrometer settings. Ordinates indicate % transmission
6 7 8 9 10 11 12 13 14 15

Fig. 2.

spaced observations were plotted between each small division of the graph. Many of the bands were faint and we have not attempted to list those concerning whose existence there appeared any doubt. It is possible that many bands have been overlooked due to the weak absorption.

TABLE III. *Ethylene chloride* ($CH_2Cl \cdot CH_2Cl$).

Spectrometer No. 1 Setting	λ in μ	Spectrometer No. 2 Setting	λ in μ	Waves per cm
		2793	1.1306	8844.8
618	1.137	2809	1.1361	8802.0
632	1.167	2885	1.1670	8568.9
		3352	1.3506	7404.1
		3367	1.3567	7370.8
		3392	1.3667	7316.8
		3442	1.3860	7215.0
		3472	1.3978	7154.0
776	1.428	3551	1.4286	6999.8
792	1.456	3580	1.4400	6944.4
		3650	1.4673	6815.2
820	1.507	3750	1.5065	6637.9
906	1.668	4170	1.6675	5997.0
928	1.707	4255	1.7062	5860.9
938	1.720	4300	1.7195	5815.6
		4355	1.7382	5753.0
		4407	1.7580	5688.2
966	1.778	4510	1.7760	5630.6
987	1.816			5506.6
1015	1.866			5359.0
1032	1.888			5305.0
1050	1.930			5181.3
1064	1.956			5112.4
1077	1.978			5055.6
1090	2.004			4990.0
1114	2.046			4887.5
1138	2.095			4773.2
1224	2.250			4444.4
1232	2.265			4415.0
1254	2.304			4340.2
1268	2.332			4288.1
1286	2.368			4222.9
1310	2.407			4154.5
1350	2.487			4020.9
1374	2.525			3960.3
1389	2.560			3906.2
1400	2.571			3889.5

DISCUSSION

The particular sequence of compounds was chosen for the following reasons: to learn what effect the hydrogen in the molecule had on the absorption, what effect symmetry in the molecule produced, what effect in the absorption an interchange of the halogens produced, and to attempt to derive series relationship among the absorption bands with a view to a possible clue to the molecular structure.

At present the explanation of infra-red spectra of liquids has not the completeness of those of gases and solids. In gases the effects of collisions and neighboring molecules may be neglected. In solids we imagine charged

centers in lattice arrays, vibrating about positions of equilibrium. In liquids there are probably no constraints keeping the charged centres in oscillation about positions of equilibrium which, taken in conjunction with the relationships between neighboring molecules, complicates any attempt to put the subject on a theoretical basis.

In comparing the spectra, certain conclusions are obvious. For example, as we progressively replace the hydrogen by the halogens, the spectra

TABLE IV. *Ethylene chlorobromide* ($CH_2Cl \cdot CH_2Br$).

Spectrometer No. 1 Setting	λ in μ	Spectrometer No. 2 Setting	λ in μ	Waves per cm
610	1.126	2785	1.1273	8870.7
616	1.136	2807	1.1361	8802.0
		2863	1.1583	8633.3
633	1.167	2885	1.1670	8568.9
		2925	1.1830	8453.0
732	1.351	3350	1.3502	7406.3
742	1.369	3395	1.3678	7311.0
		3420	1.3775	7259.5
753	1.387	3440	1.3854	7218.1
761	1.402	3485	1.4030	7127.5
768	1.414	3512	1.4135	7074.6
779	1.435	3560	1.4322	6982.2
		3590	1.4439	6925.6
		3632	1.4600	6849.3
		3675	1.4770	6770.4
903	1.666	4160	1.6635	6011.4
925	1.706	4255	1.7062	5881.6
931	1.716	4300	1.7175	5822.4
943	1.738	4350	1.7362	5759.7
982	1.809			5527.9
994	1.833			5455.5
1009	1.861			5373.4
1020	1.880			5319.1
1033	1.908			5241.0
1049	1.928			5186.7
1077	1.984			5040.3
1090	2.008			4980.0
1108	2.044			4892.3
1118	2.061			4852.0
1130	2.083			4800.7
1222	2.247			4450.3
1230	2.260			4424.7
1270	2.338			4277.1
1320	2.428			4118.6
1362	2.510			3984.0
1379	2.540			3937.0

become less complicated. When all of the hydrogens are replaced, no bands appear. No bands were found for C_2Cl_6 and $CCl_2 \cdot CCl_2$, though bands are found for these substances by others beyond the region of this investigation.

A glance at the figures reveals close resemblances between the spectra of C_2H_5Br and C_2H_5I; yet on examination, no systematic differences appear. When bromine is substituted for iodine, shifts in similar bands are evident; shifts are noted toward the longer wave-lengths and also toward the shorter wave-lengths. There appears no quantitative relationship in the shifts.

The spectra of such substances as $CH_2Cl:CH_3Cl$, $CH_2Cl:CH_2Br$, and $CH_2Br:CH_2Br$ show very close resemblances and here again no systematic changes were revealed. The substitution of bromine for chlorine changed completely the intensities of the bands, as well as the frequencies.

TABLE V. *Ethylene bromide* ($CH_2Cl \cdot CH_2Cl$).

Spectrometer No. 1 Setting	λ in μ	Spectrometer No. 2 Setting	λ in μ	Waves per cm
612	1.128	2793	1.1308	8843.2
616	1.440	2811	1.1376	8790.4
628	1.160	2867	1.1597	8622.9
		2886	1.1672	8567.5
733	1.352	3352	1.3509	7402.4
742	1.369	3394	1.3673	7313.6
753	1.387	3442	1.3861	7214.4
762	1.403	3485	1.4029	7128.0
769	1.414	3517	1.4154	7065.1
781	1.436	3569	1.4357	6965.2
		3603	1.4499	6897.0
		3647	1.4661	6820.8
		3685	1.4809	6752.6
814	1.496	3728	1.4976	6677.3
820	1.507	3762	1.5106	6619.8
828	1.522	3802	1.5261	6552.6
905	1.662	4152	1.6605	6022.2
923	1.704	4257	1.7010	5878.8
933	1.712	4287	1.7125	5839.4
943	1.738	4355	1.7381	5753.4
956	1.758	4414	1.7605	5680.2
983	1.809			5527.9
995	1.834			5452.5
1017	1.870			5347.5
1027	1.893			5282.6
1042	1.923			5200.2
1058	1.949			5130.8
1094	2.010			4975.1
1129	2.080			4807.6
1158	2.140			4672.8
1175	2.166			4616.8
1219	2.244			4456.3
1233	2.262			4420.8
1243	2.288			4370.6
1267	2.340			4273.5
1282	2.365			4228.3
1298	2.390			4184.1
1307	2.407			4154.5
1325	2.443			4093.3
1346	2.480			4032.2
1368	2.520			3968.2
1388	2.555			3913.8

Comparing $CH_3 \cdot CHCl_2$, $CH_2Cl \cdot CH_2Cl$ and CHCl:CHCl, all of which contain two atoms of chlorine but placed in different positions in the molecule, wide differences in the spectra appear.

Taking any given spectrum, attempts were made to find series relationships. Some success was obtained in arranging the bands in series, if one assumed four fundamental frequencies for the molecule. Sufficient data were not available in the region beyond this investigation to make the re-

lationships sufficiently convincing. The problem is an exceedingly complicated one, not only because of the relationships between molecules, but also because of the complex molecular arrangement. An analysis of the spectra of vapors of methane derivatives and of some of the substances

TABLE VI. *Ethylidene Cloride* ($CH_3 \cdot CHCl_2$).

Spectrometer No. 1 Setting	λ in μ	Spectrometer No. 2 Setting	λ in μ	Waves per cm
		2210	.8980	1113.5
		2260	.9182	1089.0
		2448	.9932	1006.8
		2480	1.0060	9940.3
		2508	1.0175	8948.5
616	1.136	2805	1.1355	8806.6
630	1.159	2868	1.1605	8616.9
645	1.177	2912	1.1775	8492.5
		2960	1.1967	8356.3
657	1.216	3010	1.2162	8222.3
672	1.242			8051.5
700	1.287			7770.0
714	1.320			7575.7
726	1.343			7446.0
736	1.354	3355	1.3520	7396.4
745	1.372	3410	1.3735	7280.6
		3440	1.3852	7219.1
766	1.412	3510	1.4128	7078.1
780		3590	1.4439	6925.6
794	1.462	3635	1.4613	6843.2
		3695	1.4847	6735.3
874	1.607	4010	1.6062	6225.8
910	1.675	4195	1.6770	5963.0
918	1.690	4230	1.6906	5915.0
927	1.708	4280	1.7095	5849.6
		4315	1.7230	5803.8
953	1.758	4410	1.7590	5685.0
		4435	1.7685	5654.5
982	1.813	4560	1.8158	5507.2
1006	1.852	4660	1.8532	5396.0
1016	1.867	4700	1.8685	5351.8
		4770	1.8947	5277.8
1034	1.909	4805	1.9077	5241.9
1085	1.995	5045	1.9968	5008.0
1108	2.041			4899.5
1121	2.070			4830.9
1136	2.094			4775.5
1162	2.140			4672.8
1176	2.166			4616.8
1230	2.270			4405.2
1244	2.295			4357.2
1268	2.242			4269.8
1288	2.378			4205.2
1330	2.452			4078.3
1344	2.480			4032.2
1364	2.510			3984.0
1390	2.560			3906.2

investigated here in this region reveals the fine structure characteristic of this vibration-rotation spectra. The spectra of the vapors of liquids and vapors taken in conjunction will probably throw more light on the absorbing mechanism.

TABLE VII. *Ethylidene Bromide*, $CH_3 \cdot CHBr_2$.

Spectrometer Setting	λ in μ	Waves per cm	Spectrometer Setting	λ in μ	Waves per cm
2785	1.1270	8873.1	3650	1.4670	6816.6
2862	1.1580	8635.5	3875	1.5543	6433.3
2932	1.1855	8435.2	4025	1.6120	6203.4
3035	1.2262	8155.2	4200	1.6790	5955.9
3365	1.3560	7374.6	4245	1.6964	5894.4
3390	1.3657	7325.4	4320	1.7245	5798.7
3418	1.3766	7264.2	4410	1.7590	5685.0
3450	1.3890	7199.4	4435	1.7685	5654.5
3485	1.4030	7127.5	4595	1.8290	5467.4
3535	1.4225	7029.8	4685	1.8630	5367.6
3590	1.4438	6926.1	4710	1.8720	5341.8
3635	1.4615	6842.2	4835	1.9190	5211.0

TABLE VIII. *Trichlorethane* ($CCl_2 \cdot CH_3$).

Spectrometer No. 1 Setting	λ in μ	Spectrometer No. 2 Setting	λ in μ	Waves per cm
631	1.162	2875	1.1632	8596.9
736	1.355	3360	1.3538	7386.6
740	1.362	3385	1.3637	7332.9
		3415	1.3757	7269.0
767	1.412	3485	1.4030	7427.5
774	1.424	3535	1.4225	7029.8
906	1.668	4170	1.6675	6097.0
930	1.712	4290	1.7135	5836.0
937	1.724			5800.4
956	1.758	4410	1.7590	5685.0
977	1.797	4515	1.7987	5559.5
987	1.816	4560	1.8157	5507.5
		4605	1.8327	5456.4
1002	1.842	4630	1.8420	5428.8
1014	1.864	4670	1.8645	5363.3
1046	1.924			5197.5
1055	1.940			5154.6
1076	1.978			5055.6
1090	2.004			4990.0
1130	2.078			4812.3
1152	2.118			4721.4
1164	2.140			4672.8
1196	2.201			4543.3
1227	2.256			4432.6
1258	2.314			4321.5
1268	2.242			4269.8
1300	2.390			4184.1
1352	2.485			4024.1
1378	2.534			3946.3
1397	2.568			3894.0
1418	2.604			3840.2
1434	2.632			3799.3
1470	2.699			3705.0
1482	2.722			3673.7

TABLE IX. *Tetrachlorethane* ($(HCl_2)\cdot CHCl_2$).

Spectrometer No. 1 Setting	λ in μ	Spectrometer No. 2 Setting	λ in μ	Waves per cm
631	1.164	2880	1.1650	8583.6
766	1.412	3515	1.4145	7069.6
772	1.424	3540	1.4243	7020.9
927	1.709	4285	1.7117	5842.1
974	1.792	4500	1.7932	5576.6
985	1.811	4550	1.8119	5519.0
996	1.834	4610	1.8345	5451.0
1018	1.872	4710	1.8720	5341.8
1031	1.896	4780	1.8985	5267.3
1090	2.004			4990.0
1107	2.035			4914.0
1115	2.050			4878.0
1146	2.106			4748.3
1232	2.264			4416.9
1264	2.329			4293.6
1272	2.346			4262.5
1290	2.372			4215.8
1302	2.392			4180.6
1355	2.496			4006.4
1376	2.518			3971.4
1409	2.587			3865.4
1435	2.634			3796.5
1465	2.690			3717.4
1493	2.741			3648.3
1536	2.820			3546.0

TABLE X. *Pentachloethane* ($CCl_3\cdot CHCl_2$).

Spectrometer No. 1 Setting	λ in μ	Spectrometer No. 2 Setting	λ in μ	Waves per cm
633	1.163	2875	1.1630	8598.4
656	1.210			8264.4
769	1.415	3520	1.4162	7062.1
		3550	1.4280	7002.8
930	1.711	4285	1.7125	5839.4
995	1.831	4606	1.8320	5458.5
1015	1.866	4700	1.8685	5351.8
1032	1.898			5268.7
1084	1.993			5017.5
1095	2.014			4965.2
1109	2.037			4909.1
1130	2.077			4814.6
1148	2.092			4780.1
1165	2.142			4668.5
1288	2.368			4222.9
1305	2.400			4166.6
1356	2.492			4012.8
1384	2.545			3929.2
1392	2.558			3909.3
1428	2.622			3813.8
1432	2.630			3802.2
1465	2.690			3717.4
1522	2.793			3580.3

TABLE XI. *Tetrabromethane* ($CHBr_2 \cdot CHBr_2$).

Spectrometer No. 2 Setting	λ in μ	Waves per cm	Spectrometer No. 2 Setting	λ in μ	Waves per cm
2885	1.1670	8568.9	3640	1.4633	6833.8
3025	1.2222	8181.9	3810	1.5290	6540.2
3085	1.2462	8024.3	3865	1.5505	6449.5
3370	1.3580	7363.7	3965	1.5890	6293.2
3385	1.3637	7332.9	4275	1.6180	6180.4
3410	1.3735	7280.6	4540	1.8082	5530.3
3440	1.3852	7219.1	4620	1.8383	5439.8
3475	1.3990	7147.9	4655	1.8517	5400.4
3515	1.4145	7069.6	4710	1.8720	5341.8
3545	1.4262	7011.6	4825	1.9155	5220.5
3575	1.4382	6953.1			

TABLE XII. *Dichlorethylene*, (CH_2:CCl_2).

Spectrometer No. 1 Setting	λ in μ	Spectrometer No. 2 Setting	λ in μ	Waves per cm
		2768	1.1208	8922.1
610	1.126	2785	1.1275	8869.1
618	1.139	2812	1.1380	8787.3
710	1.310	3245	1.3090	7639.4
740	1.364	3390	1.3657	7322.2
753	1.385	3400	1.3855	7217.6
		3477	1.3995	7145.4
770	1.410			7092.1
		3585	1.4420	6934.1
788	1.449	3607	1.4505	6894.1
806	1.482	3695	1.4846	6735.8
		3755	1.5080	6644.5
842	1.550	3860	1.5485	6457.8
868	1.602	4000	1.6025	6240.3
		4055	1.6236	6159.1
		4122	1.6487	6065.3
898	1.654	4140	1.6565	6036.8
		4170	1.6675	5997.0
		4215	1.6847	5935.7
918	1.690	4235	1.6925	5908.4
		4290	1.7135	5836.0
936	1.720	4312	1.7216	5808.5
		4445	1.7610	5678.5
960	1.782	4500	1.7932	5676.6
982	1.810	4550	1.8120	5518.7
		4605	1.8327	5456.4
1000	1.844	4635	1.8440	5422.9
		4770	1.8947	5277.8
1038	1.910	4815	1.9117	5230.9
		4835	1.9190	5211.0
1046	1.925	4855	1.9265	5190.7
		4905	1.9450	5141.3
1064	1.965	4955	1.9636	5092.6
1094	2.016			4960.3
1117	2.056			4863.8
1134	2.090			4784.6
1152	2.125			4705.8
1161	2.140			4672.8
1228	2.262			4420.8
1250	2.297			4353.5
1277	2.352			4251.7
1382	2.540			3937.0
1434	2.638			3790.7

TABLE XIII. *Trichlorethylene*, ($CHCl:CCl_2$).

Spectrometer No. 1 Setting	λ in μ	Waves per cm	Spectrometer No. 1 Setting	λ in μ	Waves per cm
608	1.443	8748.9	1148	2.113	4732.6
748	1.378	7256.8	1156	2.146	4659.8
877	1.613	6199.6	1180	2.169	4610.4
894	1.652	6053.2	1270	2.321	4308.4
916	1.684	5938.2	1334	2.460	4065.0
924	1.706	5861.6	1356	2.495	4024.1
956	1.755	5698.0	1384	2.550	3921.5
982	1.810	5524.8	1412	2.598	3849.1
1038	1.909	5238.3	1436	2.641	3786.4
1054	1.943	5146.6	1464	2.695	3710.5

THE DISSOCIATION OF NITROGEN BY ELECTRON IMPACT

By Louis A. Turner and E. W. Samson
Palmer Physical Laboratory, Princeton University

(Received July 17, 1929)

Abstract

The $2p^23s\ {}^4P - 2p^23p\ {}^4P^\circ$ N I lines near 8200 A.U. are produced by bombarding N_2 molecules with electrons having energies of 23 ± 1 volts or more. Experiments with different currents and pressures indicate that the rate of production of excited atoms depends on a single impact and not upon successive double impacts. A discussion is given of the possibility that the lines are emitted following the recombination with electrons of N^+ ions, shown by positive ray experiments to be produced at this voltage.

IN THE course of an investigation of active nitrogen produced by the electrodeless discharge Herzberg[1] found that certain lines of the N I spectrum were emitted with great intensity. These lines belonged to the various multiplets in the region near 8000 A.U. emitted by transitions from the $2p^23p$ configuration to the $2p^23s$ configuration. They were emitted with undiminished intensity even when the condition of the walls of the tube was such that the afterglow of the active nitrogen was quenched. On the assumption that this quenching was an indication of a great reduction in the concentration of atomic nitrogen Herzberg came to the conclusion that, because of the undiminished intensity of the red lines, their production must be independent of the concentration of the nitrogen atoms, i.e., the $2p^23p$ excited atoms must be produced by some primary process of excitation of nitrogen molecules and not by excitation of nitrogen atoms already present. The purpose of the experiments here described was to test this conclusion by a more direct experiment and to endeavor to determine the minimum energy of bombarding electrons which would cause the appearance of these lines. The experiment is essentially the same as that of Kondratjew[2] who investigated the appearance of certain of the violet N I lines. Because of the relative lack of sensitivity of the photographic plate for the infra-red lines, however, we did not find it feasible to work with such low pressures as did Kondratjew.

Fig 1. Diagram of electrodes.

The electrodes of the experimental tube were arranged as indicated in Fig. 1. The source of the bombarding electrons was the filament F_1, an oxide-coated, notched strip of either platinum or nickel. C was a closed cylinder with platinum gauze on the bottom towards F_1, and a slit in the side for spectroscopic observation. The electrons from F_1 were accelerated into C by a variable applied accelerating voltage, V_a. The correction to this applied

[1] G. Herzberg, Zeits. f. Physik **49**, 512 (1928).
[2] V. Kondratjew, Zeits. f. Physik **38**, 346 (1926).

voltage, necessary on account of the potential drop in F_1, contact difference of potential, etc., was found by determination of the apparent ionizing potential of mercury vapor always present in the tube. The Hertz[3] method was used. F_2 was a fine tungsten filament from which the space-charge limited current was drawn for this purpose. Nitrogen generated by the reaction between bromine and ammonia was stored over P_2O_5 and then flowed through a liquid air trap and the experimental apparatus, the pressure and rate of flow being regulated by adjustable capillary leaks. Mercury vapor was always present in the tube. The Hg^+ ions formed served to prevent the setting up by space-charge effects of strong fields in C. The spectrum was photographed with a Steinheil glass spectrograph of large light power(1:3). Eastman infra-red plates, ammonia bathed, were used.

It was found that of all the lines emitted in the $2p^23s-2p^23p$ transition only those of the $^4P-{}^4P^\circ$ multiplet, all of wave-lengths close to 8200 A.U., were sufficiently separate from strong first positive bands to be detected readily when weak. Fortunately, this is the region of maximum sensitivity of the Eastman infra-red plates. In all that follows "the infra-red lines" will refer solely to those of the $^4P-{}^4P^\circ$ multiplet.

The question as to whether these lines were emitted as the result of a primary dissociation was investigated by varying the bombarding current and the pressure. Two exposures were made on the same plate, the pressure being 0.04 mm and the voltage 40, one with a current of 7 milliamperes for 18 hours, the other with an average current of 40 milliamperes for 3 hours. These two exposures gave almost identical results, the intensity of the infra-red lines and of every band being practically the same in both. Another such pair of exposures was made with the higher pressure of 0.24 mm and at 40 volts, one with a current of 4.5 milliamperes for 4 hours, the other with a current of 35 milliamperes for 1/2 hour. Again the two exposures gave practically the same results. The plate was not quite so heavily exposed as was the first one made at the lower pressure, but the intensity of the infra-red lines relative to the bands was apparently the same in all four spectra. If successive electron impacts with molecules or molecular ions or excitation of already formed atomic nitrogen had been of importance in the production of these lines the exposures with higher currents and at the higher pressure would presumably have shown the lines stronger with respect to the bands. The concentration of atoms present in the tube must have been fairly small, and dependent upon the current, since there was a great clean-up effect of the gas by such a discharge. It appears then that either the excited atoms which emit the infra-red lines are produced by a dissociation of the nitrogen molecules immediately upon collision with electrons having sufficient velocity, or that metastable excited molecules are produced which break up to give the excited atoms upon collision with other molecules, or that atomic ions are somehow produced and give rise to the excited atoms upon recombination with electrons.

[3] G. Hertz, Zeits. f. Physik **18**, 311 (1923).

The only other N I line which can be distinguished on these plates (region from 4700 to 9000 A.U.) is a line at 4935.0 A.U., one of those identified by Kiess.[4] It is the $2p^3 3s\ ^2P_{1\frac{1}{2}} - 2p^3 4p\ ^2S$ line. The companion $2p^3 3s\ ^2P_{\frac{1}{2}} - 2p^3 4p\ ^2S$ line at 4915 A.U. is presumably obscured by the very heavy broad Hg line at 4916. On these plates the 4935 line appears weaker than the infra-red lines but its intensity also seems to behave the same way and to bear the same relation to the intensities of the bands in the four exposures described above.

A series of exposures at different voltages was made in the attempt to determine the critical energy necessary to cause the appearance of the infra-red lines. For these the pressure was kept at about 0.04 mm, the time of the exposure being about 15 to 20 hours. It is, of course, difficult under the most favorable circumstances to determine the exact voltage for disappearance of a spectrum line, but it was even more difficult in this work because of the extremely low intensity of the infra-red lines and especially because of changes of several tenths of a volt in the contact difference of potential in the course of an exposure. These changes are presumably connected with the formation of layers on the electrodes by atomic nitrogen. They could be followed by frequent observation of the apparent ionizing potential of the mercury vapor. The changes were greater the higher the pressure of nitrogen. The final conclusion is that the infra-red lines appear at 23 ± 1 volts. This is 0.7 volt higher than the value reported at the Washington meeting of the American Physical Society[5] because it was found later in the course of the work on the negative bands, described in the following paper, that the method of correcting the voltage scale was giving too large a correction and, therefore, low corrected voltages.

Unfortunately, the presence of the 4935 line was not detected until after this work was completed so that the exposures do not give any very exact idea of the minimum voltage for the appearance of that line. It does not appear on the plates in which the infra-red lines are just barely visible, but being much weaker would not be expected to appear even if the light were present with the same relative intensity as at higher voltages. One plate, taken at 25.3 volts shows the 4935 line with much the same intensity relative to that of the infra-red lines as at higher voltages.

This critical value of 23 ± 1 volts is just 7 volts higher than the new value of the ionizing potential of nitrogen discussed in the following paper and agrees, therefore, with the critical voltage for the appearance of N^+ ions in the positive ray experiments of Smyth[6] and of Hogness and Lunn.[7] They give a value of 24.1 ± 1 volts, but that is based on the assumption of a value of 16.9 volts for the ordinary ionizing potential of nitrogen. The agreement of these critical voltages suggests that the appearance of the N^+ ions in those experiments and of the infra-red lines in these may be different mani-

[4] C. C. Kiess, Jour. Op. Soc. Am. **11**, 1 (1925).
[5] Louis A. Turner and E. W. Samson, Phys. Rev. **33**, 1085 (1929) (Abstract).
[6] H. D. Smyth, Proc. Roy. Soc. **104A**, 121 (1923).
[7] T. R. Hogness and E. G. Lunn, Phys. Rev. **26**, 786 (1925).

festations of the same original process. The positive ray experiments indicate that the primary process is the formation of excited molecular ions which dissociate into atoms and atomic ions upon collision. The infra-red lines would appear, then, following the recombination of the N^+ ions with electrons. The available energy is not great enough for the production of molecular ions which could dissociate into atomic ions and excited atoms in the $2p^2 3p$ configuration. The behavior of the infra-red lines with changes of current and pressure discussed above shows that if they are emitted as the result of recombination, the probability that an atomic ion once produced will recombine in the cylinder must be independent of the electron density and of the pressure. This is quite plausible since the region within the cylinder is presumably nearly field-free, the positive ions are not drawn out rapidly, and a high concentration of slow electrons can be built up. The atomic ions which are all neutralized eventually must nearly all be neutralized in the cylinder in the gas or at the walls. The recent experiments of Oliphant[8] show that helium ions, at least, are neutralized to give excited helium atoms upon contact with a metal tube through which they are passing.

This agreement of the critical voltage with that for the production of the N^+ ions may, however, be merely a coincidence. The infra-red lines may be produced by an immediate dissociation of molecules into normal and excited atoms or by the dissociation of metastable highly excited molecules. The behavior of the 4935 lines suggests that the immediate dissociation can give rise to various types of excited atoms or that various metastable highly excited molecules can be formed. It is also consistent with the hypothesis of recombination. Further experiments will have to be performed before the question can be settled. Both direct production of excited atoms and recombination may take place.

In many experiments with this tube with various pressures of nitrogen the currents showed a tendency to become unsteady near 23 volts. Often there was an increase in the current from F_1 accompanied by a decrease in the thermionic current from F_2. This is apparently the same effect as the decrease of the thermionic current caused by ordinary active nitrogen in an arc found by Kenty and Turner.[8] In the present experiment, however, the phenomenon seems to occur at the voltage at which atomic lines appear and is thus most definitely and directly connected with the appearance of atomic nitrogen. It is of interest in this connection to recall that Storch and Olsen[9] found a great increase in the rate of formation of ammonia in mixtures of hydrogen and nitrogen at this voltage.

[8] M. L. E. Oliphant, Proc. Roy. Soc. **A124**, 228 (1929).
[8] Carl Kenty and Louis A. Turner, Phys. Rev. **32**, 799 (1928).
[9] H. H. Storch and A. R. Olsen, J. Am. Chem. Soc. **45**, 1605 (1923).

THE EXCITATION POTENTIAL OF THE NEGATIVE BANDS OF NITROGEN

By Louis A. Turner and E. W. Samson
Palmer Physical Laboratory, Princeton University

(Received July 17, 1929)

Abstract

The energy of excitation of the $0 \rightarrow 1$ negative band of nitrogen at 4278.1 A.U. is found to be 19.0 volts, by comparison with the energy of excitation of neon lines. This gives a value of 15.8 volts for the ionizing potential of nitrogen, and of 8.4 volts for the heat of dissociation. Peculiar effects in the excitation of the $2s-2p$ lines of neon are discussed.

IN THE work on the excitation of the infra-red N I lines, described in the preceding paper, the correction to the voltage was found by determining the apparent ionizing potential of Hg in the tube, by the Hertz method. In order to check the results so obtained an attempt was made to determine the excitation potential of the negative bands of nitrogen, in particular of the band at 4278.1 A.U. which was the strongest on the plate. It is emitted in the transition from $n'=0$ to $n''=1$, so that the determination of its excitation potential gives the energy of the 0 vibration level of the upper A' state of the molecular ion with respect to the 0 level of the normal molecule. A value of 18.3 volts was obtained by the method, radically different from the value of 19.6 volts determined by Miss Sponer.[1] This discrepancy would arise if the ionizing potentials determined by the Hertz method were too great, or if Miss Sponer's value were too great. It did not seem probable that either could be in error by the full amount of the discrepancy. In this work, in which repeated determinations of the correction to the voltage scale were made, it appeared that the discharge in nitrogen produced considerable changes of the contact difference of potential and, therefore, of this correction. It seemed possible that some such effect might have introduced an error in Miss Sponer's determination. She calibrated the voltage scale of her tube by determining the apparent excitation potential of neon lines, the true values being known from spectroscopic data. The neon was then pumped out and the tube filled with nitrogen for the experiments with that gas. She pointed out explicitly that it was being assumed that no important change of the contact difference of potential was introduced by changing the gas.

It seemed desirable, therefore, to make a new determination of this excitation potential, especially in view of the fact that it offers the best method of determining the ionizing potential of nitrogen and the heat of dissociation of nitrogen, as discussed below. The method used was to determine the critical potential of excitation of both the negative band of nitrogen and appropriate neon lines in the same series of exposures made by excitation of a suitable mixture of nitrogen and neon. The apparatus was the same

[1] H. Sponer, Zeits. f. Physik **34**, 622 (1925).

as that described in the preceding paper except that F_1 was replaced by an oxide-coated button of nickel 5 mm in diameter and 1 mm thick, spot-welded to a tungsten filament, somewhat like the cathode described by Hertz and Kloppers.[2] This was used in order to be sure of having an equipotential source of electrons. Various mixtures of nitrogen and neon containing from 5 percent to 35 percent of nitrogen were flowed through the apparatus, a total pressure of about 0.25 mm being maintained in the tube in all experiments. The same Steinheil spectrograph of large light power, but refocussed for the visible and near ultra-violet regions, was used, with Ilford panchromatic plates. Series of exposures were made, changing the accelerating voltage by 0.1 volt for each exposure. With 5 percent of nitrogen in the mixture it was found that the negative band at 4278.1 A.U. was much weaker than the neon lines in the red. Increasing the proportion of nitrogen strengthened the negative band but also increased a disturbing background of first positive bands in the region of the neon lines. In the last sets of exposures the strength of the 4278.1 band was enhanced by widening the slit of the spectrograph and giving long exposures, a narrower slit and shorter exposures being used at the somewhat lower voltages where the neon lines first appear. The constancy of the contact difference of potential was checked by making a determination of the apparent excitation potential of the yellow neon line of wave-length 5852.5 A.U., by visual observation, both before and after making the set of exposures. Currents ranging from 1.5 to 2.5 milliamperes were used. Mercury vapor was always present, giving positive ions to remove disturbing effects of negative space charge.

Fig. 1 is made from one of the plates taken with a mixture containing 5 percent of nitrogen. The exposures at the higher voltages were made longer and with a wider slit in order to bring out the relatively weak negative band at 4278.1 A.U. It is probable that in the reproduction this band will not be visible as far down as it is on the original plate, as indicated in Fig. 1. In order to try to bring out the negative band in the reproduction without making the neon lines and their background too dark in all the spectra, the ones taken at the lower voltage have been given a lighter exposure in making the print. The strong lines which appear in all the spectra are those of mercury, and the strong bands which come out in the upper set are the second positive bands of nitrogen. A few volts higher the 4278.1 band and other negative bands become much stronger than these second positive bands.

Four different plates showed the appearence of the 4278.1 band of N_2^+ at 0.5, 0.6, 0.5, and 0.5 volts, respectively, above the first appearance of the 6402.2 line of neon. The excitation potential of this line being 18.5 volts,[3] a value of 19.0 volts in thus obtained for the energy of excitation of the 0 vibration level of the A' state of N_2^+. The reasons for the choice of this particular neon line for the standard is discussed below. This value

[2] G. Hertz and R. K. Kloppers, Zeits. f. Physik **31**, 463 (1925).

[3] The 6402.2 line is the $2s_5 - 2p_9$ line. The term value of the p_9 level is $24{,}272 \Rightarrow 3.00$ volts (Paschen-Götze, Seriengesetze der Linienspektren p. 40). The I. P. of neon is 21.47 volts (G. Hertz, Zeits. f. Physik **32**, 933 (1925)). The difference, 18.47 volts, is the energy of excitation of the p_9 level and 6402.2 line.

of 19.0 volts may be 0.1 volt or so too high because the intensity of the nitrogen band drops off with decreasing voltage more slowly than does that of

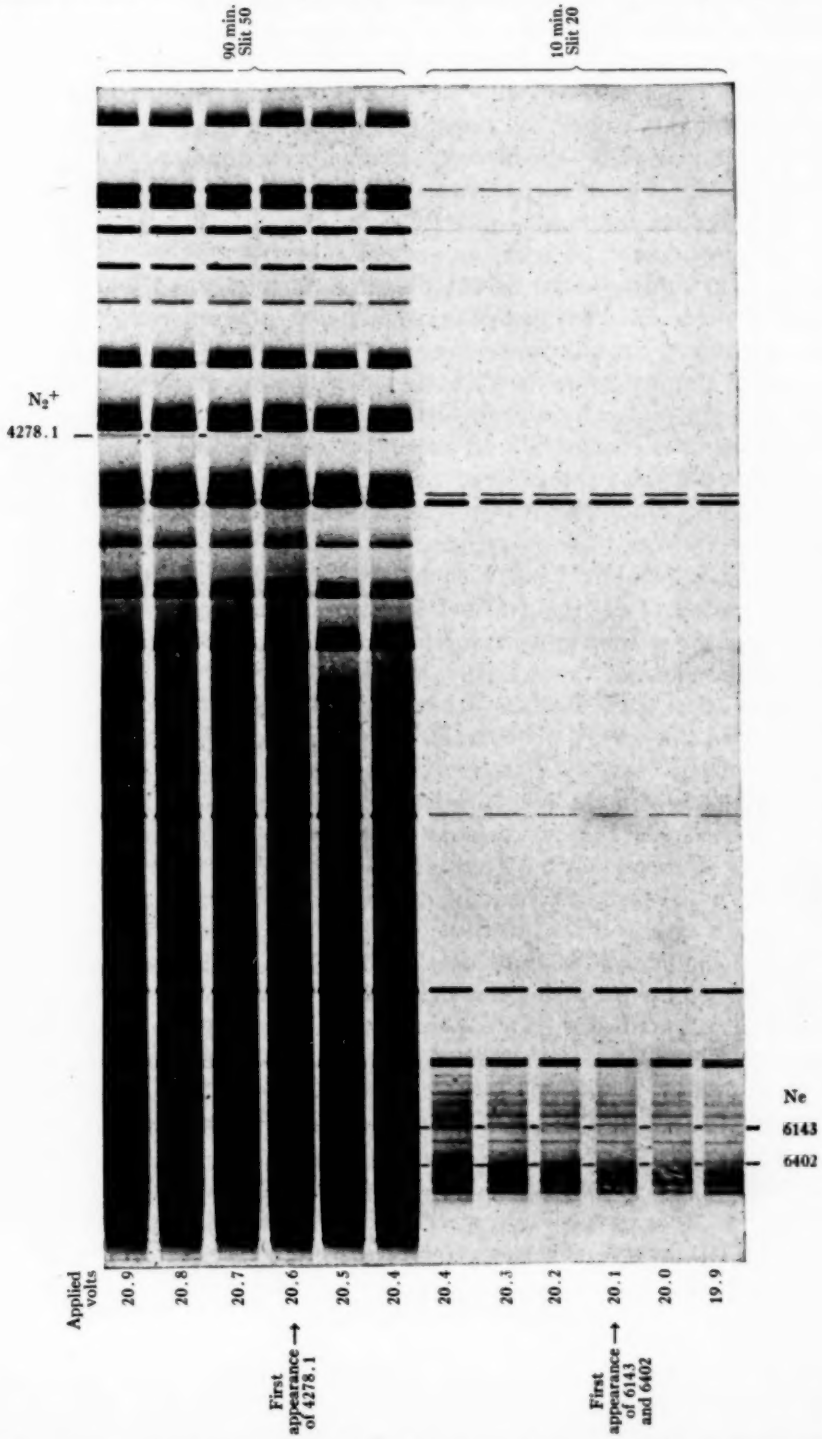

Fig. 1. Neon lines and the negative band.

the neon lines, making it less certain that greatly increased exposures would not bring it out at a slightly lower voltage. The agreement of the results

from four separate plates is the best evidence for the correctness of the determination.

The 0−0 member of the negative bands has a wave-length of 3914 A.U., corresponding to an energy of 3.15 volts. The energy of the normal state of the molecular ion is thus 19.0−3.2=15.8 volts with respect to the normal molecule. This is, of course, by definition, the ionizing potential of the molecule. This value of 15.8 volts is considerably lower than most of the previous determinations.[4] The direct, electrical methods would tend to yield somewhat higher values since they usually give automatically weighted means of the energies of excitation of the various vibrational levels of the normal electronic configuration of the molecular ion. It might be thought that the low value was obtained because of occasional excitation of vibrating nitrogen molecules already containing some energy to the upper vibrationless state. The relative number of such vibrating molecules in the $n''=1$ state of the normal nitrogen molecule is negligible[5] as far as the proportion in temperature equilibrium is concerned. If, however, the effective temperature were sufficiently increased by the electron current such an effect might take place. One would expect, in that case, that it would be enhanced by nearly doubling the current. No effect of increased current in lowering the appearance of the negative band with respect to the neon line was observed.

This lowering of the ionizing potential of the nitrogen molecule also involves a lowering of the value for the heat of dissociation in the normal state. Birge[6] calculated from the extensive analysis of the negative band system by Herzberg[7] that the heat of dissociation of the A' state of the ion is 3.9 volts. Adding this to the energy of 19.0 volts for excitation of the 0 vibration level of the A' state gives 22.9 volts as the energy necessary for production of an atom and an atomic ion from a normal molecule. This final state could also be reached by first dissociating the molecule into atoms and then ionizing one of them. The latter process requires 14.5 volts so that the difference, 8.4 volts, is the heat of dissociation of the nitrogen molecule. This is merely a repetition of Birge's calculation using the new value of the energy of the A' state instead of a value of 20.1, which would be consistent with 16.9 volts for the ionizing potential which he uses.

The 6402.2 line of neon is one of the stronger of a large number of lines emitted by the various transitions from the ten so-called $2p$ levels of the $(2p)^5 3p$ configuration to the four $2s$ levels of the $(2p)^5 3s$ configuration.[8] Two other particularly strong lines are the $2s_2-2p_1$ yellow line of wave-length 5852.5 A.U., and the $2s_5-2p_6$ red line of wave-length 6143.1 A.U. Since the $2p_1$ and $2p_6$ levels lie 3315 and 659 units, respectively, above the $2p_9$ level these two lines should appear at 0.4 and 0.1 volts above the $2s_5$

[4] J. Franck und P. Jordan, Anregung von Quantensprüngen durch Stösse, p. 269.

[5] The ratio, $e^{-(E_1-E_2)/kT}$ becomes in this case

$$\exp\left[-\frac{2331\times 3\times 10^{-10}\times 6.55\times 10^{-27}}{1.372\times 10^{-16}\times 400}\right]=e^{-8.3}=0.0021.$$

$\Delta\nu=2331$ from R. T. Birge and J. J. Hopfield, (Astrophys. J. **68,** 257 (1929)).

[6] R. T. Birge, Nature **122,** 842 (1928).

[7] G. Herzberg, Ann. d. Physik **86,** 189 (1928).

[8] For Paschen's analysis and the term values see Paschen-Götze, Seriengesetze der Linienspektren.

$-2p_9$, 6402.2 line. It was found, however, that the 6143.1 line appeared at the same voltage as the 6402.2 line, and the 5852.5 line only 0.1 or 0.2 volts higher. Hertz and Scharp de Visser[9] found by visual measurements that the 6143.1 and 6402.2 lines appeared at the same voltage and the 5852.5 only 0.3 volts higher. It seemed possible that some sort of a secondary excitation of the atoms in the lower $2p$ states by slow electrons was giving this effect. Accordingly, a series of exposures was made with a current of 4.2 milliamperes. All three lines appeared at the same voltage on this plate, thus giving evidence for the occurrence of such secondary processes. The theoretically ideal line to use for a standard of reference would, then, be one emitted upon transitions from the lowest $2p$ state, the $2p_{10}$. There are four such lines but they are all fairly weak and lie at longer wave-lengths where the plate is insensitive and the stray reflected light from the filament strong, so that their use was not feasible. The 6402.2 line, being emitted with transitions from the $2p_9$ state, the next to the lowest (0.2 volt above $2p_{10}$) was, therefore, taken as the best to use for a standard. If the slow electrons which cause the secondary effect come from the excitation of neon atoms to the $2p_{10}$ state by electrons having somewhat more than enough energy for this excitation, no secondary excitation of atoms to the $2p_9$ state will occur until the electrons have enough energy to excite the atoms to this state directly, for until the energy reaches such a value the amount left over in the slow electrons will not be sufficient to raise the excited atoms from the $2p_{10}$ to the $2p_9$ state. The occurrence of such a secondary process would at first sight seem to be highly improbable in view of the presumably short mean life of the excited atoms. The assumption of some sort of a secondary process seems, however, to be necessary in order to account for the observations. The metastable excited neon atoms in the $2s_3$ and $2s_5$ states may be involved in some way.

On one early plate made with the old strip filament the $2s_3-2p_{10}$ line at 7032.4 A.U. appears with fair intensity and without a disturbing continuous background. It increases in intensity for about 0.6 volts and then shows a sudden and considerable drop at a voltage where the N_2^+ band is beginning to appear. It then increases in intensity slowly with increasing voltage. It looks as though the fast electrons were suddenly being used to excite nitrogen rather than neon. The other neon lines were so much over-exposed on this plate that the effect would not be noticeable for them even if it occurred. No such effect was found on any of the later plates. Time did not permit a further investigation of this phenomenon.

The excitation potential of 19.0 volts being 0.7 higher than the apparent value of 18.3 volts obtained by using the ionizing potential of Hg as a standard indicates that this method was giving too high a value for the ionizing potential of Hg, presumably due to some sort of a negative space charge effect. A correction of this amount was, therefore, made to the voltages in the experiments on the excitation of the N I lines, as was mentioned in the preceding paper. This same error was found in comparing the apparent ionizing potential of Hg with the excitation of the neon lines by visual observation.

[9] G. Hertz and J. C. Sharp de Visser, Zeits. f. Physik **31**, 470 (1925).

A SEARCH FOR ELEMENT 87 BY ANALYSIS OF POSITIVE RAYS

By K. T. Bainbridge
Princeton University

(Received April 25, 1929)

Abstract

The methods used in previous attempts to discover eka-caesium are briefly examined and their limitations pointed out. *Estimates are given for the sensitivity of detection and identification of element 87* by atomic weight determinations, radioactive means, physiological effects, x-ray and optical spectrum analysis. *Predictions of spectral values* by Moseley's Law and an empirical relation give: $V_i = 4.05 \pm 0.05$ volts, $7^2P_{\frac{1}{2}} = 21340 \pm 200$ cm^{-1}, $7^2P_{3/2} = 19670 \pm 200$ cm^{-1}, $\Delta\nu$ separately determined 1675 ± 50 cm^{-1}, principal series resonance lines 8720 ± 200A and 7600 ± 200A. The large uncertainty is due to uncertainty in the iso-electronic Ra II spectrum. No absorption lines were found in the sun's spot spectrum, although possible, as element 87 should be less highly ionized than Cs. A tungsten filament heated to 1200°–1300°K converts into ions all caesium atoms which strike the tungsten surface and eka-caesium should behave the same way. By this means, first investigated by Langmuir and Kingdon, and Ives, an intense homogeneous source of positive ions is secured. This positive ion source was incorporated into a tube similar to Dempster's mass spectrograph in method of focussing and ray analysis, and positive ions were looked for of mass number 223 or 224. *Chemical separation* of caesium and any admixed eka-caesium was made from pollucite and lepidolite ores from Oxford County, Maine. Eka-caesium was not existent to an extent greater than 3.5×10^{-7} part of the caesium from pollucite or greater than 7.3×10^{-6} part of the caesium from lepidolite.

Vapor Pressure of K, Rb, Cs.—Na_2 was detected, but no K_2, Rb_2, Cs_2 or any intermetallic alkali compounds or doubly charged atomic ions were found. From this it is concluded that the vapor pressure determinations of Cs, Rb, and K by Langmuir, Kingdon, and Killian are the most accurate available. Attention is called to possible uses of a positive ion source of the type utilized in the present investigation, for separation of isotopes and determinations of isotope intensity ratios.

Introductory Review

A CRITICAL survey of the attempts to discover eka-caesium showed that the sensitivity of detection and quantitative estimation by previous methods could be greatly improved by a modified method of positive ray analysis. Following chemical fractionation to increase the concentration of eka-caesium, if existent in the preparations used, the final fractions have been compared by previous investigators and tested for the presence of element 87 by atomic weight determinations,[1,2] radioactive [2,7,8,9] methods, by observa-

[1] T. W. Richards and E. H. Archibald, Proc. Am. Acad. **38,** 443 (1903).
[2] G. P. Baxter, J. Am. Chem. Soc. **37,** 286 (1915).
[3] L. M. Dennis and R. W. G. Wyckoff, J. Am. Chem. Soc. **42,** 985 (1920).
[4] H. Zwaardemaker, W. E. Ringer and E. Smits, K. Akad. Amsterdam Proc. **26,** 575 (1923).
[5] J. G. F. Druce, Chem. News **131,** 273 (1925); F. H. Loring and J. G. F. Druce, Chem. News **131,** 289, 305, 337, (1925); F. H. Loring, Chem. News **131,** 338, 371, (1925) **132,** 101, (1926).

tion of physiological effects,[4] x-ray spectra,[5,6,10] flame, [1,2] spark,[2] and arc[3] spectra.

The concentration of eka-caesium may be increased in any chemical preparation by proper manipulation. Chemical means of separation can therefore be considered as a common factor to increase the sensitivity for all methods of identification. Atomic weight determinations of caesium from the final fractions of a caesium preparation believed to contain eka-caesium can not detect the presence of element 87 if it is present to less than one ten thousandth, assuming that its atomic weight is 223, and that 132.81 for caesium can be definitely distinguished from 132.82 for a caesium and eka-caesium mixture.

The existence of eka-caesium is, of course, dependent on its nuclear conformation and radioactive characteristics. Fajans[11] has pointed out that isotopes of atomic weight $4n$ and odd nuclear charge are very unstable, and in some cases non-existent within the limits of observation. Th D 208, Z 81, Th C 212, Z 83, and Ms Th_2 228, Z 89, are very unstable short-lived β radiators. The possibility exists that eka-caesium, Z 87, and eka-iodine, Z 85, may come under this grouping. The predictions of the atomic weight of eka-caesium do not confirm this hypothesis. The atomic weight has been variously given as 224[12] and 223[13] on the basis of empirical relationships between atomic number and atomic weight, 221[14] has been proposed after consideration of the known isotopes and radioactive disintegration series. The speculative and unconfirmed nature of the many theories of nuclear structure does not allow a confident prediction of the radioactive characteristics of eka-caesium. However, Hahn and Erbacher[8] determined from a Ms Th and Ms Th_2 preparation the non-existence of more than 10^{-7} admixed eka-caesium if the half life period lies between ten minutes and ten years. Hevesy[7] examined Ms Th_2 and decided less than 5×10^{-6} disintegrated to give 87.

The occurrence of physiological effects agreeing with the behavior predicted for eka-caesium might enable a competent investigator to detect the presence of element 87, but confirmatory identification would always have to be referred to one of the other methods.

Hevesy[15] has given a very excellent discussion of chemical Röntgen spectroscopy and agrees with Thomassen[16] that an element must be present at

[6] J. N. Friend, Nature **117,** 789 (1926).
[7] G. Hevesy, Danske Videnskab Selskab. **7,** 1 (1926).
[8] O. Hahn and O. Erbacher, Phys. Zeits. **27,** 531 (1926).
[9] O. Hahn, Naturwiss. **14,** 158 (1926).
[10] Herzfinkiel, Comptes Rendus **184,** 968 (1927).
[11] K. Fajans, Composition of Atom Nuclei, Chap. X, Radioactivity (1923).
[12] F. Loewinson-Lessing, Comptes Rendus **176,** 307 (1923).
[13] E. W. Washburn, J. Am. Chem. Soc. **48,** 2351 (1926).
[14] A. S. Russell, Phil. Mag. **47,** 1121 (1924); W. P. Widdowson and A. S. Russell, Phil. Mag. **48,** 293 (1924).
[15] G. Hevesy, Chem. Reviews **3,** 321 (1927).
[16] L. Thomassen, Kgl. Dept. Handel, Sjofart, Ind. og Friskeri Statens Raastoffkomite Publ. **21,** 108 (1925).

the anode at least to 0.1 percent, or better 1 percent, for positive identification.

In the case of the alkali metals spectroscopic methods of analysis are not the most sensitive due to the band and continuous spectra accompanying the line emission and absorption spectra.[17] Walter and Barratt observed that rubidium and caesium both have bands in the far red and that most of the alkali intermetallic compounds possess a diffuse band with no fine structure, probably a true continuous spectrum. It is this continuous background that renders difficult the identification of an alkali metal present in a small quantity when admixed with one or more of the alkalis. Gooch and Hart[18] found that one hundred parts of sodium were sufficient to mask one part of potassium in the flame spectrum. Gooch and Phinney[19] determined that for rubidium in the presence of sodium, the glare due to the band and continuous spectra made the rubidium lines invisible for a ratio as low as one part rubidium to ten parts sodium. Only one part rubidium in fifty parts potassium could be detected. Band spectra accompany the line emission spectra of the alkalis for all modes of excitation except the undamped electrodeless discharge.[20] Spectroscopic identification of eka-caesium has not been tried by this method.

Spectroscopic identification also has disadvantages in that the ultimate lines of eka-caesium would lie in the infra-red in a region of low photographic sensibility.

Ionization potential and resonance lines of eka-caesium: The ultimate and persistent lines of the alkali metals are the first doublet lines of the principal series. Radium II provides an iso-electronic system which, by application of Moseley's law, allows a prediction of the ionization potential and the term values for the first doublet of the principal series of eka-caesium. A great uncertainty is introduced due to the uncertainty of the Ra II spectrum. The term values for Ra II were taken as selected in Fowler's Report. The ionization potential of Ra II is greater than that of Ba II, consequently for Eka-Cs I, V_i is probably greater than for Cs I. The $(\nu/R)^{1/2}$ was plotted against an arbitrary abscissa length for all the alkalis and their iso-electronic counterparts in the alkaline earth metals. This was done to obtain a satisfactory value for the slope to be used for the Eka-Cs I, Ra II plot. A more satisfactory relation, without a simple theoretical basis however, was supplied by plotting as ordinates the ratio ν alkaline earth/ν alkali, for all iso-electronic systems, against a constant abscissa separation, while progressing from one ratio to the next for the successive elements. This method was also extended to the doublet separation ratios in order to get $\Delta\nu$ for eka-caesium. A smooth curve of decreasing slope resulted in every case which could be extrapolated with confidence to νRa II/νEka-Cs I. The weighted spectroscopic values

[17] J. M. Walter and S. Barratt, Proc. Roy. Soc. **119A,** 257 (1928).
[18] F. A. Gooch and T. S. Hart, Am. J. Sci. **42,** 3rd series, 448, (1891).
[19] F. A. Gooch and J. I. Phinney, Am. J. Sci. **44,** 3rd series, 392 (1892).
[20] G. Balasse, Comptes Rendus **184,** 1002 (1927).

for eka-caesium obtained by these means are: $V_i = 4.05 \pm 0.05$ volts, $7^2P_{\frac{1}{2}} = 21340 \pm 200$ cm^{-1}, $7^2P_{\frac{3}{2}} = 19670 \pm 200$ cm^{-1}, $\Delta\nu$ separately determined was 1675 ± 50 cm^{-1}, $\lambda 7^2S_{\frac{1}{2}} - 7^2P_{\frac{1}{2}} = 8720 \pm 200$A, $\lambda 7^2S_{\frac{1}{2}} - 7^2P_{\frac{3}{2}} = 7600 \pm 200$A. If the ionization potential value for Ra II is correct, then the ionization potential of eka-caesium being greater than that of caesium, element 87 would not be as highly ionized as caesium near the sun's surface[21] and the absorption lines of the first doublet of the principal series might appear in the sun's spot spectrum.[22] A search was made from 7000A to 9000A[23] for two lines with the proper intensity ratio and wave number separation, but no lines were found that could not be properly assigned to some other element. The wave-number separation is more reliable than the wave-lengths predicted, as the latter of course depend on two extrapolations introducing large uncertainties.

Positive ray analysis method. Positive ion source. Preliminary calculations of the sensitivity possible by a method of positive ray analysis showed that this method would exceed in sensitivity all but the radioactive system of identification and detection of eka-caesium, provided an efficient method of production of ions could be secured. Positive ray analysis of a likely source of eka-caesium would be independent of the radioactive properties (if the half life period were great enough to allow a concentration of eka-caesium within the limit of detection of the method), and would give definite identification from measurement of the e/M ratio. Moreover, a quantitative estimate could be made of the amount present. An efficient method of producing positive ions has been investigated by Langmuir and Kingdon,[24] and Ives.[25] Langmuir and Kingdon have shown that a tungsten filament heated to 1200°K or more converts into ions all caesium atoms which strike the tungsten surface. Together with Killian[26] they have utilized this phenomenon to determine the vapor pressure of caesium, rubidium and potassium, and have shown experimentally that ionization occurs in accord with Saha's equation. The equilibrium constant $K_n = n_e n_p / n_a$, where n_e, n_p, and n_a denote the number of electrons, positive ions, and atoms per cm^3 respectively, is given by Saha's equation,

$$\log_{10} K_n = 15.368 + \frac{3}{2}\log_{10} T - \frac{5040 V_i}{T},$$

T is expressed in degrees Kelvin and V_i is the ionization potential of the vapor. Langmuir and Kingdon pointed out that in the case of thermal ionization on the surface of a filament there is no necessary relation between n_e and n_p as occurs when the ionization of the vapor is not influenced by the

[21] M. N. Saha, Phil. Mag. **40**, 472, 809 (1920).
[22] H. N. Russell, Astrophys. J. **55**, 119 (1922).
[23] Solar spectrum wave-lengths, Carnegie Inst. Publ. **396**, (1928).
[24] I. Langmuir and K. H. Kingdon, Proc. Roy. Soc. **107A**, 61 (1925).
[25] H. E. Ives, Frank. Inst. J. **201**, 47 (1926).
[26] T. J. Killian, Phys. Rev. **27**, 578 (1926).

enclosure walls or other surfaces. n_e is dependent on the temperature and filament characteristics as given by Richardson's equation $I = AT^2\epsilon^{-b/T}$. The electron density is obtained from the relation

$$n_e = \left(\frac{2\pi m}{e^2 kT}\right)^{1/2} I = 4.034 \times 10^{13} \frac{I}{T^{1/2}},$$

I being expressed in amperes per cm^2. n_e, obtained by the elimination of I in the second and third equations, when substituted in the first equation yields the simple expression

$$\frac{n_p}{n_a} = \frac{57.93}{A} \times 10^{(b-11{,}600V_i)/2.3T}$$

for the ratio of the number of positive ions to the number of neutral atoms per unit volume. The most useful and stable thermionic surfaces have the following values for A and b: thorium on tungsten,[27] $A=7$, $b=31{,}200°$; tungsten,[28] $A=60.2$, $b=52{,}600°$; oxygen on tungsten,[28] $A=5\times10^{11}$, $b=107{,}000°$. A has the dimensions amp cm^{-2}deg^{-2}. In the present experiment the positive ions were produced thermally at the surface of a tungsten strip by this very efficient method. For eka-caesium with an ionization potential of 4.05 volts and tungsten filament at 1300°K, n_p/n_a is 71 or practically complete ionization of the incident atoms occurs. No two stage ionization can occur as the removal of the outer electron leaves a rare gas shell whose ionization potential is too great to permit ionization on the filament surface.

Apparatus design. This positive ion source was incorporated into a tube, Fig. 1, similar to Dempster's[29] mass spectrograph as regards focussing, but differing in the method of production of the ions, and in one arrangement used differing in the method of their measurement. A is the positive ion source and at the same time acts as a collimating slit as all the ions originate on the surface of A and so the beam is defined by the field distribution between A and B. With the design used, the field distribution approximated the uniform distribution between two parallel planes. For the potential differences used, the beam spread due to non-uniformity of the field was negligible and is smaller the greater the atomic weight.[30] A was a tungsten strip rolled 0.01 cm thick from a 0.051 cm diameter filament. This was heated by a ten volt secondary, center tap transformer. Connections to this filament were made to the center tap thereby eliminating lead potential differences to a large extent and acting in effect as if the connection had been made directly to the center of the strip filament. The temperature of the strip was measured by a L and N optical pyrometer. The "brightness

[27] S. Dushman, H. N. Rowe, Jessie Ewald and C. A. Kidner, Phys. Rev. **25**, 338 (1925).
[28] K. H. Kingdon, Phys. Rev. **24**, 510 (1924).
[29] A. J. Dempster, Phys. Rev. **11**, 316 (1918).
[30] L. Tonks, H. M. Mott-Smith Jr., I. Langmuir, Phys. Rev. **28**, 104 (1926)

temperature" measured this way was corrected using Forsythe and Worthing's[31] data. Due to the cooling effect of the leads there was a considerable temperature gradient This is not important as the percentage ionization at the surface of the filament does not appreciably differ from 100 percent over the range 1200°−1300°K. Only the center half centimeter was actually utilized. A strip of large cross section was used so as to minimize the voltage gradient along the filament for a given temperature. The increased surface area of the strip above a cylindrical filament of the same cross section and the cooling effect of the leads necessitated a current of 9 amperes for a temperature of 1300°K at the center of the strip. The voltage gradient was then approximately 0.14 volts per cm which was not enough to interfere with the definition of the ion beam. The transmitting slit in *B* was 0.071 cm wide and 0.54 cm long, the receiving slit at *D* being 0.64 cm long and 0.075 cm wide cut in 0.011 cm thick sheet molybdenum. The radius of curvature of the beam path was about 3.2 cm. The surface of *F* was silvered chemically and then coated with a crystalline electrolytic deposit of copper by slow deposition from an acid bath. By this means specular reflection of the beam from the walls is reduced and consequently no collimating baffles were placed in *F*. The small amount of reflection still remaining could be minimized by "spraying" the walls with the ion beam before taking readings. Evidently the walls were then covered with a film of the same metal as the vapor and instead of reflection condensation with loss of charge and re-evaporation occurred. Connection to *F* was made from a side tube not shown in Fig. 1. *D* is a thoriated tungsten filament 0.005 cm radius totally enclosed by a nickel cylinder of 1 cm radius and 2 cm long. The slit in *D* placed above the slit *C* was 0.75 cm long and 0.12 cm wide approximately.

When all the electrodes had been incorporated the preparation to be tested for the presence of eka-caesium was enclosed in the appendix connected by *H* to *G*. Caesium chloride was used prepared from two sources, as will be described later, and was mixed with calcium filings. This mixture was placed in a small vacuum fired nickel cylindrical container. The tube was evacuated by a Langmuir condensation pump backed by a Cenco Hyvac, with a liquid air trap interposed between the tube and the mercury pump. Exhaust was continued for four hours with the tube enclosed in a furnace at 260°C, higher temperatures being prohibited by the tendency of the silver copper coating to leave the walls of *F*. The bake out temperature was higher than any subsequent temperature. The pellet containing the caesium chloride and calcium was then heated inductively by a high frequency coil, the caesium distilling to the walls and then later was redistilled into appendix *G*. The tube was sealed off at a pressure less than 0.001 barye, the limit of the McLeod gauge and was then ready for test.

Chemical preparation of material. Two series of tests were made. The first trial was made using caesium chloride supplied and prepared through the courtesy of the General Electric Company. The method of separation

[31] W. E. Forsythe and A. G. Worthing, Astrophys. J. **61**, 146 (1925)

from pollucite from Oxford County, Maine, followed Browning essentially.[32] The finely powdered mineral was decomposed with strong hydrochloric acid. The acid solution was then treated with antimonous trichloride which precipitates the double chloride of antimony and caesium. This precipitate is filtered out and then hydrolyzed, the antimonous oxide precipitates leaving caesium chloride in solution, the dissolved antimony being separated with hydrogen sulphide. From the predicted chemical solubilities the eka-caesium salts should accompany the caesium salts throughout this process. No further concentration was essayed. The caesium chloride obtained in this way from pollucite was used for the first test.

Dobroserov[33] has suggested that the radioactivity of potassium is due to admixed eka-caesium. Kracke[34] doubts the existence of any potassium radiation. Although these suppositions are hardly tenable in view of the

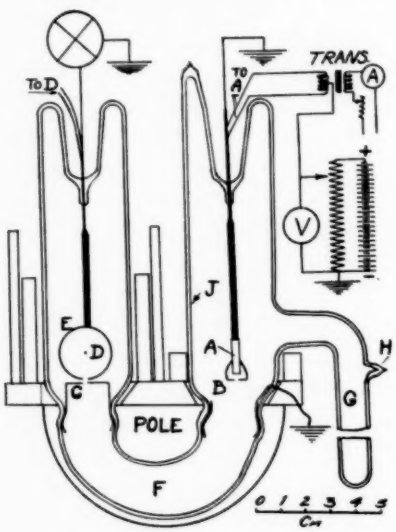

Fig. 1. Mass spectrograph.

careful work of Campbell and Wood[35] Hoffman,[36] and Ringer,[37] a potassium and caesium ore was sought. All five known alkalis occur together in lepidolite, the usual ore containing 10 to 12 percent K, 1 to 3 percent Na, 1 to 2 percent Li., 0.5 to 1 percent Rb., 0.2 to 3 percent Cs. This ore then constitutes a likely source for eka-caesium. The method of separation differed slightly from that for pollucite. The powdered mineral, also from Oxford

[32] P. E. Browning, Introduction to the Rarer Elements, 9, (1917).

[33] D. Dobroserov, Ukrainskii Khem. Zhurnal **1,** 491 (1925); Chem. Zentr. *II,* 162 (1926).

[34] B. Kracke, Phys. Zeits. **27,** 290 (1926).

[35] N. Campbell and A. Wood, Proc. Camb. Phil. Soc. **14,** 15 (1907); N. Campbell **14,** 211, 557 (1907); **15,** 11 (1909).

[36] G. Hoffman, Phys. Zeits. **24,** 475 (1923).

[37] W. E. Ringer, Onderz. physiol. Scheikunde **1,** 23 (1921).

County, Maine, was heated with a mixture of calcium carbonate and ammonium chloride, and the chlorides resulting from treatment were distilled onto a cool iron pipe and the hard chloride cake chipped off. The material was received in this form from the General Electric Company. The mixed chlorides were dissolved in a minimum quantity of water and treated with antimonous chloride as before. Only a few grams were treated at a time so that the antimonous oxide resulting from hydrolysis could be reconverted to antimonous chloride by solution in hydrochloric acid. In this way if the eka-caesium chloride should be partially adsorbed on the antimonous oxide it would go back into solution and eventually most of it would appear with the caesium chloride in the final solution. This was merely a precautionary measure, no trouble from adsorption was expected as eka-caesium chloride from its predicted solubility, hardly admitting of error, should fulfill the radioactive precipitation[38] rules, and should accompany caesium salts in solution or crystallization. The final preparation was not completely purified but intentionally included Li, Na, K, and Rb to the extent of about 25 percent. In both cases no concentration was attempted beyond the separation of caesium and eka-caesium from the ores.

Procedure and results. After the tube had been prepared it was placed between the poles of the DuBois magnet and adjusted to secure the optimum focus and connected as in Fig. I. The magnetic field was maintained constant while the accelerating voltage was varied to bring the ion beams of different e/M ratios to the receiving cylinder. The positive ion current may be limited by space charge[39] or by the rate of arrival of atoms at the filament surface. The current limited by space charge for parallel planes and singly charged ions is given by $I_s = 5.43 \times 10^{-8}\ (1/M^{1/2})\ (V^{3/2}/x^2)$, where I is the maximum current density in amp. cm^{-2}, V the potential difference in volts, x the distance of separation of the planes and M is the atomic weight of the ions. The current limited by vapor pressure is given by kinetic theory as $I_p = 10ep/(2\pi m_H MkT^{1/2})$ where e is the electronic charge, p the pressure in baryes, m_H the mass of the hydrogen atom, k the Boltzman constant, and T is the absolute temperature of the vapor. For caesium at 20°C, $p = 1.07 \times 10^{-3}$ baryes[24] and $I_p = 21.8 \times 10^{-6}$ amp. cm^{-2}. The transmitter slit, area 0.038 cm^2, allows a current of 83×10^{-8} amp., if the currents were not limited by space charge. The radius of curvature of the ion beam is

$$R = 1/H(2Mm_H V/e)^{1/2} \text{ cm.}^{29}$$

The allowable accelerating potential and so the space charge current for any ion is limited by the magnetic field strength and radius of curvature. R was 3.2 cm, so the present apparatus with a slit width of 0.075 cm had a resolution of 1/42 approximately. The magnetic field was held constant for any one run but different runs were taken with H from 3000 to 5000 gauss. MV is then constant for any run with R and H

[38] O. Hahn, Ber. **59B**, 2014 (1926).
[39] I. Langmuir, Phys. Rev. **2**, 450 (1913).

constant and the quantitative sensitivity of detection of any ion may be calculated if it is known whether or not the ion current is limited by space charge or by the rate of arrival of the atoms at the filament surface. For a magnetic field of 3050 gauss an accelerating potential of 60 volts brings the caesium beam to a focus at the receiving slit. At this accelerating potential for caesium the received current, if limited only by space charge, should be 209×10^{-8} amp. The current actually obtained at the receiving slit for caesium was 6.25×10^{-8} amperes. By varying the magnetic field and thereby the potential required to bring caesium into position, $V^{3/2}/I_{Cs}$ was found to be constant. So under the conditions obtaining in the tube the current was limited by space charge and was only 3.3 percent of the theoretical. This was not due to poor definition of the beam as the peaks observed, plotting current against accelerating potential or atomic weight, were very close to the ideal that would be obtained if the positive ion beam were defined by the first slit and perfect focussing occured. As the current was space charge limited the quantitive estimation of the sensitivity of the apparatus for detecting eka-caesium was made on this basis.

$$V_{Eka-Cs}=\frac{M_{Cs}}{M_{Eka-Cs}}\times V_{Cs}$$

for constant magnetic field strength. From space charge considerations I is proportional to $V^{3/2}/M^{1/2}$. From kinetic theory considerations the rate of arrival of atoms at the source surface is proportional to $1/M^{1/2}$. By combination of these controlling factors, the fraction of eka-caesium present in the vapor state admixed with caesium is equal to $(I_{Eka-Cs}/I_{Cs})\times(M_{Eka-Cs}/M_{Cs})^{5/2}$ I in this case referring to the received currents at D. Currents were measured with a Compton electrometer of sensitivity 10,900 mm per volt, and a L and N galvanometer. The minimum current that could be read with the electrometer by observing the rate of deflection was 5×10^{-15} amp.

In one run E was made several volts electropositive with respect to C, with D ten or twelve volts negative. The field distribution was such that positive ions could enter the slit in E. The current from the filament D was limited by space charge which was partially neutralized by the incoming positive ion beam resulting in a great increase in current through a galvanometer in the circuit D to E, the normal emission current being balanced out in the local galvanometer circuit. To permit the electrons from D to reach E[40] the tube was shielded from the magnetic field by two concentric soft iron pipes as shown in Fig. 1. The neutralization of space charge[41] occasioned by the entering positive ions resulted in an increase of current in the case of caesium which was 5,700 times greater than the positive ion beam current. The ultimate sensitivity of this arrangement was less than could be obtained with the electrometer so that this method of amplification of the received beam was abandoned.

[40] A. W. Hull, Phys. Rev. **18**, 31 (1921).
[41] K. H. Kingdon, Phys. Rev. **21**, 408 (1923).

Six trials were made to detect eka-caesium in the caesium prepared from the pollucite ore. A globule of molten caesium was held on the walls of J by cooling with an air blast and the potential was varied over the range required to bring ions between 200 to 250 mass units into focus as the globule was evaporating. Readings were made until the globule had completely evaporated so that the determination would be independent of the vapor pressure of the eka-caesium. No eka-caesium was present to an amount greater than 3.5×10^{-7} of the caesium metal from the pollucite ore. With the lepidolite caesium two runs were made and no eka-caesium was present to an amount greater than 7.3×10^{-6}. The temperature of the molten caesium was approximately 40°C in these trials. At this temperature peaks were observed for Ca, K and Rb. At higher temperatures Na and Na_2 occured in almost equal amount, but to a very small extent when using the pollucite caesium. There was no evidence of any Cs^+_2 present to more than 10^{-6}. The only molecular beam detected was Na_2. Any other molecular configurations or intermetallic compounds were dissociated if present at all. This appears anomalous in view of the fact that Na_2 has the smallest heat of dissociation[17] of any of the alkalis or their intermetallic compounds. No satisfactory explanation has yet been formulated.

Discussion. The sensitivity of the method described is of the same order as the radioactive test results obtained by examining Ms Th and Ms Th_2. The positive ray analysis method is based on a more secure foundation being dependent chiefly on eka-caesium having a low ionization potential and being independent of its radioactive characteristics providing the half-life period is great enough to allow a small concentration of the element. In view of the uncertain knowledge of nuclear structure this method appears to be superior to any system of detection depending on highly speculative predictions of the radioactive properties of eka-caesium or possible parent elements, and at least provides a new and sensitive mode of attack in seeking for the interesting element 87. If eka-caesium is found to be present to a small extent in any preparation tested by this means, a quantitative estimate is easily made which can direct the amount of fractionation required to provide a quantity of this element sufficient for confirmatory identification by methods allowing a permanent and incontestable record.

No doubly charged alkali ions were detected at all. The measurements of the vapor pressures of the alkali metals by Langmuir and Kingdon,[24] and Killian[26] by measurement of the positive ion current thermally produced from tungsten filaments in the vapor of the elements K, Rb, and Cs have been criticised by Rowe[42] on the grounds that multiple ionization did occur. From the present examination of the products of ionization this criticism is unfounded in fact and it is believed that the above vapor pressure determinations are the most accurate available. Disagreement is found with Ives'[25] results who reported molecular ions of K, Rb and Cs, besides

[42] H. Rowe, Phil. Mag. **3**, 534 (1927).

Na. Ives' results were probably due to the filament not being coaxial with the cylinder.

A new apparatus is being constructed that will be able to separate completely ions differing in mass by 1/250. The ion source in this case is an oxygen coated filament which Kingdon[43] has shown can ionize Ca, Cu, and Bi ($V_i=8$). On this surface many of the metallic elements which are difficult to deal with by the usual methods of positive ion production can be ionized and examined for isotopes and the isotope intensity ratios can be obtained. Particularly those elements of very low vapor pressures, even at temperatures of 2000°K, are amenable to this method if their ionization potentials are not greater than eight volts. An attempt is also being made to use an apparatus essentially like the present one in principle to separate the isotopes of Li and K.

In conclusion I wish to thank Professor H. D. Smyth for valuable criticisms and suggestions, and the General Electric Company for the materials and ores supplied.

[43] K. H. Kingdon, Phys. Rev. **23**. 778 (1924).

CONDUCTIVITY OF IONS IN CROSSED ELECTRIC AND MAGNETIC FIELDS

By Leigh Page
Sloane Physics Laboratory, Yale University

(Received May 13, 1929)

Abstract

The effect of collisions of ions moving through crossed electric and magnetic fields is investigated. (*a*) Collisions of ions with one another are shown to be without effect, the transverse current at right angles to the fields having the same value neu, where u is the velocity of progression, as would exist in the absence of collisions. (*b*) Collisions of free ions with neutral particles are investigated for the case where u is small compared to the speed v of thermal agitation. As the mean free path is increased the current parallel to the electric field increases to a maximum and then falls asymptotically to zero, the transverse current parallel to u rising from zero to the limiting value neu for infinite mean free path. Calculation of the Hall coefficient on the present theory, which differs from the usual theory in that it takes account of long free paths, shows that the coefficient increases with increasing magnetic field.

IN AN earlier paper[1] it was shown that ions in constant electric and magnetic fields progress at right angles to the plane of the fields with the constant velocity

$$u = c[\boldsymbol{E}\times\boldsymbol{H}]/H^2 \tag{1}$$

the projection of the path of each ion on the plane perpendicular to $\boldsymbol{H}$ being a prolate, common or curtate cycloid in accordance with the magnitude and direction of its initial velocity. In the investigation referred to, the ions were supposed to suffer no collisions. The object of the present paper is to examine the effect of collisions on the paths of the ions and to calculate the current densities and conductivities both in the direction of the electric field and in the direction of the velocity of progression u. We shall limit ourselves to the case where the electric and magnetic fields are at right angles, since nothing essentially new is to be gained by including a component of the electric intensity parallel to the magnetic lines of force. Then the velocity of progression at right angles to the fields is

$$u = cE/H. \tag{2}$$

We shall consider separately (1) the case where the only collisions are between one ion and another, and (2) the case where the collisions are between ions and neutral particles, the number of collisions of one ion with another being negligible in comparison.

(1) *All collisions between ions.* This case is easily disposed of. We transform to a set of axes XYZ moving with the velocity u given by Eq. (1) rela-

[1] L. Page, Phys. Rev. **33**, 553 (1929).

tive to the observer's inertial system. By so doing we eliminate the electric field, as was shown in the paper[1] to which reference has already been made. Therefore we have a magnetic field alone in the system XYZ. Obviously this field can give rise to no general drift of the ions. Whether they collide with one another or not no current can exist relative to XYZ. Consequently the ions drift relative to the observer's inertial system with the same velocity of progression $\boldsymbol{u}$ at right angles to the fields whether they suffer collisions with one another or not. If n is the number of ions per unit volume and e the charge on each, the current density is simply

$$j=neu=necE/H \tag{3}$$

in a direction at right angles to the plane of $\boldsymbol{E}$ and $\boldsymbol{H}$.

Of course the above reasoning is valid only for $u<c$ and therefore $E<H$.

(2) *Collisions between ions and neutral particles.* Now we shall treat the case where the collisions are between free ions and particles which are unaffected by the fields, such as neutral particles in the case of gaseous conduction or fixed positive ions in the case of electronic conduction in a metal. We shall assume that the collision of one free ion with another is too infrequent to require consideration. In order to handle the problem analytically it will be necessary to disregard the Maxwellian distribution of velocities and follow Clausius' method of treating the particles as if they all had the mean speed of thermal agitation. This approximation, however, can hardly do more than introduce a small error in the numerical coefficients involved in the expressions for the conductivities. In order to avoid consideration of the drag which would be exerted on the free ions by a stream of neutral particles drifting relative to the observer, all calculations will be made relative to the inertial system in which the neutral particles, as a whole, are at rest. Finally, we shall confine ourselves to cases where the normal velocity of progression u relative to this inertial system is small compared to the velocity v of thermal agitation. This condition is undoubtedly satisfied in the upper atmosphere for electrons and protons if not for heavier ions, as the electric field in that region is small compared to the magnetic field.[2]

If we orient axes so that the y axis is parallel to $\boldsymbol{E}$, the z axis to $\boldsymbol{H}$, and therefore the x axis to $\boldsymbol{u}$, and put

$$\omega\equiv -eH/mc\ ;$$

$$v_x=v\sin\theta\cos\phi=V\cos\alpha+u,$$

$$v_y=v\sin\theta\sin\phi=V\sin\alpha,$$

$$v_z=v\cos\theta,$$

the integrated equations of motion[3] take the form

$$x=\frac{V}{\omega}[\sin(\omega t+\alpha)-\sin\alpha]+ut, \tag{4}$$

[2] L. Page, Phys. Rev. **33**, 823, (1929).

[3] L. Page, Phys. Rev. **24**, 284 (1924), Eqs. (1), (2), (3).

$$y=\frac{V}{\omega}[-\cos(\omega t+\alpha)+\cos\alpha], \tag{5}$$

$$z=v\cos\theta\cdot t. \tag{6}$$

An element of path is therefore

$$ds=vdt[1+2(uV/v^2)\{\cos(\omega t+\alpha)-\cos\alpha\}]^{1/2}.$$

As u is small compared to v by hypothesis we can expand the radical as a power series in u/v, retaining only the first order term.[4] Integrating we have

$$s=vt+(uV/\omega v)\{\sin(\omega t+\alpha)-\sin\alpha\}-(uV/v)\cos\alpha\cdot t,$$

and solving for t we get

$$t=s/v[1-(uV/\beta v^2)\{\sin(\beta+\alpha)-\sin\alpha-\beta\cos\alpha\}],$$

where β has been put for $\omega s/v$. In the term containing u we can put $v\sin\theta$ for V and ϕ for α. Hence

$$t=\frac{\beta}{\omega}\left[1-\frac{u}{\beta v}\sin\theta\{\sin(\beta+\phi)-\sin\phi-\beta\cos\phi\}\right]. \tag{7}$$

Substituting this value of t in the expressions (4), (5), (6) for x, y, z we get

$$x=\frac{v}{\omega}\sin\theta[\sin(\beta+\phi)-\sin\phi\ ]$$
$$+\frac{u}{\omega}[\beta-\sin\beta-\sin^2\theta\cos(\beta+\phi)\{\sin(\beta+\phi)-\sin\phi-\beta\cos\phi\}], \tag{8}$$

$$y=\frac{v}{\omega}\sin\theta[-\cos(\beta+\phi)+\cos\phi]$$
$$+\frac{u}{\omega}[-(1-\cos\beta)-\sin^2\theta\sin(\beta+\phi)\{\sin(\beta+\phi)-\sin\phi-\beta\cos\phi\}] \tag{9}$$

$$z=\frac{v}{\omega}\beta\cos\theta-\frac{u}{\omega}\sin\theta\cos\theta\{\sin(\beta+\phi)-\sin\phi-\beta\cos\phi\}. \tag{10}$$

Equations (8), (9) and (10) give the components of displacement of an ion as functions of the direction of its initial velocity—specified by the angles θ and ϕ—and of the length of arc traversed, $s=\beta v/\omega$.

In order to find the x component of the current density we must calculate the number of ions passing through a unit cross-section perpendicular to the x axis. Considering x, y and z as functions of s, θ and ϕ we find that if x is kept constant

[4] This approximation is also valid for small magnetic fields even if u is large compared to v, provided the electric field is small enough so that its square can be neglected. For if H is small the radical becomes: $1+(e/mv)Et\sin\theta\sin\phi+$terms in H and E^2 and higher powers.

$$[dydz]_x = \frac{J}{\frac{\partial x}{\partial s}} d\theta\, d\phi,$$

where J is the Jacobian

$$J = \frac{\partial(x,y,z)}{\partial(s,\theta,\phi)}.$$

Therefore the value of $d\theta d\phi$ corresponding to a unit cross-section AB (Fig. 1) perpendicular to the x axis is

$$d\theta d\phi = \frac{\partial x/\partial s}{J}.$$

If N represents the number of collisions made by the ions per unit volume per unit time and if as many ions start off in one direction as in any other after suffering a collision, the number of ions starting off on new free paths

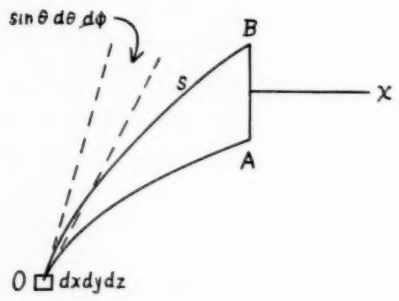

Fig. 1.

inside the conical angle $\sin\theta d\theta d\phi$ is $(N/4\pi)\sin\theta d\theta d\phi$ per unit volume per unit time. Hence the number originating in a unit volume at O per unit time so directed as to pass through the unit cross-section AB is

$$\frac{N}{4\pi}\frac{\partial x}{\partial s}\frac{\sin\theta}{J},$$

and the number originating in a volume $dx\,dy\,dz$ at O per unit time so directed as to pass through AB is

$$\frac{N}{4\pi}\frac{\partial x}{\partial s}\frac{\sin\theta}{J} dx\,dy\,dz.$$

But

$$dx\,dy\,dz = J\,ds\,d\theta\,d\phi.$$

Therefore this number is

$$\frac{N}{4\pi}\frac{\partial x}{\partial s}\sin\theta\, ds\, d\theta\, d\phi.$$

If all the ions had exactly the same free path l the x component of the current density would be

$$j_x=\frac{Ne}{4\pi}\int_0^{2\pi}\int_0^{\pi}\int_0^{l}\frac{\partial x}{\partial s}\sin\theta\,ds\,d\theta\,d\phi \tag{11}$$

with corresponding expressions for j_y and j_z, the letter e standing for the charge on each ion.

The chance of an ion colliding before reaching AB, however, must be taken into account, giving for j_x the integral

$$j_x=\frac{Ne}{4\pi}\int_0^{2\pi}\int_0^{\pi}\int_0^{\infty}e^{-s/l}\frac{\partial x}{\partial s}\sin\theta\,ds\,d\theta\,d\phi \tag{12}$$

instead of (11), where l is the mean free path. Corresponding expressions hold for j_y and j_z.

While Eq. (11) does not correspond to the physical conditions actually existing, the current will be calculated on the basis of this equation for the purpose of comparison with the current calculated from Eq. (12).

Differentiating (8), (9) and (10), substituting in (11) and the corresponding equations for j_y and j_z and integrating, we get

$$j_x=neu\left[1+\frac{1}{3}\cos\gamma-\frac{4}{3\gamma}\sin\gamma\right], \tag{13}$$

$$j_y=neu\left[-\frac{1}{3}\sin\gamma+\frac{4}{3\gamma}(1-\cos\gamma)\right], \tag{14}$$

$$j_z=0. \tag{15}$$

where

$$\gamma\equiv-\beta=\frac{elH}{mcv}, \qquad n\equiv\frac{Nl}{v}=\text{ number of ions per unit volume.}$$

Furthermore if we denote by σ the conductivity

$$\sigma=\frac{1}{3}\,\frac{ne^2l}{mv}$$

which would exist in the absence of the magnetic field, and define the conductivities σ_x, σ_y, σ_z in the x, y, z directions in the presence of both fields by the relations

$$\sigma_x=\frac{j_x}{E_y}, \qquad \sigma_y=\frac{j_y}{E_y}, \qquad \sigma_z=\frac{j_z}{E_y},$$

we find

$$\frac{\sigma_x}{\sigma}=\frac{3}{\gamma}\left[1+\frac{1}{3}\cos\gamma-\frac{4}{3\gamma}\sin\gamma\right], \tag{16}$$

$$\frac{\sigma_y}{\sigma}=\frac{3}{\gamma}\left[-\frac{1}{3}\sin\gamma+\frac{4}{3\gamma}(1-\cos\gamma)\right], \tag{17}$$

$$\frac{\sigma_z}{\sigma}=0. \tag{18}$$

Figure 2 shows j_x and j_y plotted against γ. The curves in this figure show how the currents change with increasing free path, the magnetic field as well

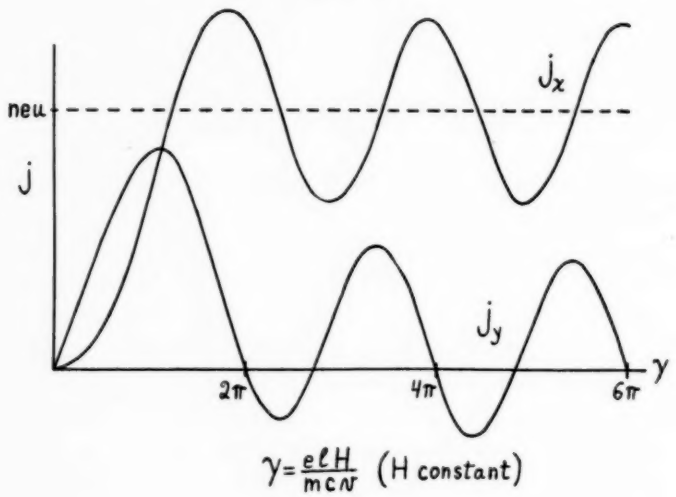

Fig. 2.

as the electric field remaining constant. The current j_y parallel to the electric field increases from zero to a maximum, decreases to zero and reverses in direction, finally oscillating about the value zero for very long free paths. The

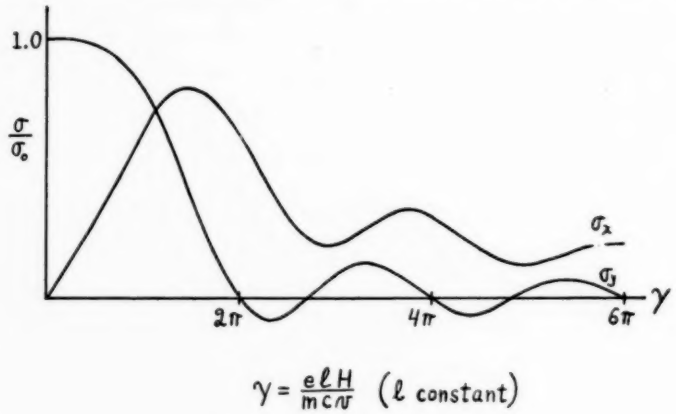

Fig. 3.

transverse current j_z, on the other hand, mounts from zero to a maximum greater than that of the current in the direction of the electric field, and finally

oscillates about the normal value *neu* of the current of progression at right angles to the two fields.

In Figure 3 the conductivities σ_x and σ_y are plotted against γ. These curves show how the conductivities change with increasing magnetic field for a constant free path l. It is to be noted that while the transverse conductivity σ_x is less than the conductivity σ_y parallel to the electric field for small magnetic fields, the reverse is true for large magnetic fields. Again currents in the direction opposite to the electric field are found for certain values of the magnetic field. Both conductivities approach zero as the magnetic intensity is indefinitely increased.

Next we will evaluate (12) and the corresponding expressions for j_y and j_z. Obtaining the partial derivatives from (8), (9) and (10) as in the previous case and evaluating the integrals we get

$$j_x = neu\left[1-\frac{1}{1+\gamma^2}-\frac{2}{3}\,\frac{\gamma^2}{(1+\gamma^2)^2}\right], \tag{19}$$

$$j_y = neu\gamma\left[\frac{1}{1+\gamma^2}-\frac{1}{3}\,\frac{1-\gamma^2}{(1+\gamma^2)^2}\right], \tag{20}$$

$$j_z = 0, \tag{21}$$

and denoting by σ the conductivity

$$\sigma = \frac{2}{3}\,\frac{ne^2l}{mv}$$

which would exist in the absence of the magnetic field in this case,

$$\frac{\sigma_x}{\sigma} = \frac{3}{2\gamma}\left[1-\frac{1}{1+\gamma^2}-\frac{2}{3}\,\frac{\gamma^2}{(1+\gamma^2)^2}\right], \tag{22}$$

$$\frac{\sigma_y}{\sigma} = \frac{3}{2}\left[\frac{1}{1+\gamma^2}-\frac{1}{3}\,\frac{1-\gamma^2}{(1+\gamma^2)^2}\right], \tag{23}$$

$$\frac{\sigma_z}{\sigma} = 0. \tag{24}$$

Figure 4 shows how the currents change with increasing mean free path, the fields being kept constant. The current j_y parallel to the electric field rises to a maximum at a value of γ equal to 1.335 and then falls, approaching zero asymptotically. The transverse current j_x increases more slowly at the start, becoming equal to the current parallel to $\boldsymbol{E}$ for a value of γ of 1.427 and then approaching asymptotically the normal current of progression *neu*. Comparison of Figs. 2 and 4 shows how the curves have been ironed out by taking into account the variations in the free paths of the ions. In this connection it must be remembered that the scale of abscissae is different in the two figures.

Finally Fig. 5 shows how the conductivities change with increasing magnetic field for a constant mean free path. The conductivity parallel to the electric field falls steadily with increasing H while the transverse conductivity rises to a maximum at γ equal to 1.468. Both conductivities

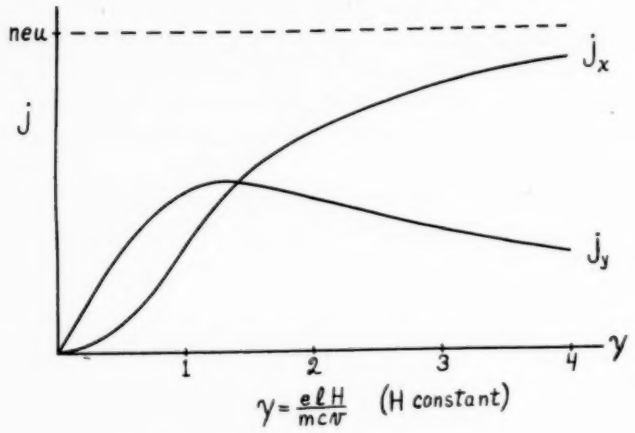

Fig. 4.

approach zero for large magnetic fields. In fact a sufficiently large magnetic field exerts a grip on the ions which makes the electric field impotent to produce appreciable motion in any direction. Again comparison of Figs. 3 and 5 shows the ironing-out effect of variations in the free paths of the ions.

Heretofore we have considered ions of one sign only. If ions of both signs are present, the total current in the direction of the electric field is the *sum*

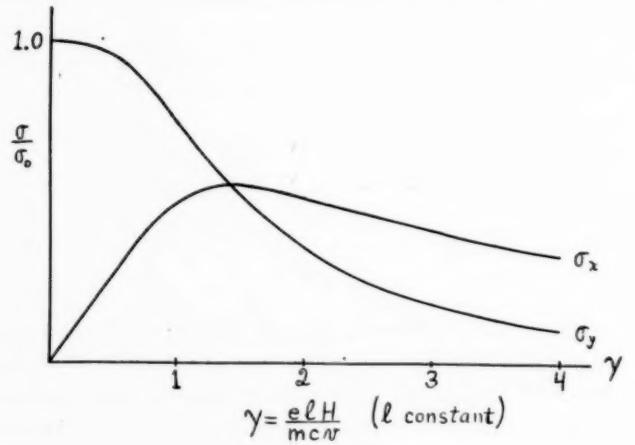

Fig. 5.

of the currents due to the two sets of ions. Ions of both signs, however, progress in the same sense perpendicular to the plane of the field, and therefore the transverse current is the *difference* of the currents due to the two sets. As the quantity denoted by γ may have a different value for the one set from

what it has for the other, either on account of a difference in mass or a difference in mean free path or both, the transverse current need not vanish even when equal numbers of ions of each sign are present, except in the case of infinitely large $\boldsymbol{H}$.

If we put σ_E for the conductivity parallel to $\boldsymbol{E}$—our previous σ_y as given by Eq. (23)—and σ_H for the conductivity at right angles to $\boldsymbol{E}$—the σ_x given by Eq. (22)—we can express the current density in vector form by the equation

$$\boldsymbol{j}=\sigma_E\boldsymbol{E}+\sigma_H\frac{\boldsymbol{H}}{c}\boldsymbol{u}.$$

Therefore, for any orientation of the xy axes in the plane perpendicular to $\boldsymbol{H}$,

$$j_x=\sigma_E E_x+\sigma_H E_y,$$
$$j_y=-\sigma_H E_x+\sigma_E E_y.$$

If, now, the current is entirely in the x direction j_y vanishes and

$$E_y=\frac{\sigma_H}{\sigma_E}E_x,$$
$$j_x=\frac{\sigma_E^2+\sigma_H^2}{\sigma_E}E_x,$$

and the Hall coefficient obtained from the present theory is

$$\pi\equiv\frac{E_y}{Hj_x}=\frac{\sigma_H}{H(\sigma_E^2+\sigma_H^2)}. \tag{25}$$

Putting in the values of the conductivities given by Eqs. (22) and (23) we find

$$\pi=\frac{3}{4nec}\,\frac{1+3\gamma^2}{1+\frac{9}{4}\gamma^2}, \tag{26}$$

indicating that the Hall coefficient increases with the field, approaching for very large magnetic intensities a value 4/3 of its value for zero field.

In contradiction to observation the computed resistance shows a slight decrease with increasing magnetic field, approaching a limiting value 8/9 of its value for zero field as the magnetic intensity is indefinitely increased.

BARKHAUSEN EFFECT IN IRON, NICKEL AND PERMALLOY. I. MEASUREMENT OF DISCONTINUOUS CHANGE IN MAGNETIZATION

By Richard M. Bozorth
Bell Telephone Laboratories, New York

(Received July 24, 1929)

Abstract

These experiments show that the changes in magnetization which take place suddenly in large groups of atoms account quantitatively for the whole change in magnetization which corresponds to the steeper part of the hysteresis loop. Since it is estimated that discontinuities corresponding to groups of 10^{10} atoms (10^{-13} cm^3) or less will not appreciably affect the measuring system, it is concluded that the magnetic moments of only a very small number of atoms are reversed in groups smaller than this. The maximum size of the discontinuities for all materials examined, independent of crystal size, is found to be about the same, corresponding to the complete reversals of the elementary magnets contained in a volume of about 10^{-6} cm^3. The discordance of the results of previous measurements by others is explained as due to the different rates of decay of eddy-currents in the samples used.

Introduction

EXPERIMENTS have shown that the Barkhausen effect is due to discontinuities in magnetization,[1] and that the larger discontinuities correspond to the reversal of as many magnetic elements as are contained in a volume[2] of 10^{-5} or 10^{-6} cm^3. But it has not been known whether the observed discontinuities account for any considerable fraction of the total change in induction, or whether this change can best be accounted for by a very large number of discontinuities most of which correspond to the simultaneous reversals of but a few atoms. It has been proposed[3] that each single crystal reverses its magnetic moment at once, and on this view one would expect that in annealed materials the whole change in induction could be accounted for by discontinuities large enough to observe. The size of the larger discontinuities also suggested to early observers that each crystal in the metal changed its magnetization as a unit. On the other hand, Tyndall[2] found that the size of the discontinuities did not depend on the grain size in silicon steel, and recently Sizoo[4] has come to a similar conclusion for electrolytic iron. The observation has frequently been made that there is a larger effect in hard-worked than annealed materials, from which it might be inferred that the groups are as large, or larger in material with very small crystals than they are in the comparatively coarse grained annealed materials.

[1] H. Barkhausen, Phys. Zeits. **20**, 401–403 (1919); Zeits. Tech. Phys. **5**, 518–519 (1924). B. van der Pol, Proc. Acad. Sci. Amsterdam **23**, 637–643, 980–988 (1920).

[2] B. van der Pol, reference 1; E. P. T. Tyndall, Phys. Rev. **24**, 439–451 (1924).

[3] P. Weiss and G. Ribaud, Journal de physique **3**, 74–80 (1922).

[4] G. J. Sizoo, Physica **9**, 43–50 (1929).

Not only are there these different possibilities as to the average size of the discontinuities, but there is also a great variety of experimental data[5] for the Barkhausen effect observed as the noise in a telephone receiver or the current output from an amplifier, in various materials having different shapes and sizes and permeabilities. The lack of an explanation of these differences in the effect, and the uncertainty as to the average size of the discontinuities, made it desirable to investigate these questions further.

It is the purpose of this paper to describe experiments which show that on the steep part of the hysteresis loop practically the whole change in induction takes place in steps large enough to detect with an amplifier in the usual way, and only a very small part of the change in induction occurs in steps corresponding to the simultaneous action of 10^{10} or fewer atoms.[6] The different estimates of the magnitude of the Barkhausen effect observed as the noise in a telephone receiver, or as the current output from an amplifier, are seen to depend on the different rates of decay of eddy-currents in the materials of different sizes and permeabilities. A following paper[7] will describe the determination of the volume of the material which corresponds to one discontinuous change in magnetization of average size, assuming that this change is from saturation in one direction to saturation in the other.

The Experimental Procedure

Principle of the method. The magnetic material to be examined is placed in a slowly and uniformly changing magnetic field. When a discontinuous change in the induction B occurs, an e.m.f. is created in a coil of wire surrounding the sample. This e.m.f. is proportional to dB/dt, and rises quickly to a maximum and then decreases to zero as illustrated in Fig. 16. The area under the e.m.f.-vs.-time curve is proportional to the change in B which occurred as a single Barkhausen impulse. A great many such single impulses occur during a complete magnetic cycle, perhaps a million per cm^3, and the problem is to integrate the areas under the dB/dt-vs.-time (or e.m.f.-vs.-time) curves. This is done by amplifying the e.m.f.'s, and arranging the amplifier output so that the current measured is the average value, over a period of several seconds, of currents which are at all times proportional to dB/dt. This average current, multiplied by the time, gives the whole change in B which occurs during this time in discontinuities large enough for the apparatus to detect.

Description of apparatus. The apparatus used is shown diagrammatically in Fig. 1. A slowly changing magnetic field is produced in the magnetizing coil M by means of the apparatus shown at the left. Here a condenser C

[5] W. Gerlach, E. T. Z. **42**, 1293 (1921); W. Gerlach and P. Lertes, Zeits. f. Physik **4**, 383–392 (1921), Phys. Zeits. **22**, 568–569 (1921); K. Zschiesche, Zeits. f. Physik **11**, 201–214 (1922); S. Procopiu, Comptes rendus **184**, 1163–1165 (1927); E. P. T. Tyndall and J. M. B. Kellogg, Phys. Rev. **30**, 354–356 (1927); J. Pfaffenberger, Ann. d. Physik **87**, 737–768 (1928).

[6] A preliminary report of this work was given at the New York Meeting of the American Physical Society, February 23, 1929, Phys. Rev. **33**, 636–7 (1929).

[7] A preliminary report was given at the Washington Meeting of the American Physical Society, April 18, 1929, Phys. Rev. **33**, 1071 (1929).

is slowly charged by a small current flowing through a vacuum tube V_1. The potential on the condenser controls the grid bias of another vacuum tube V_2, the space current of which flows in the windings of the coil. A battery and resistance in parallel with the coil permit the strength of the magnetic field to be changed between -10 and $+10$ gauss at a rate proportional to the current charging the condenser C. By shorting this condenser the process may be repeated. The rate of change of field can easily be changed from 0.001 to 10 gauss/sec. by changing a resistance R_1 in the filament circuit of V_1. The magnetizing coil surrounds the sample and the two search coils S_1 and S_2, which are wound on spools 2.5 cm long and 2.5 cm in outside diameter and are connected to the amplifier in series opposition. The amplifier has four stages and is resistance-capacity-coupled with 200,000 ohms and 1 microfarad, and has one-half megohm grid leaks. Its performance was tested up to 10,000 cycles per second at which point its efficiency was found to have decreased but slightly. The output current from the amplifier is passed through a resistance R_2 of about 50,000 ohms, and the constant potential produced in this, when there is a constant voltage on the input, is neutralized by a battery B_1. In series with this battery and resistance are

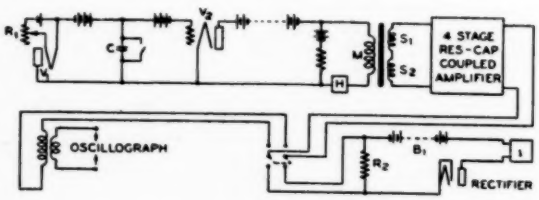

Fig. 1. Diagram of apparatus.

a rectifier[8] and a meter which registers the current. On account of the high resistance R_2 and the characteristics of the rectifier the relation between the input voltage on the amplifier and the current read on the meter is approximately linear. The battery in series with the rectifier is adjusted until the current indicated by the meter is 10 microamperes. When a variable alternating voltage is applied to the first stage of the amplifier the output current is very nearly proportional to the average value of this voltage for currents ranging from 20 to 300 microamperes. The range usually used is from 20 to 200 microamperes.

The whole apparatus is shielded by enclosing it in iron boxes electrically connected together. The first stage vacuum tube of the amplifier and the tube through which the magnetizing current passes are suspended by rubber bands in small lead boxes mounted on springs, to protect them from mechanical vibrations.

Operation. When a sudden change in magnetization, characteristic of the Barkhausen effect, occurs in the sample inside of one of the search coils, the electromotive force which acts on the amplifier is proportional to dB/dt, the rate of change of induction in the sample, which is determined by the

[8] Western Electric Vacuum Tube 244-A with grid connected to plate.

rate of decay of the eddy-currents. For calculating dB/dt for a spontaneous change in magnetization we may use the expression given by Rayleigh[9] or that given by Wwedensky.[10] According to the early calculation of Rayleigh the change in induction takes place in accordance with the equation:

$$B=B_0\left[1-\exp\left(-\frac{1.44\times10^9\rho t}{\pi r^2\mu}\right)\right]$$

where B_0 is the total change in induction, ρ the resistivity in ohm-cm, and μ the permeability, in this case the reversible permeability or permeability for small alternating forces. Wwendensky's calculation indicated that the initial rate of change of induction is infinite but drops rapidly to the value given by Rayleigh, following his equation after $B/B_0=0.1$.

If the apparatus is distortionless the output current i is proportional to dB/dt. If the meter reads i_1, the average of the instantaneous values of i, the total change in induction which takes place discontinuously may be calculated from the equation

$$B'=A_1\int i_1dt,$$

so that by observing i_1 as a function of t, integrating, and multiplying by the appropriate constant A_1, we may determine B' and compare it with B, the total change in induction observed in the ordinary way. Or, more simply, dB'/dH due to Barkhausen changes of induction may be calculated from i_1 and compared with the total dB/dH as ordinarily determined.

Although it has been shown that eddy-currents decay approximately according to the equation of Rayleigh given above, nevertheless it should be emphasized that dB'/dH may be calculated from i_1 quite independently of the validity of that equation.

When a sudden change in induction occurs in the second search coil, surrounding another portion of the sample, an electromotive force is produced in the opposite direction to that produced in the first coil, but the rectifier prevents current so produced from passing through the meter. The purpose of the second coil is two-fold, first to neutralize the effect of any stray alternating magnetic field which penetrates the two shields of 1/4 inch copper and 3/8 inch annealed permalloy surrounding the magnetizing coil; and second to make the mean voltage applied to the amplifier equal to zero so that the charges on the coupling condensers produced by many successive impulses in one direction will not be lost by discharging through the grid leaks. A test was made to ensure that the same sudden change in induction did not affect both search coils. The coils were placed various distances apart and i_1 observed for a certain change in induction for each separation. It was found that i_1 increased as the separation increased until the separation was 4 or 5 cm, after which i_1 became practically constant. Accordingly measurements were made with the coils about 7 cm apart.

[9] Rayleigh, Rep. Brit. Assn. **52**, 446–447 (1882).

[10] B. Wwedensky, Ann. d. Physik **64**, 609–620 (1921).

When the times between successive voltage impulses, caused by successive discontinuities, are short enough the voltage impulses from one search coil will overlap those from the other and the current i_1 will be too small. Consequently, in order to measure the whole discontinuous change in induction the field must be changed very slowly, and in reality it is necessary to make measurements for various speeds and extrapolate to zero speed.

When making measurements the strength of the magnetic field is changed at a convenient rate and the output current i_1 noted for various values of the current through the solenoid as indicated by the meter H. The rate of change of field strength is determined at the same time, using a stop-watch. For most samples in the form of wires 1 mm in diameter and 20 cm long, i_1 is noted each time the field-strength changes by 0.1 gauss. Although the current i_1 fluctuates considerably between readings the average value can usually be determined with considerable accuracy. For any given value of the field strength, dB'/dH is obtained from i_1, dH/dt, and a constant determined by calibrating the apparatus.

Calibration. The apparatus is calibrated by removing the sample and placing coaxially with one of the search coils a long single layer coil through which is passed a small measured sinusoidal current of known frequency. Complete flux linkage between this calibrating coil and one of the search coils, and the absence of flux linkage with the other search coils, were ensured. The current through the calibrating coil produces a calculable mean rate of change of flux in the place occupied later by the sample, and it is assumed that the same rate of change of flux will produce a current i_1 whether that change is produced in a coil containing air or in a sample of ferromagnetic material.

Denoting by A the ratio of the mean rate of change of flux in maxwells per second, to the output current i_1 in microamperes,

$$\frac{d\phi}{dt}=A i_1,$$

and

$$A=0.8\pi 2^{\frac{1}{2}} n f A_c \alpha$$

where f is the frequency of the current, n is the number of turns of wire per cm on the calibrating coil, A_c is its cross-sectional area, and α is the ratio of the r.m.s. current in amperes in the coil to the output current i_1 which flows at the same time. Then

$$\frac{dB'}{dt}=\frac{A i_1}{S}$$

where S is the cross-sectional area of the sample. For the apparatus used, $A=3.40\times 10^{-3}$ maxwells/second/microampere. In the experiments described in this paper $S=0.0081$ cm^2, so that $dB'/dH=0.420\, i_1\, dH/dt$.

A sample calibration curve is shown in Fig. 2.

The Experimental Results

The following materials were examined:

Armco iron, hard drawn.

Armco iron, vacuum annealed 3 hrs. at 1100°C, 1 hr. at 880°C, cooled 300°/hr.

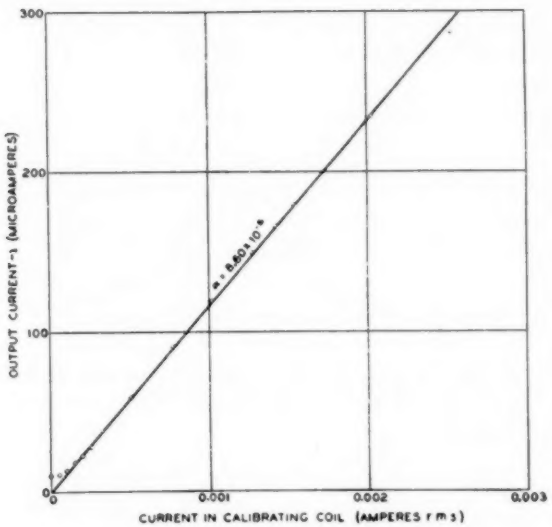

Fig. 2. Typical calibration curve.

Permalloy, 81 percent Ni, hard drawn from 3 mm diameter.

Permalloy, 81 percent Ni, vacuum annealed 3 hrs. at 1100°C, cooled 300°/hr.

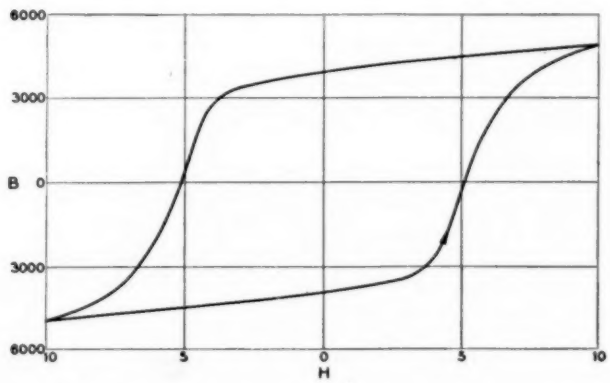

Fig. 3. Hysteresis loop for hard drawn permalloy wire composed of 81 percent Ni and 19 percent Fe.

Permalloy, 50 percent Ni, vacuum annealed 3 hrs. at 1100°C, cooled 300°/hr.

Nickel, vacuum annealed 3 hrs. at 1100°C, cooled 300°/hr.

The specimens in each case were 1 mm in diameter and 20 cm long.

The data for hard permalloy are shown in Figs. 3 and 4. Fig. 3 is the hysteresis loop and Fig. 4(a) indicates the slope of the lower branch of the loop for various values of H. These curves were both taken with a ballistic

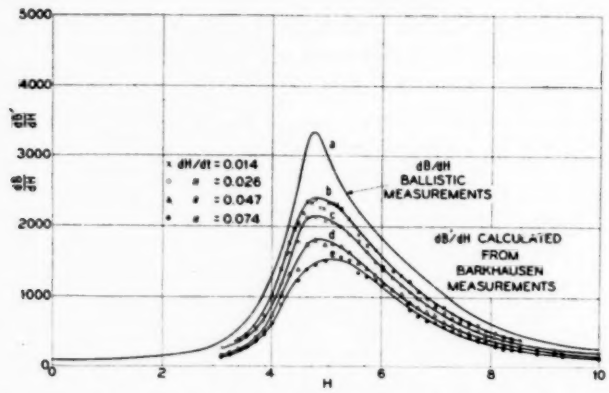

Fig. 4. (a) represents the slope of the lower branch of the hysteresis loop of Fig. 3. The other curves show dB/dH calculated from Barkhausen measurements using different time rates of change of magnetic field.

galvanometer, using the same coils in the same positions as for the measurements of the Barkhausen effect, the only difference being that the leads from one of the coils were reversed so that they were aiding instead of opposing

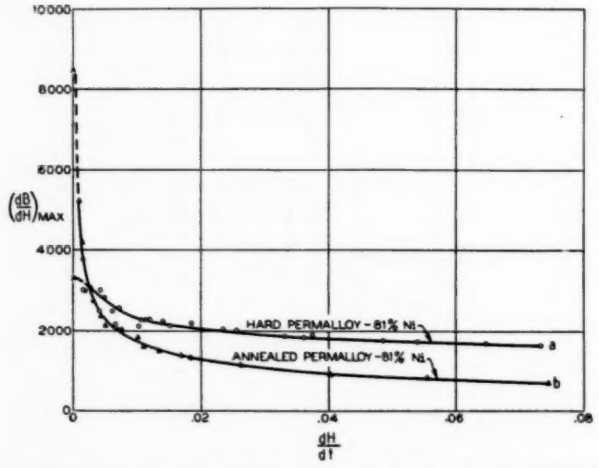

Fig. 5. This shows that when the field-strength is changed more and more slowly the peaks of curves such as (b) to (e) in Fig. 4, approach the peak of curve (a) in Fig. 4. Similar data are shown for annealed permalloy of the same chemical composition.

each other. Curves (b), (c), (d) and (e) represent for various values of H the values of dB'/dH calculated as described above from the output current i_1. These four curves are taken with various rates of change of field-strength as shown in the figure, and do not coincide because there are differ-

ent amounts of overlapping of the impulse in the two coils, as already described under "Operation." But even when the overlapping is considerable, over half of the total change in flux is accounted for by the measured discontinuities. The largest values of dB'/dH for various values of dH/dt, are plotted [11] in Fig. 5(a) against the appropriate value of dH/dt, and the curve connecting them is drawn to the point for $dH/dt=0$, corresponding to the maximum of curve (a) of Fig. 4, determined with a ballistic galvanometer. The course of this curve is in entire agreement with the idea that the whole change in magnetization is discontinuous, and that the increased overlapping of the impulses accounts for the lowering of the curve as dH/dt increases as shown in Fig. 4.

The data for annealed permalloy containing 81 percent Ni are shown in Figs. 6 and 7. As before, Fig. 6 is the hysteresis loop and the upper curve

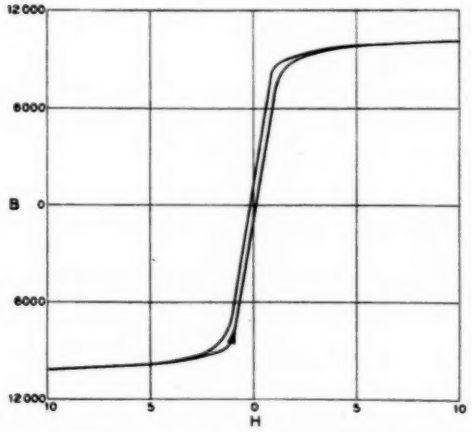

Fig. 6. Hysteresis loop for a sample of annealed permalloy (81 percent Ni, and 19 percent Fe) 1 mm in diameter and 20 cm long.

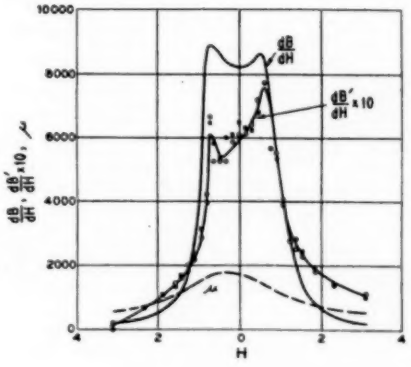

Fig. 7. Barkhausen data for annealed permalloy, the hysteresis loop for which is shown in Fig. 6, $dH/dt=0.047$ gauss/sec.

in Fig. 7 represents the total dB/dH as determined with a ballistic galvanometer, and the next lower curve dB'/dH calculated from the current i_1 produced by the Barkhausen discontinuities. The relatively flat top of the upper curve is a result of the demagnetizing effect of the induced poles at the ends of the specimen. For this material only a small fraction of the total dB/dH is recorded by the apparatus, but it must be remembered that the overlapping will be much greater here than in hard permalloy. The reason for this is the slower decay of eddy-currents due to the greater reversible permeability, which is about 2000 in annealed permalloy as compared with 80 in hard permalloy. The maximum values of the calculated dB'/dH, for different rates of change in field-strength, are shown in Fig. 5(b).

[11] For this series of measurements the calibration was made so that the output current was 4 microamperes when the current in the calibrating coil was zero, instead of 10 microamperes as shown in Fig. 2.

The dB'/dH curve in Fig. 7 differs from the total dB/dH curve in shape as well as height. This seems to be due to two causes: the center of gravity of the permeability curve, shown as a dotted line in the figure, is displaced towards lower (or more negative) fields with respect to that of the total dB/dH curve, causing an increase in the calculated dB'/dH towards the right because of less overlapping due to smaller permeabilities; and an increase in the average size of the discontinuities for higher fields, resulting also in increased calculated dB'/dH for higher fields because of less overlapping. For example, if the average size of the discontinuities is twice as great in one case as in another, the current for one impulse of the first average size will be twice as great as for the second for corresponding parts of the

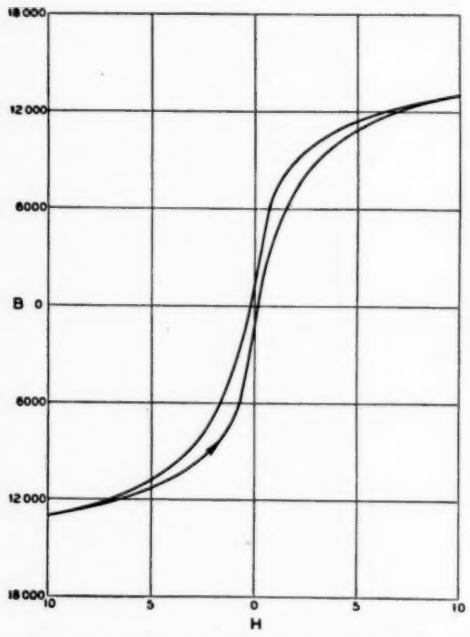

Fig. 8. Hysteresis loop for annealed permalloy containing 50 percent Ni and 50 percent Fe.

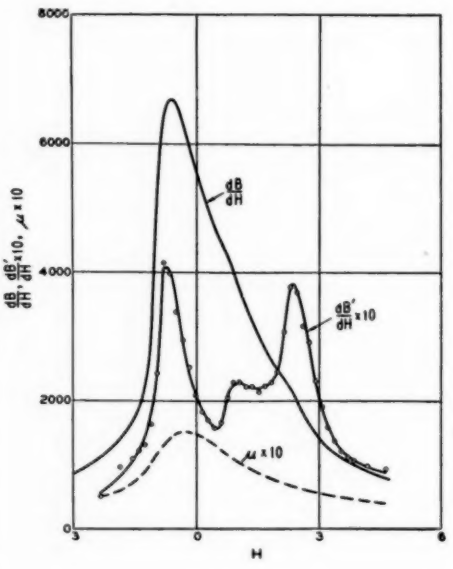

Fig. 9. Barkhausen data for permalloy containing 50 percent Ni and 50 percent Fe, $dH/dt = 0.046$ gauss/sec.

impulse, but the time constant for the two cases will be the same. The chance of overlapping of two impulses in opposite directions will be one-fourth as great in the first case as the second because the total number of impulses of each kind is one-half as great, but for each time that overlapping occurs the amount of overlapping will be twice as great. On the average, then, the loss by overlapping will be less for the larger impulses and the ratio of calculated dB'/dH to total dB/dH will be greater. Other experiments show that the largest discontinuities for 81 permalloy also occur where the calculated dB'/dH is a maximum.

Data for annealed permalloy containing 50 percent Ni are shown in Figs. 8 and 9. As shown in the latter figure the maximum of the μ-*vs*-H curve

is displaced with respect to the maximum of the ballistic dB/dH-*vs*-H curve in the direction opposite to that for 81 Ni permalloy. This helps to explain

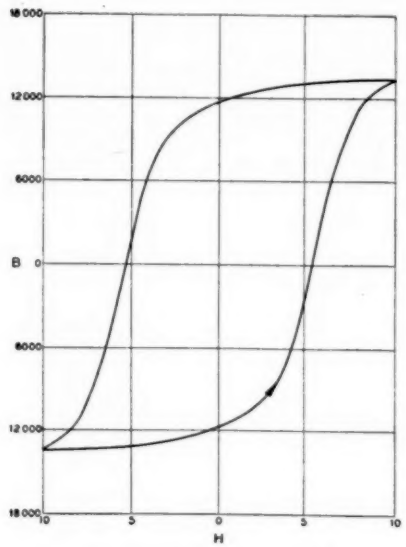

Fig. 10. Hysteresis loop for hard drawn iron wire.

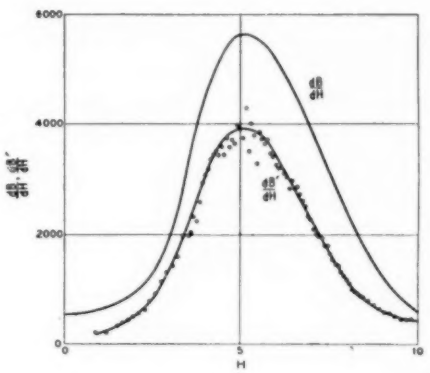

Fig. 11. Barkhausen data for hard drawn iron wire, $dH/dt=0.011$ gauss/sec.

the greater relative prominence of the peak in dB'/dH at $H=2.6$ gauss. A more direct influence, however, seems to be the different average size of

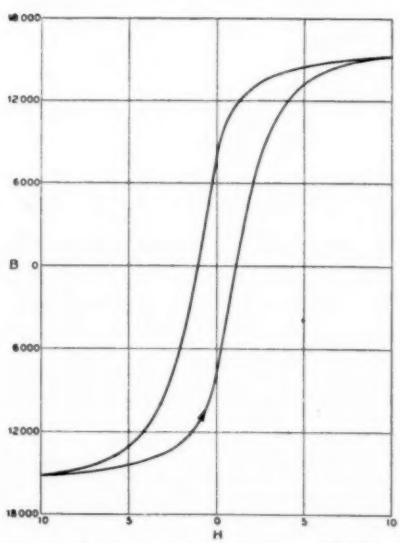

Fig. 12. Hysteresis loop for annealed iron.

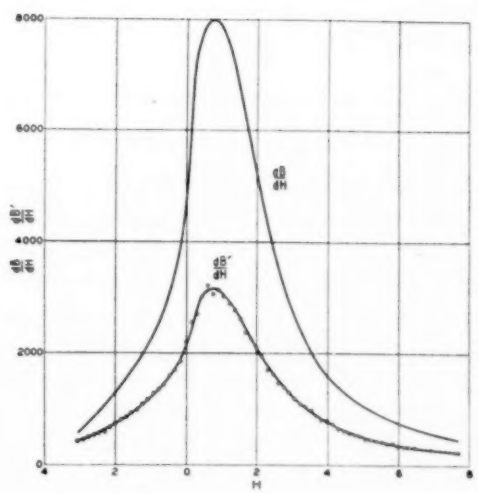

Fig. 13. Barkhausen data for annealed iron, $dH/dt=0.032$ gauss/sec.

the discontinuities at the two peaks. Experiments to be reported later show that the average size for this specimen is a maximum at about 2.6 gauss,

corresponding to the last maximum of dB'/dH shown in Fig. 9. The two maxima in the dB'/dH curve as well as the constricted "wasp-waisted" hysteresis loop of Fig. 8 suggest an inhomogeneous[12] magnetic structure, and suggest also the possibility of learning more about the nature of such inhomogeneities by measurements of the Barkhausen effect.

Data for hard and annealed Fe and for annealed Ni are shown in Figs. 10 to 15. For hard Ni the fields available were not as great as the coercive force, so quantitative measurements were not made.

To illustrate the decay of eddy-currents in hard and annealed permalloy, and the effect of overlapping of impulses produced in the two search coils, oscillograph records were made, as shown in Fig. 16. The output of the amplifier was passed through the primary of a transformer, the secondary of which was connected to a Westinghouse oscillograph, type N. The upper trace is for a 2 mm wire of well annealed permalloy containing 78 percent Ni. Here the decay of eddy-currents is relatively slow on account of the large

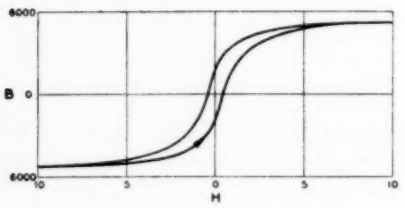

Fig. 14. Hysteresis loop for annealed nickel.

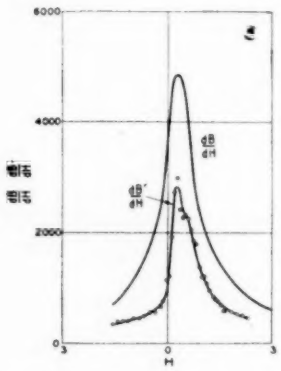

Fig. 15. Barkhausen data for annealed nickel, $dH/dt = 0.012$ gauss/sec.

diameter and high permeability. This should be contrasted with the middle trace which shows the effect in hard-drawn permalloy 1 mm in diameter. In the latter case the decay is so rapid that the oscillograph does not record properly the form of the curve; nevertheless, the area under the curve is a true measure of the size of the discontinuity in magnetization, and can be compared with the area under the impulses in the upper trace. The volumes of material corresponding to the separate impulses have been calculated in a few cases for these specimens and also for other materials in both the hard drawn and annealed conditions, and found to be about 10^{-6} cm^3 for the larger impulses in all cases. This volume is about the same as that observed by Tyndall for silicon steel. The rate of decay of eddy-currents as determined from the upper trace and the 1000 cycle timing wave given in the lower trace, may be compared with the rate calculated from Wwedensky's

[12] E. Gumlich, Arch. f. Electrot. **9**, 153–166 (1920); G. Elmen, J. Franklin Inst. **206**, 317–338 (1928).

formula given above. The calculated time constant for this sample is 0.0015 sec., and agrees tolerably well with that estimated from the oscillographic record.

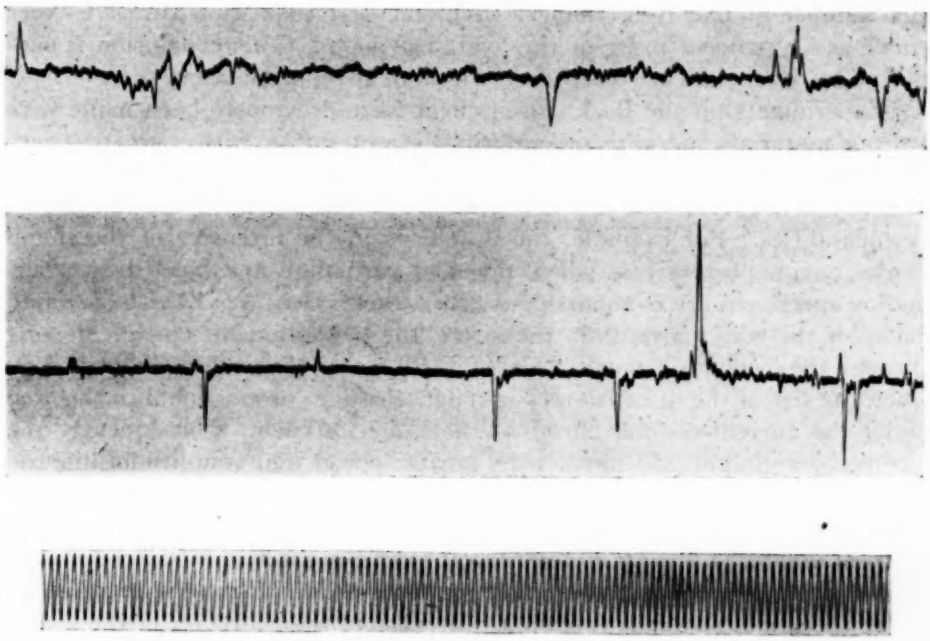

Fig. 16. Retouched oscillographic records of Barkhausen effect. Upper trace, record for sample 2 mm in diameter containing 78 percent Ni and 22 percent Fe. Middle trace, record for sample 1 mm in diameter containing 81 percent Ni and 19 percent Fe. Lower trace, timing line of frequency 1000 cycles per second.

Discussion of the Results

These experiments show that the whole change in magnetization on the steeper parts of the hysteresis loops of hard worked samples of iron and permalloy is accounted for by the magnetic discontinuities detected and measured by the apparatus. The larger discontinuities correspond to the complete reversal of magnetization of about 10^{17} atoms, or a volume of 10^{-6} cm^3. Since it is estimated that discontinuities corresponding to groups of 10^{10} atoms will not appreciably affect the measuring system, it is concluded that a very small proportion of the discontinuities correspond to groups containing less than this number of atoms. In other words, the Barkhausen discontinuities which account for practically the whole change in magnetization are due to the simultaneous action of a great many atoms and the magnetization of only a relatively small number of atoms is reversed in groups of less than 10^{10}. This conclusion applies, of course, only to changes in magnetization on the steeper parts of the hysteresis loop. Although for annealed permalloy the rate of change of magnetization calculated from

Barkhausen measurements is never more than about two-thirds of the total rate of change, this would be expected because the reversible permeability of the material is very high and the loss due to overlapping is correspondingly great. The most reasonable conclusion is that in all of the materials examined the number of magnetic changes involving less than 10^{10} atoms is very small on the steeper parts of the hysteresis loops. This conclusion is supported by other evidence of a different kind to be reported later.

Experiments on the Barkhausen effect have previously been made with various materials and with several kinds of apparatus, with a great variety of results. These results can now be explained as due to the different rates of decay of eddy-currents in these materials of different sizes and shapes and permeabilities. For example, the difference in the intensity of the sound in the telephone receivers when annealed permalloy and hard drawn permalloy specimens are compared, is very marked. Because of the more rapid decay of the eddy-currents in the latter, the instantaneous current flowing through the receivers is much greater for this material than for soft permalloy when the size of the discontinuity in magnetization, proportional to the area under the current-*vs*-time curve, is the same for each. Consequently the receiver diaphragm will move with greater speed and amplitude and the noise will be many times greater for hard worked permalloy with a reversible permeability of 80 than for annealed permalloy with a reversible permeability of 2000. This great difference cannot be attributed to different sizes of discontinuities because the larger impulses on oscillographic records are about the same for each. A similar difference in the character of the sound is observed for thick and thin wires of the same material having similar hysteresis loops. In the experiment using fine wires a sharp crackling sound is observed in contrast to a rustling sound observed using thicker wires. This is because the decay of eddy-currents is more rapid in the fine wires and the output current from the amplifier is correspondingly greater and fluctuates more rapidly.

The general parallelism between the Barkhausen effect and hysteresis[13] is apparently due to the character of the eddy-current decay, for when the hysteresis is low the reversible permeability is generally high and the Barkhausen effect as measured by ear is consequently low.

I take pleasure in acknowledging the benefit I have derived from technical discussions with Dr. O. E. Buckley, and from the assistance of Mr. Joy F. Dillinger with the apparatus.

[13] W. Gerlach and P. Lertes, and K. Zschiesche, reference 5.

TOTAL RADIATION FROM NICKEL AND COBALT

By C. L. Utterback
University of Washington, Seattle

(Received July 19, 1929)

Abstract

Measurements have been made on the total radiation from nickel between 630°K and 1600°K and from cobalt between 672°K and 1590°K. The radiation was measured by means of a platinum-tellurium thermocouple and a high sensitivity galvanometer. A constant deflection method was used. The temperature of the metal was measured by means of a Holborn-Kurlbaum type of optical pyrometer, calibrated at the gold and palladium points, and by means of a platinum platinum-rhodium thermocouple. A comparison of the radiation with other properties of the metals is given.

IN A study of the total radiation of metals, Suydam[1] found that the radiation from nickel could be fairly well represented, between 463°K and 1283°K, by an equation of the Stefan-Boltzmann form, and that the exponent of T in

$$E=cT^n \tag{1}$$

has a constant value.

Kahanowicz[2] determined that, between 273°K and 903°K, the same form of equation could be used for nickel but the value of the exponent was very different from that found by Suydam.

In the present work observations have been made on the radiation from nickel, extending the temperature nearer the melting point. Observations have been made on the radiation from cobalt.

The method employed in this experiment consisted in allowing the radiation from the metal to fall on the thermocouple and, by means of a rotating sector, comparing the energies at the different temperatures.

The metallic radiators were in the form of a V-shaped wedge as described by Mendenhall.[3] The characteristic radiation of the metal was taken from the outer surface of the wedge. Two methods were used to determine the temperature of the radiators. A platinum platinum-rhodium thermocouple, as described by Spence,[4] was used for temperatures extending from 630°K to the gold point. Temperatures extending from 1200°K to 1600°K were measured by means of an optical pyrometer. This gave a range of 135°, from 1200°K to 1335°K, for which the temperatures were measured with both the pyrometer and the thermocouple.

[1] V. A. Suydam, Phys. Rev. **5**, 497 (1915).
[2] M. Kahanowicz, Accad. Lincei. Atti. **30**, 132 (1921).
[3] C. E. Mendenhall, Astrophys. J. **33**, 91 (1915).
[4] B. J. Spence, Astrophys. J. **37**, 194 (1913).

A water-jacketed brass base, *U*, about 20 cm in diameter and 4 cm deep was mounted as shown. A water-jacketed cylinder, *A*, contains a platinum tellurium thermocouple, *T*. The blackened receiver of the couple is at the center of curvature of a hemispherical silver mirror, B. The mirror is to better the black body conditions of the receiver. *A* is connected by means of a curved brass tube to a fixed diaphragm, *E*, the latter being mounted by means of the brass tube, *F*, extending through the bottom of the base. A movable diaphragm, *H*, also water cooled, was mounted directly in front of the fixed diaphragm.

The V-shaped metal strip, *L*, was about 4.5 cm long 1 cm wide and 0.0025 cm thick and has an opening of about 8 degrees. This strip was mounted in such a manner that the expansion of the strip, when heated, could be taken up from the outside of the apparatus. The supports for the

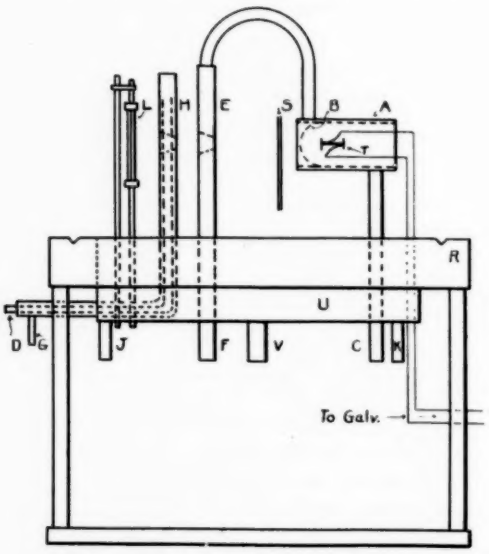

Fig. 1. A diagram of the apparatus.

filament were insulated from the base and served also as conductors for the current used to heat the filament. Storage cells were used for the heating current.

A rotating sector, *S*, having two known apertures, was mounted on the shaft of a small motor. The motor was mounted on a rod which extended through a packed joint to the outside of the tank. By this means the sector could be placed in such a position that the full beam of radiation through the diaphragms could fall on the thermocouple or, so that this radiation was reduced by passing through either of the apertures of the sector. The motor operating the sector was driven by two dry cells placed outside the base.

The base was provided with a solid brass ring, *R*, 3 cm square, in which was cut an annular V-shaped groove. A brass cover was provided which had a similar ring so cut that when the cover was in position the two grooves

were in exact register. A solid ring of solder was placed in the lower groove, the cover placed in position, and the solder squeezed into the grooves by means of 0.5″ cap screws which were threaded into the base.

The vessel was evacuated through the tube V by means of a mercury vapor pump which was backed by a Cenco oil pump. The working pressure, as measured by a McLeod gauge, was never more than 3×10^{-5} mm of mercury and frequently during the observations lower pressures were obtained.

The cover of the tank was provided with a side tube having a glass window through which optical pyrometer measurements of the temperature were taken.

Method of Making Observations

The wedge of the metal to be studied was mounted in the supports. The thermocouple was connected to a Leeds and Northrup galvanometer which had a sensitivity of 482 megohms and a resistance of 20 ohms.

After the apparatus had reached equilibrium, which required from two to four hours, the metal strip was heated to some desired temperature. The full beam of radiation was allowed to fall on the thermocouple and the deflection of the galvanometer was adjusted to some convenient value, usually around 20 to 30 cm.

The receiver of the couple was exposed to the beam of radiation for one minute, then the beam was cut off for one minute by means of the movable diaphragm, thus enabling a correction for any slight shift in the zero position of the galvanometer during an exposure. After recording the deflection and the temperature, the rotating sector was moved into such a position that the beam of radiation from the metal passed through the first aperture of the sector, thus reducing the energy falling on the receiver of the couple by a known fraction of its original value. The temperature of the filament was then raised until the galvanometer showed the *same deflection* as before. Then the second, (smaller), aperture of the sector was moved into the beam of radiation and the temperature again raised until the galvanometer gave the *same deflection* as before. A sector having but two apertures could be used. To proceed to higher temperatures, the last observed temperature of the filament was kept constant, the sector moved out of the beam of radiation, and the deflection of the galvanometer was adjusted to nearly its original value. No attempt was made exactly to reproduce the last deflection although in some cases it was possible to do so. This adjustment of the deflection was accomplished by means of several resistances placed in parallel and in series with the galvanometer coil. The temperature of the filament was again raised by two steps, keeping the deflection of the galvanometer *constant* by means of the rotating sector as before. These operations were repeated as many times as necessary to cover the temperature range being studied. A great many such sets of observations were made both for nickel and for cobalt. The initial, or starting, temperature was selected in many instances so that the data from one set of observations would overlap the

data of other sets of observations. A typical set of observations is shown in Table I.

TABLE I. *A set of observations for cobalt in the temperature range for which the optical pyrometer was used.*

Pyrometer current	Temp (°K)	Deflection	Sector H_1
0.2688		31.24	Full aperture
0.2689		31.24	
0.2688	1208	31.26	
0.2853		31.24	Second aperture
0.2853		31.24	
0.2855	1278	31.23	
0.3021		31.22	Third aperture
0.3023		31.25	
0.3019	1338	31.23	
0.3020		30.15	Full aperture
0.3022	1338	30.17	
0.3281		30.16	Second aperture
0.3282		30.15	
0.3281	1424	30.15	
0.3525		30.14	Third aperture
0.3522		30.15	
0.3522	1495	30.15	

Two sectors were used. H_1 had apertures of 215° 41′ 20″ and 269° 51′ 40″. Sector A_1 had apertures of 52° 07′ 40″ and 34° 09′ 00″. These apertures were measured on a Societe Genevoise spectrometer which read to ten seconds of arc. In order further to investigate the possibility of having introduced some cumulative error in the process of building up the temperatures, another sector, H_2, having apertures of 80° 40′ 10″ and 81° 33′ 00″ was used. These apertures were calculated so that the following relations held,

$$(2\pi/{}^1H_1)^2 < 2\pi/{}^1H_2$$

and

$$2\pi/{}^2H_2 < (2\pi/{}^1H_1)^2$$

where ${}^1H_1$ refers to the first aperture of sector H_1, etc. That no error was found is evidenced by the fact that the points determined by the use of sector H_2 fell exactly on the energy-temperature curve obtained with the other sectors. From the known apertures of the sectors the energy corresponding to each temperature was computed. The logarithm of the energy is plotted in Fig. 2 against the logarithm of the corresponding temperature.

The curve for nickel is a straight line from 653°K to about 1400°K. Over this temperature range n in Eq. (1) is found to be 5.29. From 1450°K to 1600°K the curve is also a straght line but of different slope. The value of n for this range is 4.75. From around 1400°K to 1450°K the value of n changes rapidly from 5.29 to 4.75. Similar results obtain with cobalt. The value of n, for cobalt, is constant from 672°K to about 1320°K and equal

to 5.20. From this latter temperature to around 1380°K n is not constant but decreases in value to 4.62. Above 1380°K the value of n remains constant and equal to 4.62 up to 1590°K. The following equations express the relation between energy and temperature:

For nickel $E = C_1 T^{5.29}$ for all values of T from 650 to 1400°K
$E = C_2 T^{4.75}$ for all values of T from 1450 to 1600°K
For cobalt $E = C_3 T^{5.20}$ for values of T from 672 to 1320°K
$E = C_4 T^{4.62}$ for values of T from 1380 to 1590°K

The results of these experiments are not in agreement with those of Suydam[1] or Kahanowicz.[2] The first of these experimenters finds an average value of n for nickel, between 463°K and 1283°K, to be 4.648 with the individual values varying from 4.6 to 4.7. It is stated that an equation of the form of Eq. (1) does not hold very well for nickel over the range studied. In Suydam's experiments the radiation was not directly measured but was

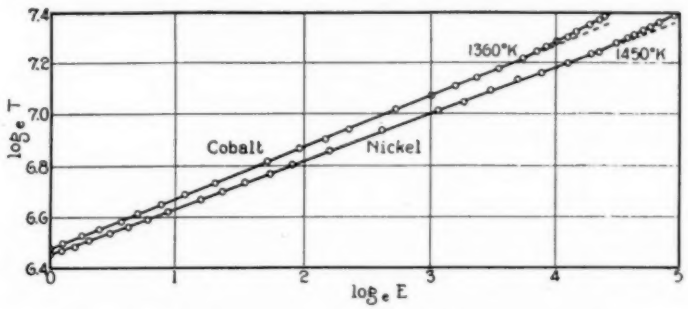

Fig. 2. Logarithmic plot of energy against temperature.

computed from the energy put into the sample. This, in comparison with the method of the present experiments, is not so direct and might easily lead to differences in results.

Kahanowicz also finds that an equation of the form of Eq. (1) will hold for nickel between 273°K and 905°K and that the average value of n for that region is 5.5. The writer's value of n over the lower temperature range is in fair agreement with this, while for temperatures nearer the melting point it is more nearly in agreement with the value found by Suydam.

So far as the writer knows, no observations have been made on cobalt.

The internal structure is one of the factors affecting the radiation and as this varies with the temperature, especially so at the Curie point, it is not to be expected that the emission from these metals can be simply expressed. At the Curie point for cobalt, 1348°K, a rapid change in the emission is indicated by the curve in Fig. 2. It is known that at this temperature, the susceptibility, the permeability, the resistance, and thermal expansion undergo rapid changes and it is to be expected that the specific heat, at this point, behaves in a similar manner. The fact that a sudden decrease in the specific heat may be expected at this temperature is a direct consequence of the Langevin-Weiss theory of magnetism.

There is no known transition point for nickel in the region of rapid variation of n, that is, around 1400°K. However some internal change may occur here. The possibility that such might be the case is indicated, not only by the present data, but also by measurements of other experimenters.

Terry[5] finds that around 1430°K susceptibility measurements show a change in the β form of nickel. His results are in general agreement with those of Foëx[6] and of Weiss and Foëx[7] who also find a change in the β form of nickel.

The fact that n is found to have a smaller value for the higher temperatures is in general agreement with the work of Hagen and Rubens.[8] These authors arrive at the result that the radiation from metals, with increasing temperature, approaches black-body radiation.

The above results are in agreement with that of Aschkinass[9] who, in a treatment of the radiation of metals, shows that the radiation approaches that of a perfect radiator as the temperature rises.

Hase,[10] in some not very precise measurements, finds that the radiation from iron, up to 1200°C approaches black body radiation with rising temperature.

Jones[11] has computed the rate of emission of energy from tungsten for various temperatures. His results show an approach toward black-body radiation as the temperature nears the melting point.

It is proposed to make a further study of the properties of nickel in the region of temperature where the radiation is changing.

The greater part of this work was done at the University of Wisconsin. This opportunity is taken to express my appreciation to Professor C. E. Mendenhall for his helpful suggestions and for his interest in the work.

[5] E. M. Terry, Phys. Rev. **9**, 394 (1917).
[6] Foëx, Ann. d. Physik **16**, 174 (1921).
[7] Weiss and Foëx, Arc. Des Sc. Phys. et Nat. **31**, 89 (1911).
[8] Hagen and Rubens, Ann. d. Physik **11**, 873 (1903).
[9] E. Aschkinass, Ann. d. Physik **17**, 960 (1905).
[10] Hase, Zeits. f. Physik **15**, 54 (1923).
[11] H. A. Jones, Phys. Rev. **28**, 206 (1926).

THE INFLUENCE OF SURFACE CONDITIONS AND SPACE CHARGES ON THE CONDUCTIVITY OF POOR CONDUCTORS

By K. F. Herzfeld
Physics Department, The Johns Hopkins University

(Received May 31, 1929)

Surface conditions.—To keep a substance non-conducting it is necessary not only that it does not itself generate carriers of electricity, but that these are prevented from entering if good conductors are brought into contact with it. Vacuum and crystals are insulators because the electrons from metal electrodes cannot leave the metal on account of the work function. Water has electrolytic, not electronic conductivity, because ions can be discharged at the electrodes, while electrons cannot permeate the surface directly.

Space charge.—The possible types of space charge in a medium containing ions of constant and equal mobility are discussed. It is pointed out that for the potentials which are of interest diffusion plays a role only in the immediate neighborhood of the electrode, and space charge is entirely due to insufficient recombination. Methods of determining the data of interest from space charge curves are given. The number of ions present is always below the equilibrium number.

1. The Nature of Poor Conductors

A GOOD conductor is a substance which contains a sufficient number of electric carriers (electrons or ions) having a sufficient mobility. What groups of substances satisfy these conditions will ultimately be answered only by the new quantum theory, but a qualitative answer is well known at present in that electronic conductors are, in the main, metals and a number of salts, while ionic conductors are other salts in the solid state and a number of solutions in which dissociation occurs. The physical conditions under which dissociation occurs have been treated extensively, and shall not be taken up here. But it is not quite sufficient that carriers are generated in the substance, the substance must also be able to keep them. In the case of a metal, this is due to an attraction between the ionic lattice and the electron. The energy of this attraction has recently been estimated by Bethe[1] and found to be of the order of magnitude of 15 volts. (We are going to measure energy in the familiar manner in volts). This energy is sufficient to keep the electrons in the metal in spite of a large internal pressure, which is, according to Sommerfeld,[2] due to their highly degenerated state. The resultant of the two, the work function, is still of the order of magnitude of about 5 volts, and accordingly is sufficient to make the equilibrium concentration of the electrons outside negligibly small at normal temperatures, as each volt difference decreases the equilibrium concentration by a factor $e^{-Ve/kT}=10^{-18}$. Therefore, if we put two metal plates opposite each other,

[1] H. Bethe, Ann. d. Physik **87**, 55 (1928).
[2] A. Sommerfeld, Zeits. f. Physik **47**, 1, (1928).

the vacuum between them is an insulator because the work function prevents electrons from passing in sufficient number through it. In the same manner a solution of sodium chloride is a conductor because the ions are prevented from evaporating by the heat of hydration which according to Fajans[3] is about 70 k-cal., or about 3 volts. It is an interesting problem, which has not yet been solved, to determine why the condition which makes for the generation of carriers makes, at the same time, for a sufficient energy to keep them in the substance.

If now we put a substance which we call an insulator between two metallic plates it is not sufficient that the substance does not contain carriers, but it is necessary in addition that no carriers from the electrodes can pass through. Let us first consider electrons and take as insulator a salt such as sodium chloride. The experiments of Gudden and Pohl[4] have shown that if electrons are generated by light in the salt they can move freely so that the mobility of electrons would be sufficient.

Next, the conditions at the surface, that is the potential distribution, have to be examined. When the electrons get to the boundary of the crystal plate, they are able to enter the metal without a prohibitive resistance. This means that the potential energy inside the crystal is not less than the potential

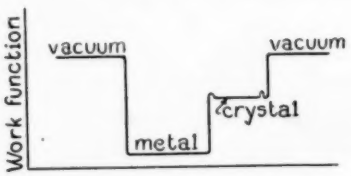

Fig. 1. Work function for different surfaces.

energy (plus internal pressure) of the electrons in the metal. Furthermore, it seems that they cannot enter the metal quite freely,[5] but only if either a sufficient electron concentration or a sufficiently high field has been reached at the surface of contact. The same seems to be true for the discharge of calcium ions if we electrolize solid calcium carbonate.[6] From this it would follow that there is a small hump of energy between the interior of the crystal and the metal. As the results of thermionic emission do not seem to indicate that on the side of the metal there is a hump preventing the free entrance of electrons,[7] it is probable that this hump lies on the surface of the crystal. The same conclusion can be reached from the fact that the elementary experience shows that it is possible to charge the surface of the crystal without making this crystal conducting. This means that a small hump of potential energy prevents electrons on the surface from penetrating

[3] K. Fajans, f. e., Ber. d. D. Phys. Ges. **20**, 712 (1918).

[4] B. Gudden and W. Pohl, many papers in Zeits. f. Physik. See B. Gudden, Hand. d. Physik **13**, 103, Berlin (1928).

[5] B. Gudden, Forschr. d. Ex. Naturwis. **3**, 150, Berlin (1924).

[6] A. Joffe, The Physics of Crystals, New York, 1928.

[7] L. Nordheim, Zeits. f. Physik **46**, 833 (1927).

into the space of lower potential energy inside. But this hump cannot be very large as moderate fields can overcome it as mentioned before.

The fact that electrons do not pass straight through from one metal into the salt and then out again must, therefore, be due to a high resistance to the entrance of electrons from the metal into the crystal. [It can easily be shown that this entrance is not prevented sufficiently by a space charge which would be set up in the crystal. (See Mathematical Appendix I)]. This means that the potential energy of an electron in the crystal must be considerably higher (its work function lower) than the work function of the metal. Unfortunately there is no way at present to know accurately the amount of work necessary. Joffe[8] has tried to estimate the work function of the crystal, and found it to be 3.9 volts which then would make the difference about 1 volt.

Coehn[9] has experimented with contacts between metals and dielectrics. He finds that metals in contact with diamond are always charged positively, which he explains by the assumption that a few electrons enter the diamond. With other dielectrics metals giving off electrons easily are charged positively, nobler metals negatively, which result Coehn explains by an over-compensation of the electron effect through positive ions. It seems quite possible that the very few electrons sufficient to give a measurable charge can be in equilibrium even at room temperature with the metal in presence of a work-function-difference of 1 volt (corresponding to the state at 1500° for 5 volts), but, on the other hand, the apparently rather high potential measured by Coehn makes such an explanation doubtful. Besides, the surfaces with which he experiments are moved against each other.

In a similar manner we can discuss the question why, if we put two metallic electrodes in water and apply to them a potential difference, the current is entirely carried by ions (which fact guarantees the fulfillment of Faraday's law) instead of being carried by electrons which move simply out of the cathode. These would then probably be attached to a water molecule forming a negative ion H_2O^- which would move with the same speed that ions normally have and then be discharged on the anode. The reason that this does not happen must then be that the work (here we always assume the effects of the internal pressure of the electrons in the metal to be already subtracted) for bringing the electrons from the metal into the water is too high. The work function of the metal being about 5 volts, we can divide the amount of energy to be gained by immersion of the electron into the water into two parts: First, the work gained by attaching an electron to a gaseous water molecule (the electron affinity of water vapor: nothing is known about it except that it is very probably positive). Second we gain the heat of hydration by bringing this negative molecule ion into the liquid water. If we assume this

[8] A. Joffe, The Physics of Crystals, p. 142, New York (1928); P. Tartakovsky, Jour. Russ. Phys. Chem. Soc. (1926).

[9] A. Coehn and A. Lotz, Zeits. f. Physik **5**, 242 (1921); A. Coehn and A. Curs, Zeits. f. Physik **29**, 186 (1924); A. Coehn, Fortschr. Ex. Naturwiss. **1**, 174 Berlin (1922).

to be of the same order of magnitude as for Cl^- it will correspond to about 3 volts.

We have then finally to inquire[10] how ions are discharged on the surface of the electrode (we restrict ourselves to ions different from the metal ions of the electrode itself). Assume that we have a positive ion of an electron affinity higher than the metal itself. The following will be a simplified picture of the surface of the cathode: The interior of the metal with a certain potential energy (minus effect of internal pressure); on the surface a rapid rise of potential energy corresponding roughly to the work function; at a distance of about atomic dimensions a layer of positive ions in the liquid in which the potential energy is lower even than in the metal; in the sheet between the surface of the metal and the center of the ions, a strong field

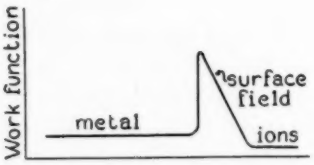

Fig. 2. Work function near an electrode with a layer of positive ions.

simplified as being linear, and of the order of magnitude of the ratio of the electron affinity of ions to atomic dimensions. The new quantum mechanics[11] has shown that it is possible for electrons to pass through this rather high energy hump (of about 5 volts)provided that it is sufficiently thin,[12] in other words, that the field is sufficiently high. The ease of transition is very sensitive to the field, just in the range which appears reasonable for the magnitude of this field, It can than easily be understood that the discharge will go smoothly for small ions or for media where the hump is small, while in less fortunate cases it might be possible to raise the field artificially either by an accumulation of ions or by an outside field of sufficient strength.

In the case of negative ions, where the transition occurs from the ion to the electron the qualitative statement is quite similar.

2. Space Charges in Liquid or Solid Insulators

The general equations for the distribution of charges in an electric field as determined by this field, diffusion and the normal processes of generation and recombination of these ions can easily be stated but their exact integration in the general case has been impossible. According to the circumstances, different assumptions for the purpose of simplification have to be made. Many of them have already been applied to gas discharges and we can simply take over the result. We start with a systematic discussion.

[10] K. F. Herzfeld, to appear shortly in Zeits. f. Phys. Chem. Abt. B.

[11] R. H. Fowler and L. Nordheim, Proc. Roy. Soc. **A119**, 173 (1928).

[12] Physically this comes about as a result of the fact that electrons behave like waves. A wave can pass through a plate to some extent however high its absorption coefficient, provided the plate is thin enough.

A. The velocity of the carriers is mainly determined by the field. This case applies to discharges in highly rarefied gases with long free paths. It has been worked out especially by Child, Langmuir and Schottky,[13] and gives the familiar results for vacuum tubes, but does not apply to liquids or solids where the friction is large.

B. Due to frictional effects, the main velocity of the ions is the thermal velocity, only slightly modified by the electric field. In this case, as has been shown by Townsend,[14] the ratio between the diffusion coefficient D and the electric mobility K is given by

$$\frac{K}{D}=\frac{e^2\epsilon}{kT}=\frac{F^2\epsilon}{NRT} \tag{1}$$

where e is the charge of an ion, ϵ the dielectric constant, $k=R/N$ the Boltzmann constant (=gas constant R divided by number of molecules per mol N) and e (=the Faraday equivalent F divided by N), the charge of an ion.

For the following we assume that q positive and negative ions are produced per cm³ per second, which recombine at a rate given by $\alpha n_+ n_-$.

We assume an infinite condenser with parallel plates at a distance 1 from each other, so that everything depends only on the coordinate at right angles to them which we call x, and measure from an origin in the middle between the plates.

In the appendix we have made a study of the space charge distribution which follows from the different approximations which have to be made. The result is the following: Except for a potential drop of the order of magnitude of a few volts the effect of diffusion can be neglected. This can be seen if we consider the relative importance of the current due to diffusion and the current due to the electric field in the equation for the stream of ions passing a certain cross section (V potential, h field):

$$D\left(\frac{dn}{dx}-\frac{F}{RT}nh\right)=Dn\left(\frac{d\ln n}{dx}-\frac{F}{RT}h\right)=Dn\frac{1}{\Delta x}\left[\Delta\ln n+\frac{F}{RT}\Delta V\right] \tag{2}$$

Here the first member is due to diffusion, the second to the electric field. Now even if n should change in the region considered from 10^{20} to 1 ion per cm³ log n would change only by 86, which corresponds to a potential of 2.1 volts. This means that if we are interested in space charges corresponding to hundreds of volts we can leave diffusion out of consideration. But, then, the space charge must be due to the fact that the electric current disturbs appreciably the equilibrium between dissociation and recombination of ions. This means further that we can have appreciable space charges only if the current has values which lie in a restricted range near the saturation current. If it were infinitely small compared with the saturation current, the ionization—recombination equilibrium is sustained in the main, except in

[13] C. D. Child, Phys. Rev. **32**, 492 (1911); I. Langmuir, Phys. Rev. **21**, 419 (1923); W. Schottky, Phys. Zeits. **15**, 526, 624 (1914).

[14] Townsend, Phil. Trans. **193**, 129 (1900).

the immediate neighborhood of the electrodes. If the current is very close to saturation, we have again a constant field, as the ions are then removed so quickly that no space charge can accumulate, as has been shown by Seeliger.[15] We can say that if we want a space charge amounting to the order of magnitude of 100 volts or more, not restricted to a layer very thin compared with the distance between the plates, the current must be between the limits:[16]

$$j_{sat}/10 < j < j_{sat}(1-\gamma/15\beta) \tag{3}$$

The methods of getting from space charge and current measurements, both in the stationary state, and if possible, measurements of the initial current, all the data of interest, namely, number of ions present, mobility, number of ions generated per second, and the recombination coefficient, are discussed in the appendix.

One more point of interest should be mentioned. Joffé has found that after cutting off a field which has acted long enough to build up a considerable space charge, there is an increased conductivity which disappears slowly. The same is true for insulating oils after reversal of the field.[17] Joffé interprets this by assuming that there is an accumulation of ions which is set free after the field is cut off, diffuses back into the main space between the electrodes, and increases there the conductivity until it disappears slowly through recombination. We have shown in the appendix that in the whole region where space charge is considerable, the number of ions is always less than without current. It is possible that there is an excess of ions present, but this must then be due to a resistance to the discharging of ions at the electrode, and they must be concentrated in an extremely thin layer close to the electrode, so thin that the potential drop in it is only a few volts.

Appendix I.

Space Charge Due to Electrons Between Parallel Plates

The point of origin is between the two plates, the distance of which is $2l$. If F is the Faraday equivalent, A and B are constants, then Laue[18] gives the following formula for the electrical density ρ and the potential:

$$\rho = \frac{RT}{F}\,\frac{2A^2}{\cos^2 Ax} \tag{4}$$

$$V = \frac{RT}{F}\log\cos^2 Ax + B. \tag{5}$$

In the center where the electron density is lowest, ρ is given according to (4) by

$$\rho = 2A^2RT/F.$$

For not too small a distance between the plates the constant A is approximately $\pi/2l$. This gives at room temperature in the center a number of about $NRT\pi^2/2l^2F^2 = 10^6/l^2$ electrons per

[15] R. Seeliger, Ann. d. Physik **33**, 319 (1910).

[16] The first limit meaning space charge limited to about $\frac{1}{5}$–$\frac{1}{10}$ of the condenser space, the latter a variation in the field of about 10 percent. [(46) and (48′)].

[17] Private communication of Professor Whitehead and Dr. Marvin of The Johns Hopkins University.

[18] M. v. Laue, Jahr. der Radio. u. Elekt. **15**, 205, (1918).

cm³ as the number present if it were limited by the space charge and not by the surface forces. This number is high enough to give measureable electron conductivity. Accordingly we conclude from its absence that the surface forces are responsible for the absence of these electrons.

Appendix II.

Space Charge in an Ionized Medium Between two Plates

We assume a uniform generation of q pairs of ions per second per cm.³ We call the number of positive ions present in 1 cm³ n_+, the number of negative ions n_-. The recombination per cm³ and second is given by $\alpha n_+ n_-$. We call the diffusion coefficient of the positive ions D_+ for the negative ions D_-, and recall relation (1) between K and D. Let h be the electric field, V the potential, $y = VF/RT$. We assume both ions to have the same charge which might be a multiple of the charge of the electron, in which case F must be taken as a multiple of the Faraday equivalent. ϵ shall be the dielectric constant of the medium. All quantities referring to the left plate ($x = -l$) shall be designated by the subscript 1, all quantities referring to the right plate ($x = +l$) by the subscript 2. The zero point of the potential is taken at the origin in the middle between the plates, the potential difference accordingly $2V_1$. The current density shall be j.

The equations of motion of the ions are

$$D_+\left(\frac{d^2n_+}{dx^2} - \frac{F}{RT}\frac{d}{dx}hn_+\right) = \alpha n_+ n_- - q$$
$$D_-\left(\frac{d^2n_-}{dx^2} + \frac{F}{RT}\frac{d}{dx}hn_-\right) = \alpha n_+ n_- - q \tag{6}$$

$$\frac{dh}{dx} = \frac{4\pi F}{\epsilon N}(n_+ - n_-) \tag{7}$$

where the last equation is the Poisson equation.

As an exact integration is impossible, approximations have to be made, but can be made in different ways, which shall now be discussed.

1. *Langevin's approximation.*[19] Langevin assumes the number of generated ions to be small, and develops accordingly everything in a power series in q. He shows that this assumption is the more justified the smaller the expression $(ql^2/n_0 D)^2$ becomes, because in this case the loss of ions through diffusion to the plate becomes more and more important compared with recombination. Accordingly he puts

$$n_+ = n_+'q + \cdots$$
$$n_- = n_-'q + \cdots$$
$$h = (V_1/l) + h'q + \cdots .$$

In our calculations we are going to be satisfied with this approximation. The introduction of these expressions into the equations of motion amount to a neglecting of the recombination term because it would contain q^2. It is then possible to give a first integral of the following form

$$D_+\left(\frac{y_1}{l}n_+' - \frac{dn_+'}{dx}\right) = -C_+ + x \tag{8}$$
$$D_-\left(\frac{y_1}{l}n_-' + \frac{dn_-'}{dx}\right) = C_- - x$$

where the left hand sides express the stream of positive or negative ions, respectively (divided by q). The Poisson equation can then be written

$$\frac{dh'}{dx} = \frac{4\pi F}{\epsilon N}(n_+' - n_-'). \tag{9}$$

We introduce, then, the following abbreviation

$$\alpha_+ = D_+ y_1^2/l^2 \qquad \alpha_- = D_- y_1^2/l^2$$

[19] P. Langevin, Le Radium **10**, 113 (1913).

and the integration of Eqs. (8) with Langevin's method, but taking into account a generalized surface condition leads to the following formula for the distribution of charges

$$n_+=(n_+)_2\,e^{-y_1}\frac{e^{y_1x/l}-e^{-y_1}}{1-e^{-2y_1}}+(n_+)_1\frac{1-e^{y_1(x/l-1)}}{1-e^{-2y_1}}-\frac{2y_1qe^{-y_1}}{\alpha_+}\frac{e^{y_1x/l}-e^{y_1}}{1-e^{-2y_1}}+\frac{y_1q}{\alpha_+}\left(\frac{x}{l}-1\right)$$

$$=\left[(n_+)_2-(n_+)_1-\frac{2y_1q}{\alpha_+}\right]\frac{e^{-y_1}}{1-e^{-2y_1}}e^{y_1x/l}+\frac{y_1q}{\alpha_+}\frac{x}{l}+\left[(n_+)_1-(n_+)_2e^{-2y_1}+\frac{y_1q}{\alpha_+}(1+e^{-2y_1})\right]\frac{1}{1-e^{-2y_1}} \quad (10)$$

$$n_-=\left[(n_-)_1-(n_-)_2-\frac{2y_1q}{\alpha_-}\right]\frac{e^{-y_1}}{1-e^{-2y_1}}e^{-y_1x/l}-\frac{y_1q}{\alpha_-}\frac{x}{l}+\left[(n_-)_2-(n_-)_1e^{-2y_1}+\frac{y_1q}{\alpha_-}(1+e^{-2y_1})\right]\frac{1}{1-e^{-2y_1}} \quad (10')$$

These introduced into Poisson's equation permit a solution of the latter which gives the following formula for the distribution of the potential

$$\begin{aligned}V=\frac{V_1x}{l}+\frac{4\pi F}{\epsilon N}\frac{l^2}{y_1^2}\frac{e^{-y_1}}{1-e^{-2y_1}}&\left\{\left[(n_+)_2-(n_+)_1-\frac{2y_1q}{\alpha_+}\right](1-e^{y_1x/l})\right.\\&\left.-\left[(n_-)_1-(n_-)_2-\frac{2y_1q}{\alpha_-}\right](1-e^{-y_1x/l})\right\}\\&+\frac{2\pi F}{3\epsilon N}ly_1q\left(\frac{1}{\alpha_+}+\frac{1}{\alpha_-}\right)\left(\frac{x^2}{l^2}-1\right)x+\frac{2\pi}{\epsilon}\frac{F}{N}\frac{1}{1-e^{-2y_1}}\left\{(n_+)_1-(n_+)_2e^{-2y_1}\right.\\&\left.-(n_-)_2+(n_-)_1e^{-2y_1}+y_1q(1+e^{-2y_1})\left(\frac{1}{\alpha_+}-\frac{1}{\alpha_-}\right)\right\}x(x-l)\\&+\frac{4\pi Fl}{\epsilon Ny_1^2}\left\{(n_+)_2-(n_+)_1-\frac{2y_1q}{\alpha_+}+\left[(n_-)_1-(n_-)_2-\frac{2y_1q}{\alpha_-}\right]e^{-y_1}\right\}x.\end{aligned} \quad (11)$$

Furthermore, we get from (8) as the components of the current carried by the two types of ions separately, if N means again the number of molecules per mol.

$$\begin{aligned}\frac{F}{N}(-C_+q+qx)&=\frac{FD_+}{N}\frac{y_1}{l}\frac{[(n_+)_1-(n_+)_2e^{-2y_1}]}{1-e^{-2y_1}}+\frac{F}{N}ql\left(\frac{1+e^{-2y_1}}{1-e^{-2y_1}}-\frac{1}{y_1}+\frac{x}{l}\right)\\\frac{F}{N}(C_-q-qx)&=\frac{FD_-}{N}\frac{y_1}{l}\frac{[(n_-)_2-(n_-)_1e^{-2y_1}]}{1-e^{-2y_1}}+\frac{F}{N}ql\left(\frac{1+e^{-2y_1}}{1-e^{-2y_1}}-\frac{1}{y_1}-\frac{x}{l}\right).\end{aligned} \quad (12)$$

In (11) there is one term, the one multiplied with $x(x-l)$, which is symmetric to the center, while all others are anti-symmetric. This term is due to difference in the behavior of the two ions, either in mobility or at the surfaces.

We assume now first that all ions are discharged immediately upon reaching the electrodes, as in the case of gases. This means

$$(n_+)_1=(n_+)_2=(n_-)_1=(n_-)_2=0$$

The potential distribution then takes the form

$$\begin{aligned}V=\frac{V_1x}{l}-\frac{8\pi F}{\epsilon N}\frac{l^2}{y_1}q\frac{e^{-y_1}}{1-e^{-2y_1}}&\left(\frac{1-e^{y_1x/l}}{\alpha_+}-\frac{1-e^{-y_1x/l}}{\alpha_-}\right)\\&+\frac{4\pi Fl^2}{6\epsilon N}y_1q\left(\frac{1}{\alpha_+}+\frac{1}{\alpha_-}\right)\frac{x}{l}\left(\frac{x^2}{l^2}-1\right)\\&+\frac{2\pi F}{\epsilon N}y_1q\frac{1+e^{-2y_1}}{1-e^{-2y_1}}x(x-l)\left(\frac{1}{\alpha_+}-\frac{1}{\alpha_-}\right)-\frac{8\pi Fl}{\epsilon Ny_1}q\left(\frac{1}{\alpha_+}+\frac{e^{-y_1}}{\alpha_-}\right)x.\end{aligned} \quad (11')$$

Again we have the symmetric term with $x(x-l)$ which disappears if the two ions have equal mobility ($\alpha_+=\alpha_-$), but otherwise is present even without external field.

$$\begin{aligned}\frac{F}{N}(-C_+q+qx)&=\frac{F}{N}\left(\frac{ql}{1-e^{-2y_1}}(1+e^{-2y_1})-\frac{ql}{y_1}+qx\right)\\\frac{F}{N}(C_-q-qx)&=\frac{F}{N}\left(\frac{gl}{1-e^{-2y_1}}(1+e^{-2y_1})-\frac{gl}{y_1}-qx\right)\end{aligned}$$

give the components of the current

$$j=2ql\frac{F}{N}\left(\frac{1+e^{-2y_1}}{1-e^{-2y_1}}-\frac{1}{y_1}\right)$$

For very weak fields this gives Ohm's law $j=2qlFy/3N$ but in the cases with which we are concerned, where y_1 is several hundred, the current is approximately

$$j=2ql\frac{F}{N}\left(1-\frac{1}{y_1}\right)$$

or almost saturation current $2qlF/N$, where all the $2ql$ ions generated are discharged at the plates.

Another possible assumption would be that at the positive plate the current is carried entirely by negative ions; at the negative plate, entirely by the positive ions. This means that for $x=-l$ the left hand side of the first equation (8) would be zero; for $x=+l$ the left hand side of the second equation would be zero. This leads to the following connection between the number of ions at the two plates

$$D_+\frac{y_1}{l}[(n_+)_1-(n_+)_2e^{-2y_1}]=ql\left[\frac{1}{y_1}-\frac{2e^{-2y_1}}{1-e^{-2y_1}}\right](1-e^{-2y_1})$$

$$D_-\frac{y_1}{l}[(n_-)_2-(n_-)_1e^{2y_1}]=ql\left[\frac{1}{y_1}-\frac{2e^{-2y_1}}{1-e^{-2y_1}}\right](1-e^{-2y_1})$$

But in this case the current is exactly saturation current since the diffusion is completelv overshadowed by the effect of the field.

It might be remarked in general that for the case (11′) as well as for the general case (11) (except if the expressions $(n_+)_2-(n_+)_1-2y_1q/\alpha_+$, $(n_-)_1-(n_-)_2-2y_1q/\alpha_-$ are very small) a large part of the space charge will be restricted to a narrow layer adjoining the plates on account of the very small values $e^{y_1(x/l-1)}$ takes, except for x very close to l.

As Langevin's approximation gives so nearly saturation current for the voltages with which we are concerned, it does not apply in our case.

2. *Jaffé's approximation.*[20] Jaffé gives for relatively small voltages a power development in respect to V_1, for high voltages a development of inverse powers. But we have to assume with him that the mobilities are equal for both ions.

A) Region of Ohm's lqw. We put:

$$\begin{aligned} n_+&=n_+'+n_+''V_1+\cdots \\ n_-&=n_-'+n_-''V_1+\cdots \\ h&=h_+'V+\cdots . \end{aligned} \tag{13}$$

Inserting this into Eq. (6) and (7) we get first equations for n_+' and n_-', the numbers of the ions that would be present without outside potential

$$D\frac{d^2n_+'}{dx^2}=\alpha n_+'n_-'-q \tag{14}$$

$$D\frac{d^2n_-'}{dx^2}=\alpha n_+'n_-'-q$$

$$0=n_+'-n_-'\,;\quad n_+'=n_-'=n'. \tag{15}$$

These values are then determined entirely by diffusion, dissociation and recombination, and it is clear that the number of both kinds of ions should be equal.

$$\begin{aligned} D\left[\frac{d^2n_+''}{dx^2}-\frac{F}{RT}\frac{d}{dx}(n'h')\right]&=\alpha(n_-'n_+''+n_-''n_+')=\alpha n'(n_+''+n_-'') \\ D\left[\frac{d^2n_-''}{dx^2}+\frac{F}{RT}\frac{d}{dx}(n'h')\right]&=\alpha(n_-'n_+''+n_-''n_+')=\alpha n'(n_+''+n_-'') \end{aligned} \tag{14′}$$

[20] G. Jaffé, Ann. d. Physik **43**, 249 (1914).

are the next approximations for the number of ions with the Poisson-equation:

$$\frac{dh'}{dx}=\frac{4\pi F}{\epsilon N}(n_+''-n_-''). \tag{15'}$$

As we are not interested in the number of ions, we subtract the two equations (14') and integrate once

$$\frac{d}{dx}(n_+''-n_-'')-\frac{2F}{RT}(n'h')=\frac{jN}{DFV_1}.$$

That the letter j, which we have used in the integration constant, is justified follows from the fact that the left hand side multiplied with DV_1 gives the difference of the streams of positive and negative ions. We eliminate then $n_+''-n_-''$ with the help of (15'), and find for the field:

$$\frac{d^2}{dx^2}h=\frac{8\pi F^2}{\epsilon NRT}n'h+\frac{4j\pi}{\epsilon D}. \tag{15''}$$

In this equation n' is to be found from the single equation into which the two equations (14) merge if (15) is taken into account.

$$D\frac{d^2n'}{dx^2}=\alpha n'^2-q. \tag{14''}$$

This equation gives in general upon integration n' as an elliptical function of x, as Jaffé has shown, but a numerical evaluation is very inconvenient, and accordingly we pursue another method.

(a) All ions are discharged on the plates as assumed in gas discharges and by Jaffé. We have then the border conditions

$$(n_+)_1=(n_+)_2=(n_-)_1=(n_-)_2=0$$

If we introduce now as abbreviation n_0 the number of ions that would be present without discharge on the plate,

$$\frac{q}{\alpha}=n_0^2, \tag{14'''}$$

we get

$$\frac{Dn_0}{q}\frac{d^2(n'/n_0)}{dx^2}=\frac{n'^2}{n_0^2}-1. \tag{14''''}$$

We assume now that $(q/Dn_0)^{1/2}x<1$ (16) and make for n'/n_0 a power development according to this expression, stopping with the first member. We find then,

$$\frac{n'}{n_0}=\frac{1}{2}\frac{q}{Dn_0}(l^2-x^2)+\cdots. \tag{17}$$

This, introduced into (15''), leads to the following differential equation for the field h

$$\frac{d^2h}{dx^2}=\frac{4\pi F^2q}{\epsilon RTND}(l^2-x^2)h+\frac{4\pi j}{\epsilon D} \text{ or}$$

$$\frac{d^2h}{d(x/l)^2}=\frac{4\pi F^2q}{\epsilon RTND}l^4\left(1-\frac{x^2}{l^2}\right)h+\frac{4\pi jNl^2}{\epsilon D}. \tag{18}$$

We find the following border condition from (15'): $(dh/dx)=0$ for $x=\pm l$. We then use the abbreviation

$$A=\frac{4\pi F^2}{\epsilon RTN}\frac{q}{D}l^4=\frac{4\pi F^2n_0}{\epsilon RTN}l^2\frac{q}{Dn_0}l^2 \tag{19}$$

and assume that A is not large compared with 1. Except in the case in which n_0l^2/ϵ is larger than 10^4 this is a weaker restriction than (16). We develop the solution in a power series of A stopping with the third and find

$$V=\frac{3}{2}\frac{RT}{Fql^2}jx\left\{C+\frac{A}{6}\frac{x^2}{l^2}\left(C-\frac{2}{3}\right)-\frac{A}{60}\frac{x^4}{l^4}\left(C-\frac{AC}{2}+\frac{A}{3}\right)\right.$$
$$\left.-\frac{A^2}{360}\frac{x^6}{l^6}\left(C-\frac{AC}{14}-\frac{4}{7}+\frac{A}{21}\right)+\frac{A^2}{6048}\frac{x^8}{l^8}\left(C-\frac{11}{15}AC+\frac{7A}{15}+\frac{A^2C}{60}-\frac{A^2}{90}\right)\right\} \tag{20}$$

where C means the abbreviation

$$C=1+\frac{A}{360}\,\frac{7-(A^2/16)}{1+\frac{29}{320}A+\frac{A^2}{960}+\frac{A^3}{3840}}\cdot \tag{20'}$$

The current j in (20) is then determined by the condition that $V=V_1$ for $x=l$. But formula (20) does not give any stronger space charges with A not large compared with 1 than would Langevin's approximation; in fact, the condition (16) is identical with the latter's condition on page 797, and accordingly (20) is identical, at least in the first order, with (11') for small values of A.

We try next the opposite surface condition, namely that no ions are discharged on the plates under normal conditions without field. Then the number of ions without field is uniformly the equilibrium number throughout space.

$$n_+'=n_-'=n_0=(q/\alpha)^{1/2}.$$

We find then in the same manner which led to (18)

$$\frac{d^2h}{dx^2}=\frac{8\pi F^2}{\epsilon NRT}n_0h+\frac{4\pi j}{\epsilon D}\cdot \tag{21}$$

But this equation is even accurate to a somewhat higher approximation. If we put namely

$$\begin{aligned} n_+&=n_0+n''V_1+n_+''V_1+\cdots \\ n_-&=n_0-n''V_1+n_-''V_1+\cdots \end{aligned} \tag{22}$$

the value of n_++n_- is not affected by the existence of $n''V$, and so (21) remains unchanged even if we take these members in. The integration of (21) leads then to

$$h=-\frac{jNRT}{2F^2n_0D}-A\kappa\ \mathrm{ch}\ \kappa x \tag{23}$$

where κ^2 is the constant introduced by Debye[21] into the theory of strong electrolytes

$$\kappa^2=\frac{8\pi F^2n_0}{\epsilon NRT}\cdot \tag{23'}$$

It appears there for the same reason as here. $1/\kappa$ has the dimensions of a length. A is an integration constant. sh x and ch x mean the hyperbolic sin and cosine. Eq. (23) can then be integrated and gives

$$V=-h_0x+A\ (\mathrm{sh}\ \kappa x-\kappa x). \tag{24}$$

There h_0 means the electric field at the origin which is, according to (23)

$$-h_0=\frac{jNRT}{2F^2n_0D}+A\kappa. \tag{25}$$

If this field were present uniformly between the plates the potential difference would be

$$V_1'=-h_0l.$$

The constant A is then defined by the excess in potential

$$V_1-V_1'=A(\mathrm{sh}\ \kappa l-\kappa l). \tag{26}$$

We can then rewrite (24)

$$V=V_1'\frac{x}{l}+(V_1-V_1')\frac{\mathrm{sh}\ \kappa x-\kappa x}{\mathrm{sh}\ \kappa l-\kappa l}. \tag{27}$$

From (9) and the assumption that the deviations from the uniform distribution are antisymetric for both ions ($n_+''=n_-''=0$) it follows

$$n_+=n_0+\frac{\epsilon N}{8\pi F}A\kappa^2\ \mathrm{ch}\ \kappa x=n_0\left[1+\frac{F}{RT}(V_1-V_1')\frac{\mathrm{sh}\ \kappa x}{\mathrm{sh}\ \kappa l-\kappa l}\right]. \tag{28}$$

[21] P. Debye u. E. Hückel; Phys. Zeits. **24**, 185, 305 (1923). See also E. Hückel, Erg. der Ex. Nat. **3**, 199 (1924).

But then the condition that (22) should be a convergent series would demand that

$$F(V_1-V_1')/RT<1$$

which would again make the space charge potential V_1-V_1' smaller than a fraction of a volt.

(B) The current is close to saturation. The formulas for this case are completely given by Jaffé. They are

$$h=\frac{V_1}{l}+\frac{2\pi}{\epsilon V_1}ql^2\frac{RT}{N}\left[2\left(\frac{1}{D_-}-\frac{1}{D_+}\right)\frac{x}{l}+\left(\frac{1}{D_+}+\frac{1}{D_-}\right)\left(\frac{x^2}{l^2}-\frac{1}{3}\right)\right] \tag{12'}$$

$$j=\frac{2qFl}{N}-\frac{RT}{N}\frac{2ql}{V_1}-\alpha\left(\frac{qRT}{N}\right)^2\frac{1}{D_+D_-}\frac{4}{3}\frac{l^5}{V_1^2}.$$

3. *Space charge in equilibrium.* Another possible approximation would be given in the case in which we assume that the equilibrium between dissociation and recombination is practically established everywhere, and the action of the electric field is just counter-balanced by diffusion. We neglect then the influence of the current on the space charges. This assumption would be justified if the transfer resistance at the electrodes were very large so that the drain due to the current is small compared with the exchange by diffusion, dissociation and recombination. This case is present in the normal galvanic cells, and has been worked out there.[22]

The distribution of ions will then be given by Boltzmann's formula which states the equilibrium between external (for example electric) forces and diffusion, and which does not violate the dissociation—recombination equilibrium.

$$\alpha n_+n_-=q \tag{29}$$

$$n_+=n_0e^{-FV/RT}=n_0e^{-v} \tag{29'}$$

$$n_-=n_0e^{v} \tag{29''}$$

The Poisson equation then takes the form

$$\frac{d^2V}{dx^2}=-\frac{4\pi F}{\epsilon N}n_0(e^{-v}-e^{v}) \tag{30}$$

which can be rewritten

$$\frac{d^2y}{dx^2}=\kappa^2\,\mathrm{sh}\,y. \tag{30'}$$

A first integration of this gives, with A as a constant of integration

$$\frac{1}{2}\left(\frac{dy}{dx}\right)^2=\kappa^2\,\mathrm{sh}\,y+A\kappa^2. \tag{31}$$

This equation can be easily integrated only if A is put $-\frac{1}{2}$. This turns out to represent the case in which the electrodes are infinitely far apart. That shall therefore be assumed and x here calculated from one of the plates, instead of from the middle.[23] We then get

$$\left(\frac{d(y/2)}{dx}\right)^2=\kappa^2\,\mathrm{sh}^2(y/2)\quad\text{or}\quad\frac{d(y/2)}{d(\kappa x)}=-\mathrm{sh}\,(y/2). \tag{32}$$

We find as a result of integration

$$e^{FV/2RT}=\mathrm{ctgh}\,\frac{\kappa}{2}(x+x_0)=1+\frac{2e^{-\kappa x+x_0}}{1-e^{-\kappa(x+x_0)}} \tag{33}$$

where x_0 is determined by the conditions at the electrode

$$e^{-\kappa x_0}=\frac{1-e^{-FV_1/RT}}{1+e^{-FV_1/RT}} \tag{33'}$$

[22] Gouye, Comptes rendus **146**, 612 (1908); Journ. d. Phys. **9**, 457 (1910); D. L. Chapman, Phil. Mag. **25**, 475 (1913); K. F. Herzfeld, Phys. Zeits. **21**, 28, 61 (1920); M. von Laue, and N. Sen, Ann. d. Physik **75**, 182 (1924).

[23] For other values of A the solution has to be made by two different developments for y. The calculation is rather lengthy and does not change the conclusions.

or for a considerable value of FV_1/RT

$$\kappa x_0 = 2e^{-FV_1/RT}. \tag{33''}$$

But formula (33) shows that most of the potential drop, apart from a fraction of a volt, is concentrated in a narrow sheet near the electrode. If we call V' the value of the potential at any place where it is higher than 1 volt, we can write for the position of that place

$$\kappa x \sim 2(e^{-FV'/RT} - e^{-FV_1/RT}).$$

From this equation it follows that even if V' is not more than 10 volts κx will be negligibly small, or in other words even with the lowest possible value of κ the whole potential drop, except a few volts, is concentrated in a sheet of very small dimensions.

All the cases considered up to now have shown that whenever diffusion is considered as of preeminent importance while approximations are made in other respects the space charge apart from a few volts is concentrated in the immediate neighborhood of the electrode. In the next case we are accordingly to neglect diffusion completely and will follow a method first outlined by J. J. Thomson.[24]

4. *Neglection of diffusion.* In this case subtraction of the two Eqs. (6) and integration shows immediately that the electric field is inversely proportional to the sum of the number of ions. If we assume namely that the mobilities of all the ions are equal, the conductivity is proportional to this sum, and the neglecting of diffusion makes the current dependent only on the electric field.

In this case it is shorter to use directly the electric mobility K instead of the diffusion coefficient D. The formula for the current density is then

$$j = eK(n_+ + n_-)h_0 \tag{35}$$

J. J. Thomson then expresses the n's with the help of this and Poisson's formula through h, and eliminates n from one of the Eqs. (6). The result is

$$\frac{d^2h^2}{dx^2} = \frac{16\pi e}{K\epsilon}\left\{q - \frac{\alpha}{4e^2K^2h^2}\left[j^2 - \frac{K^2\epsilon^2}{64\pi^2}\left(\frac{dh^2}{dx}\right)^2\right]\right\} \tag{36}$$

We introduce a new constant

$$\beta^{-1} = \alpha\epsilon/8\pi eK. \tag{37}$$

Langevin[25] has shown that β is always larger than 1, and should not vary very much with the material. For air, it is about 4; for quartz, it would come out with Joffe's values about 1. Thomson integrates (36) and finds

$$\frac{K^2\epsilon^2}{64\pi^2}\left(\frac{dh^2}{dx}\right)^2 = j^2 + \frac{qeK\epsilon}{2\pi(1-1/\beta)}h^2 + Ch^{2/\beta} \tag{38}$$

where C is an integration constant. Furthermore, we have for the number of ions the equation

$$n_\pm = \frac{1}{2eKh}\left(j \pm \frac{K\epsilon}{8\pi}\frac{dh^2}{dx}\right). \tag{39}$$

If we now neglect diffusion, there can be no negative ions on the positive plate, and no positive ions on the negative plate. It follows then for the plates if we call h_m the maximum value of the field, which is always located at the plate

$$\frac{K\epsilon}{8\pi}\left(\frac{dh^2}{dx}\right)_{h=h_m,\, x=l} = j$$

With the help of this relation, we can eliminate the integration constant C. We get namely

$$0 = \frac{qeK\epsilon}{2\pi(1-(1/\beta))}h_m^2 + Ch_m^{2/\beta}$$

and find the following differential equation

$$\frac{K^2h_m^4\epsilon^2}{64\pi^2j^2}\left[\frac{d(h^2/h_m^2)}{dx}\right]^2 = 1 + \frac{qeK\epsilon}{2\pi(1-1/\beta)}\frac{h_m^2}{j^2}\left[\frac{h^2}{h_m^2} - \left(\frac{h^2}{h_m^2}\right)^{1/\beta}\right]. \tag{40}$$

This integration has been treated by Thomson[24] himself and many others.[25] We try a more convenient development in the following manner: we introduce a numerical constant γ, to be defined later, and furthermore the following abbreviations—

$$G^2=\frac{q\epsilon K\epsilon}{4\pi\beta}\frac{h_m^2}{j^2} \tag{41}$$

$$\lambda=\gamma^{1/2}G\frac{8\pi j}{Kh_m^2\epsilon}=\frac{2}{h_m}\left(\frac{4\pi q\epsilon\gamma}{K\beta\epsilon}\right)^{1/2} \tag{41'}$$

$$u=(h_m^2-h^2)/h_m^2 \quad 0\leqq u<1. \tag{41''}$$

With these we rewrite (40) in the following form

$$\frac{\gamma G^2}{\lambda^2}\left(\frac{du}{dx}\right)^2=1+\frac{2\beta G^2}{1-1/\beta}[1-u-(1-u)^{1/\beta}]. \tag{40'}$$

We then develop the last expression into a power series up to the second power of u

$$\frac{\gamma G^2}{\lambda^2}\left(\frac{du}{dx}\right)^2=1+2\beta G^2(-u+u^2/2\beta)=1-G^2\beta^2+G^2(\beta-u)^2 \tag{40''}$$

But instead of $u-(u^2/2\beta)$ we are going to use $u-\frac{\gamma u^2}{2\beta}$ where γ is a pure number adapted to the value of β, because the table below shows that we get in this manner a better approximation.

u	$(1-u)^{1/\beta}-(1-u)$			$\gamma=1$, $(u-u^2/2\beta)$ $(1-1/\beta)$			$\gamma=2$, $(u-u^2/\beta)$ $(1-1/\beta)$		
	$\beta=2$	$\beta=4$	$\beta=10$	$\beta=2$	$\beta=4$	$\beta=10$	$\beta=2$	$\beta=4$	$\beta=10$
0.25	0.116	0.181	0.222	0.117	0.181	0.235	0.109	0.186	0.219
0.50	0.207	0.341	0.431	0.219	0.352	0.475	0.198	0.327	0.427
0.75	0.250	0.457	0.621	0.305	0.510	0.686	0.235	0.457	0.624
0.80	0.247	0.468	0.651	0.320	0.540	0.730	0.240	0.480	0.662

Accordingly one sees that in the range between $\beta=2$ and $\beta=10$ $\gamma=2$ gives a very satisfactory representation up to $u=0.8$, or an h^2 higher than $h^2_m/5$. Accordingly we write, instead of (40'')

$$\frac{\gamma G^2}{\lambda^2}\left(\frac{du}{dx}\right)^2=1+2\beta G^2\left(-u+\frac{\gamma u^2}{2\beta}\right)=1-\frac{\beta^2G^2}{\gamma}+\gamma G^2\left(u-\frac{\beta}{\gamma}\right)^2 \tag{40'''}$$

or

$$\frac{\gamma G^2}{G^2\beta^2/\gamma-1}\left[\frac{d(u-\beta/\gamma)}{\lambda dx}\right]^2=\frac{\gamma G^2}{G^2\beta^2/\gamma-1}\left(u-\frac{\beta}{\gamma}\right)^2-1. \tag{40''''}$$

This equation can be easily integrated. If we take into account that the field must be symmetrical in respect to the center between the plates if the two ions have equal mobility, as is assumed here, we find

$$\frac{h^2}{h_m^2}=1-\frac{\beta}{\gamma}+\left(\frac{G^2\beta^2-\gamma}{\gamma^2G^2}\right)^{1/2}\operatorname{ch}\lambda x. \tag{42}$$

The square root is determined by the condition that the field h must take the value h_m at the electrodes, $x=\pm l$.

$$\left(\frac{G^2\beta^2-\gamma}{\gamma^2G^2}\right)^{1/2}=\frac{\beta}{\gamma}\frac{1}{\operatorname{ch}\lambda l}. \tag{43}$$

[24] J. J. Thomson and G. P. Thomson, Conduction of Electricity through Gases, Cambridge, 1928, page 193 and the following.

[25] P. Langevin, Comptes rendus **131**, 177 (1903); O. W. Richardson, Phil. Mag. **10**, 242 (1905).

[26] G. Mie, Ann. d. Physik **13**, 857 (1904); G. W. Walker, Phil. Mag. **8**, 650 (1904); A. A. Robb, Phil. Mag. **10**, 237, 164 (1905); R. Seeliger, Ann. d. Physik **33**, 319 (1910).

The solution of this is

$$\beta G/\gamma^{1/2}=\operatorname{ctgh}\lambda l \tag{44}$$

As the field h_m close to the plates is rather difficult to measure we introduce instead the field h_0 in the middle, which is according to (42)

$$\frac{h_0^2}{h_m^2}=1+\frac{\beta}{\gamma}\left(\frac{1}{\operatorname{ch}\gamma l}-1\right) \tag{45}$$

We have then

$$h^2=h_0^2\frac{1+\frac{\beta}{\gamma}\left(\frac{\operatorname{ch}\lambda x}{\operatorname{ch}\lambda l}-1\right)}{1+\frac{\beta}{\gamma}\left(\frac{1}{\operatorname{ch}\lambda l}-1\right)}. \tag{46}$$

If we want now to evaluate a measured field, we try to determine λ by comparing the field h at a given place x with h_0 and calculating λ for an assumed β from the equation

$$\frac{1-(1-\gamma/\beta)\operatorname{ch}\lambda l}{\operatorname{ch}\lambda x-\operatorname{ch}\lambda l}=\frac{h_0^2}{h^2-h_0^2}$$

We can test our assumed β by repeating the process at different places. Knowing then λ, we determine the number of ions n_0 present without field by using (41′) and (37)

$$\lambda=\frac{8\pi\epsilon n_0}{h_0\beta}(2\gamma)^{1/2}\left(1+\frac{\beta}{\gamma}\left(\frac{1}{\operatorname{ch}\lambda l}-1\right)\right)^{1/2}. \tag{47}$$

Knowing then n_0 we can get K from the conductivity at very low fields, as we have then Ohm's law $j=h_0\epsilon K 2n_0$. β will then permit the calculation of α and (14‴) that of q. The equation for the current is found in (44) and (41)

$$j=\left(\frac{q\epsilon K\beta\epsilon}{4\pi\gamma}\right)^{1/2}h_m\operatorname{tgh}\lambda l. \tag{48}$$

If λl is sufficiently small we can develop the hyperbolic tangent and find

$$j=q\epsilon 2l\left(1-\frac{16\pi q\epsilon\gamma}{3K\beta\epsilon h_m^2}+\cdots\right)=2q\epsilon l\left(1-\frac{\lambda^2 l^2}{3}+\cdots\right) \tag{48′}$$

where $2q\epsilon l$ is the saturation current.

But we get impossible results, namely a negative value for h_0^2 from (45) if

$$1+\frac{\beta}{\gamma}\left(\frac{1}{\operatorname{ch}\lambda l}-1\right)<0 \quad \text{or} \quad \operatorname{ch}\lambda l>\frac{\beta}{\beta-\gamma}.$$

This is due to the fact that our approximation (40‴) gives too small results for the gradient of the field for large values of u, and to get this gradient to be zero at $x=0$, too small a value is assumed for G. As we have mentioned on page 804 we have to limit ourselves to values of u up to 0.8 or

$$\frac{h_m^2-h_0^2}{h_m^2}<0.8, \quad \operatorname{ch}\lambda l<\frac{1}{1-0.8\gamma/\beta}=$$

5/3 for $\beta/\gamma=2$ or $\lambda l\sim 1{,}1$

or according to (48) $0.73 j_{sat}<j<j_{sat}$.

To see what has to be done for lower currents we remember that J. J. Thomson[25] in his discussion had divided the region between the electrodes into three parts. In the central part the space charge was neglibible, the field constant, adjoining the two condenser plates, there are layers in which the field increases to the value h_m due to the space charges mainly restricted to these layers. For the thickness of these layers and for h_m Thomson gives as approximate formulas

$$l-x_k>\frac{j}{2eq} \text{ or } \frac{l-x_k}{l}>\frac{j}{j_{sat}} \tag{49}$$

$$\frac{h_m^2}{h_0^2}=\beta^{\beta/(\beta-1)}=c \tag{49′}$$

At this critical point therei s a decided bend in the curve. From (49) one sees that the closer the current is to saturation, the shorter the flat bottom of the curve, that is the region without space charges, becomes. At sufficiently high currents the flat part disappears completely, and the two layers merge in the middle. This is the case for which our preceding discussion applies accordingly.

For the case of weak currents, we have to use Mie's[26] approximation. He is forced to use two different expressions for the central part where the space charges are small, and for the parts close to the electrodes where the space charge is large. In his more accurate discussion, the space charge in the center is not completely negligible, and accordingly the curves there are not completely flat. He introduces then a field H defined by

$$H^2=\frac{j^2}{4e^2K^2n_0^24l^2}. \tag{50}$$

This is the field necessary to uphold the current j if Ohm's law were valid up to the current j with the resistance present at low current. It would also be the initial field if we kept the current constant in time. The general formula is then

$$h^2=H^2[1+2(c-1)e^{+f}]. \tag{51}$$

Here c is a constant defined by (49′)
We give a table for c.

β:	1	1.5	2	3	4	6	8	10
c:	$e(=2.72)$	3.38	4	5.20	6.35	8.59	10.77	12.92

f has two different expressions, one in the flat part of the curve, one in the steep part. The two are separated by the point x_k where the bend is located. The values of f are:

$$\text{Flat part, } x<x_k \quad f=\frac{c-1-(2\beta)^{1/2}}{2(2\beta-c+1)}-(2\beta)^{1/2}\frac{j_{sat}}{j}+\ln \operatorname{ch}\left[(2\beta)^{1/2}\frac{j_{sat}}{j}\frac{x}{l}\right] \tag{52}$$

$$\text{Steep part } x>x_k \quad f=-\frac{2\beta}{c-1}\frac{j_{sat}}{j}-\frac{\beta(2\beta-c+1)}{(c-1)^2}\frac{j_{sat}}{f^2}\left(1+\frac{x^2}{l^2}\right)$$
$$+\ln \operatorname{ch}\left\{\frac{2\beta}{c-1}\frac{j_{sat}}{j}\left[1+\frac{2\beta-c+1}{c-1}\frac{j_{sat}}{j}\right]\frac{x}{l}\right\} \tag{52′}$$

The position of the dividing point is given by

$$\frac{l-x_k}{l}=\frac{j}{j_{sat}}\frac{(c-1-(2\beta)^{1/2})(c-1)}{(2\beta)^{1/2}(2\beta-c+1)}. \tag{53}$$

The value of the coefficient of j_{sat}/j in (53) is shown in the following table:

β:	1	1.5	2	3	4	6	8	10
Coeff.:	1.34	1.08	1.50	1.66	1.79	2.05	2.27	2.45

We remark that (53) differs from Thomson's estimate (49) just by this coefficient.

The evaluation of a given space charge curve will then proceed so: We first decide whether the curve has a flat bottom or a continuous curvature. In the latter case, formula (46) will apply, the current is above $\frac{3}{4}$ of the saturation current. The method of discussion mentioned in connection with (46), (47) will allow the determination of β and λ, (48) will then give the saturation current and from this we get q. In the former case we locate the position of the bend, and then with an estimated value of β, the degree of saturation j/j_{sat} can be calculated from (53). Then we test the two values by comparing more closely the fit of the curve to (52), (52′). A method of trial and error will then lead to the actual values of β and the degree of saturation. Knowing the degree of saturation and the actual current, we can calculate the saturation current, and accordingly q. $q\beta=8\pi n_0^2eK$ and either H from (51) or a direct measurement of the initial conductivity which give n_0eK will allow the calculation of n_0, the number of ions present without current, and K the mobility separately.

To give an example we investigate the middle curve[27] for quartz in Joffe's book, page 103. The data given are scarce so that only a very rough calculation is feasible. We assume the curve

[27] Treating it as stationary.

to be symmetric (which seems not to be quite true). Then h_0 is found to be $44/2l$ volts/cm. At the place marked by a circle, which is given by $x=0.8l$, the field on the left side is found to be $124/2l$ volts/cm, on the right $140/2l$ volts/cm. We take as average $132/2l$ volts/cm, or $h^2=9h_0^2$ for $x=0.8l$. We take the bend at $x=0.5l$, and evaluate the formulas for $\beta=1.5$, 4, 8. The corresponding degree of saturation would be $j/j_{sat}=0.45$, 0.3, 0.22. For the ratio h_0^2/H^2 we get from (54) 1.12, 1.003, and 1.0002. This means that for this value of β the reduction of the number of ions in the center compared with the equilibrium number would be 6 percent, 0.15 percent, 0.01 percent. For the field at $x=0.8l$, we find $h^2=1.75h_0^2$, $4.59h_0^2$, $50h_0^2$. Accordingly the suitable value of β lies around 6, the degree of saturation around 0.26. If the current under these conditions were given we could then calculate j_{sat} and q and proceed as mentioned above.

We show finally that the number of ions present under these conditions is no where larger than the equilibrium number n_0. According to (35) the ratio h/j is inversely proportional to the number of ions (positive plus negative) present at the place. Formula (50) if applied to the center of the field

$$h_0^2=H^2\left\{1+2(c-1)\exp\left[\frac{c-1-(2\beta)^{1/2}}{2(2\beta-c+1)}-(2\beta)^{1/2}\frac{j_{sat}}{j}\right]\right\} \tag{54}$$

shows that even there h_0 is never smaller than H, and accordingly the number of ions never greater than n_0. As the field has its lowest value in the center, the same is true for the number of ions anywhere in even greater measure. To prove that this statement holds also when we make the transition to currents close to the saturation current, we proceed in the following manner: If we call h_a the average value of the field taken over the condenser, that is, the total potential difference divided by $2l$, we know that with increasing saturation the ratio of h/j continuously increases. This means that the ratio h_a/H continuously increases. In any case the minimum field is in the center, but we can now write

$$\frac{h_0}{H}=\frac{h_0}{h_a}\frac{h_a}{H}$$

In the preceding analysis, we have seen that close to the saturation current, the variation in the field is less than for low currents (49′), and accordingly for strong currents h_0/h_a is larger than for moderate currents.[28] The same is true, as we have just shown, for the second factor h_a/H. We have then proved that the left hand side is always larger than 1 or even the minimum field always larger than the field corresponding to Ohm's law, and therefore the total number of ions present always smaller than the equilibrium number.

[28] This argument is not quite strict.

CONNECTORS IN ACOUSTICAL CONDUITS

By R. B. Lindsay
Sloane Physics Laboratory, Yale University

(Received July 24, 1929)

Abstract

Transmission through a connector.—Employing the horn theory of Webster the power transmission through an acoustical connector joining two conduits is calculated when the law of the change of area of the connector is of the form $S=S_0\phi(x)$. The general result is applied to the following special cases: 1. Conical connector, $S=S_0x^2$, for which it is found that the transmission approaches unity with increasing kl, where l is the length of the connector and $k=2\pi/\lambda$; curves are given showing the exact dependence of the transmission on frequency for various values of l and the expansion ratio m. 2. Bessel connectors of higher order, $S=S_0x^a$ where a can take all values, in which case it is found that the transmission for kl large approaches a value approximately independent of a. 3. Exponential connector, $S=S_0e^{ax}$, the limiting case of the Bessel connectors, with a transmission ratio showing little difference from that of the former. 4. The connector whose generating curve has a point of inflection, $S=S_0e^{-ax^2}$, for which for large kl, the transmission differs little from that of the previously discussed connectors. These theoretical results are in agreement with certain transmission experiments of G. W. Stewart.

Phase change due to a connector.—The phase change introduced by the connector is calculated for the special cases mentioned and is shown to approximate kl in the limit of increasing kl.

Introduction

WHEN sound passes through a cylindrical tube or conduit it is often desirable to change the area of cross section. If this is done abruptly, as in Fig. 1, a considerable loss in power transmission ensues. In fact a simple calculation shows that in this case if the conduits are of such size that we

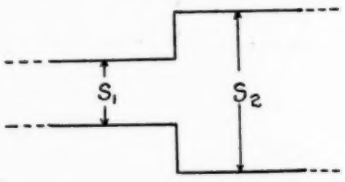

Fig. 1. Abrupt change in area.

can neglect viscosity damping the ratio of the transmitted flow of energy to the incident flow, which we may denote by P_r (power transmission ratio), is given by

$$P_r=4m^2/(m^2+1)^2 \qquad (1)$$

where m^2 is the ratio S_2/S_1 of the two areas of cross section. If m differs much from unity, i.e. if the change in area is large, P_r may become considerably less than unity. It is natural to suppose that if the transition from one

cross section to the other is made more gradually the transmission will be materially bettered. This is in fact the case. The subject has been investigated by Brillië[1] who worked out in detail the conical connector and made some general remarks about the exponential connector. It is desired in the present paper to extend his results and present the subject from a different and somewhat more unified point of view.

Transmission through a Connector

The method employed in the present calculations differs from that of Brillië in that it is based on the horn theory of Webster.[2] It is therefore subject to the approximations of this theory, which, however, so far as the author knows, has not been materially improved on in the cases to which it is proper to apply it. It is well to emphasize here the principal assumptions underlying it, viz.: 1. the cross sectional area $S \ll \lambda^2$ everywhere; 2. the fundamental acoustic equations are applicable; 3. both the particle displacement ξ and the excess pressure p are everywhere analytic functions; 4. the walls of the horn are rigid, and there is no displacement in a direction perpendicular to the axis; 5. the condensation s and the particle velocity $\dot{\xi}$ are so small that $\rho_0 s$ and $S\xi\, \partial s/\partial x$ can be neglected respectively compared with ρ_0 and $S\partial\xi/\partial x$. Under these conditions Webster showed that the differential equation for harmonic waves in the horn, in terms of the excess pressure p is

$$\frac{\partial^2 p}{\partial x^2}+\frac{\partial(\log S)}{\partial x}\cdot\frac{\partial p}{\partial x}+k^2 p=0 \tag{2}$$

where $k=\omega/c=2\pi/\lambda$; ω being 2π times the frequency and c the velocity of sound. A corresponding equation in ξ can be obtained from the equation of motion, viz.

$$\ddot{\xi}=-\omega^2\xi=-\frac{1}{\rho_0}\frac{\partial p}{\partial x}. \tag{3}$$

It is, however, for our purposes unnecessary to write the equation in ξ.

The method of the present article then is to obtain the general solution of (2) for various functional values of S corresponding to different types of

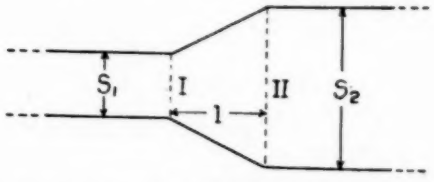

Fig. 2. Acoustical conduits joined by a connector.

connectors, apply the usual boundary conditions at the two ends of the connector and so determine P_r. The detailed analysis for the general case fol-

[1] H. Brillië, Le Genie Civil **75**, 223 (1919).

[2] A. G. Webster, Proc. Nat. Acad. Sci. **5**, 275 (1919).

lows. In Fig. 2 there is shown a conduit of cross section S_1 joined to one of cross section S_2 by a connector of length l which is here shown for simplicity as the frustrum of a cone, but which is of arbitrary nature, that is $S=S_0\phi(x)$ is the law of area change. Now let us write the general solution of Eq. (2) for harmonic waves in the form $p=[Af(x)e^{-ikx}+Bg(x)e^{ikx}]e^{i\omega t}$ corresponding to two waves progressing in opposite directions along the connector. The corresponding expression for the displacement is

$$\xi=\frac{1}{\rho_0\omega^2}\frac{\partial p}{\partial x}$$
$$=[A(f'-ikf)e^{-ikx}+B(g'+ikg)e^{ikx}]e^{i\omega t} \tag{5}$$

where the prime indicates differentiation with respect to x. We desire to discuss the transmission through the system from left to right (i.e. in the positive x direction). Let us denote the displacement amplitudes of the incident and reflected plane waves in the conduit S_1 at the boundary I (where $x=x_1$) by A_1 and B_1 respectively, where it is to be noted that B_1 is measured in the negative x direction. The transmitted displacement amplitude in the conduit S_2 at the boundary II ($x=x_2$) is denoted by A_3. As is usual in transmission problems the return wave in S_2 in the negative x direction is neglected. It should also be emphasized that viscosity damping is here left out of consideration. A_2' and B_2' denote the amplitudes in the connector. But for the sake of simplicity in writing down the boundary conditions we shall set $A_2=A_2'e^{-ikx_1}$ and $B_2=B_2'e^{ikx_1}$. Recalling now that in a plane wave the excess pressure $p=\pm\rho_0c^2\partial\xi/\partial x$, where the plus or minus sign is to be used according as the wave is progressing in the negative or positive x direction, we proceed to write the conditions of continuity of excess pressure and volume displacement (area times particle displacement) at the two boundaries as follows

Boundary I ($x=x_1$)

Displacement

$$A_1-B_1=\frac{1}{\rho_0\omega^2}[A_2(f_1'-ikf_1)+B_2(g_1'+ikg_1)]. \tag{6}$$

Pressure

$$ik\rho_0c^2(A_1+B_1)=A_2f_1+B_2g_1 \tag{7}$$

Boundary II ($x=x_2$)

Displacement

$$\frac{1}{\rho_0\omega^2}[A_2e^{-ikl}(f_2'-ikf_2)+B_2e^{ikl}(g_2'+ikg_2)]=A_3. \tag{8}$$

Pressure

$$A_2f_2e^{-ikl}+B_2g_2e^{ikl}=ik\rho_0c^2A_3 \tag{9}$$

The subscripts 1 and 2 indicate the values of the functions f, g, f' and g' at the boundaries. The solution of Eqs. (6), (7), (8) and (9) consists in the elimination of B_1, A_2 and B_2, and the expression of A_3 in terms of A_1. If this is done it is found that

$$A_1=\frac{A_3}{2}\left\{\frac{if_2'g_1'e^{-ikl}/k+(2g_2-ig_2'/k)(f_1'-2ikf_1)e^{ikl}}{(g_2f_2'-f_2g_2'-2ikf_2g_2)}\right\}. \tag{10}$$

Now the transmission through the system is the ratio of the average rate of flow of sound energy in the transmitted wave to the average rate of flow in the incident wave. That is,

$$P_r=\overline{p_t\dot{X}_t}/\overline{p_i\dot{X}_i}=S_2/S_1\cdot|A_3|^2/|A_1|^2 \tag{11}$$

where $\dot{X}_i=S_1\dot{\xi}_i$, and $\dot{X}_t=S_2\dot{\xi}_t$ denote the incident and transmitted volume currents respectively and the bars denote time average. A_3 and A_1 are, of course, in general complex and in (11) the absolute values must be taken. In order to evaluate P_r, it is necessary to reduce Eq. (10) by the introduction of the values of f_1, g_1, f_2, g_2, etc., appropriate to the special connector being used. We shall now do this for a number of special cases and discuss the results.

Conical Connector

For the conical connector we have $S=S_0x^2$ as the law of areas. The differential Eq. (2) takes the form

$$\frac{\partial^2p}{\partial x^2}+\frac{2}{x}\cdot\frac{\partial p}{\partial x}+k^2p=0 \tag{12}$$

and the solution may be put into the form (4) where

$$f=g=1/kx \tag{13}$$

and

$$f'=g'=-1/kx^2.$$

On substitution, reduction and separation of the real and imaginary parts, the relation (10) then becomes in this case

$$A_1=x_2/x_1\cdot A_3(G+iH) \tag{14}$$

where

$$G=\cos kl+kl\sin kl/2k^2x_1x_2 \tag{15}$$

and

$$H=(1+1/2k^2x_1x_2)\sin kl-kl\cos kl/2k^2x_1x_2. \tag{16}$$

Since $S_2/S_1=x_2^2/x_1^2$, the transmission ratio is then (from (11))

$$P_r=1/(G^2+H^2). \tag{17}$$

For purposes of calculation it will be convenient to express x_1 and x_2 in terms of l and $m=x_2/x_1=(S_2/S_1)^{1/2}$, since the principal points of importance about the connector are its length and expansion ratio. If this is done we have, since $x_1=l/(m-1)$,

$$G=(m-1)^2/2m\cdot\sin kl/kl+\cos kl$$
$$H=(1+(m-1)^2/2mk^2l^2)\sin kl-(m-1)^2/2m\cdot\cos kl/kl. \tag{18}$$

The form of G and H shows that the conical connector is selective in frequency, but for a given connector as the frequency increases the transmission approaches unity more or less rapidly depending on m and l. The action is perhaps best illustrated by means of the following curves in Fig. 3, which indicates the result of plotting the transmission against frequency for the cases $m=2$ and 3 and $l=10$ cm and 50 cm. It is interesting to note from the

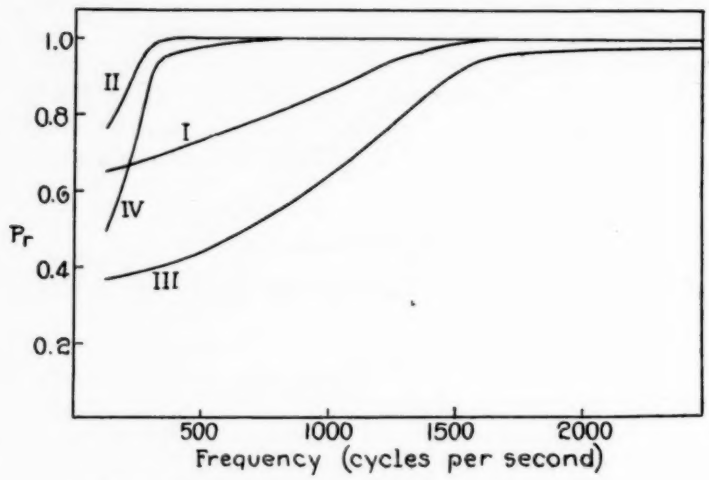

Fig. 3. Power transmission through conical connector.
I, $m=2$, $l=10$ cm; II, $m=2$, $l=50$ cm
III, $m=3$, $l=10$ cm; IV, $m=3$, $l=50$ cm.

character of the curves that in each case for very small values of kl, P_r approximates the value given by Eq. (1) for an abrupt change in cross section. This is also evident from reduction of the formulae (18) for this special case. As kl increases the transmission improves, indicating that to get good transmission for low frequencies a long connector should be employed. For high frequencies it is possible to utilize a shorter one.

It is now desirable to investigate the effect of using as connectors horns of different shape from the conical.

Bessel Connectors of Higher Order

Following Ballantine[3] we may term the connector in which the change in area follows the equation $S=S_0x^a$, a generalized Bessel connector of order a. When $a=2$ we have the special case of the conical horn already treated.

[3] S. Ballantine, Jour. Franklin Inst. **203**, 85 (1927).

Instead of treating each case separately we may now investigate the general case. The fundamental differential Eq. (2) here takes the form

$$\frac{d^2p}{dx^2}+\frac{a}{x}\cdot\frac{dp}{dx}+k^2p=0 \tag{19}$$

where we employ ordinary derivatives and discuss the equation as an ordinary one. It will be convenient to make the substitution $z=kx$, whence the equation becomes

$$\frac{d^2p}{dz^2}+\frac{a}{z}\frac{dp}{dz}+p=0. \tag{19'}$$

In the first instance it will probably suffice to consider the solutions for z large, the simpler case. As a linear second order differential equation, (19') has an essential singularity at $z=\infty$. Nevertheless we can get an asymptotic solution for z large in the usual way. Neglecting in the first instance the middle term the equation becomes

$$\frac{d^2p}{dz^2}+p=0 \tag{20}$$

with the two solutions $p=e^{iz}$ and $p=e^{-iz}$. Writing $p=ve^{iz}$, substituting into (19') and considering v as "slowly varying" so that d^2v/dz^2 and adv/zdz can be neglected compared with dv/dz etc., we have for the determining equation for v

$$\frac{dv}{dz}=-\frac{av}{2z} \tag{21}$$

whence

$$v=C/z^{a/2} \tag{22}$$

C being an arbitrary constant. The quantities f and g of the general solution (4) then are

$$\begin{aligned} f&=g=1/(kx)^{a/2}\\ f'&=g'=-ak/2\cdot(kx)^{-a/2-1}\end{aligned} \tag{23}$$

The Eq. (10) then becomes

$$A_1=(x_2/x_1)^{a/2}A_3(G+iH) \tag{24}$$

with

$$\begin{aligned} G&=\cos kl+a(m^{2/a}-1)^2/4m^{2/a}\cdot\sin kl/kl \\ H&=(1+a^2(m^{2/a}-1)^2/8m^{2/a}k^2l^2)\sin kl-a(m^{2/a}-1)^2/4m^{2/a}\cdot\cos kl/kl\end{aligned} \tag{25}$$

wherein we have made use of the relations $x_2/x_1=m^{2/a}$ and $x_1=l/m^{2/a}-1$, l being as before the length of the connector. Incidentally we note that for

$a=2$ Eq. (25) reduces to the special form (18) already discussed. Neglecting higher powers of $1/kl$ than the second we may write for the transmission ratio

$$P_r=\left\{1+a^2(m^{2/a}-1)^2/4m^{2/a}k^2l^2\cdot\left[\sin^2 kl+(m^{2/a}-1)^2/4m^{2/a}\right]\right\}^{-1}. \qquad (26)$$

For given a and m, P_r rapidly approaches unity with increasing kl. Moreover for given m, it is easily verified that

$$\lim_{a\doteq\infty} a(m^{2/a}-1)/2m^{1/a}=\log m$$

and for small m (i.e. not greater than 4) the limiting value is attained to a good approximation for relatively small values of a. Inspection of Eq. (26) then shows that acoustic connectors with cross section following the law $S=S_0x^a$ yield a transmission which is practically independent of a for reasonably large values of kl. The differences introduced by the term in the bracket in Eq. (26) can at most amount to a few percent and will in general be safely negligible in practice. Since there is no restriction on the sign of a, the above statement also applies, among others, to the *hyperbolic* connector for which $a=-2$. Indeed the expression for P_r is an even function of a and therefore has the same value for $+a$ and $-a$. Moreover, since $\lim_{a\doteq\infty} x^a=e^{-a}\,e^{ax}$, the limiting case of the Bessel connector is an *exponential* connector[4] and in this case the expression for the transmission reduces to the form

$$P_r=\left\{1+[(\log m)/kl]^2\sin^2 kl\right\}^{-1} \qquad (27)$$

precisely the form which is indicated by direct calculation based on the differential equation for the exponential horn, under the approximation mentioned. The computation of the transmission for special values of m and l is unnecessary, for it is evident that the results will not differ materially from those indicated for the conical connector, thus implying that under the conditions specified the exponential connector enjoys no preference in practice over the conical type. Of course our results apply only for $kl>\log m$ and the approximation is better the larger kl. For $kl<\log m$, and indeed for $k<m/2$, Webster's theory of the exponential horn breaks down.[5] There is thus no point in trying to extend the present work to lower frequencies and very short connectors. As a matter of fact the behavior of the conical connector for small kl is typical of that of all the Bessel connectors under like circumstances, as may be shown by a detailed calculation which will be omitted here. Indeed we see from Eq. (18) that as $kl\doteq 0$, $H\doteq 0$ and $G\doteq 1+(m-1)^2/2m$ so that the transmission approaches

$$P_r=4m^2/(m^2+1)^2$$

which is the transmission for abrupt change of cross section.

[4] So far as the writer is aware, the significance of this in horn theory was first pointed out by C. R. Hanna, Jour. Franklin Inst. **203**, 849 (1927).

[5] See, for example, Ballantine, reference 3.

CONNECTOR $S=S_0e^{-ax^2}$

The connectors previously considered have generating curves showing no point of inflection. One of the simplest types of generating curves with a point of inflection is the curve of the error function to which corresponds the connector with cross sectional area governed by the law $S=S_0e^{-ax^2}$. The fundamental Eq. (2) then becomes

$$\frac{d^2p}{dx^2}-2ax\frac{dp}{dx}+k^2p=0. \tag{28}$$

Introducing the transformation $z=kx$ and utilizing the definition of m to write $a=2(\log m)/l^2$ ($m>1$: note that we have taken $x_1=0$ for simplicity), this equation becomes

$$\frac{d^2p}{dz^2}-\frac{4\log m}{k^2l^2}\cdot z\frac{dp}{dz}+p=0. \tag{28'}$$

Now $z\leqq kl$, and if kl is large compared with $\log m$, the asymptotic solution is again $p=ve^{\pm iz}$, where by the usual scheme used above we find $v=e^{az^2/2k^2}=e^{ax^2/2}$, so that if the solution is put into the form given in Eq. (4) we have

$$\begin{aligned} f&=g=e^{ax^2/2}\\ f'&=g'=axe^{ax^2/2}. \end{aligned} \tag{29}$$

The usual procedure yields here for the transmission ratio

$$P_r=\{1+[(\log m)/kl]^2\}^{-1}. \tag{30}$$

Comparison with Eq. (27) indicates that there is no particular advantage to be gained in employing the type of connector here under consideration.

For kl small, it can be shown that in this case also, as would be expected, the power transmission approaches the limiting value for abrupt change given in Eq. (1).

The theoretical conclusions reached in this paper are confirmed to a large extent by some experiments of G. W. Stewart,[6] who investigated experimentally the transmission through three connectors of similar dimensions (i.e. same m and l); one was a conical connector, one an exponential connector, and the third a connector with the generating curve having a point of inflection, approximating the case $S=S_0e^{-ax^2}$ discussed above. It was found that the difference in transmission through the three connectors was not more than two or three percent throughout the frequency range from 600 to 3200 cycles per second.

PHASE CHANGE INTRODUCED BY CONNECTORS

In several of the practical uses of acoustical conduits the phase of the wave is of importance (e.g. conduits used in binaural localization, etc.).

[6] Unpublished.

Hence the phase change introduced by a connector is a matter of significance. Referring again to Eq. (10), if we write this in the form

$$A_1 = A_3 e^{i\theta} \tag{31}$$

the phase change due to the connector will be θ. Taking first the general Bessel connector we see from Eq. (25) that the phase change here is given by

$$\tan\theta = H/G \tag{32}$$

which for given a and m approaches $\tan kl$ as kl gets larger. For the exponential connector the corresponding expression is

$$\tan\theta = \tan kl \cdot \left[1+\frac{1}{2}\left(\frac{\log m}{kl}\right)^2\right] \tag{33}$$

which also for given m reduces to $\tan kl$ in the limit of large kl. Finally for the connector $S = S_0 e^{-ax^2}$, we have

$$\tan\theta = \frac{\tan kl - (\log m)/kl}{1+(\log m)/kl \cdot \tan kl} = \tan(kl-\psi) \tag{34}$$

where $\tan\psi = (\log m)/kl$. Again the limiting value is $\tan kl$.

LETTERS TO THE EDITOR

Prompt publication of brief reports of important discoveries in physics may be secured by addressing them to this department. Closing dates for this department are, for the first issue of the month, the twenty-eight of the preceding month; for the second issue, the thirteenth of the month. The Board of Editors does not hold itself responsible for the opinions expressed by the correspondents.

The Heat of Dissociation of Oxygen

It has recently been suggested by Gerhard Herzberg (Zeits. f. phys. Chem. **4B**, 223 (1929)) that the currently accepted value for the heat of dissociation of oxygen is too high. Herzberg concludes that the correct value is not 7.0 volts, but somewhere between 5 and 6 volts; the basis for the conclusion is a re-interpretation of the Lyman-Runge bands on the basis of a theory developed by Wigner and Witmer.

This lower value receives at least a partial confirmation from an entirely different source. The present writer has previously pointed out (Zeits. f. phys. Chem. **2B**, 264 (1929)) that it is possible to calculate a value for the heat of dissociation from the measurement by Risenfeld and Schumacher of what these authors state is a homogeneous unimolecular decomposition of ozone. The calculation is based upon the very likely assumption that the primary process in the decomposition is the step $O_3 \rightarrow O_2 + O$ and involves the not very well known heat of formation of ozone; furthermore, there is still some doubt whether the decomposition concerned is entirely homogeneous. The result of the calculation is 4.8 volts (110,000 calories) and the error can scarcely be more than 0.5 volts, if the reaction involved is homogeneous; if not, the calculations are of course of no value. In spite of this uncertainty, the agreement seems to the writer to lend support to the lower value proposed by Herzberg, and also to suggest that the correct value lies within the narrower limits of 5.0 to 5.5 volts.

Gates Chemical Laboratory
California Institute of Technology
LOUIS S. KASSEL

August 13, 1929. (National Research Fellow)

On the Possibility of Nuclear Disintegration by Artificial Sources

It has been pointed out by Atkinson and Houtermans[1] that it may be easier to transmute elements by bombarding them with protons rather than with alpha-particles. It is of interest to consider the significance of their remark for protons accelerated artificially by means of high potentials. It turns out that it is reasonable to expect them to penetrate the nuclei of the lighter elements under accelerating potentials within the experimentally readily obtainable range. Before Gamow's[2] suggestion as to the possible nature of artificial nuclear disintegration it was customary to speak of the required potentials in terms of the energies of the alpha-particles expressed in electron-volts. These energies are from 5.2×10^6 for polonium to 8.8×10^6 for ThC'. Artificial sources operating at such potentials will probably require many years of development. It will be readily seen however that protons accelerated by 2.6×10^6 volts have a greater probability of penetrating the nucleus than the 5.2×10^6 "electron-volt-equivalent" alpha particles. Whether a proton inside a light nucleus will necessarily have a disintegrating effect is of course uncertain. If no disintegration results it is reasonable to expect deviations from Rutherford's inverse square law of scattering. It should be possible to get information about the dimensions of nuclei in a better way by means of protons than has been done heretofore by means of alpha-particles.

[1] Atkinson and Houtermans, Zeits. f. Physik **54**, 656 (1929).

[2] Gamow, Zeits. f. Physik **52**, 510 (1928).

The main point of the theory of radioactive disintegration developed by Gurney and Condon and by Gamow is that the potential wall around the nucleus is partly transparent for particles having too little energy to jump the wall according to classical dynamics. The probability that a particle should penetrate the wall is given approximately by $\exp[-2\int[8\pi^2mh^{-2}(U(x)-E)]^{1/2}dx]$ where m is the mass, E the energy, and the potential energy of the wall for the particle is $U(x)$. If the particle has the charge e and is accelerated before impact by a potential V_0 its energy is $E=eV_0$ and the potential energy is $U(x)=eV(x)$ where $V(x)$ is the electrostatic potential. The important exponential factor is therefore $\exp[-(me)^{1/2}A]$ where A depends only on the nucleus and the accelerating potential. For the same A therefore the negative exponent is $2\cdot 2^{1/2}=2.82$ times smaller for a proton than for an alpha-particle.

In Gamow's treatment, particularly in his formula (7) it is not altogether clear how the sum of the cross sections of the nuclei enters in the final result. On a rough picture of the collisions the outside of the wall might be supposed to determine the effective cross section. On the other hand the electrons impinge partly from the side and obliquely. It is easy to obtain an estimate of these effects for the case of a small nuclear diameter using the exact solutions worked out for a Coulomb field of force.[3] Taking the incident beam of V_0 electrons per second per centimeter square the number of particles penetrating through a small sphere of radius r_0 is $\pi r_0^2 v_0 x/(\epsilon^x-1)$ where $x=4\pi^2ee'/v_0h$. Here e is the charge of the incident particle and e' the charge of the nucleus; v_0 is the velocity of the incident particles at infinity and $\epsilon=2.718$. It is seen that the exponential factor is still the controlling one. It is reasonable to take therefore Gamow's formula (5) as the criterion. The order of magnitude of W_1^* for Fe is $10^{-6.5}$ for Po alpha-particles and $10^{2.2}$ for 2.6×10^6 volt protons. Since according to Gamow's Fig. 5 Al has been disintegrated for values of W comparable to 10^{-1} we may expect 2.6×10^6 volt protons not only to penetrate Al nuclei but also those of heavier elements approaching in atomic number that of Fe. It must be remembered here that presumably large quantities of artificially accelerated particles can be produced. For Al the same protons would have $W_1^*\leqq10^{-0.5}=1/3$. If 1.5×10^6 volt protons are used $W_1^*\leqq10^{-1.7}$ for Al and $10^{-0.5}$ for N. Thus even 1500 kv protons should be of interest for the lighter elements. Experiments with such voltages should be not too difficult to perform.

Department of Terrestrial Magnetism
G. BREIT

August 28, 1929

[3] Gordan, Zeits. f. Physik **48**, 180 (1928); Mott, Proc. Roy. Soc. **A118**, 542 (1928),

BOOK REVIEWS

Thermodynamik. Die Lehre von den Kreisprozessen, den physikalischen und chemischen Veränderungen und Gleichgewichten. Eine Einführung zu den thermodynamischen Problemen unserer Kraft- und Stoffwirtschaft. Dr. W. SCHOTTKY, in Gemeinschaft mit Dr. H. ULICH und Dr. C. WAGNER, with 90 figures and 1 Table, xxv+619 pages, 25 x 17 cm. Julius Springer, Berlin, 1929. Price: unbound, RM56; bound RM 58.80.

It is to be said at once that this is a very notable addition to thermodynamic literature, and no adequate review of it can be given in the space available here.

The book has been largely influenced by the book of Lewis and Randall, and in fact it may be partially characterized as an attempt to formulate critically and rigorously the fundamental principles and to exhibit the full details of the practical applications of these principles to the sort of problems in chemical thermodynamics which were the chief interest of Lewis and Randall. That this is the emphasis of the book is roughly shown by the allocation of space given to various topics: the first 80 pages to general thermodynamics, the next 44 pages to physical thermodynamics, and the last 487 pages to chemical thermodynamics.

The fundamental method of treating general principles will be of the greatest interest to all those who have felt an uneasy distrust of the adequacy to meet the present enlarged situation of formulations which were satisfactory enough in the time of Gibbs. For example, many teachers of thermodynamics must have been embarrassed in formulating the concept of "component" in such a way as not to reduce to the absurd statement that every chemical system is built of just two components, electrons and protons. The new concept of "Resistente Gruppen" introduced to take the place of the old concept of "molecule" in framing the notion of component seems to offer a satisfactory way of dealing with the situation. This concept is elastic enough to apply to the newly discovered phenomena at low temperatures where internal changes in the atoms from one quantum state to another have measurable physical effects. In fact, the treatment of Nernst's theorem and general phenomena at low temperatures are perhaps one of the most interesting parts of the book to the pure physicist. In addition to the concept of Resistente Gruppen, the concept of restricted and unrestricted equilibrium plays an important part in the rigorous treatment of the phase rule.

There are many features in which the treatment offers novelties; a list of these will be found in the preface. Two of special interest were the application of thermodynamic principles to capillary-electric phenomena, and the careful formulation and extensive applications of the principle of le Chatelier-Braun.

In the attempt to secure rigor it seems to me that sometimes principles have been formulated in too restricted terms, although without doubt the formulation is broad enough for the problems treated in the book. Thus it is not clear that the fundamental definition (on page 5) of what is meant by a thermodynamic system is broad enough to permit treating a system in which electrons are being emitted from a hot body as a thermodynamic system; some modification will evidently have to be made in the way in which "transfer" temperature is associated with the concept of heat, before the transfer of heat by radiation between two bodies at different temperatures can be treated as a problem in thermodynamics (page 39); and it is not obvious in what sense it can be said (page 134) that in principle a reversible method always exists for carrying out any chemical reaction.

The book is not easy to read, but demands concentrated attention from any one who is to profit by it. The style is uneven; in places it is almost eloquent, but in others it drags and gives the impression of prolixity; perhaps this is unavoidable in a joint work by three authors. One of the most valuable parts of the book is the last chapter of 65 pages in which is given a detailed solution of 18 practical problems; the reader would have been grateful if the severe abstraction of many of the theoretical parts had been relieved by illustration by other practical applications, not necessarily worked out in such detail. P. W. BRIDGMAN

Elektrische Gleichrichter und Ventile. A. GÜNTHER-SCHULZE. Pp. 330, figs. 305. Julius Springer, Berlin, 1929. Price: RM 29.00.

The ever increasing and large variety of uses for rectifiers and electrical valves make this book particularly timely. The author's well known and wide experience in modern physics and especially in discharge devices make him a master of his subject. He first deals with the physical and chemical fundamentals of rectification and rectifying devices in a simple and lucid manner. The technique of using rectifiers in various types of circuits is taken up next. Then follows a detailed description of commercially available rectifiers. The patent literature is thoroughly reviewed. The book should be interesting to physicists, chemists and engineers who deal with rectifiers. The illustrations are clear and very numerous and the printing is good.

J. A. BECKER